EXPLOITING ALCOHOL DEHYDROGENASES IN THE ASYMMETRIC SYNTHESIS OF HYDROXY COMPOUNDS:

An easy, highly efficient and sustainable access to chiral building blocks

Marion Müller
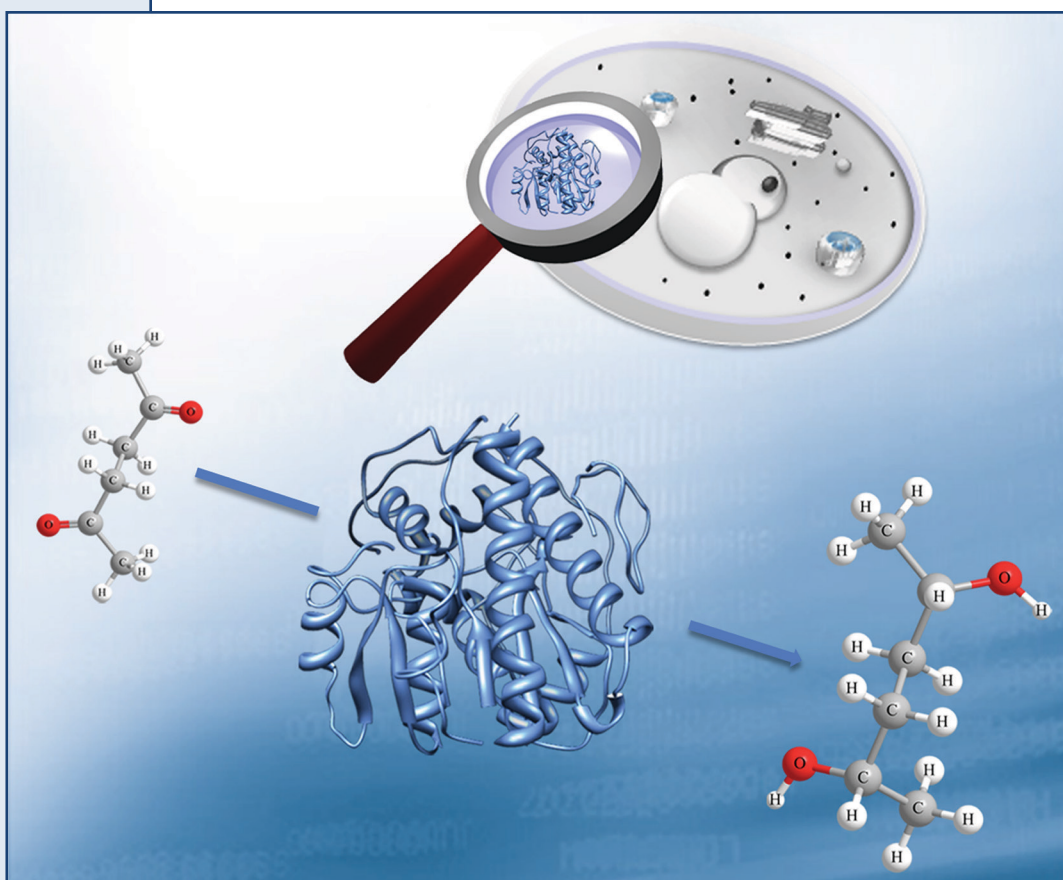
Thesis for doctoral degree (Dr. *rer. nat.*)

Exploiting alcohol dehydrogenases in the asymmetric synthesis of hydroxy compounds:
An easy, highly efficient and sustainable access to chiral building blocks

Inaugural-Dissertation

zur Erlangung des Doktorgrades
der Mathematisch-Naturwissenschaftlichen Fakultät
der Heinrich-Heine-Universität Düsseldorf

vorgelegt von

Marion Müller
aus Rostock

Düsseldorf, Oktober 2014

aus dem Institut für Molekulare Enzymtechnologie
der Heinrich-Heine Universität Düsseldorf

Gedruckt mit der Genehmigung der
Mathematisch-Naturwissenschaftlichen Fakultät der
Heinrich-Heine-Universität Düsseldorf

Referent: Prof. Dr. Werner Hummel
Korreferent: Prof. Dr. Vlada Urlacher

Tag der mündlichen Prüfung: 10.07.2015

SUMMARY

Asymmetric synthesis generates chiral compounds from prochiral ones. The former are important building blocks for the synthesis of pharmaceuticals, fine chemicals and agrochemicals. One example of a much sought-after chiral key building block is (2S,5S)-hexanediol. The compound is obtained through a two-stage reduction from 2,5-hexanedione. Chemical synthesis is both economically and environmentally unfriendly, mainly due to low atom economy, production of unwanted by-products, harsh reaction conditions and the need for a transition metal catalyst, which is both expensive and toxic. There is currently only one commercially viable biocatalytic route: biotransformation of the γ-diketone mediated by baker's yeast (*Saccharomyces cerevisiae*). However, because of the small quantities of the responsible enzyme in the cell, cell productivity is low, resulting in a low reaction velocity. The aim of the work presented in this doctoral thesis was to overcome these disadvantages by identifying the 2,5-hexanedione-reducing enzyme and then optimising (2S,5S)-hexanediol synthesis.

Through an activity-based and column-chromatographic purification of baker's yeast, NADPH-dependent Gre2p was identified as the 2,5-hexanedione-reducing enzyme. Enantiopure (2S,5S)-hexanediol was synthesised on a laboratory-scale (20 mM) through *in vitro* biotransformation using recombinant Gre2p together with glucose dehydrogenase (GDH) for cofactor recycling. Due to increased enzyme amounts, reaction velocity and space-time yield (g·L^{-1}·d^{-1}) were higher in comparison to conventional synthesis. In addition, as a large quantity of recombinant enzyme was formed as insoluble and inactive protein (so-called "inclusion bodies"), expression of *GRE2* in *E. coli* was further optimised. This was achieved by cloning a synthetic gene adapted to the bias of *E. coli* into a plasmid which reveals a lower copy-number than the pET-vector system. The enzyme thus produced revealed an approximately 600-fold increase in specific activity compared with wild-type cell-free extract. In contrast, homologous gene expression in the *S. cerevisiae* strain BY4741 resulted in only a 140-fold increase in Gre2p activity. With cell-free approaches, (2S,5S)-hexanediol was synthesised up to a concentration of 0.2 M with a space-time yield of 374 g·L^{-1}·d^{-1}. With an *E. coli* designer catalyst expressing genes for Gre2p and GDH, it was feasible to reduce even 0.5 and 1 M diketone with space-time yields of 572 and 361 g·L^{-1}·d^{-1}.

This whole-cell system resulted in significantly better cell productivity and co-substrate yield than both conventional biotransformation via baker's yeast and *in vivo* synthesis using the recombinant *S. cerevisiae* strain.

Moreover, in-depth characterisation revealed that Gre2p also reduces the reduction of *α*- and *β*-diketones, leading to optically active hydroxy ketones and diols.

To solve the three-dimensional structure of Gre2p, several screening and optimisation approaches were taken. Crystals of a Gre2p complex with NADP$^+$ were grown using polyethylene glycol (PEG) 8000 as a precipitant. The diffraction resolution was 3.2 Å.

In an attempt to identify new alcohol dehydrogenases, *in silico* screening based on the amino acid sequence of Gre2p was performed, resulting in the identification of a novel alcohol dehydrogenase (KpADH) from the yeast *Kluyveromyces polysporus*. The enzyme was shown to reduce a broad spectrum of carbonyl compounds and was successfully applied in the synthesis of several optically active compounds, such as (*S*)-2-pentanol or (*R*)-ethyl-3-methyl-2-hydroxybutanoate, which are important synthons for the production of anti-Alzheimer's drugs and protease inhibitors, respectively.

In summary, the findings presented in this thesis establish the basis for the production of (2*S*,5*S*)-hexanediol on a commercial-scale via biotransformation of 2,5-hexanedione using either isolated and recombinant enzyme or tailor-made cells. Moreover, Gre2p and a newly identified alcohol dehydrogenase were successfully applied in the synthesis of further valuable chiral building blocks.

ZUSAMMENFASSUNG

Die asymmetrische Synthese überführt prochirale Verbindungen in chirale. Letztere sind wichtige Schlüsselbausteine bei der Herstellung von Pharmazeutika und Fein- sowie Agrochemikalien. In diesem Zusammenhang ist auch der Bedarf an enantiomerenreinem (2*S*,5*S*)-Hexandiol sehr hoch. Die Verbindung wird durch eine zweistufige Reduktion aus 2,5-Hexandion gewonnen. Die chemische Herstellung ist sowohl ökonomisch als auch ökologisch unzureichend, im Wesentlichen, aufgrund niedriger Atomökonomie, der Bildung von Nebenprodukten, extremen Reaktionsbedingungen und dem Bedarf an hochpreisigem sowie toxischem Übergangsmetallkatalysator. Gegenwärtig gibt es nur eine wirtschaftlich interessante biokatalytische Synthesemethode: Die Biotransformation des *γ*-Diketons durch Bäckerhefe (*Saccharomyces cerevisiae*). Da aber nur geringe Mengen des verantwortlichen Enzyms in der Zelle vorhanden sind, ist die Zellproduktivität niedrig, so dass eine niedrige Reaktionsgeschwindigkeit resultiert. Um dem entgegenzuwirken, sollte in dieser Doktorarbeit das 2,5-Hexandion-reduzierende Enzym identifiziert und anschließend die (2*S*,5*S*)-Hexandiol-Synthese mit rekombinantem Enzym optimiert werden.

Nach einer aktivitätsbasierten und säulenchromatographischen Reinigung der Bäckerhefe wurde die NADPH-abhängige Alkoholdehydrogenase Gre2p als das 2,5-Hexandion-reduzierende Enzym identifiziert. Enantiomerenreines (2*S*,5*S*)-Hexandiol konnte im Labormaßstab (20 mM) durch *in vitro* Biotransformation mit isoliertem, rekombinantem Enzym und Glukosedehydrogenase (GDH), die zur Cofaktorregenerierung eingesetzt wurde, synthetisiert werden. Die Reaktionsgeschwindigkeit als auch die Raumzeitausbeute ($g \cdot L^{-1} \cdot d^{-1}$) konnten im Vergleich zum herkömmlichen Verfahren um ein Vielfaches gesteigert werden, was der Bereitstellung größerer Enzymmengen zuzuschreiben ist. Da ein größerer Anteil an rekombinantem Enzym als unlösliches, inaktives Protein, sog. „Inclusion bodies" gebildet wurde, wurde in der Folge die Expression das entsprechende Gens *GRE2* in *Escherichia coli* weiter optimiert. Dies wurde durch Verwendung eines synthetischen Gens mit adaptierter *E. coli* Codon Usage in ein Plasmid, das im Vergleich zum pET-Vektorsystem eine geringere Kopienzahl besitzt, erzielt. Das auf diese Weise produzierte Enzym zeigte eine etwa 600-fach höhere spezifische Aktivität als der Rohextrakt des Wildtyps. Im Gegensatz dazu führte die homologe Expression im *S. cerevisiae* Stamm BY4741 nur zu einer 140-fach erhöhten Gre2p Aktivität. In zellfreien Ansätzen konnte (2*S*,5*S*)-Hexandiol bis zu einer Konzentration von 0,2 M mit einer Raumzeitausbeute von 374 $g \cdot L^{-1} \cdot d^{-1}$ synthetisiert werden. Mit Hilfe eines

rekombinanten *E. coli*-Ganzzellkatalysators, der neben dem Gen für Gre2p auch das für die GDH co-exprimiert (sog. „Designer-Zellen"), konnten sogar 0,5 und 1 M Diketon mit 572 und 361 $g \cdot L^{-1} \cdot d^{-1}$ reduziert werden. Dieses Ganzzellsystem war in Raumzeitausbeute, Zellproduktivität und Co-Substrat-Verbrauchsrate nicht nur wesentlich besser als die herkömmliche Biotransformation mit Bäckerhefe, sondern übertraf auch die *in vivo* Synthese mit dem rekombinant hergestellten *S. cerevisiae*-Stamm.

Es konnte außerdem durch detaillierte Charakterisierung des Gre2p-Enzyms gezeigt werden, dass es in der Lage ist, auch die Reduktion von *α*- und *β*-Diketonen zu katalysieren. Hierbei wurden sowohl nahezu optisch reine Hydroxyketone als auch Diole erzielt.

Zur Aufklärung der 3D-Struktur von Gre2p wurden mehrere Screening- und Optimierungsansätze durchgeführt. Kristalle eines Gre2p-NADP$^+$-Komplexes wuchsen in Gegenwart des Präzipitats Polyethylenglycol (PEG) 8000. Die Röntgenstrukturanalyse erbrachte eine Auflösung von 3,2 Å.

Basierend auf der Aminosäuresequenz von Gre2p wurde ein *in silico* Screening durchgeführt, das zur Identifikation einer neuen Alkoholdehydrogenase aus der Hefe *Kluyveromyces polysporus* führte. Es zeigte sich, dass das Enzym in der Lage ist, ein breites Spektrum von Carbonylverbindungen zu reduzieren. Es wurde zudem erfolgreich zur Synthese einer Vielzahl optisch aktiver Verbindungen, wie z.B. (*S*)-2-Pentanol oder (*R*)-Ethyl-3-methyl-2-hydroxybutanoate, die wichtige chirale Synthons für die Herstellung von Anti-Alzheimer Medikamenten bzw. Protease-Inhibitoren sind, eingesetzt.

Zusammenfassend lässt sich sagen, das die hier erzielten Ergebnisse eine Grundlage für die Synthese von (2*S*,5*S*)-Hexandiol im industriellen Maßstab schaffen. Dabei kann die Biotransformation von 2,5-Hexandion entweder mit Hilfe von isoliertem, rekombinantem Enzym oder mit Designer-Zellen erfolgen. Des Weiteren konnten Gre2p und eine neu-identifizierte Alkoholdehydrogenase erfolgreich in der Synthese weiterer hochwertiger chiraler Schlüsselbausteine eingesetzt werden.

LIST OF PUBLICATIONS

Peer-Reviewed Journals

Katzberg M., Wechler K., **Müller M.**, Dünkelmann P., Stohrer J., Hummel W. and Bertau M. (**2009**) *Biocatalytic production (5S)-hydroxy-2-hexanone*: Org. Biomol. Chem. 7 (2) 304-314

Müller M., Katzberg M., Bertau M. and Hummel W. (**2010**) *Highly efficient and stereoselective biosynthesis of (2S,5S)-hexanediol with a dehydrogenase from Saccharomyces cerevisiae*: Org. Biomol. Chem. 8 (7) 1540-1550

this work has been featured on the front cover of the journal

Breicha K.*, **Müller M.*** Hummel W. and Niefind K. (**2010**) *Crystallization and preliminary crystallographic analysis of Gre2p, a NADP$^+$-dependent alcohol dehydrogenase from Saccharomyces cerevisiae*: Acta Cryst. F66 (7) 838-841

*authors contribute equally to this work

Manuscripts in preparation

Müller M. and Hummel W. *Functional expression of GRE2 from Saccharomyces cerevisiae and application of Gre2p in the asymmetric synthesis of various hydroxy compounds and diols*

Müller M. and Hummel W. *Asymmetric synthesis of (2S,5S)-hexanediol on a preparative-scale using a Saccharomyces cerevisiae strain expressing GRE2 encoding NADPH-dependent alcohol deydrogenase Gre2p*

Müller M. and Hummel W. *Construction and characterisation of Escherichia coli whole-cell catalyts co-producing Saccharomyces cerevisiae alcohol dehydrogenase Gre2p and glucose dehydrogenase and their application in the synthesi of (2S,5S)-hexanediol*

Müller M. and Hummel W. *A novel alcohol dehydrogenase from Kluyveromyces polysporus DSM 70294 revealing a broad range of carbonyl compounds and its application in asymmetric synthesis*

TABLE OF CONTENTS

ABBREVIATIONS

3D	three dimensional
ADH	alcohol dehydrogenase
AKR	aldo keto reductase
BLAST	Basic Local Alignment Search Tool
DNA	deoxyribonucleic acid
E.C.	enzyme commission number
ee	enantiomeric excess
GC	gas chromatography
GDH	glucose dehydrogenase
Gre2p	Genes de Respuesta a Estres (stress-response gene)
IPTG	isopropyl β-D-1-thiogalactopyranoside
Kp_i	potassium phosphate buffer
K_M	Michaelis Menten constant
MS	mass spectroscopy
MDR	medium-chain dehydrogenase
NAD(H)	nicotinamide adenine dinucleotide
NADP(H)	nicotinamide adenine dinucleotide phosphate
PCR	polymerase chain reaction
PDB	Protein Data Bank
SDR	short-chain dehydrogenase
SDS	sodium dodecyl sulfate
STY	space-time yield
TEA	triethanolamine
TFA	trifluoroacetic acid
Tris	tris(hydroxymethyl)aminomethane
U	Unit

1

INTRODUCTION

1.1 CHIRAL BUILDING BLOCKS - RELEVANCE AND SYNTHESIS

Low-molecular chiral compounds such as the ones shown in Figure 1.1 are valuable intermediates for the manufacture of fine chemicals, agrochemicals, natural products and pharmaceuticals [1-8]. Because of this, their synthesis has become of pivotal interest in organic chemistry over the past few decades.

(2R,5R)-hexanediol	(S)-2-(4-hydroxyphenoxy)propanoic acid (HOPS)	(S)-3,7-dimethyloct-6-enal ((S)-citronellal)	(3R,4S)-2-oxo-4-phenylazetidin-3-yl acetate
ligand precursor	**herbicide precursor**	**pheromone precursor**	**drug precursor**
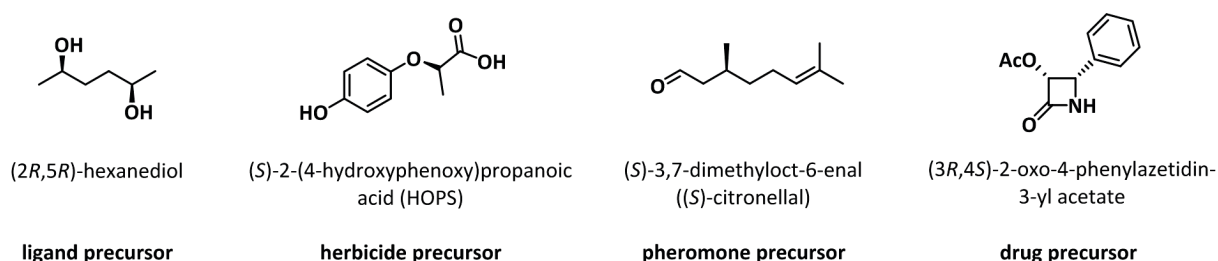
Figure 1.1. Examples of low-molecular chiral compounds which are used in the synthesis of fine chemicals, agrochemicals, natural products or pharmaceuticals.

The key drivers for innovation are the fine chemical and, in particular, the pharmaceutical market [9]. Nearly two-thirds of the drugs on today's market are chiral and contain at least one or more chiral centres [10]. Recently, it was predicted that this number will increase up to 95% by 2020 [11]. Driven by the fact that enantiomers display different biological effects, the US Food and Drug Administration (FDA) passed a law in 1992 under which it is necessary to prove that both the non-therapeutic enantiomer and the racemate of a racemic marketed drug are non-teratogenic [12]. As this requires expensive and time-consuming analysis, pharmaceutical companies have moved their attention to the production of single-enantiomer drugs only [2, 3, 13-16]. Consequently, no new racemic drugs have been placed on the market since 2001 [17, 18].

The growing demand for enantiomerically pure compounds requires efficient, sustainable, healthy and economically attractive synthesis technologies which meet the increasing strict safety, quality and environmentally requirements of industrial production processes [5]. Production of optically pure building blocks can, in principle, be synthesised either (i) from the chiral pool, (ii) by racemate separation or (iii) by asymmetric synthesis [6, 16].

(i) 10-20% of the enantiomerically pure compounds can be synthesised at an affordable price (US$ 100–250 per kg) from the chiral pool which contains of a stock of enantiopure natural compounds such as amino acids, carboxylic acids, carbohydrates, terpenes, alkaloids or

pheromones. The drawbacks of using this technology are that each compound usually has only one enantiomer, e.g. L-amino acids, and that the defined structure of natural compounds make subsequent reaction steps necessary when using them as starting material [13].

(ii) An alternative approach to optically pure compounds is the separation of racemates, which is carried out either by crystallisation, purification or kinetic resolution. The first strategy makes use of the separation of the two diastereomeric salts, revealing different chemical and physical properties. These are obtained from the reaction between the racemate and a single enantiomer that functions as resolving agent. The second technology uses chiral chromatography, mainly HPLC, for the separation of the enantiomers. Kinetic resolution can be carried out using either a chemocatalyst such as a chiral acid or base or a chiral metal complex, or enzymatically using primarily hydrolases [5, 19-26]. It's worth mentioning that the maximum yield of a racemate separation will not exceed 50%, even when 100% conversion is achieved, due to the existence of equimolar quantities of both enantiomers. Thus, the "left over" 50% comprises the "wrong enantiomer". This is especially important when the target building block has to be prepared on a large scale, since the yield will have an impact on production costs [6].

(iii) In contrast to racemate separation, a maximum yield of 100% can be achieved by asymmetric synthesis, which is the subject of this thesis. This technology uses chiral catalysts to introduce chirality stereoselectively into compounds. The catalysts are either chemical or biological in nature. The chemical ones are organometal-types including transition metals which have the ability to differentiate the enantiotopic faces of a prochiral functional group [27]. These catalysts were first developed by W.S. Knowles, R. Noyori [28] and K.B. Sharpless [29], who were awarded the 2001 Chemistry Nobel prize for their pioneering work on catalytic asymmetric synthesis.

Asymmetric synthesis using biological catalysts is predominantly performed by oxidoreductases. Other enzymes (e.g. transaminases, lyases, glycosyltransferases or nitrilases) can also be employed for the synthesis of biologically active compounds [5, 6, 19, 21, 22, 26, 30-33].

1.2 BIOCATALYSIS – THE USE OF ENZYMES OR MICROBES FOR THE PRODUCTION OF OPTICALLY ACTIVE MOLECULES

Biocatalysis is the exploitation of enzymes or microorganisms in synthetic chemistry [13, 34-36]. The first biocatalytic application was achieved by Rosenthaler over a century ago when he synthesised (*R*)-mandelonitrile from benzaldehyde and hydrogen cyanide using a plant extract [37]. Since then, many enzymes have been identified and have been applied for the production of both natural and non-natural compounds, like chiral building blocks, fuels, materials and chemical feedstocks [5, 7, 16, 19, 26, 36, 38-48]. A key step in this progress was the introduction of recombinant DNA technology, in particular the discovery of restriction enzymes allowing the transfer of genes into other organisms to enhance the production yields of the corresponding proteins [34, 46].

Another rapid catch-up of biocatalytic reactions has been observed over the past two decades, which is undoubtedly due to both the pioneering work of Frances Arnold and Pim Stemmer on their development of new protein optimisation techniques as well as the application of computational protein design. The first technique facilitates *in vitro* engineering of enzymes taking place over a much shorter timescale than natural evolution [49-51]. The second one permits rational protein design based on structural and mechanistic information [52-60]. As a result, enzymes have been improved by overcoming limitations such as temperature, solvent instability or a limited substrate range, or have even been engineered to reveal novel functions [61-65]. Many of the engineered enzymes have already found their way into commercial manufacturing plants [19, 34, 66-68].

The advantages of using biocatalysts are clear, as reactions are catalysed with high regio-, chemo- and stereoselectivity and high catalytic activities lead to accelerations in the range of 10^8-10^{10}. Moreover, they are able to work in environmentally friendly conditions and are mostly readily available, cheap, health friendly and renewable. They are also easy to handle, which facilitates their use even by non-biologists with little knowledge of microbiology. Further characteristics of enzymatic reactions are improved step and atom economy, which also makes them efficient from an economic perspective [13, 35, 40, 69, 70]. Taking all these benefits together, it is no wonder that "green" synthesis routes have been used increasingly used by the chemical and pharmaceutical industries [9, 19, 40, 42, 71-73] and many conventional routes have already been re-designed by the exploitation of biocatalysts [6, 7, 67, 72]. Accordingly, about 10% of modern drugs are generated via biocatalysis [31].

One example of the successful re-design of a chemical process is the development of an efficient enzyme-catalysed route to sitagliptin. This compound is the active ingredient in Januvia, a leading drug for the treatment of type II diabetes with global sales exceeding $4 billion in 2012 [74]. As illustrated in Figure. 1.2, the use of an *R*-selective transaminase provides the product via a direct route from prositagliptin. By contrast, the chemical manufacture involves several reaction steps, including an asymmetric hydrogenation at high pressure using a chiral Rh-based catalyst, the subsequent removal of this transition metal and a re-crystallisation to enhance the enantiomeric excess. In both cases sitagliptin is obtained in optically pure form. However, the biocatalytic process not only decreases the total waste disposal and is free of any transition metals, it also increases the overall yield and productivity, and reduces the total manufacturing costs [75, 76].
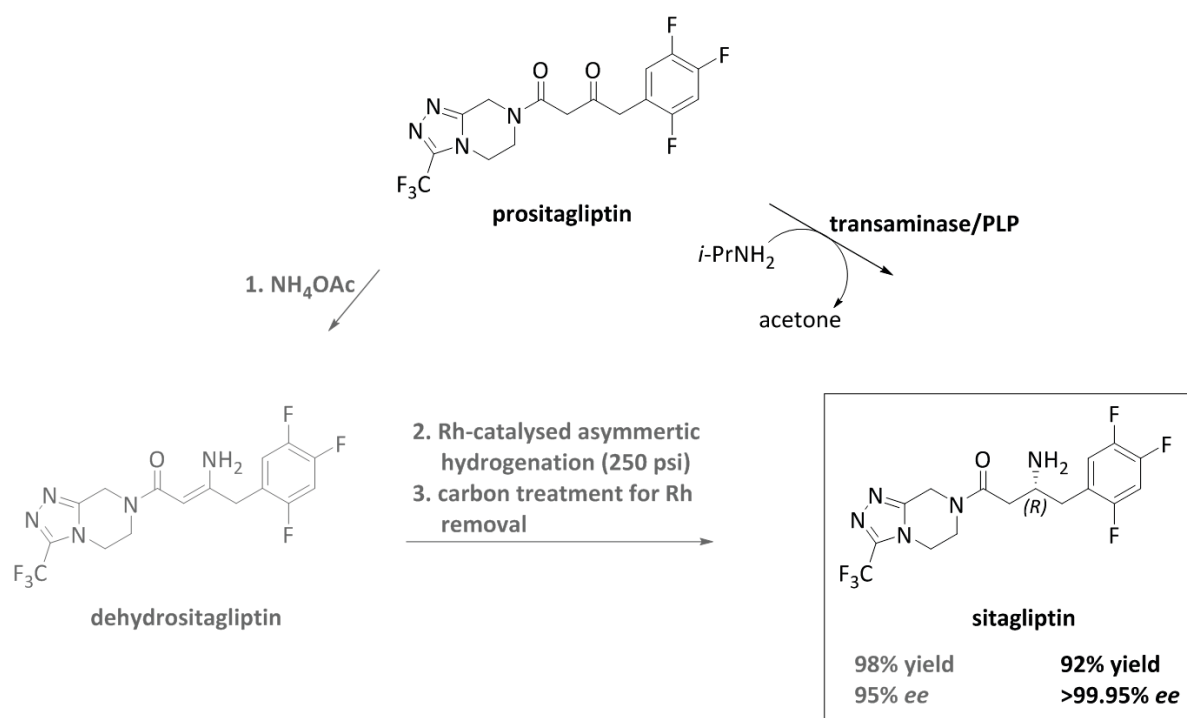
Figure 1.2. Re-design of the sitagliptin synthesis. The chemical synthesis from prositagliptin involves an asymmetric hydrogenation at high pressure catalysed by a chiral rhodium-based catalyst followed by the removal of the transition metal from the product stream. The enzymatic route offers direct synthesis from prositagliptin through a transaminase-catalysed amination. Compared to the chemical route the biocatalytic process increases the overall yield (13%) and productivity (53%), reduces the total waste produced (19%), is free of transition metals, and leads to a decrease of the total manufacturing costs [75, 76]. PLP pyridoxal 5'-phosphate; psi pressure per square inch; *i*-PrNH$_2$ isopropylamine.

Another example is the synthesis of the semisynthetic statin Simvastatin, a cholesterol lowering compound that is sold on the market as a generic drug (Figure 1.3). Traditionally, it

is manufactured from the natural product lovastatin either via hydrolysis/esterification, yielding the key intermediate monacolin J, or via direct methylation. Both routes are multi-step processes involving protection and deprotection chemistry and the use of hazardous and toxic reagents. Moreover, a number of solvents are required and the overall yield is low [7]. The identification of both LovD acyltransferase and α-acyl donor facilitates a much greener and more efficient route. Thus, an acyl moiety is transferred directly and regioselectively to the C_8 hydroxy group of monacolin J catalysed by LovD acyltransferase decreasing the number of reaction steps. Monacolin J was converted with a high conversion rate (>99%) into simvastatin which was obtained with >98% purity [77, 78]. Optimisations of both enzyme and process chemistry have been made to enable the production of simvastatin on a large scale with attractive economic results [79, 80].
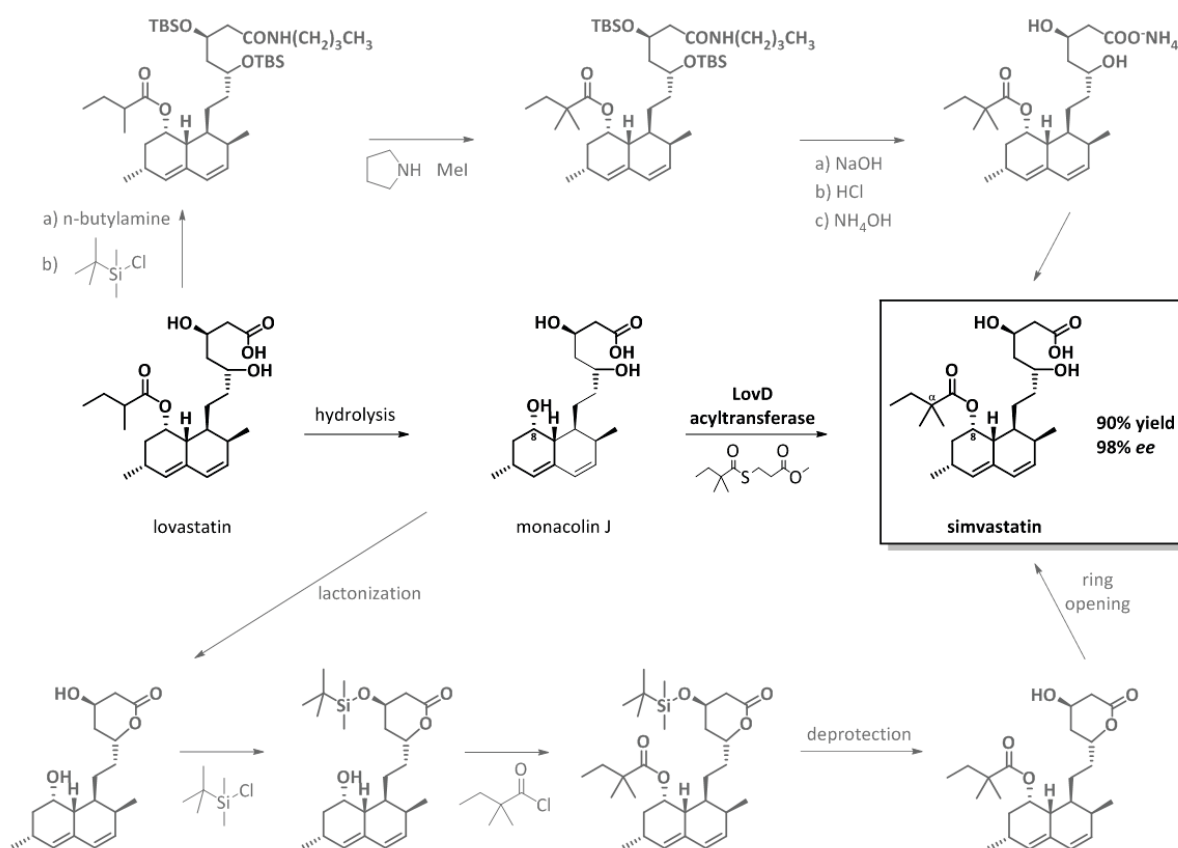
Figure 1.3. Re-design of the simvastatin synthesis. The two commonly used semisynthetic routes, hydrolysis/esterification and direct methylation are multi-step processes requiring several protection and deprotection reactions. They also involve an excess of hazardous and toxic reagents and many solvents. The overall yield is low. In contrast, in a single enzymatic step catalysed by LovD acyltransferase simvastatin is obtained from monacolin J through the transfer of an acyl moiety. This route significantly reduces hazardous waste, is cost-effective and a high conversion rate (>99%) and purity (>98%) is achieved [7, 77, 78].

1.3 OXIDOREDUCTASES

Redox reactions are catalysed by oxidoreductases, which belong to enzyme class one and comprise 22 subclasses. About 25% of all known enzymes are oxidoreductases, and thus it is no wonder that chemists have taken advantage of this class of enzymes for synthesis purposes. As a result, production of optically active compounds integrating redox biocatalysis has increased significantly over the past decade [30-33, 41, 81, 82]. Nowadays, oxidoreductases catalyse the second largest portion of all industrially relevant reactions following hydrolases [9, 20, 21]. Additionally, the number of commercially available enzymes catalysing redox reactions has increased massively during the last few years, and various screening kits for oxidation and reduction have been put on the market [21, 40, 41, 81].

1.3.1 Alcohol dehydrogenases/reductases and their application

The oxidoreductases most often applied for biocatalytic reactions are alcohol dehydrogenases/reductases (ADHs, EC 1.1.1.x.) As illustrated in Figure 1.4, they catalyse both the stereoselective reduction of prochiral carbonyl compounds into the corresponding hydroxy compounds as well as the reverse reaction, the oxidation. ADHs use nicotinamide cofactors to withdraw or supply redox equivalents during the catalytic process (see Figure 1.8a). Thus, when reduction takes place a hydride is transferred from NAD(P)H to the substrate carbonyl carbon, forming the oxidised nicotinamide cofactor NAD(P)$^+$ [31, 32, 68, 83].
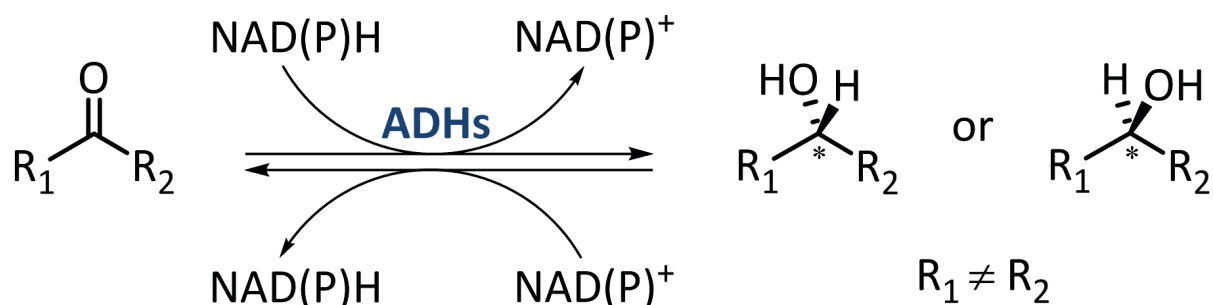
Figure 1.4. Catalytic reaction of alcohol dehydrogenases (ADHs). ADHs catalyse both the asymmetric reduction of prochiral carbonyl compounds as well as the oxidation of hydroxy compounds/alcohols. The cofactors NAD(P)H/NADP$^+$ serve as carrier of the redox equivalents. The reduction reaction is of pivotal interest for the organic chemistry as it leads to the synthesis of chiral molecules which are useful building blocks.

Because the asymmetric reduction catalysed by ADHs leads to the generation of stereogenic centres, they are in high demand in organic synthesis [40, 67]. As summarised in Figure 1.5 a-c, the spectrum of application of ADHs encompasses the synthesis of a variety of optically active hydroxy esters to numerous chiral hydroxy ketones, alcohols, and diols. A number of these products are key chiral building blocks in the production of pharmaceuticals, fine chemicals and natural products and therefore ADHs have also been increasingly used in numerous industrial processes [19, 30, 45, 84-88].

One example of using an ADH in an industrial process is the ADH-catalysed reaction step in the production of the cholesterol-lowering drug Atorvastatin, sold by Pfizer as Lipitor® with worldwide sales of $2 billion in 2011 before patent expiration later that year [177]. In combination with a halohydrin dehydrogenase, the key intermediate ethyl (R)-cyano-3-hydroxybutanoate (HN) is synthesised which had been conventionally obtained from chiral pools [1, 2, 7, 40, 67, 178]. As illustrated in Figure 1.6, an ADH is used to catalyse the asymmetric reduction of ethyl 4-cloroacetoacetate into ethyl (S)-4-chloro-3-hydroxybutanoate, which is then converted by a halohydrin dehydrogenase into HN. Using laboratory evolution techniques, both enzymes could be optimised to yield much higher STYs [86, 179], making the biocatalytic steps in the synthesis process of Atorvastatin more efficient.

Another example is the synthesis of (R)-2-hydroxy-3,3-dimethylbutanoic acid used for the preparation of a potent thrombin inhibitor (Figure 1.7). The key chiral intermediate is ethyl (R)-2-hydroxy-3,3-dimethylbutanoate which is produced by asymmetric reduction of ethyl 3,3-dimethyl-2-oxobutanoate catalysed by a commercially available ADH. The building block is then saponified into the aforementioned acid. [1, 3].
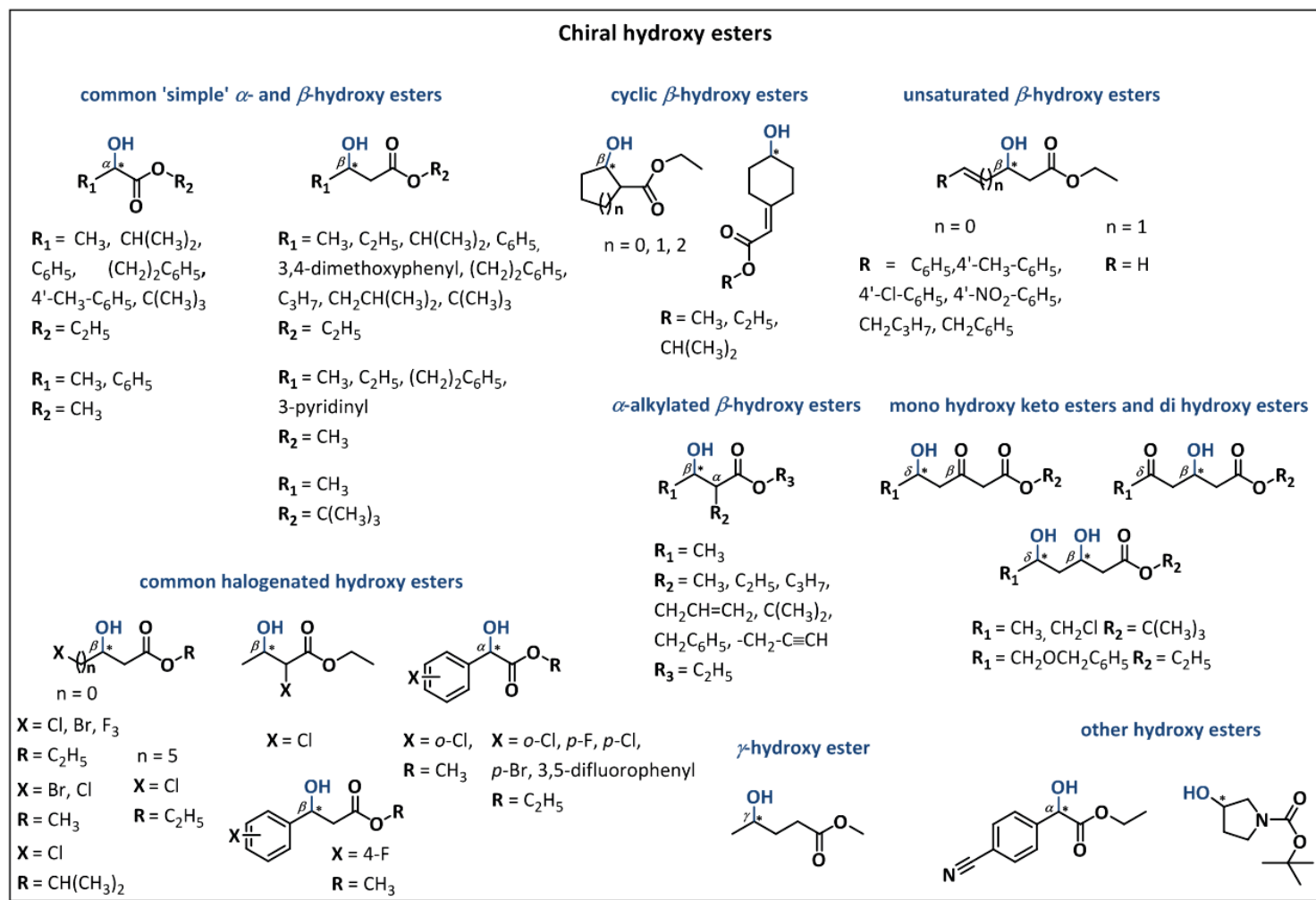
Figure 1.5a. Overview of the hydroxy esters that can be synthesised by exploiting ADHs. Common 'simple' α- and β-hydroxy esters: [89-120]; cyclic β-hydroxy esters: [114, 121, 122], unsaturated β-hydroxy esters: [100, 101, 123]; α-alkylated β-hydroxy esters: [99, 105, 114, 119, 120, 124]; mono hydroxy keto esters and di hydroxy esters: [102, 107, 125, 126]; common halogenated hydroxy esters: [90-98, 100-103, 109, 110, 112-115, 118, 127-142]; γ-hydroxy esters: [100, 101]; other hydroxy esters: [103, 115, 143].
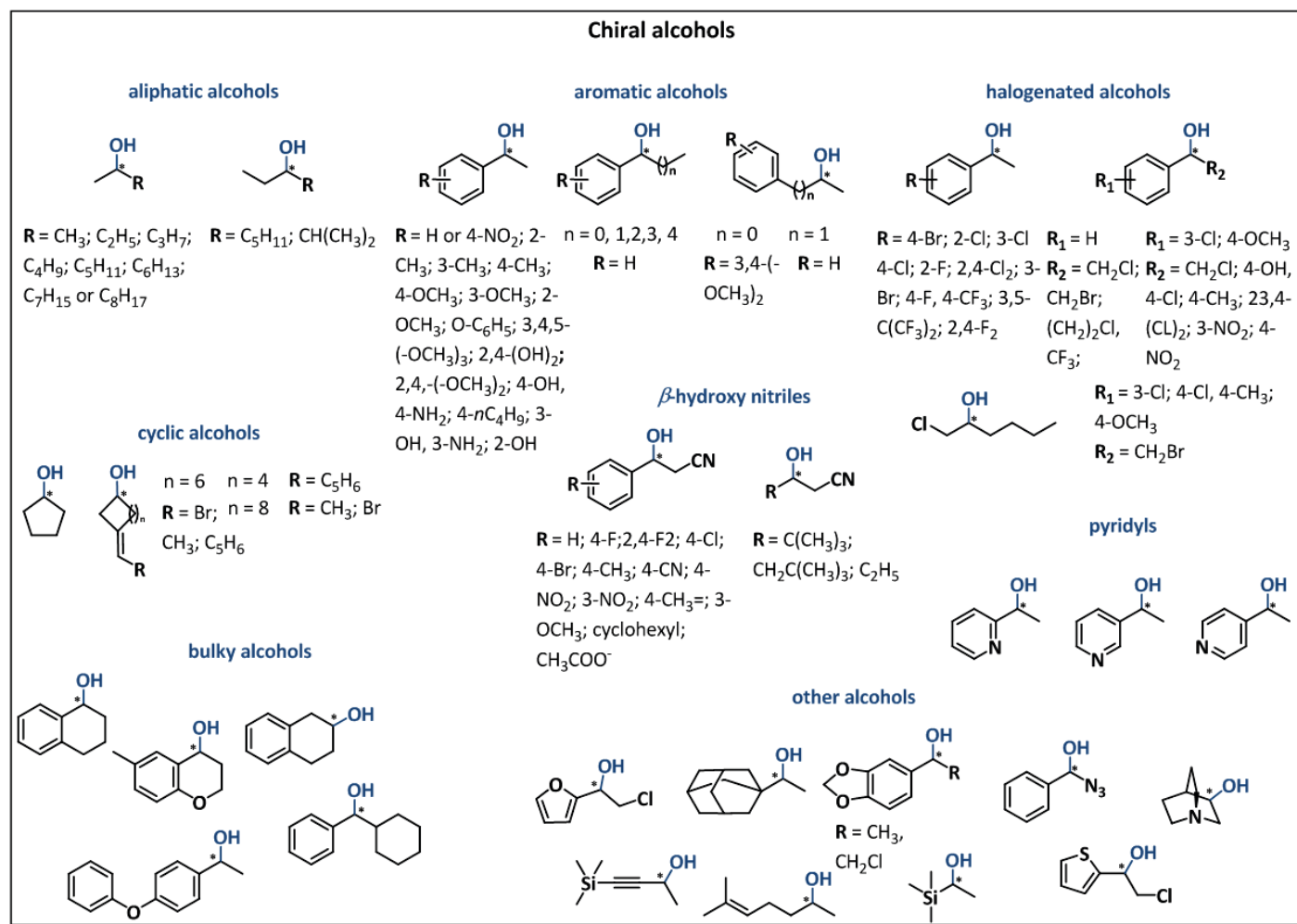
Figure 1.5b. Overview of the chiral alcohols that can be synthesised by exploiting ADHs. Common aliphatic and aromatic alcohols: [89-95, 97, 99, 102, 103, 107, 115-117, 136, 144-149]; halogen-containing alcohols: [89-95, 97, 100, 101, 103, 115-117, 121, 127, 133, 136, 145, 148-152]; cyclic alcohols: [121, 136, 143]; β-hydroxy nitriles: [90, 97, 133, 153-155]; bulky alcohols: [99, 104, 115, 116, 136, 146]; pyridyls: [92-94, 100, 107, 148], other alcohols: [89, 115, 127, 133, 156].
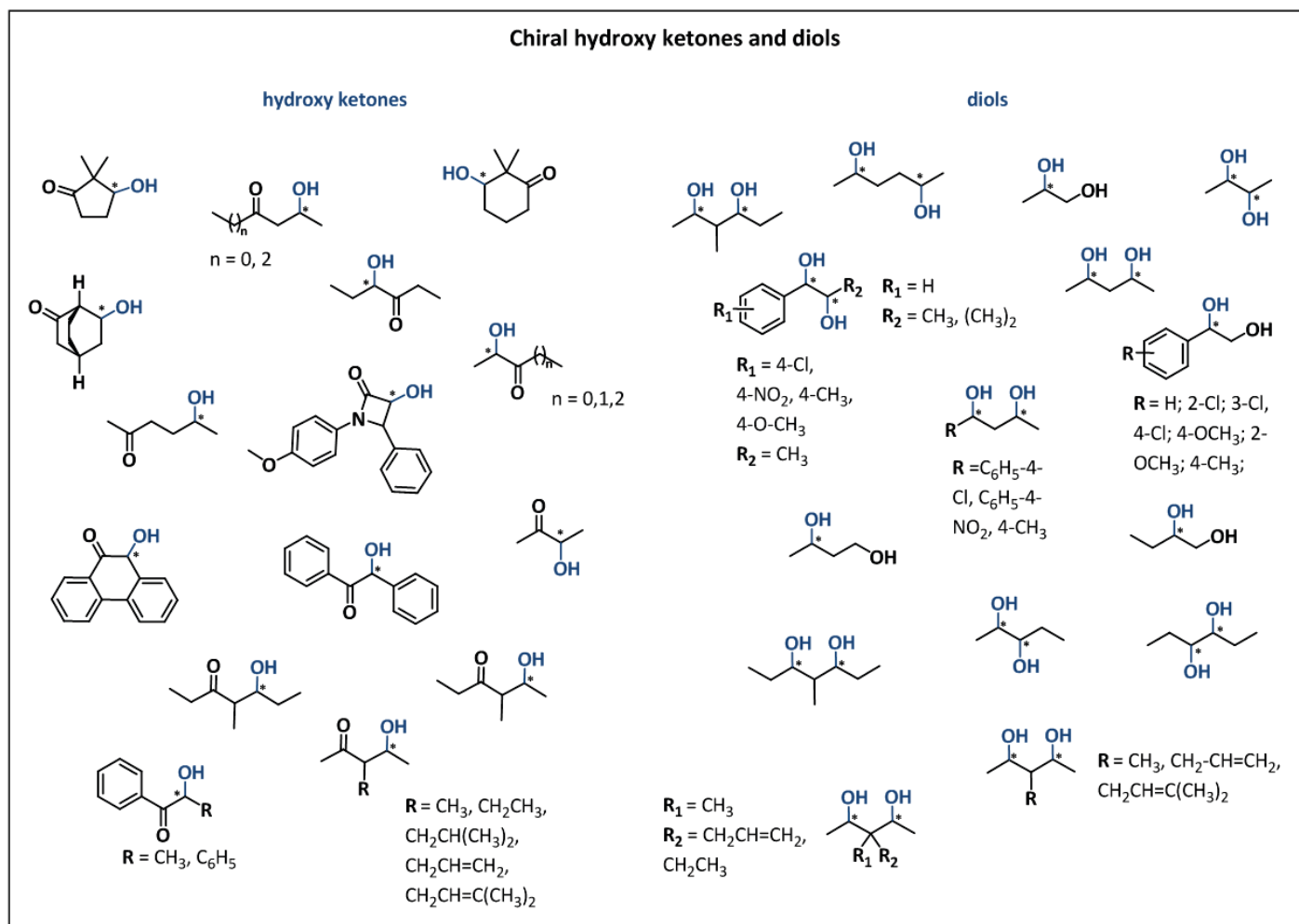
Figure 1.5c. Overview of the chiral hydroxy ketones, diols and hydroxy acids that can be synthesised by exploiting ADHs. Diols: [90, 95, 102, 145, 157-168] and hydroxy ktones: [100, 101, 160, 163, 167-176].
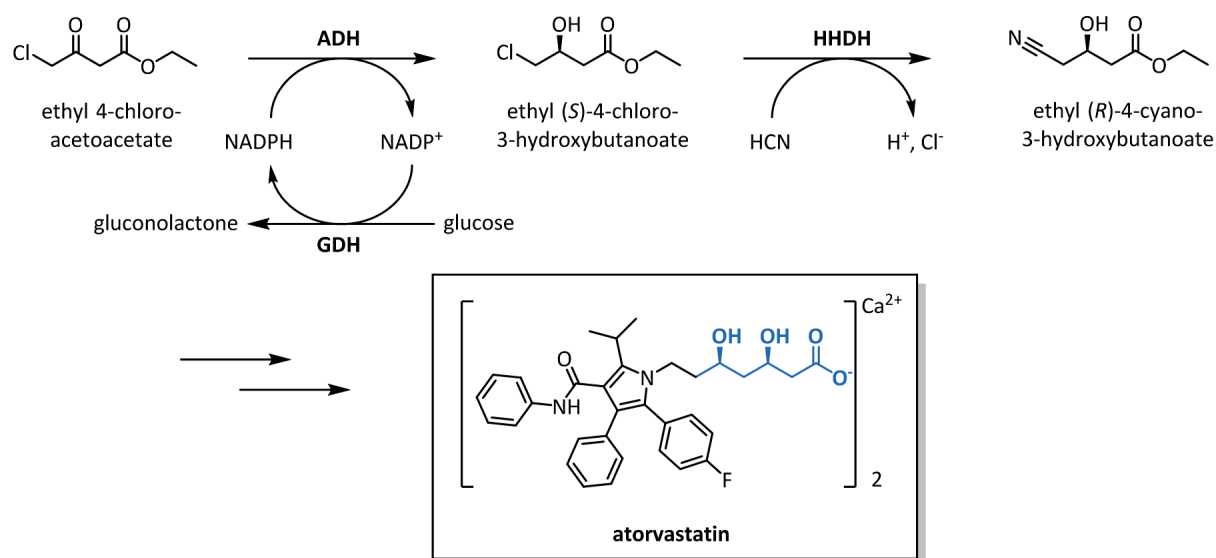
Figure 1.6. The combination of an ADH-catalysed reduction of ethyl-4-chloroacetoacetate and a halohydrin dehydrogenase (HHDH) provides ethyl (*R*)-4-cyano-3-hydroxybutanoate, the chiral key intermediate in the synthesis of the cholesterol lowering drug atorvastatin.
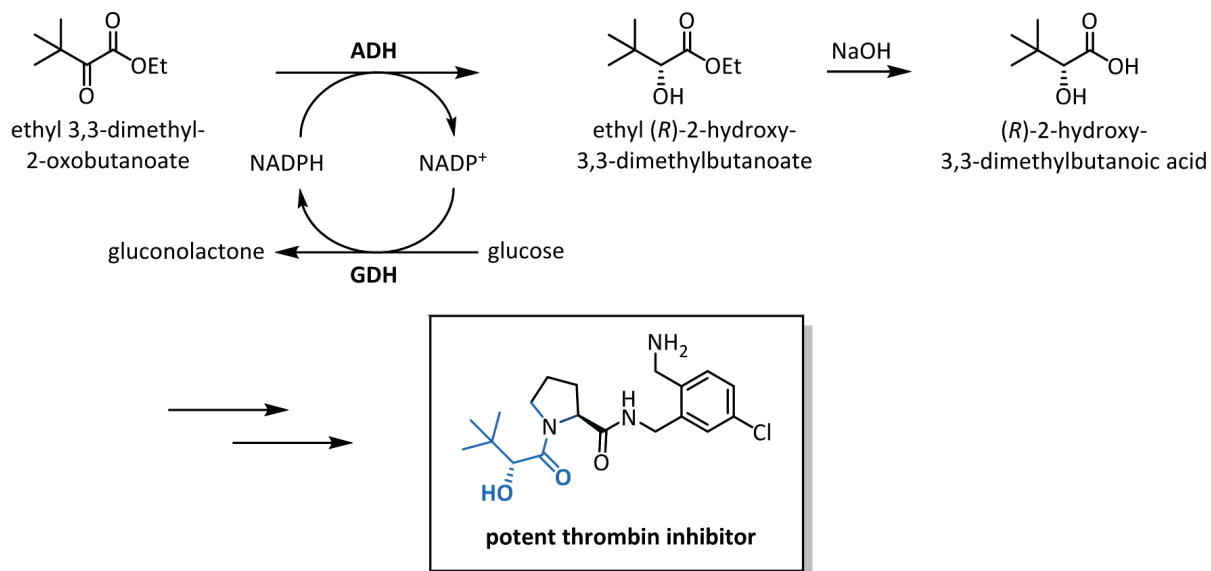
Figure 1.7. ADH-catalysed synthesis of a (*R*)-2-hydroxy-3,3-dimethylbutanoate, a chiral key intermediate in the synthesis of a potent thrombin inhibitor.

1.4 COFACTOR REGENERATION

As mentioned previously, ADHs are NAD(P)H-dependent and require stoichiometric amounts of the cofactor to maintain catalytic activity. Because an ADH-catalysed reaction is an equilibrium reaction, an excess of cofactor is required to transform the substrate completely into product. However, because of the high costs of nicotinamide cofactors, their stoichiometric use is not feasible for economic reasons. Therefore, the past two decades' have seen intensive research into solving the NAD(P)H recycling issue. As a result, many different cofactor recycling methods have been established, including chemical, photo-, electrochemical, and enzymatic regeneration. Comprehensive overviews of the different recycling techniques have been published recently by Wu *et al.* [180], Weckbecker *et al*. [181] and Berengua-Murcia [182]. The following briefly summarises the most important techniques.

1.4.1 Chemical regeneration

Chemical regeneration of NADPH can be achieved using transition-metal catalysts such as ruthenium (II) or rhodium (III) complexes which transfer hydrogen (H_2) directly to $NADP^+$. This recycling method is appropriate for *in situ* coupling the cofactor regeneration to an enzymatic reduction, for the following reasons: (i) H_2 is the cheapest reducing agent and yields no requisite by-products; (ii) the high regioselectivity, yielding 1,4-dihydropyridine, the only active form of the cofactor (see Fig. 1.8.b); (iii) the high selectivity for reduction of the nicotinamide coenzyme vs the enzymatic substrate; and (iv) the fact that reactions can be performed in an aqueous medium under mild reaction conditions (Temp. 25-65°C; pH 6.5-8.5). This regeneration system has been successfully applied to the *Thermoanaerobacter brockii* ADH-catalysed reduction of 2-heptanone. The corresponding alcohol was obtained with 18% yield and 40% *ee* [183].

Recycling of NADH can be achieveed by using a combination of both a platinum carbonyl cluster which is soluble in organic solvents only and a redox active dye that functions as shuttle carrier. Driven by H_2, the cluster reduces the redox active dye in the organic phase and the reduced dye thus obtained migrates across the phase boundary and transfers the redox equivalents onto NAD^+. This system was successfully coupled to the reduction of pyruvate to L-lactate catalysed by L-lactate dehydrogenase (L-LDH). When a ratio of 600:10:1

of pyruvate to NAD$^+$ to carbonyl cluster was used, the reaction went to completion within 48 h [183, 184].

However, chemical regeneration techniques are not considered for commercial and preparative application as they depend on both toxic and expensive reagents/catalysts and suffer from unwanted side products.

(a)

NADH	**R = H**
NADPH	**R = PO$_3$$^{2-}$**

(b)

oxidised cofactor   reduced cofactor
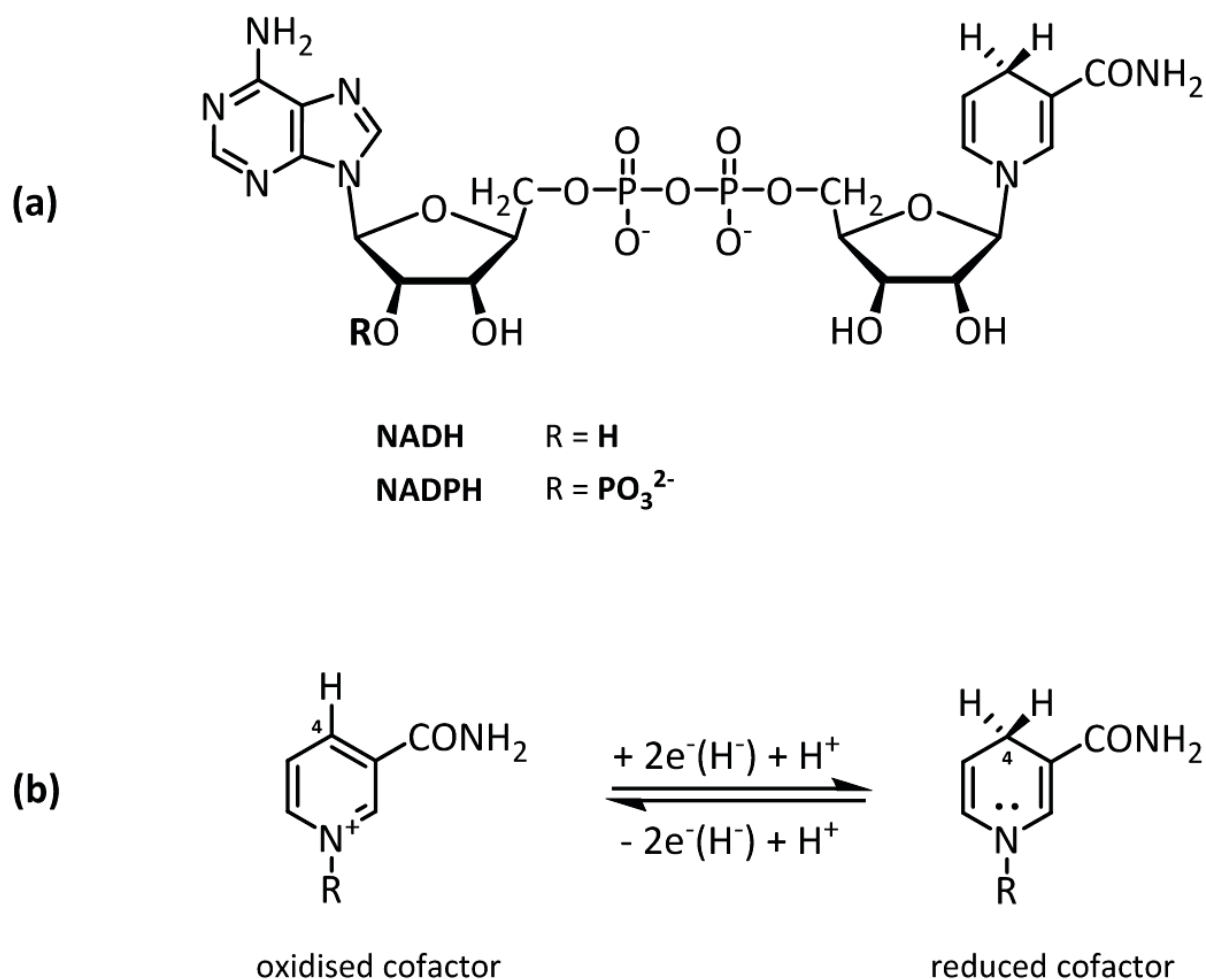
Figure 1.8. (a) Structure of NAD(P)H which consists of nicotinamide mononucleotide and adenosine monophosphate (b) Reduction of the oxidised form of cofactor (NAD(P)$^+$) to the active form 1,4-dihydropyridine.

1.4.2 Photochemical regeneration

The use of photosynthetic living organisms as biocatalysts allows an environmentally friendly and cheap recycling method by the use of light energy. Only water and light are necessary to regenerate NAD(P)H through the photosynthetic electron-transfer reactions. The reduced cofactors produced in this manner can be utilised for substrate reductions. Applying this

regeneration tool to the reduction of various acetophenone derivatives catalysed by the freshwater cyanobacterium *Synechococcus elongatus* PCC 7942 gave the corresponding alcohols with excellent enantioselectivities (*ee* 96-99%) [185-187].

If the photosynthetic living organism is replaced as catalyst, a photosensitizer is required which boosts the whole regeneration system. Examples of appropriate photosensitizers are porphyrin or metal-containing porphyrin, xanthene dyes (e.g. eosin Y), toluidine blue O or oligothiophene. The photosensitizer is irradiated by visible light and delivers the photoexcited electrons onto a mediator (e.g. methyl viologen) for reduction of $NAD(P)^+$. Unfortunately, most organic photosensitizers are not stable enough to be used repeatedly over a long period and thus this kind of regeneration has not been very widespread. However, photochemical regeneration has become an important research issue as it allows for the utilisation of cheap, clean and abundant solar energy.

1.4.3 Electrochemical regeneration

Electrochemical regeneration is, in principal, a simple and cost effective technology since "cheap" electricity is used, no co-substrates or co-enzymes are required and, because no by-products are formed, an easy downstream product recovery process is facilitated. Cofactor recycling can be direct or indirect. With respect to the first, $NAD(P)^+$ is reduced directly at the surface of an electrode which needs to have a potential which is substantially more negative than the Standard Reduction Potential (STR) of $NAD(P)^+/NAD(P)H$ of -0.320 V. An example of this regeneration method is the reduction of pyruvate to D-lactate catalysed by lactate dehydrogenase. NAD^+ can be reduced at a cholesterol-modified gold amalgam electrode with a turnover number of 1400. The NADH thus produced drives the enzymatic reduction. A resultant conversion of about 72% is observed [188]. However, direct cofactor recycling has disadvantages like cofactor dimerisation and poor regioselectivity leading to enzymatically inactive 1,6-NAD(P)H and electrode fouling. Because of these drawbacks, this method is not normally used in practice.

Alternatively, the indirect recycling method is used. Here, a mediator, an electronegative species, is added which allows for efficient electron transfer between cathode and cofactor. To facilitate a proper regeneration the mediator should meet the following four attributes: (i) transfers either two electrons or one H^- ion in one step to avoid radical formation, which otherwise would lead to cofactor dimerisation; (ii) is highly selective for the formation of 1,4-

NAD(P)H; (iii) does not transfer the electrons to the substrate; and (iv) has a electrochemical activation potential of less than -0.9 V to prevent direct reduction of NAD(P)$^+$. The most widely used mediators are rhodium complexes, like [Cp*Rh(bpy)(H$_2$O)]$^{2+}$, but enzymes like diaphorase or lipoamide dehydrogenase also function as electron shuttles (= indirect enzyme coupled regeneration). However, the chemical-based mediators can be incompatible with some enzymes and therefore their use is limited. Despite this, several examples of mediator-mediated electrochemical regenerations have been published [189-191].

1.4.4 Enzymatic regeneration of NAD(P)H

Of much greater importance than the regeneration techniques just described are enzymatic cofactor recycling systems, which have been studied extensively. The advantages of using enzymes are their higher selectivity leading to the formation of the active form of the cofactor, their higher compatibility with other reagents, and their simple detection of activity. There are two methods of regeneration: the substrate-coupled system where a second substrate is used and the enzyme-coupled system where a second enzyme is used.

1.4.4.1 Substrate-coupled

As illustrated in Figure 1.9a, substrate-coupled regeneration is accomplished via a single ADH that catalyses both reactions, the reduction of the carbonyl compound to the corresponding target alcohol and the oxidation of a co-substrate, simultaneously leading to recycled NAD(P)H. Usually, inexpensive 2-propanol or ethanol are used as auxiliary substrates which are oxidized into acetone or acetaldehyde, respectively. However, to shift the equilibrium towards the formation of alcohol the co-substrate needs to be added in excess which can lead to the inhibition of the enzyme. Despite this, a number of examples of the successful application of this regeneration method can be found in the literature [87, 97, 146, 147, 163, 192-199].
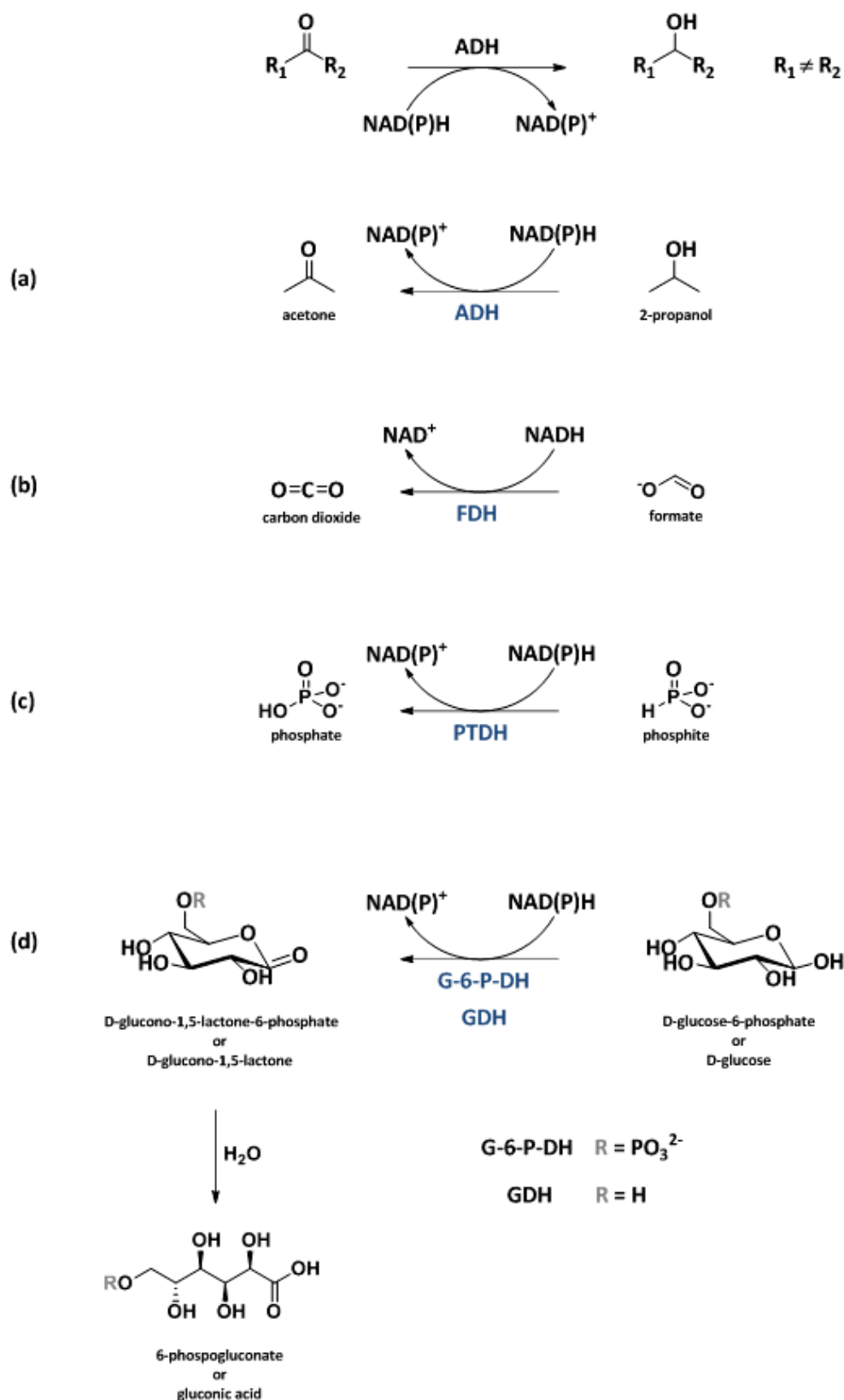
Figure 1.9. Enzymatic regeneration of NAD(P)H. (a) Substrate-coupled by a single ADH which also catalyses the oxidation of the auxiliary substrate under formation of NAD(P)H. (b-d) Enzyme-coupled NAD(P)H-regeneration methods; (b) formate dehydrogenase (FDH) (c) phosphite dehydrogenase (PTDH), (d) glucose-6-phosphate dehydrogenase (G-6-P-DH) or glucose dehydrogenase (GDH).

1.4.4.2 Enzyme-coupled

This regeneration method makes use of coupling two independent ADH-catalysed reactions which act simultaneously. Several enzymes are commonly used for regeneration of reduced nicotinamide cofactors. The most common ones are described in the following.

1.4.4.2.1 Formate dehydrogenases (FDHs)

Formate dehydrogenase (FDH) catalyses the oxidation of formate to carbon dioxide (Figure 1.9b). FDH is attractive for cofactor regeneration because the oxidation product is volatile and thus the thermodynamic equilibrium is shifted almost completely towards the desired direction. In addition, easier product isolation and purification is facilitated as carbon dioxide can be easily removed from the reaction mixture. Formate is also inexpensive and inert, and the enzyme is commercially available and active across a wide pH range (6.0-9.0). However, because of the higher affinity for NAD^+ than for the phosphorylated nicotinamide cofactor, application of FDH is mainly restricted to the regeneration of NADH. In addition, the enzyme displays very low specific activity (4-7.5 Umg^{-1}) compared to other enzymes, requiring either large quantities of enzyme or longer reaction times. Nevertheless, coupling FDH to an enzymatic reduction has been one of the most widely used methods for regenerating NADH, as shown by the many examples found in the literature [107, 108, 117, 130, 139, 143, 149, 194, 200-203].

1.4.4.2.2 Phosphite dehydrogenase (PTDH)

An alternative method to regenerate reduced nicotinamide cofactor is achieved through phosphite dehydrogenase (PTDH) (Figure 1.9c). This oxidoreductase was first isolated from *Pseudomonas stutzeri* and catalyses the oxidation of phosphite to phosphate with simultaneous reduction of NAD^+ to NADH. Because of the reaction's high thermodynamic equilibrium constant, the catalysed reaction is almost irreversible. Further advantages are the cheap substrate phosphite, the innocuous nature of both phosphite and phosphate and the fact that they act as buffer, as well as the wide pH range of PTDHs. Additionally, if needed the co-product phosphate can be readily removed by calcium precipitation. Because of its low activity towards $NADP^+$, the enzyme was engineered yielding a mutant that reduces both NAD^+ and $NADP^+$ with high efficiencies. The mutant was further evolved towards increased temperature and also displays a higher expression and activity level than

the wild-type. The highly stable NADP$^+$-accepting PTDH was then used to regenerate NADPH during the xylose-reductase catalysed xylitol synthesis and the alcohol dehydrogenase-catalysed (R)-phenylethanol synthesis [204].

1.4.4.2.3 Glucose-6-phosphate dehydrogenase and glucose dehydrogenase (G-6-P-DH & GDH)

Glucose-6-phosphate dehydrogenase (G-6-P-DH) catalyses the oxidation of glucose-6-phosphate to 6-phosphogluconolactone (Figure 1.9d). The reaction is exothermic and irreversible due to the spontaneous formation of 6-phosphogluconate. The system has been used to regenerate NAD(P)H in the synthesis of chiral α-hydroxy acids and alcohols [170, 171, 205, 206]. The enzyme has been isolated from many animals, plants and microbes. Some G-6-P-DHs were shown to accept only one of the two nicotinamide cofactors, while others display dual nucleotide specificity with either comparable activities or a preference for either NADP$^+$ or NAD$^+$. However, disadvantages of this system are the high costs of glucose-6-phosphate and its instability in water. In some cases, it is also difficult to isolate the target product from 6-phosphogluconolactone. Further, it is observed that NAD(P)H is decomposed by both 6-phosphogluconolactone and glucose-6-phosphate as they act as general acid catalysts. Therefore, its use on large-scale applications is prevented. Alternatively, glucose-6-sulfate can be used instead of glucose-6-phosphate as it is easily prepared and does not cause inactivation of the nicotinamide cofactors.

Glucose dehydrogenase (GDH) catalyses the strongly exothermic oxidation of glucose to gluconolactone which spontaneously hydrolyses irreversibly to gluconic acid (Figure 1.9d). GDHs from *Bacillus subtilis* and *Bacillus megaterium* are well-characterised and accept either NAD$^+$ or NADP$^+$ with high specific activities. As a result, GDH can be applied for the regeneration of both nicotinamide cofactors. A further advantage is that, in contrast to glucose-6-phosphate, glucose is cheap and readily available. Moreover, it is stable and strongly reducing. However, the formation of the by-product gluconic acid is disadvantageous as it decreases the pH in the reaction mixture which may complicate the reaction work-up. Nevertheless, application of GDH has proven an excellent coenzyme regenerating tool in many enantioselective reduction reactions [90-94, 96, 100-102, 108-110, 112-115, 126, 131, 139, 141, 142, 144, 164, 194, 207-214].

1.5 WHOLE-CELL BIOTRANSFORMATIONS

In general, the use of whole cells in biotransformation reactions is favoured over isolated enzymes. Nowadays, the majority of biocatalytic mediated redox reactions are carried out using metabolising cells [6]. The major advantages of whole-cell approaches are the increased stability of the used enzymes due to the surrounding of their natural environment and the internal cofactor regeneration [215]. As a result, bacteria, yeast or fungi have been employed for many decades in asymmetric synthesis [33, 124, 146, 197, 198, 216-229].

However, the presence of other reductases with counteracting stereoselectivities may lead to diminished enantiomeric excess values. Also, both the substrate and the product can be metabolised by the cells, decreasing the product yield. Moreover, the use of non-physiological substrates (xenobiotics) can cause different cell stress responses which also affect the reaction negatively [230]. Another disadvantage of microbial cell transformations is the low reaction velocity due to low quantities of the involved enzyme in the cells. This drawback is typically overcome by applying a recombinant expression system, which allows production of the target enzyme in larger amounts. Generally, *E. coli* is chosen as expression host because of its easy handling and fast growth [193, 194, 199, 231, 232]. It also displays no relevant reducing activities [138] and is therefore ideal when used as a catalyst in the asymmetric synthesis of chiral hydroxy compounds.

Even more efficient are *E. coli* catalysts that co-express a NAD(P)H recycling gene, like *fdh* or *gdh*, along with the *adh* gene in a single cell, which facilitates simultaneous cofactor regeneration. These so-called "designer" or "tailor-made" cells are constructed using a one- or two-plasmid strategy, carrying both the *adh* and the cofactor recycling gene (Fig 1.10). Regulation of the individual specific activities can be easily facilitated by varying the cultivation conditions, the plasmid's copy-number or promoter strength. Activities within the same range have been shown to be an important issue in achieving optimised whole-cell catalysis [233]. "Tailor-made" whole cell catalysts are much simpler in their application and are more cost-efficient than the use of isolated enzymes, since there is no stringent need for external cofactor addition, isolation, or purification of the enzymes [234, 235]. These advantages are reflected by the markedly increasing number of publications in the past few years using "designer cells" as catalysts [93, 94, 100, 101, 112, 113, 116, 126, 128, 130, 139, 141-143, 194, 200-203, 208-211, 213, 214, 236].
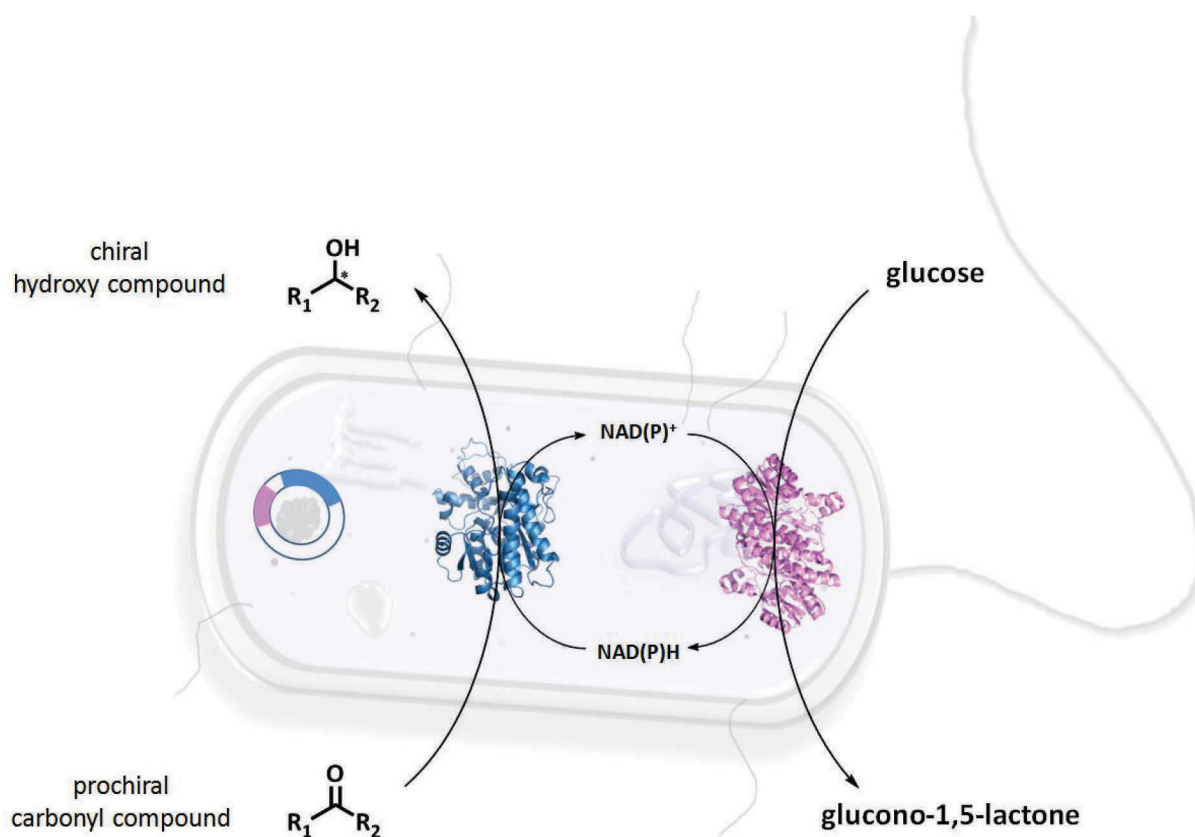
Figure 1.10. Example of a "tailor-made" *E. coli* whole-cell catalyst, expressing the *adh* (blue) and *gdh* (magenta) genes simultaneously using a one-plasmid strategy. A prochiral compound passes the cell membrane and is reduced by the ADH to the corresponding chiral product which is subsequently released from cell. The consumed cofactor, NAD(P)H is recycled immediately by the GDH-catalysed oxidation of glucose under the consumption of NAD(P)$^+$ leading to the reduced cofactor, NADP(H).

As well as *E. coli*, engineered *S. cerevisiae* strains have also been employed in asymmetric synthesis [169, 237-240]. These strains were engineered to enhance the intracellular cofactor pool. This will be discussed in more detail in section 7.3.1.

1.6 IDENTIFICATION OF NATURALLY OCCURING BIOCATALYSTS

The increasing use of biocatalytic reactions in synthetic chemistry requires a steady supply of novel biocatalysts. Several methods for the identification of naturally occurring enzymes have been reported, which, in general, can be divided into activity- and sequence-based routes.

A conventional activity-based method for which no sequence knowledge is required is the screening of various microorganisms or enzymes based on the target reaction [241, 242]. When the cell-free extract of a microbe is found to display the desired activity, the enzyme

responsible can then be purified from the extract. The pure protein solution can then be analysed either via Edman sequencing or Maldi-TOF mass spectrometry. This will provide information about the amino acid sequence. Application of this identification tool has recently led to the discovery of ADHs from *Nocardia globerula*, *Saccharomyces cerevisiae* and *Penicillium citrinum* [98, 108, 160]. However, there are major disadvantages such as the facts that most microbes are not culturable under standard laboratory conditions and that a recombinant expression system still needs to be developed to obtain high quantities of the biocatalyst.

One way to overcome these drawbacks is the metagenome approach, another activity-based method for identifying naturally occurring enzymes. In this case, the complete DNA from an environmental source (e.g. the sea or soil) is extracted, followed by the construction of recombinant DNA-libraries (also called metagenomic libraries). These are then screened either for enzyme activity (phenotype-based search) or for conserved regions that are in the nucleotide sequences of genes coding for enzymes which are known to possess the ability to catalyse the target reaction (genotype-based search). This is, generally, done via medium or high-throughput screening. However, development and establishment of such a screening assay is not easy and requires considerable time and effort [67, 243-245]. Knietsch *et al*. combined enrichment technology and metagenomics to find enzymes from four different environments with the ability to oxidize short-chain polyols or to reduce the corresponding carbonyl compounds, respectively. This led to the identification of nine novel genes responsible for the formation of carbonyls from short-chain polyols, among them three genes encoding hypothetical alcohol dehydrogenases [246].

Massive progress in sequence technologies in combination with metagenome libraries has increased the amount of available sequence data exponentially. Nowadays, databases contain approximately 20 million sequences and over 1,700 complete microbial genomes [68, 243]. Annotation of both genes and proteins occurs automatically and is mainly derived from information that has been obtained experimentally [247]. However, because this is a very costly and laborious process, the majority of sequences have not been annotated. As a result, public databases contain a large number of putatively and hypothetically annotated proteins. To find novel and suitable biocatalysts among them, two sequence-based identification methods can be used: genome hunting and database mining.

In genome hunting a genome-wide expression library is screened. Over-expression strains, carrying the genes of all putative annotated or known ADHs from one genome-sequenced organism are examined for special or desired traits. A typical example was the systematic investigation of bakers' yeast reductases catalysing the reduction of various keto esters [105, 119, 122, 138]. An analogous screening method was performed for the identification of synthetically useful reductases from *Bacillus* sp. ECU0013. Investigation of *E. coli* strains expressing 11 recombinant oxidoreductases for their ability to synthesise optically active *α*- and *β*-hydroxyl esters resulted in the identification of three ADHs [92, 93].

Homology-driven individual genome screening is another powerful tool. Here, the sequence of a known enzyme is used as template to search for homology in the entire genome of a selected organism. For example, a sequence-similarity search with an ADH of known stereospecificity in the *Candida parapsilosis* genome revealed three novel anti-Prelog ADHs catalysing the (*S*)-specific reduction of 2-hydroxyacetophenone [95]. Another example was the discovery of a novel NADH-dependent ADH in the genome of the extremely thermophilic and halotolerant *Thermus thermophilus* HB27 using NADP-dependent (*R*)-specific ADH from *Lactobacillus brevis* for the homology search [111].

The database mining approach is a further useful strategy for quickly finding early clues about novel enzymes within the public databases [248]. This method is based on the search for matches using amino acid sequences of enzymes with known activity as template [249]. A target reaction-oriented mining, for example, was used to find new ADHs displaying ethyl 4-chloro-3-oxo-butanoate reducing activity. Thus, ADHs reported to display activity towards this compound were employed in a BLAST (Basic Local Alignment Search Tool) search which resulted in the discovery of a novel highly *S*-selective ADH from *Streptomyces coelicolor* [97]. Another example was the recent identification of a *Neurospora crassa* ADH based on the sequence of $NADP^+$-dependent glycerol dehydrogenase from *Gluconobacter oxydans*. The enzyme was shown to synthesise a number of *α*- and *β*-hydroxy esters with high conversion and stereoselectivity and is thus believed to be a useful biocatalyst in synthetic chemistry [96].

1.7 ENANTIOPURE HYDROXY KETONES AND DIOLS

Chiral hydroxy ketones and vicinal (=1,2- or *α*-diols), *β*-(=1,3-diols), *γ*-(=1,4-diols) and longer diols are of particular interest because of the presence of two asymmetric centres which can

be easily transformed to other functionalities to produce many complex chiral systems [250-252].

As shown in Figure 1.11, they are an essential part of a variety of natural products, of which some have proven to be antifungal (e.g. (+)-Roxaticin) [253], antibiotic (e.g. Bafilomycin A₁) [254], anti-carcinogenic (e.g. epothilones) [255] or anti-inhibitory (e.g. farnesyltransferase inhibitors, kurasoin A and B) [256, 257]. In addition, their structural subunits are also frequently encountered in many pheromones [176, 258-260].

Synthetic hydroxy ketones and diols are also useful intermediates for synthesising a number of pharmaceutical active and nutriceutical products. For example, the α-hydroxyphenylketone (R)-1-(3-chlorophenyl)-2-hydroxypropan-1-one is an intermediate in the synthesis of the anti-depressant (S)-bupropion [261], while (1S,2S)-3-chlorocyclohexa-3,5-diene-1,2-diol is useful for preparing L-ascorbic acid [262]. Furthermore, enantiopure diols serve as the backbone in a number of chiral ligands which are used in asymmetric catalysis [263-267].

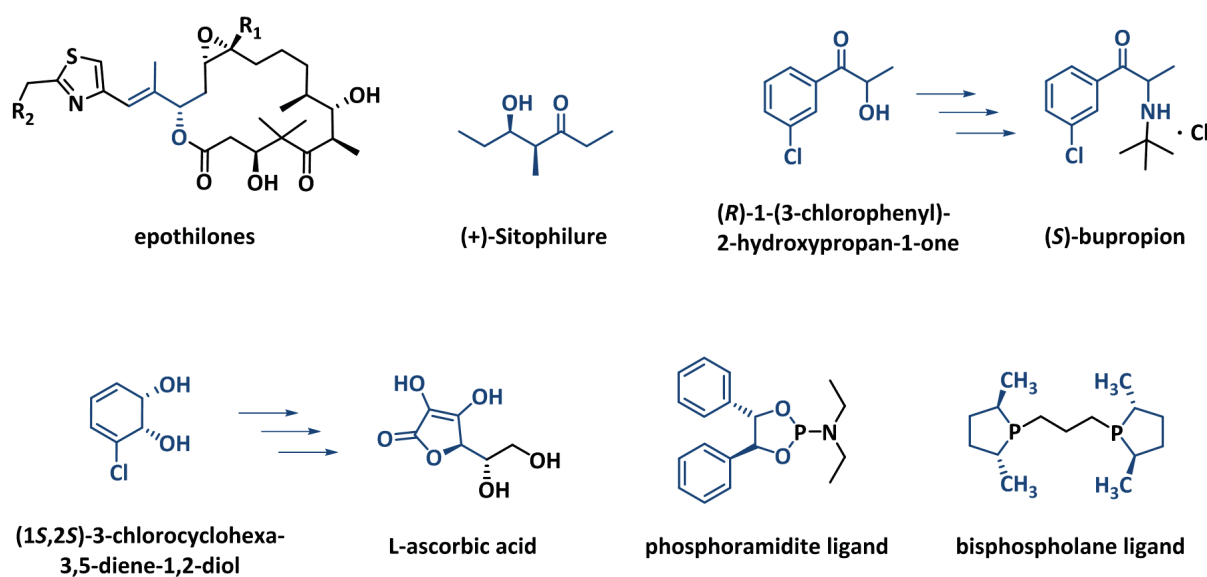**Figure 1.11.** Examples of compounds bearing hydroxy ketones or diols as well as some products derivatised thereof.

1.7.1 Synthesis of chiral hydroxy ketones and diols

In virtue of their importance, much effort has been made into developing efficient synthesis routes to chiral hydroxy ketones and diols and several chemical approaches have been described. The most common include the asymmetric reduction of the corresponding

diketones or hydroxy ketones via hydrogenation [268-271] or borane reduction [272-275], the oxidative kinetic resolution of the corresponding racemic hydroxy ketone or diol [276-278], the asymmetric hydrosilylation of the corresponding diketones [279] or asymmetric carbon-carbon bond forming reactions [161, 280, 281]. Common synthesis routes to optically active α-hydroxy ketones and *syn*-1,2-diols are the α-hydroxylation of ketones through enantioselective enolate oxidation [282] and the Sharpless asymmetric dihydroxylation of (*E*)-olefins, respectively [29].

However, in many cases these synthesis routes require a significant number of chemical steps, frequently involve the use of dangerous and toxic catalysts, produce hazardous waste, and result in low product yields and stereoselectivities. Therefore, enzymatic approaches are an attractive alternative. Various biocatalytic routes to optically active hydroxy ketones and diols have been described. They include the application of oxidoreductases, hydrolases and lyases, and have been carried out either with isolated enzymes or whole cells [250, 251, 283, 284].

The use of ADHs has proven to be very efficient as they are able to introduce two chiral centres through the bio-reduction of two carbonyl groups [250, 251]. For example, Kulig *et al.* have successfully used an ADH from *Ralstonia* sp. to synthesise chiral bulky 1,2-diols with excellent enantio- (>99% *ee*) and diastereoselectivities (>99% *de*) from the corresponding 2-hydroxy ketones [158]. Kalaitzakis *et al.* have used ADHs in the stereoselective synthesis of α-substituted β-hydroxy ketones and -diols from the corresponding diketones [166-168, 175, 176] and ADHs from *Lactobacillus kefir* and *Rhodococcus* sp. were used to synthesise all four stereoisomers of the β-diol 1-(4-chlorophenyl)butane-1,3-diol with *ee*≥95% [161]. In addition, several reports have been published on the stereoselective reduction of dicarbonyl compounds using microbial transformations [217, 221, 225, 226, 229, 285, 286].

1.7.2 The γ-diol (2*S*,5*S*)-hexanediol

The chiral C_2-symmetric compound (2*S*,5*S*)-hexanediol is a γ-diol and a valuable building block, as illustrated in Figure 1.12. It is used in the preparation of a variety of chiral auxiliaries (**1-8**), being used in various synthesis reactions. One prominent example is (-)-(2*R*,5*R*)-2,5-dimethylpyrrolidine (**6**) which has wide-ranging applications in asymmetric synthesis [287].

The *γ*-diol also serves as starting material for the synthesis of a variety of chiral phosphorus (III) ligands (**9-12**), which are used in transition metal homogeneous catalysis. One example is the (*S,S*)-DuPHOS-Rh catalyst that is applied in asymmetric synthesis reactions [288].

(2*S*,5*S*)-hexanediol is also a precursor in the production of hydrazones, like 3-amino-4-alkylazetidin-2-ones (**14**); these are the key substructures of the monocyclic *β*-lactam antibiotics aztreonam and carumonam [289]. It is also a structural element in the non-imidazole-based H_3 antagonist, A-349821 (**13**). This compound is considered a useful drug candidate in the treatment of neurodegenerative diseases such as Alzheimer, as it has shown promising efficiency in enhancing cognition and attention and regulating wakefulness in animal models [290].

1.7.2.1 Synthesis of (2*S*,5*S*)-hexanediol

Because of the great potential of (2*S*,5*S*)-hexanediol, efficient synthesis routes are required. So far, several chemical routes, one chemoenzymatic method and baker's yeast-mediated synthesis have been reported. The following two sections summarise the various synthesis reactions.

1.7.2.1.1 Chemical and chemoenzymatic routes to (2*S*,5*S*)-hexanediol

As previously mentioned, asymmetric hydrogenation leads to chiral hydroxy ketones or diols. With respect to (2*S*,5*S*)-hexanediol synthesis, three different reduction reactions exist (Figure 1.13). The first allows direct access to the diol through hydrogenation of the corresponding *γ*-diketone 2,5-hexanedione using Noyori's (*S*)-Ru-BINAP catalyst (**1**). The outcome of this reaction is a 4:1 (yield 84-26%) mixture of (*S,S*)- and *meso*-diol [271]. However, the fact that a significant amount of *meso*-diol is formed reveals the low stereoselectivity of the catalyst towards the diketone. This issue can be overcome by replacing 2,5-hexanedione with methyl 3-oxobutanoate since the catalyst is much more selective towards this compound, yielding the corresponding (*S*)-*β*-hydroxy ester with >99% *ee* (**2**) [300]. A subsequent saponification leads to the corresponding (*S*)-*β*-carboxylic acid. This is then subjected to electrochemical Kolbe coupling, yielding enantiomerically pure (2*S*,5*S*)-hexanediol in reasonable amounts (40-70%) [296, 301].
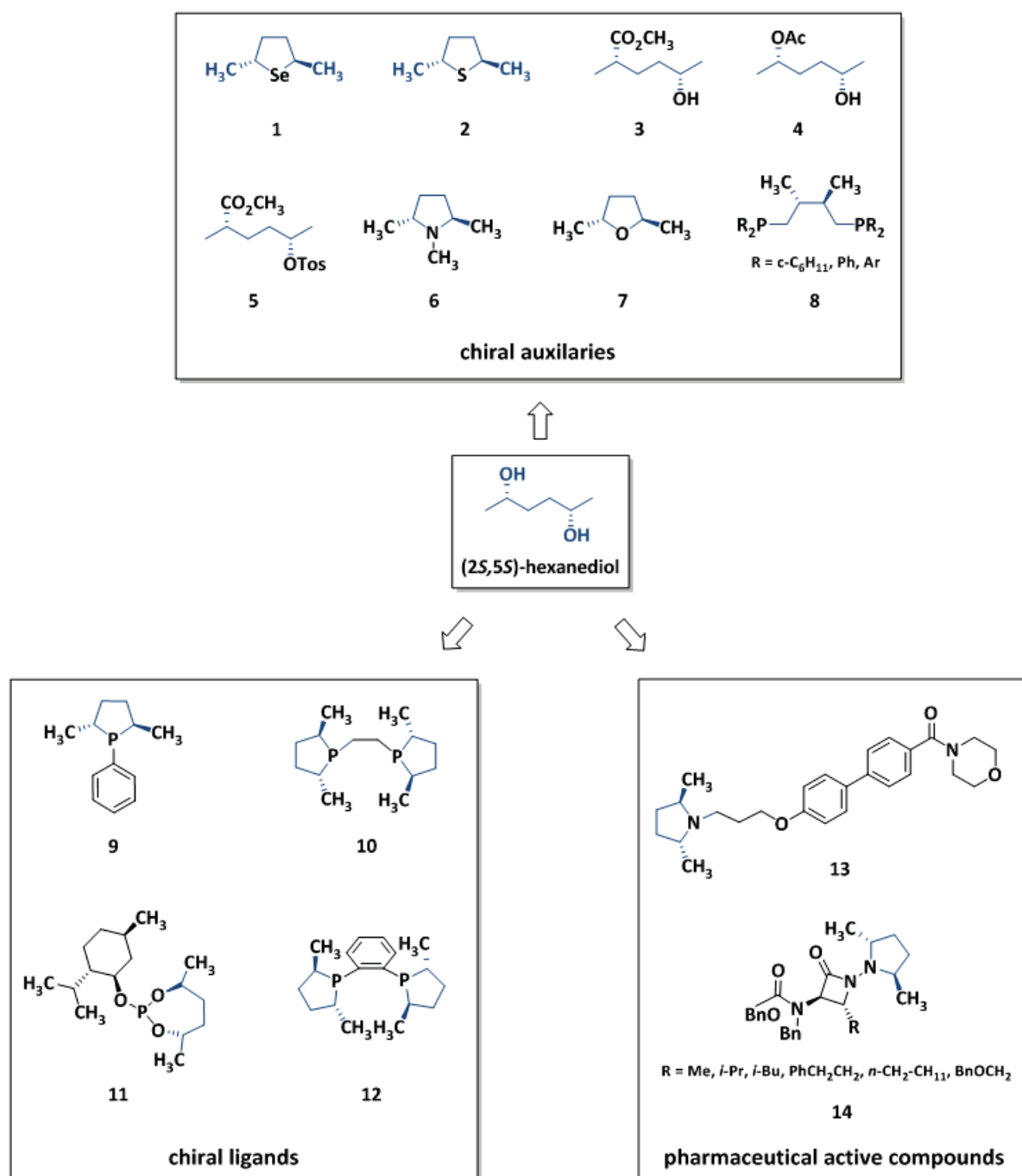
Figure 1.12. Overview of the application of (2S,5S)-hexanediol. It is a key chiral building block in the preparation of chiral auxilaries **1** [291], **2** [292], **3** [293], **4**, **5**, **7** [294], **6** [287], **8** [295]; chiral ligands **9** [296], **10**, **12** [297, 298] **11** [299] and pharmaceutical active compounds **13** [290], **14** [289].

In a third hydrogenation route, 2,5-hexanedione is reduced by oxazaborolidine (**3**). However, in comparison to reaction **1** and **2**, both the yield (34.5%) and enantiomeric excess (17% *ee*) are significantly lower [274].

Asymmetric hydrosilylation is another possibility for synthesising diols. To prepare (2*S*,5*S*)-hexanediol, the *γ*-diketone is hydrosilylated by an EtTRAP-rhodium complex into a silyl ether which is then solvolysed to 2,5-hexanediol. The reaction proceeds with a high enantioselectivity (97% *ee*) but only moderate diastereoselectivity ([(*S,S*)+(*R,R*)] : *meso* = 75:25) and (2*S*,5*S*)-hexanediol is obtained with an approximate yield of 70.6% [279].
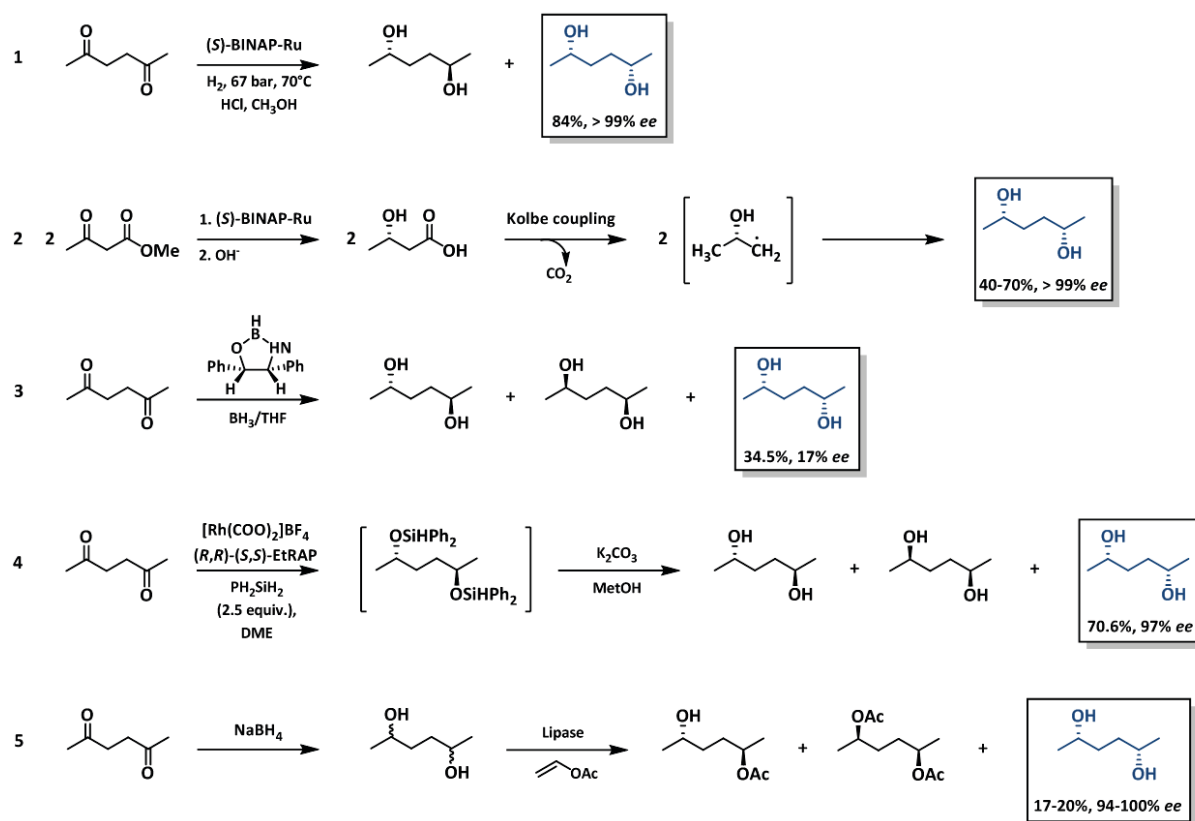
Figure 1.13. Chemical and chemoenzymatic synthesis of (2*S*,5*S*)-hexanediol. (**1**) Enantioselective hydrogenation of 2,5-hexanedione using Noyori's (*S*)-Ru-BINAP catalyst (**2**) enantioselective hydrogenation of methyl 3-oxobutanoate using (*S*)-Ru-BINAP followed by saponification into the corresponding carboxylic acids which are then subjected to electrochemical Kolbe coupling, (**3**) oxazaborolidine-catalysed reduction of 2,5-hexanedione, (**4**) asymmetric hydrosilylation of 2,5-hexanedione, (**5**) lipase-catalysed esterification of *rac/meso*-2,5-hexanediol with vinyl acetate catalysed by a lipase from *Pseudomonas* sp. or *Alcaligenes* sp.

The chemoenzymatic approach (**5**) to (2*S*,5*S*)-hexanediol makes use of a lipase reaction. The starting material is a mixture of *rac*- and *meso*-2,5-hexanediol, which can be purchased or obtained through reduction of the *γ*-diketone with sodium borohydride. Then, a lipase from *Pseudomonas* sp. or *Alcaligenes* sp. catalyses the esterification of *rac*- and *meso*-2,5-hexanediol with vinyl acetate. The lipases used are *R*-selective and thus di- and mono-acylated product is achieved while (2*S*,5*S*)-hexanediol remains inert. This is then extracted

and re-crystallised. Thus, highly enantiopure (94-100% *ee*) (*S*,*S*)-diol with a yield of 17-20% out of max. 25% is attained [302].

1.7.2.1.2 Biocatalytic access to (2*S*,5*S*)-hexanediol

The biocatalytic route to (2*S*,5*S*)-hexanediol was first described by Lieser in 1983 and is mediated through baker's yeast, which catalyses the di-reduction of 2,5-hexanedione via the hydroxy intermediate (5*S*)-hydroxy-2-hexanone (Figure 1.14). After incubation for 48-72 h at room temperature, using sucrose as energy source to maintain the intracellular cofactor pool, the diol was obtained with an isolated yield of 57% and an enantiomeric excess of at least 95% [229]. Ever since, attempts have been made to optimise this biotransformation regarding higher enantioselectivity, overall yield and space-time yield (STY). By varying the yeast/substrate ratio, higher yields (up to 90-94%) and a slightly enhanced stereoselectivity (>99% *ee* and *de*) were achieved. The STY was also improved by a factor of 4.4 to 4 g L^{-1}·d^{-1} [225, 286].

Figure 1.14. Stereoselective baker's yeast-mediated bioreduction of 2,5-hexanedione. The reduction proceeds via the mono-reduction product (5*S*)-hydroxy-2-hexanone.
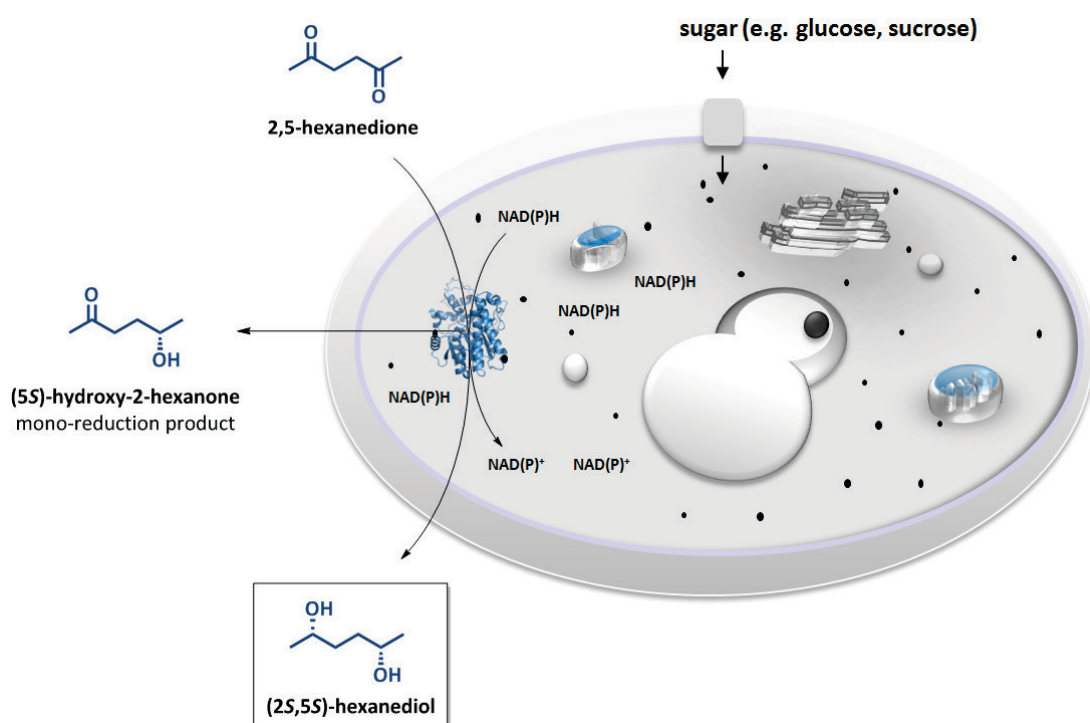
Nowadays, baker's yeast reduction is the most powerful tool to synthesise (2*S*,5*S*)-hexanediol on a preparative-scale. It is more economical than the chemical approaches, and

allows the preparation at high atom economy. Additionally, the catalyst is readily available and cheap, easy to handle and possesses the GRAS status (generally recognized as safe) [237]. However, despite these benefits, this whole-cell biotransformation suffers from several disadvantages. Thus, it is observed that the mono-reduction product accumulates during the course of reduction due to low enzyme activity [225]. This, in turn, is the result of low quantities of diketone reducing enzyme present in the cells. This also limits the use of high diketone concentrations. Accordingly, regardless of any process optimisation carried out in the past, cell productivity (70 $mg_{diol} \cdot g^{-1}_{cells}$) and STY remain low and could be improved significantly by using a recombinant catalyst. This was successfully demonstrated for the synthesis of the opposite enantiomer, (2R,5R)-hexanediol. Wild-type biotransformation of 2,5-hexanedione performed in a continuously operated process using whole resting cells of *Lactobacillus kefir* resulted in a STY of 64 $g \cdot L^{-1} \cdot d^{-1}$ [226]. In contrast, application of recombinant *E. coli* cells producing an alcohol dehydrogenase from *Lactobacillus brevis*, which was shown to synthesise (2R,5R)-hexanediol with a similar activity [303], gave the product with a threefold increase in STY (>170 g $L^{-1} \cdot d^{-1}$) [304].

1.8 AIM OF THIS THESIS

As explained above, (2S,5S)-hexanediol is a versatile chiral building block and thus there is high demand for efficient synthesis routes. Chemical synthesis approaches usually require a significant number of chemical steps, reveal low overall yields or poor stereoselectivity and are also carried out under harsh reaction conditions. In contrast, biotransformation using baker's yeast is more efficient in terms of both product outcome and stereoselectivity. However, the process is limited to the use of low diketone concentrations and results in low space-time yields (STYs). Because of this, the major focus of the present thesis is to develop powerful biocatalytic synthesis routes to optically pure (2S,5S)-hexanediol. To meet this objective, the reductase responsible for the reduction of 2,5-hexanedione in *S. cerevisiae* must first be identified. Afterwards, suitable expression systems will be generated to allow production of the reductase in large quantities.

Subsequent *γ*-diol synthesis will be accomplished with both isolated enzyme, coupled to a cofactor recycling system, and whole cells, which include the application of *E. coli* "designer cells" and a *S. cerevisiae* strain expressing the 2,5-hexanedione reductase gene. Additionally,

attempts will be made to produce (2*S*,5*S*)-hexanediol on a preparative scale and to investigate whether this approach would enable its commercial application.

The 2,5-hexanedione reductase will also be fully characterised and its substrate scope will be examined, particularly with respect to the stereoselective reduction of other diketones. Moreover, to get a mechanistic understanding of how the reductase catalyses the reduction of carbonyl compounds, an attempt should be made to solve the three dimensional structure.

Because ADHs are used for the production of numerous chiral hydroxy compounds, some of which are used in various technical applications, a further aim of this thesis is the expansion of the biocatalytic toolbox by novel ADHs. To meet this purpose, a database mining approach on the sequence of the 2,5-hexanedione reductase will be carried out to find novel reductases among the putative annotated oxidoreductases. The ability to synthesise chiral hydroxy compounds and diols will finally be investigated via small scale reactions using recombinant enzyme.

2

IDENTIFICATION OF THE

2,5-HEXANEDIONE REDUCTASE

2.1

Highly efficient and stereoselective biosynthesis of (2*S*,5*S*)-hexanediol with a dehydrogenase from *Saccharomyces cerevisiae*

Marion Müller, Michael Katzberg,
Martin Bertau and Werner Hummel

Highly efficient and stereoselective biosynthesis of (2*S*,5*S*)-hexanediol with a dehydrogenase from *Saccharomyces cerevisiae*[†]

Marion Müller[a], Michael Katzberg[b], Martin Bertau[b] and Werner Hummel[a]*

The enantiopure (2*S*,5*S*)-hexanediol serves as a versatile building block for the production of various fine chemicals and pharmaceuticals. For industrial and commercial scale, the diol is currently obtained through bakers' yeast-mediated reduction of 2,5-hexanedione. However, this process suffers from its insufficient space-time yield of about 4 g L^{-1} d^{-1} (2*S*,5*S*)-hexanediol. Thus, a new synthesis route is required that allows for higher volumetric productivity. For this reason, the enzyme which is responsible for 2,5-hexanedione reduction in bakers' yeast was identified after purification to homogeneity and subsequent MALDI-TOF mass spectroscopy analysis. As a result, the dehydrogenase Gre2p was shown to be responsible for the majority of the diketone reduction, by comparison to a Gre2p deletion strain lacking activity towards 2,5-hexanedione. Bioreduction using the recombinant enzyme afforded the (2*S*,5*S*)-hexanediol with >99% conversion yield and in >99.9% *de* and *ee*. Moreover, the diol was obtained with an unsurpassed high volumetric productivity of 70 g L^{-1} d^{-1} (2*S*,5*S*)-hexanediol. Michaelis–Menten kinetic studies have shown that Gre2p is capable of catalysing both the reduction of 2,5-hexanedione as well as the oxidation of (2*S*,5*S*)-hexanediol, but the catalytic efficiency of the reduction is three times higher. Furthermore, the enzyme's ability to reduce other keto-compounds, including further diketones, was studied, revealing that the application can be extended to α-diketones and aldehydes.

Introduction

Chiral alcohols and hydroxyl ketones are versatile building blocks and thus of steadily increasing interest for the fine and agrochemical as well as the pharmaceutical industries.[1,2] In particular, the γ-diol (2*S*,5*S*)-hexanediol is of special interest, as it is the key starting material for the production of chiral catalysts[3–5] and pharmaceuticals.[6] The demand for the enantiopure diol is high and can only be satisfied through the development of an efficient synthesis technology.

Probably the most convenient chemical method to synthesize the (*S*,*S*)-diol is the asymmetric reduction of the corresponding diketone, 2,5-hexanedione, *via* selective hydrogenation using an (*S*)-Ru–BINAP catalyst.[7] Besides this, alternative routes do exist. Among them, the chemoenzymatic route described by Nagai *et al.*[8] uses resolution of racemates through enantioselective esterification catalysed by lipases from *Pseudomonas* sp. or *Alcaligenes* sp. to obtain enantiopure (*S*,*S*)-hexandiol. Furthermore, Burk *et al.*[9] developed a method based on the asymmetric hydrogenation and saponification of methyl 3-oxobutanoate, yielding the corresponding carboxylic acid, which is subjected to Kolbe electrolysis to generate the (*S*,*S*)-diol. Although all these methods afford the desired product in high enantiomeric excess (>99%), yields are only moderate (17–86%). Furthermore, the mentioned processes are not very efficient, because they exhibit low atom economy[10], show numerous side reactions or have a high energy demand due to harsh reaction conditions. Thus, a more efficient

[a]   Marion Müller, Prof. Dr. Werner Hummel
      Institute of Molecular Enzyme Technology
      Research Center Juelich
      52426 Juelich, Germany
      Tel: (+49)24641 613790
      E-mail: w.hummel@fz-juelich.de

[b]   Michael Katzberg, Prof. Dr. Martin Bertau
      Institute of Technical Chemistry
      Freiberg University of Mining and Technology
      09596 Freiberg, Germany

synthesis technology is needed. Recently, Machielsen *et al.* reported on a biocatalytic process to produce *S*-selective 2,5-hexanediol, as they had used an engineered alcohol dehydrogenase (AdhA) from *Pyrococcus furiosus*[11]. However, this AdhA shows little activity towards the corresponding diketone. By contrast, good yields of (2*S*,5*S*)-hexanediol were obtained with an alcohol dehydrogenase (AdhT)[12] isolated from *Thermoanaerobacter* sp.

Nevertheless, up to now, the most powerful enzymatic synthesis route is the bakers' yeast-mediated *in vivo* (*S*)-selective reduction of 2,5-hexanedione furnishing the stereoselective (*S*,*S*)-diol (*ee*, *de* > 99.9%) in up to 90% yield.[13,14] The process is furthermore suitable for commercial scale-up as yeast is readily available, easy to handle and possesses the GRAS status (generally recognized as safe).[15] However, major drawbacks are the long reaction time and the low substrate concentration that can be used. For example, complete reduction of 80 mM 2,5-hexanedione with 125 g L^{-1} yeast (wet weight) takes 2–3 days. The reason for this insufficient reaction rate is most likely the low intracellular activity of the enzyme responsible for the reduction of 2,5-hexanedione and possible diffusion problems of the substrate through the cell membrane. The rate limiting step of this two-stage reaction seems to be its second step, namely the reduction of the intermediate (*S*)-5-hydroxy-2-hexanone,which leads to a transient accumulation of the intermediate product during the course of the reaction.[12] These hurdles may be overcome by applying the isolated enzyme catalysing 2,5-hexanedione reduction *in vitro*, since in this case, the activity will be increased due to a higher amount of enzyme available.[1,16] However, up to now, there have been no attempts to identify the dehydrogenase responsible for this reduction in yeast cells.

In order to overcome the bottlenecks of bakers' yeast-mediated production of (2*S*,5*S*)-hexanediol and to establish an *in vitro* synthesis, we were encouraged to identify the dehydrogenase involved in the 2,5-hexanedione reduction by bakers' yeast. Moreover, in a view of the enzyme's biotechnological power to synthesise chiral hydroxy compounds, the enzyme was employed to reduce other keto-compounds than the γ-diketone, in particular other diketones.

Results and discussion

Cofactor dependence of the enzyme reducing 2,5-hexanedione

Since dehydrogenases require NADH or NADPH as an electron donor for their reduction,[17] the cofactor dependence of the enzyme catalysing the consecutive reduction of 2,5-hexanedione had to be determined first. Thus, yeast crude cell extract was analyzed spectrophotometrically with NADH and NADPH, and hexanedione as the substrate. By this means, an approximately 6-fold higher activity with NADPH (0.12 U mg^{-1}) compared to NADH (0.02 U mg^{-1}) was obtained, suggesting that at least the first step of diketone reduction depends on NADPH. However, this assay was restricted, since only the decrease of cofactor at 340 nm was measured, and no information about the second step, reducing the hydroxy ketone, was feasible because this compound is not available.

In order to obtain more information about this two-stage reaction, cell-free bioreductions were conducted with both cofactors, followed by product analysis with gas chromatography. Glucose and glucose dehydrogenase (GDH) were used for cofactor regeneration. Fig. 1 shows the formation of the mono-reduced intermediate hydroxyhexanone and the diol (2*S*,5*S*)-hexanediol with reaction time, highlighting an approximately 5-fold enhancement in the hydroxy ketone synthesis already after fifteen minutes, when using NADPH (a) over NADH (b). The afore-mentioned low affinity of the enzyme for the hydroxyketone was observed as well, since it led to an accumulation of this compound (Figure 1a). 2,5-Hexanediol synthesis was only achieved in the presence of NADPH, reaching up to 30% after 3 h. These experiments agreed well with the spectrophotometrically measured data, suggesting that the reduction of the diketone is mainly dependent on NADPH. The occurrence of the hydroxyketone, reaching a conversion rate of around 45% after 3 h, in cell-free bioreductions utilizing NADH points out that yeast either harbors multiple dehydrogenases reducing 2,5-hexane-

dione with different activities and cofactor dependences, or that a single 2,5-hexanedione-reducing dehydrogenase is present in the cells lacking absolute cofactor specificity.
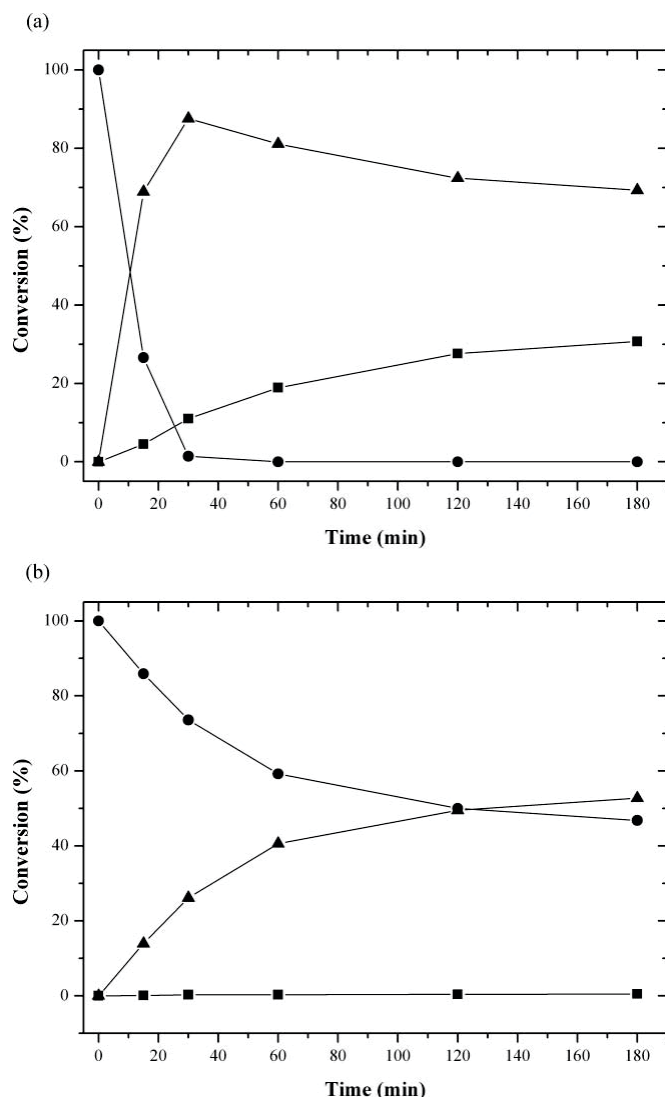

(a)

(b)

Figure 1. Conversion of 20 mM 2,5-hexanedione using bakers' yeast crude cell extract (2.5 units) and NADPH (1 mM) **(a)** or NADH (1 mM) **(b)**. For regeneration of the coenzyme, glucose (100 mM) and glucose dehydrogenase were added. Reactions were performed at 30 °C, pH 7.5 under shaking, and reactant and product concentrations were analysed by gas chromatography. ● 2,5-hexanedione, ▲ 5-hydroxy-2-hexanone, ■ (2S,5S)-hexanediol.

Identification of the 2,5-hexanedione reductase by purification

In order to identify the yeast dehydrogenase responsible for the NADPH-dependent 2,5-hexanedione reduction, the enzyme was purified from crude cell extract. After ammonium sulfate precipitation, five further steps of purification were needed to obtain the protein in an almost homogeneous form, with a specific activity of 68 U mg^{-1} (Table 1). A representative SDS polyacryl-

amide gel documenting the purification is shown in Figure 2. The purified protein could now be subjected to N-terminal amino acid sequencing by means of automated Edman degradation.[18] However, this approach failed, probably due to a modification of the N-terminal amino acid, which has been reported in the literature for a majority of eukaryotic intracellular proteins.[19,20] Alternatively, MALDI-TOF mass spectrometry can be applied in this case due to the fact that the whole genome sequence of *S. cerevisiae* is available in databases.[21] Thus, the observed mass prints, obtained from a tryptic in-gel digestion, were compared with those found in the database and fitted best according to subunit size (Figure 2) and cofactor dependence, with the NADPH dependent methylglyoxal reductase Gre2p[22] (Table 2). Since the SDS gel still shows additional bands in the purest solutions (Figure 2, lane 7–9), these bands were analysed by MALDI-TOF mass spectrometry as well. However, none of these bands could be assigned to a known or putative dehydrogenase present in *S. cerevisiae*, which underlines that the 2,5-hexanedione reductase activity found in the purest solutions is, with the most probability, due to Gre2p alone.

Gre2p is responsible for the majority of yeast's 2,5-hexanedione reductase activity

The question arises if there are additional 2,5-hexanedionereducing enzymes contributing to the total activity of whole-cells. As in the case of most substrates investigated in *S. cerevisiae* bio-reductions, it is quite likely that more than one enzyme is responsible for reduction of a substrate. As an example, ethyl 3-oxo-butanoate is reported to be reduced by 15 *S. cerevisiae* dehydrogenases.[24] However, just a few of them are expressed in sufficient amounts, and hence approximately four reductases are responsible for catalyzing the reduction of ethyl 3-oxo-butanoatein wild-type bakers' yeast.[25] In order to address the question if there is more than one dehydrogenase catalysing reduction of 2,5-hexanedione in wildtype *S. cerevisiae*, we used a *GRE2*-deficient mutant.

Table 1. Purification of 2,5-hexanedione reductase from bakers' yeast. Activity was measured photometrically reducing 15 mM 2,5-hexanedione using NADPH.

Purification step	Activity /U	Specific activity / U mg^{-1}	Yield (%)	Purification (-fold)
Crude cell extract	504	0.100	100	1.00
Crude cell extract[a]	500	0.102	99.2	1.02
Butyl-Sepharose	229	0.96	45.4	9.6
Q-Sepharose	215	3.7	42.6	37
Hydroxyapatite	32.3	34.7	6.4	347
Superdex 75	10.9	68.1	2.2	681

[a]After ammonium sulfate precipitation.

Table 2. Properties of mass fragments obtained from a tryptic in-gel digestion. MOWSE-Score is a similarity score based on the molecular weight search (MOWSE) scoring system described by Papin.[23]

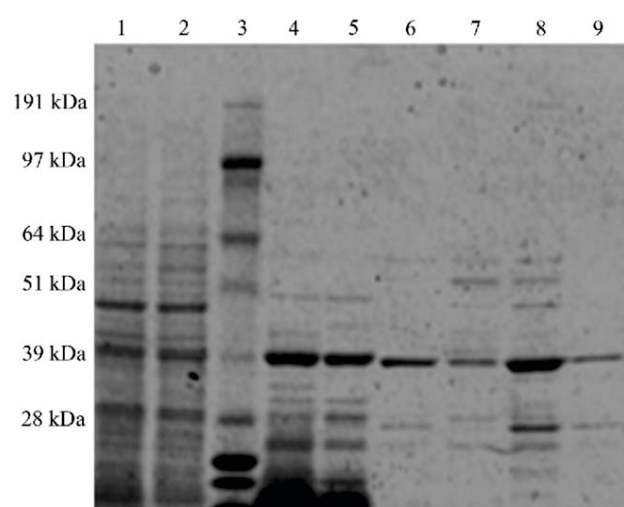| Parameter	Result
MOWSE -Score	1.73e + 6
Identical masses	11 (8)
Sequence identity (%)	41.2
Protein MW (Da) /PI[a]	38170/5.8
Gene locus	YOL151W
Gene name	*GRE*2
Protein name	Grw2p

[a]After ammonium sulfate precipitation.

Figure 2. SDS-PAGE analysis of the enrichment steps of 2,5-hexanedione reducing activity from bakers' yeast. Lane 1: yeast crude cell extract. Lane 2: yeast crude cell extract after ammonium sulfate precipitation. Lane 3: protein standard (SeeBlue® Plus2 pre-stained). Lane 4: pool Butyl-Sepharose. Lane 5: pool Q-Sepharose. Lane 6: pool hydroxyapatite. Lanes 7–9: active fractions after Superdex 75.

As is evident from Figure 3a, no 2,5-hexanedione reducing activity was detectable in crude extracts of the exponentially growing *gre2*-Δ strain whereas cells of the same strain showed some activity when they had reached stationary phase. It can be concluded from this experiment that

Gre2p is responsible for the majority of the 2,5-hexanedione-reductase activity in wild-type yeast cells. However, there are some dehydrogenases which are capable of 2,5- hexanedione-reduction in stationary phase cells. These enzymes seem to be induced during the transition to stationary phase, and catalyse reduction of 2,5-hexanedione at a slow rate, or are poorly expressed. This result is underlined further by observations from Biotransformations carried out with resting cells of *S. cerevisiae gre2*-Δ (Figure 3b). The strain, which lacks Gre2p, reduced less 2,5- hexanedione than the corresponding wild-type in 24 h. But as there was some reduction of 2,5-hexanedione even with the *gre2*-Δ strain, it is evident that there are additional 2,5-hexanedione reductases present in wild-type *S. cerevisiae* which are not yet identified.
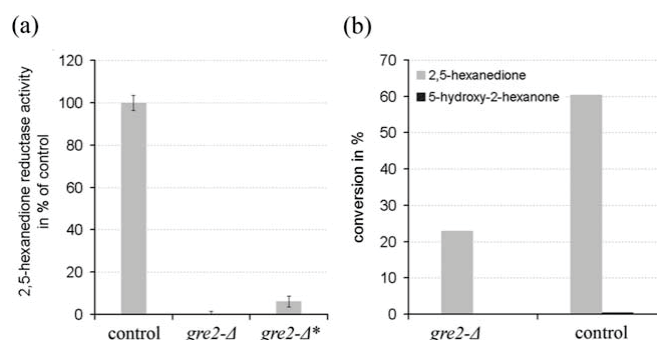
Figure 3. *gre2*-Δ Mutants and their ability to reduce 2,5-hexanedione. Reductase activity on 2,5-hexanedione in crude extracts of exponentially growing *S. cerevisiae gre2*-Δ and of cells in stationary phase (*gre2*-Δ*), respectively. Activities are referenced to the activity of wild-type cells (control) (**a**). Conversion of 40 mM 2,5-hexanedione (≈ 0.5% v/v) by resting cells of *S. cerevisiae gre2*-Δ and wild-type cells (control), respectively after 24 h (**b**).

Recombinant expression of *GRE2*

To facilitate the production of Gre2p in amounts sufficient for *in vitro* biotransformations, the gene *GRE2* (systematic name: YOL151W), located on chromosome XV and without introns, was cloned and expressed in *E. coli* BL21(DE3), which lacks 2,5-hexanedione reductase activity.

However, only low yields of recombinant Gre2p (*rec*Gre2p) were obtained, as most of it was present as inactive insoluble aggregates (inclusion bodies). Although expression was accomplished in

various *E. coli* host strains, and at different temperatures as well as incubation times, none of these altered parameters enhanced the amount of soluble protein. However, sufficient amounts of *rec*Gre2p (up to 50 U mg^{-1}) could be gained after two-step purification (>95% purity) so that the enzyme could be used for characterisation studies and in biotransformations.

Effect of pH and temperature

To determine the dependence of Gre2p's activity on pH, reduction of 2,5-hexanedione and oxidation of (2*S*,5*S*)-hexanediol activity were measured in different buffers (100 mM each) covering the range pH 4–12. At pH 7.0, partially purified Gre2p (after Butyl Sepharose^{TM} column,

>90% purity) exhibited the maximal specific activity of 16.6 U mg^{-1} for the reduction of 2,5-hexanedione (Figure 4a). This pH optimum seems to be optimal for the conditions in yeast cells for which an intracellular pH$_i$ of 6.5 has been reported,[26] and underlines that Gre2p potentially serves as a reductase *in vivo*. For the oxidation of (2*S*,5*S*)-hexanediol, the pH optimum was observed at pH 10.0, resulting in an oxidation activity of 9.7 U mg^{-1} (Figure 4b). At pH values greater than 10, a sharp decrease in the enzyme's activity could be observed. Thus, the pH optima of Gre2p for reduction and oxidation are observed at well separated values, in which the optimum of reduction activity is prevalent over a broader pH range than the optimum of oxidation activity. In the temperature range between 10 and 60 °C,
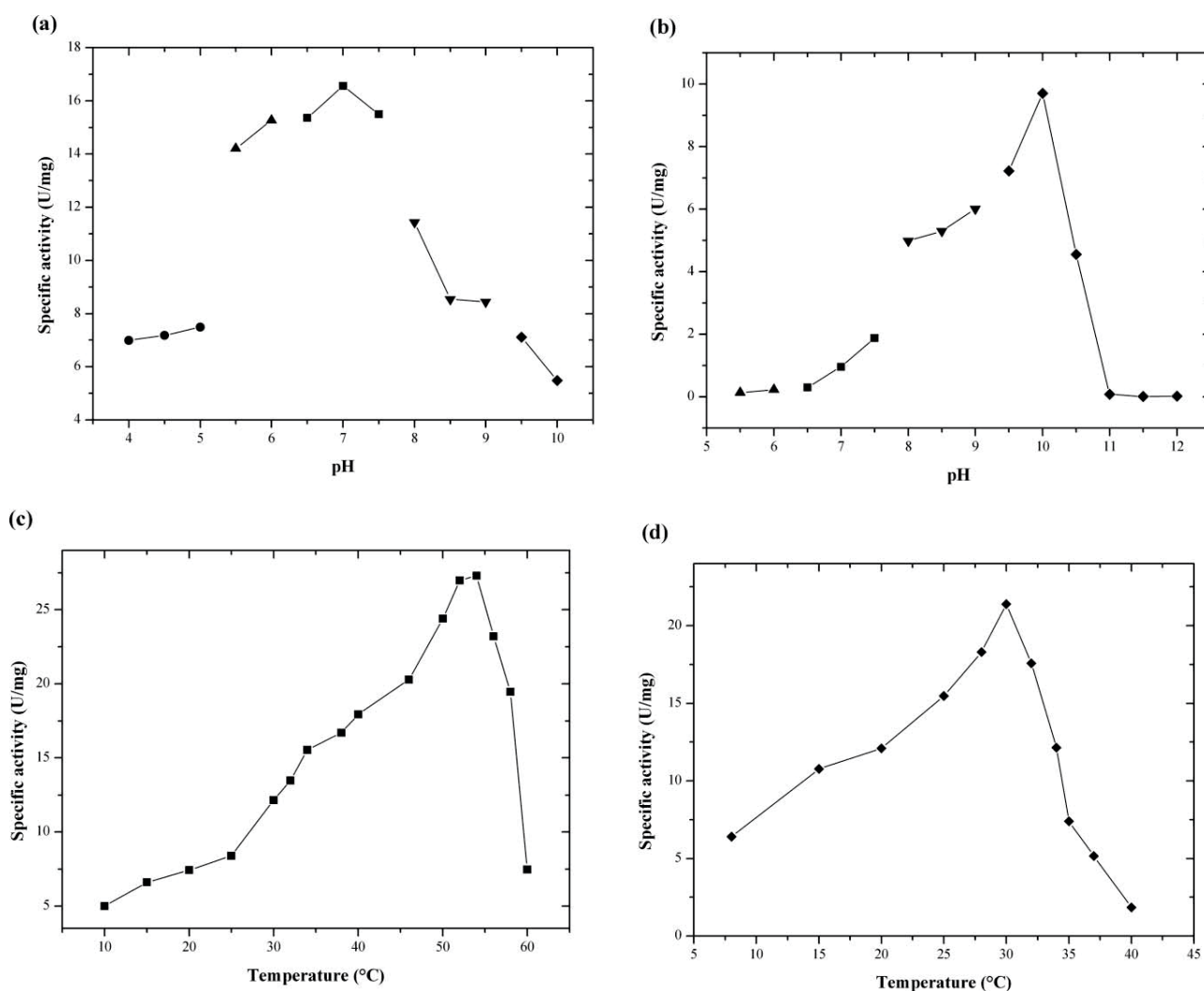
Figure 4. Effect of pH and temperature on 2,5-hexanedione reduction (**a, c**) and (2*S*,5*S*)-hexanediol oxidation (**b, d**). ● Sodium acetate buffer, ▲ 4-morpholine ethanesulfonic acid (MES), ■ TEA, ▼ TRIS/HCl, ◆ Glycine buffer; assay concentration of 2,5-hexanedione was 15 mM, and (2*S*,5*S*)-hexanediol was employed at 20 mM in both experiments. The determination of the optimum temperature was carried out using TEA buffer (pH 7.0) and glycine buffer (pH 10.0) for the reduction and oxidation, respectively.

enzyme activity was determined for the reduction of 2,5-hexanedione, with an optimum activity of 27.3 U mg^{-1} at 54 °C. Further increases in temperature resulted in a fast decay in activity (Fig. 4c). For the oxidation of (2S,5S)-hexanediol, the temperature optimum was observed at 30 °C, with 21.3 U mg^{-1} (Figure 4d). An explanation for the optimum difference could be that the enzyme is better stabilised by both 2,5-hexanedione and the reduced cofactor than it is by the diol and by NADP$^+$, or by the buffer TEA used in the reduction experiments (Figure 4c).

Determination of the molecular weight and group classification

To determine the molecular weight of the native Gre2p, size exclusion chromatography, coupled with activity-based detection, was applied to attain a molecular mass of about 39 kDa. The subunit size estimated by SDS-PAGE (Figure 2) was about 42 kDa. Since both values are in fair agreement with the calculated molecular mass of 38.139 kDa for a single subunit of the enzyme, it can be concluded that Gre2p has a monomeric structure. According to Persson et al[27] and Jörnvall et al,[28] the enzyme can be classified into the extended short-chain-dehydrogenase/reductase
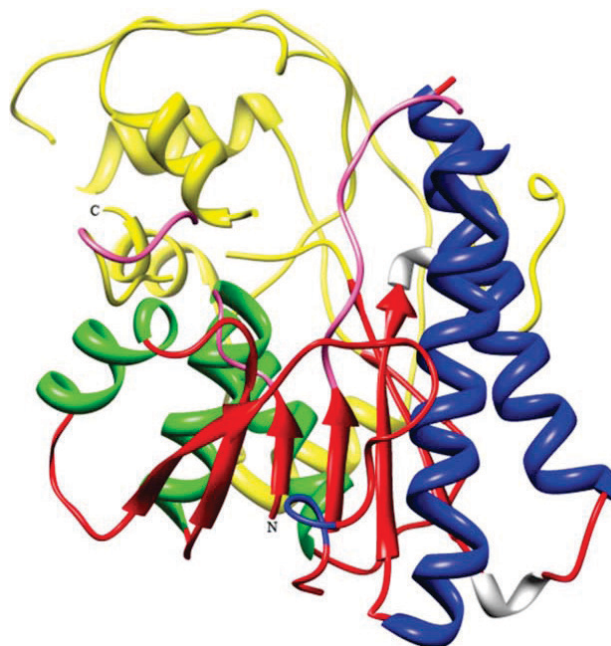
Figure 5. Stereoview of the overall model structure of Gre2p based on the PDB homologous SsAKIIp, illustrated by the UCSF Chimera program. The colouring is the same as used for Fig. 6.

superfamily, as the primary sequence length of Gre2p consists of 342 amino acids, it exhibits a Rossmann-fold cofactor binding motif and the three catalytic residues, Ser-Tyr-Lys,[29] are in the active site as well as the characteristic PFAM domain, PF01370.
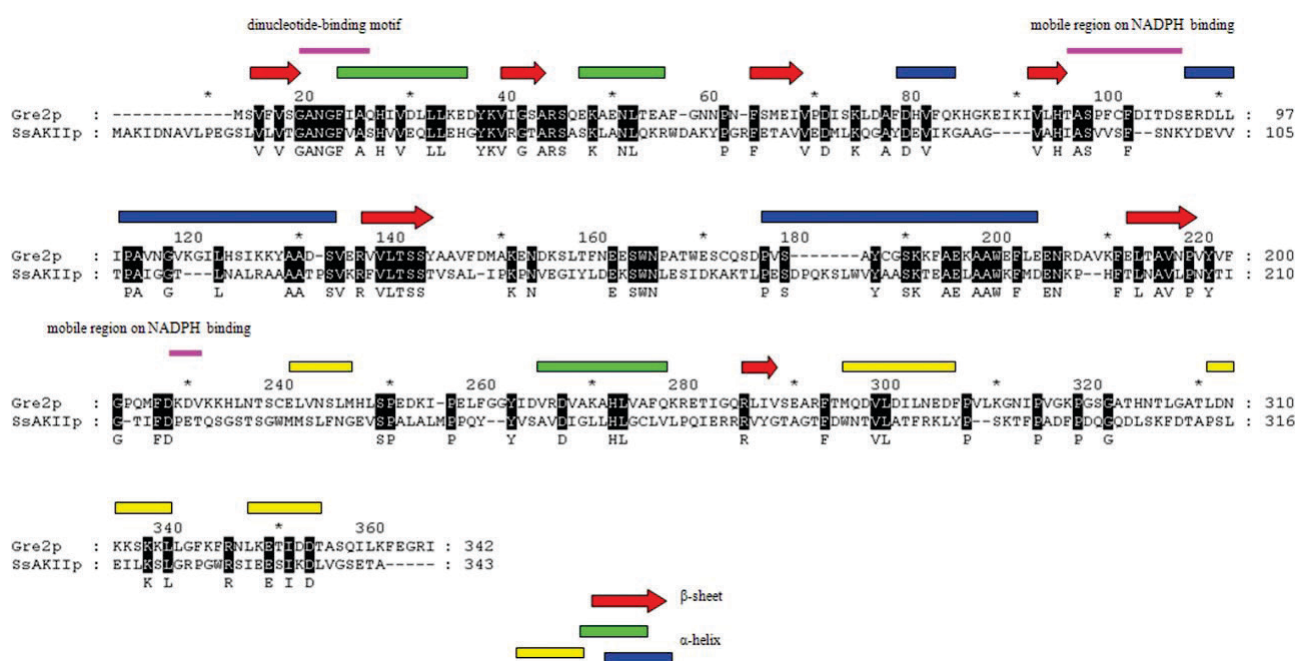
Figure 6. Alignment of Gre2p with the aldehyde reductase II from *Sporobolomyces salmonicolor* (SsAKIIp) and illustration of Gre2p's predicted secondary structure elements, based on the model structure. β-sheets are marked in red, and α-helices are marked in green, blue and yellow.

To gain insights into the proposed mechanism of cofactor binding, a structure model (Figure 5) of Gre2p was obtained, based on the X-ray structure of the aldehyde reductase II from *Sporobolomyces salmonicolor* AKU4429 (abbreviated as SsAKIIp)[30], to which Gre2p shares 30% homology, as displayed in the amino acid sequence alignment (Fig. 6). Thus, the cofactor-binding domain is expected to be highly conserved, but does not contain the typical two-halves of the β-α-β-α-β motif (Rossmann fold) as well, since the cofactor domain contains a seventh β-sheet. The β-sheets (red) form a parallel structure and six α-helices (green, blue) are located on both sides of the β-sheet. The amino residues Gly^7-Ala^{13} (magenta), interacting most probably with the dinucleotide, and the positive charged residues Arg^{32} and Lys^{36} are expected to play a role in the affinity of the enzyme on NADPH, rather than NADH, since they most likely form salt-bridges with the phosphate moiety at the 2'-position of AMP. Moreover, the model predicts the presence of two mobile regions (Thr^{81}-Ser^{92} and Asp^{206}-Val^{209}; magenta), which are proposed to also play a role in the cofactor-binding, as is the case for the aldehyde reductase II. Compared to the cofactor-binding domain, the substrate binding domain (yellow) shares only minor similarity with SsAKIIp, although primary sequence alignment gives high homology. However, it is undoubted that Ser^{126}, Tyr^{165} and Lys^{169} are the residues that are indispensable for the catalytic reaction.

In vitro biocatalysis of (2*S*,5*S*)-hexanediol

The synthesis of (2*S*,5*S*)-hexanediol through bioreduction of 2,5-hexanedione was achieved by using *rec*Gre2p after one step purification on Butyl Sepharose[TM] (>90% purity). In this experiment, 20 U mL^{-1} of Gre2p was sufficient to reach complete conversion of 20 mM 2,5-hexanedione into the diol (≥99%) within 1 h (Figure 7). The product (2*S*,5*S*)-hexanediol was obtained in >99.9% *de* and *ee*, which underlines the absolute stereoselectivity of Gre2p. Compared to the use of whole-cells, application of the isolated dehydrogenase markedly increased reaction rates, because the

applicable amount of active enzyme (in this experiment 2 U mL^{-1}) is much higher now.
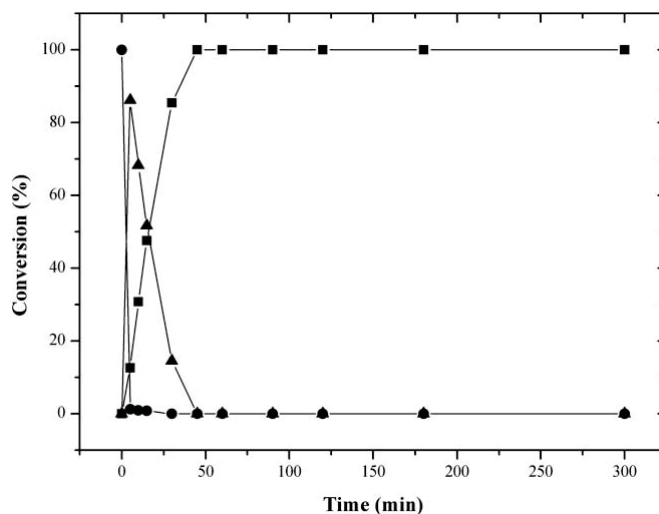
Figure 7. Conversion of 20 mM 2,5-hexanedione using single-purified recombinant Gre2p (after Butyl-Sepharose column) (20 units). Reaction was performed at pH 7.5, 30 ℃ and with gentle shaking. NADPH was recycled by glucose dehydrogenase (GDH). ● 2,5-hexanedione, ▲5-hydroxy-2-hexanone, ■ (2*S*,5*S*)-hexanediol.

For example, the theoretical 2,5-hexanedione reductase activity in high-cell-density (125 g L^{-1} (wet weight)) whole-cell biotransformations is around 1–1.5 U mL^{-1},[12] disregarding effects which further slow down the reaction rate, like non-saturating intracellular concentration of NADPH and possible transport limitations of the substrate through the cell membrane. Thus, the use of isolated *rec*Gre2p allows for a significantly improved space-time yield of about 70 g L^{-1} d^{-1} (2*S*,5*S*)-hexanediol, which is 17 times higher than the one observed in whole-cell-biotransformations (about 4 g L^{-1} d^{-1} (2*S*,5*S*)-hexanediol). Moreover, even higher concentrations of Gre2p are applicable in bioreductions, thus enabling even higher space-time yields, which makes the process transferable to a commercial scale, in which a volumetric productivity of about 100 g L^{-1} d^{-1} is required on average.[31] A further advantage of the process is the full conversion of the starting material to the product, which is achievable because reduction of 2,5-hexanedione is favoured over reoxidation of 2,5- hexanediol at pH 7.5 (pH of the reaction mixture). At this pH value, the reduction activity of Gre2p towards 2,5-hexanedione is about 7 times higher than the

oxidation activity towards (2*S*,5*S*)-hexanediol (Figure 4a and b). Furthermore, the cofactor regeneration system drives the reaction to completion if the co-substrate is used in excess of the starting material. Thus, a high NADPH:NADP$^+$ ratio is sustained throughout the reaction, favoring reduction over oxidation.

To characterise the reduction of 2,5-hexanedione and oxidation of (2*S*,5*S*)-hexanediol through Gre2p, the kinetic constants of both reactions obeying Michaelis–Menten kinetics were determined (Table 3). The results show that the enzyme's affinity towards the diketone 2,5-hexanedione is higher than the affinity towards (2*S*,5*S*)-hexanediol. This means that the substrate concentration required for reaching the maximal reaction rate is three times smaller in the direction of reduction than in the direction of oxidation. However, as both K_M values are in the lower millimolar range, the affinity of the enzyme towards these xenobiotic compounds can be assessed to be quite good. Moreover, Gre2p catalyses formation of products in either direction (oxidation or reduction) with a similar turnover number (k_{cat}), whereas it is catalytically more efficient in the direction of reduction, *i. e.* the catalytic efficiency (K_M/k_{cat}) of the reduction is three times higher than the one for oxidation.

Table 3. Kinetic parameters for the reduction of hexanedione and oxidation of (2*S*,5*S*)-hexanediol

Substrate	K_M/mM	V_{max}/ U mg^{-1}	k_{cat}/s^{-1}	k_{cat}/K_M s^{-1} mM^{-1}
2,5-hexanedione	4.33 ±0.28	14.03 ± 0.34	9.13^a	2.11
(2*S*,5*S*)-hexanediol	10.48 ±0.56	12.90 ± 0.50	8.40^a	0.80

^{a} Calculated in reference to the empirically determined molecular weight of 39 kDa.

Substrate spectrum

In this work, the yeast dehydrogenase Gre2p was identified as being responsible for the reduction of the γ-diketone 2,5-hexanedione in cells of *S. cerevisiae*. It has been known that Gre2p serves as a versatile biocatalyst, which has been also reported by Ema *et al.*[32,33] and Kaluzna *et al.*[24] However, reduction of diketones was only sparsely addressed in previous works. Moreover, to the best of our knowledge, the ability of Gre2p to reduce γ-diketones such as 2,5-hexanedione has not been reported before, and thus extends the range of possible applications of Gre2p in biocatalysis. Based on this fact, the enzyme maybe able to reduce a number of other diketones. Thus, the substrate specificity of Gre2p was investigated, including not only diketones, but also aliphatic and cyclic α- and β-keto esters and aldehydes, as well as ketones. The activities of Gre2p towards various substrates were measured spectrophotometrically at a substrate concentration of 15 mM in 0.1M TEA buffer (pH 6.5) at 30°C, and were referenced to the activity of the enzyme towards 2,5-hexanedione, which was set to be 100%.

As given in Table 4, Gre2p catalyses the reduction of α- and β-diketones at a slower rate than reduction of the γ-diketone 2,5-hexanedione. In the group of all diketones studied, 2,4-pentanedione is the worst substrate. Furthermore, it appears that methyl-ketones (*e. g.* 2,3-hexanedione) are better substrates than ethyl-ketones (*e. g.* 3,4-hexanedione), indicating that the latter is possibly not as accessible for hydrogen transfer through the enzyme.

The dehydrogenase also shows good to moderate activity with β-keto esters, in which the activity increases if the molecule features electron-withdrawing substituents. For example, the activity almost quadruples if ethyl 3-oxo-butanoate is substituted with chlorine at position 2. Furthermore, activity declines with increasing size of the alcohol part as well as the acid part of the ester. Thus, benzyl 3-oxo-butanoate and ethyl 3-oxo-hexanoate are poorer substrates than ethyl 3-oxo-butanoate. Also cyclic β-ketoesters are reduced by Gre2p. However, activity markedly drops by almost a factor of ten if the ring size is increased from five to six carbon atoms. In contrast to β-keto-esters, the activity of Gre2p towards α-keto-esters was observed to increase with the size of the acid part of the ester. Accordingly, activity increases from ethyl 2-oxo-propanoate (ethyl pyruvate) being the worst substrate to ethyl 4-phenyl-2-oxo-butanoate being the best.

Table 4. Substrate specificity of Gre2p reducing diketones, α- and ß-keto esters, and aldehydes. (* 100 % correspond to 50 U mg^{-1}; activity was measured in a photometric assay by reducing 15 mM substrate using NADPH as the coenzyme.)
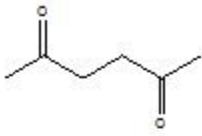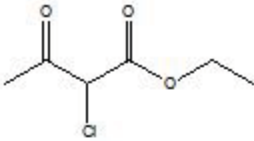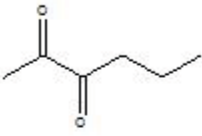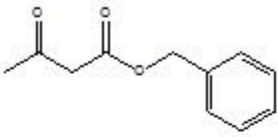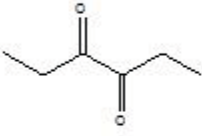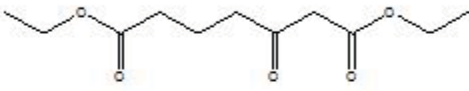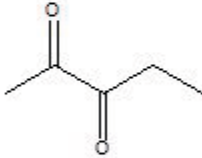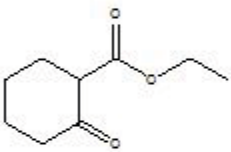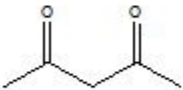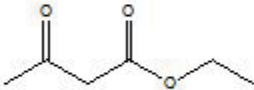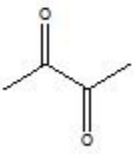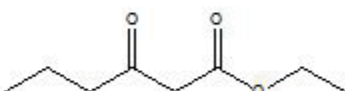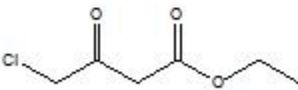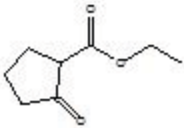
Substrates	Relative activity (%)
Diketones	

2,5-hexanedione — 100*

2,3-hexanedione — 32.0

3,4-hexanedione — 4.84

2,3-pentanedione — 5.74

2,4-pentanedione — 2.10

2,3-butanedione — 10.1

ß-Keto esters

ethyl 2-chloro-3-oxo-butanoate — 63.2

benzyl 3-oxo-butanoate — 2.30

diethyl 3-oxo-heptanoate — 2.53

ethyl 2-oxo-cyclohexanecarboxylate — 1.97

ethyl 3-oxo-butanoate — 16.3

ethyl 3-oxo-hexanoate — 0.67

ethyl 4-chloro-3-oxo-butanoate — 71.5

ethyl cyclopentanone-2-carboxylate — 18.5

Table 4. (continued)

α-Keto esters
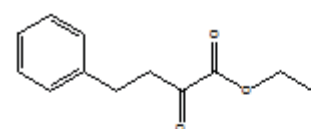
ethyl 4-phenyl-2-oxobutanoate   26.3
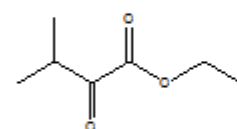
ethyl 3-methyl-2-oxo-butanoate   7.86
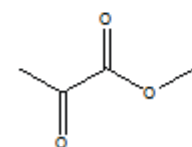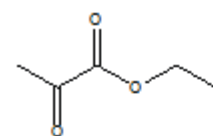
methyl pyruvate   0.83

ethyl pyruvate   0.71
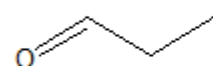
Aldehydes

propanal   31.7

butanal   169

Pentanal   68.0

hexanal   18.1
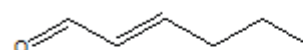
trans-2-hexenal   62.5
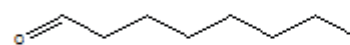
octanal   122

nonanal   39.7

decanal   63.4
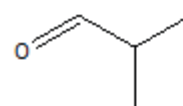
2-methyl-propanal   153

3-methyl-butanal   174

benzaldehyde   32.5

phtaldialdehyde   1.62
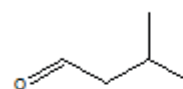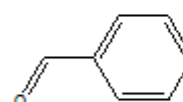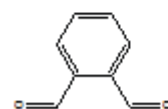
Since Gre2p is thought to work *in vivo* as an isovaleraldehyde reductase,[34] a number of aldehydes have been included in this study. Indeed, among all compounds investigated, Gre2p exhibits the highest reductase activity with isovaleraldehyde (3-methylbutanal) as the substrate (174% referenced to the activity towards 2,5-hexanedione), underlining that Gre2p may indeed be a 3-methylbutanal reductase *in vivo*. The consequence of this finding is that substrates which resemble the structure of 3-methylbutanal, such as butanal or 2-methylpropanal, will in turn be good substrates for Gre2p, which was confirmed here. Other aliphatic aldehydes are also accepted as substrates, but reduced at a slower rate, with the exception of butanal and octanal. There seems to be no trend connecting the chain length of aliphatic aldehydes with activity, as it increases from propanal to butanal, but drops then to hexanal and increases once more if octanal is used as the substrate. Furthermore, it is quite interesting that introduction of a double bond into the molecule increases the activity of Gre2p towards the substrate. Thus, *trans*-2-hexenal is reduced 3.5 times faster than its saturated analogue, hexanal. Also, aromatic aldehydes like benzaldehyde are reduced by Gre2p, whereas only a marginal activity was observed with *o*-phthaldialdehyde, possibly because this compound is known for its ability to modify and crosslink proteins,[35] and thus may inactivate the enzyme.

In the course of this study ketones were also investigated. However, significant activity of Gre2p was only observed towards methylglyoxal (53.3%) and hydroxylacetone (9.8%). Activity towards the former substrate was therefore expected, as Chen *et al.*[22] have shown that Gre2p is probably involved in *in vivo* methylglyoxal detoxification. Surprisingly, Gre2p poorly accepted 2-hexanone (3.4%), which indicates that efficient substrate binding may only be possible if a second keto group or other hydrophilic moiety is present in the molecule.

Since all these substrates are accepted by the enzyme, it is difficult to propose a substrate binding pattern for Gre2p. However, it can be concluded from this substrate spectrum that large hydrophobic moieties next to the carbonyl carbon atom are tolerated by Gre2p (*e. g.* decanal, ethyl 4-phenyl-2-oxobutanoate), and that activity increases if electron-withdrawing groups are present next to the carbonyl group to be reduced (*e. g.* ethyl 3-oxobutanoate *vs.* ethyl 2-chloro-3-oxo-butanoate). Moreover, the presence of a second keto group in the molecule seems to increase the enzyme's activity towards such a substrate (*e. g.* 2-hexanone *vs.* 2,5-hexanedione), possibly through improved substrate binding by formation of additional hydrogen bonds. Apart from any speculations, crystallisation and determination of the three-dimensional structure of Gre2p in the future will be a prerequisite to elucidate the molecular fundamentals of the enzyme's substrate specificity.

Gre2p lacks cofactor specificity

Although Gre2p is reported as being dependent on NADPH[36], it was observed that the recombinant enzyme also catalyses reductions using NADH as a cofactor, however, at a slower rate (10–20% referenced to the reduction activity in the presence of NADPH). This behaviour of Gre2p may be the reason why conversion of 2,5-hexanedione was also observed in *in vitro* biotransformations utilizing yeast crude extract with NADH as a cofactor (Figure 1b). Thus, Gre2p is not only responsible for the majority of the NADPH-dependent but also for the NADH dependent 2,5-hexanedione reductase activity in wild-type cells of *S. cerevisiae*.

Conclusion

In the present study, it was shown that the dehydrogenase Gre2p is responsible for the *in vivo* reduction of 2,5-hexanedione, forming (2*S*,5*S*)-hexanediol, as the activity-based purification yielded Gre2p, and as a strain lacking Gre2p showed little or no activity towards 2,5-hexanedione. However, whole-cell biotransformations with the deletion mutant strain *S. cerevisiae gre2-Δ* point to the existence of additional 2,5-hexanedione reducing enzymes with low activity in yeast. In the future, these enzymes will be identified and it has yet to be

proven if their activity towards different diketones and other xenobiotic substrates is sufficient for a successful utilisation in bioreductions.

In vitro biosynthesis of enantiopure (2*S*,5*S*)-hexanediol, using *rec*Gre2p, achieved a signifycantly improved space-time yield compared to the usage of whole-cells. This fact was now possible due to a higher amount of active enzyme available, which is the key for the use of this process on an industrial scale. Further improvement will be achieved through a more efficient production of the dehydrogenase, enabling higher volumetric activities of *rec*Gre2p and thus even higher space-time yields of chiral products. Investigation of the substrate specificity complements the knowledge about the substrate spectrum of Gre2p, which, to date, focused mainly on α,β-ketoesters and some β-diketones and ketones. Here, we have displayed that Gre2p not only catalyses the reduction of the γ-diketone, 2,5-hexanedione, but α-diketones and aldehydes as well.

Taken together, this study illustrates that Gre2p is a highly valuable biocatalyst whose efficient heterologous synthesis allows for efficient production of enantiopure (2*S*,5*S*)-hexanediol with a high space-time yield. Due to its broad substrate specificity, utilisation of Gre2p in bioreductions will spread in the future.

Experimental

Chemicals, coenzymes, and materials

All chemicals used in this study were of analytical grade or higher quality and were purchased from Sigma-Aldrich (Buchs, Switzerland) and Roth (Karlsruhe, Germany). Nicotinamide cofactors were obtained from Biomol GmbH (Hamburg, Germany). For purification and molecular weight determination chromatographic resins, prep grade columns and calibration proteins were purchased from GE Healthcare (Amersham, UK) and Bio-Rad (Munich, Germany). Medium components were from BD Bioscience (Franklin Lakes, USA).

Microorganisms

Industrially produced bakers' yeast was obtained from Uniferm (Werne, Germany). *S. cerevisiae* BY4741 *gre2*-Δ and the corresponding wild-type strain was obtained from Euroscarf, Frankfurt. The strain was grown in YPD at 30 ℃ and harvested by centrifugation. The *E. coli* expression strain BL21(DE3) [F⁻ompT hsdS$_B$(r$_B$⁻ m$_B$⁻) gal dcm rne131 (DE3)] was purchased from Novagen (Madison, USA). For clonal plasmid production *E. coli* DH5-α [F⁻ φ80lacZΔM15 Δ(lacZYA⁻argF)U169 recA1 endA1 hsdR17(r$_k$⁻, m$_k$⁺) phoA supE44 thi-1 gyrA96 relA1 λ⁻] was used from Invitrogen (Karlsruhe, Germany).

Disruption and purification of bakers' yeast

Bakers' yeast was suspended (2 mL buffer per 1 g cells) in triethanolamine hydrochloride (TEA) buffer (100 mM, pH 6.5 with 1 mM MgCl$_2$ and 1 mM dithiothreitol (DTT)). To this mixture twice the amount of glass beads (∅ 0.5–0.7 mm) was added. Cells were disrupted under cooling at 2000 rpm for 20 min using the Cell Disintegrator-S from Innomed-Konsult AB (Stockholm, Sweden). The crude extract was obtained after centrifuging the suspension at 27 000 x g for 1 h at 4 ℃. A part of the yeast crude extract's proteins was removed by addition of 1.5 M ammonium sulfate, gentle stirring on ice for 1.5 h and subsequent centrifugation (27 000 x g; 1 h; 4 ℃). The resulting supernatant was applied to a Butyl Sepharose™ 4 Fast Flow column, which had been equilibrated with 10 column volumes (CV) TEA buffer, 100 mM, pH 6.5, with 1 mM MgCl$_2$, 1 mM DTT and 1.5 M ammonium sulfate. The protein was eluted with the same buffer containing no ammonium sulfate, with a linear gradient from 1.5–0 M. Active fractions were pooled and concentrated with an Ultrafiltration membrane (M_r 10 000 Da). After, the protein solution was applied to CM Q Sepharose™ Fast Flow material, which had been previously equilibrated with 10 CV TEA buffer, 100 mM, pH 6.5, with 1 mM MgCl$_2$ and 1 mM DTT. The protein did not bind to this material and was determined in the flow. Hence, ion exchange chromatography was applied as a "negative chromatography". Active, dialysed and concentrated protein was then applied to a Macro-Prep® Ceramic Hydroxyapatite Typ I (40

mm) column, which had been equilibrated with 10 CV potassium phosphate buffer, 5 mM, pH 6.5, with 150 mM NaCl, 1 mM $MgCl_2$ and 1 mM DTT. A linear gradient (5–50 mM potassium phosphate buffer) was used to elute the protein, which was detected in fractions eluting at a buffer concentration of 45 mM. For the final purification step, active fractions were applied to a Superdex[TM] 75 column. Elution was accomplished with TEA buffer, 100 mM, pH6.5, with 150 mM NaCl, 1 mM $MgCl_2$ and 1 mM DTT. Purified protein was used either immediately or stored at 4 °C until further processing.

Isolation of genomic yeast DNA

Genomic DNA from yeast was isolated from frozen cells as described by Harju et al.[37] Thawed yeast cells were resuspended in 200 mL TE buffer (100 mM tris(hydroxymethyl)aminomethane (TRIS), 1 mM ethylenediamintetraacetate (EDTA) pH 8.0 with 2% Triton X-100, 1% sodium dodecyl sulfate (SDS) and 100 mM NaCl). To this suspension, 0.3 g glass beads and 200 mL of chloroform were added. The tube was vortexed vigorously for 8 min at room temperature. After addition of 200 mL TE buffer pH 8.0 the tube was centrifuged at 15 000 x g for 5 min. For precipitation of DNA, 1 mL ethanol (abs.) was added to the aqueous layer and the sample was centrifuged for 2 min at 15 000 x g. The DNA pellet was dissolved in 400 mL TE buffer, including RNase A, and incubated for 5 min at 37°C, followed by addition of 20 mL 7.5 M ammonium acetate and 1 mL 100% ethanol. The tubes were centrifuged again for 20 min at 15 000 x g. The pellet was washed with 1 mL 70% ethanol followed by centrifuging for 3 min at 15 000 x g. The DNA pellet was dried under vacuum and resuspended in 100 mL TE buffer pH 8.0. For further processing the DNA was stored at -20 °C.

Cloning of GRE2

The GRE2 gene was amplified from genomic DNA by PCR (Forward 5'-GGAATTCCATATGTCAG-TTTTCGTTTCAGGTG-3' T_M: 65.6 °C; Reverse 5'-CGCGGATCCTTATATTCTGCCCTCAAATTTTAAAA-3' T_M: 66.0 °C) and cloned into pET-21a(+) from

Novagen. PCR was performed according to a standard protocol using TripleMaster® Polymerase from Eppendorf (Hamburg, Germany). The amplified gene and pET-21a(+) were restricted with NdeI and BamHI from Fermentas (St. Leon-Rot, Germany) and ligated using the Rapid DNA Dephos & Ligation Kit from Roche Diagnostics (Mannheim, Germany) according to the manufacturer's instructions. Sequence identity had been confirmed by Sequiserve (Vaterstetten, Germany) before transformation of E. coli BL21(DE3) using the heat shockmethod as described by Chung et al.[38]

GRE2 expression, disruption and purification

E. coli cells were cultivated in lysogeny Broth (LB) medium (NaCl 1%, tryptone 1% and yeast extract 0.5%) supplemented with ampicillin (100 mg mL^{-1}). For expression of GRE2, LB medium was inoculated from an overnight culture. Cells were grown with shaking (120 rpm) at 37 °C and their optical density was monitored by measuring the absorbance at 600 nm using a UV 1602 spectrophotometer from Shimadzu (Duisburg, Germany). Enzyme induction was started when cells had reached an optical density of 0.5–0.6 by addition of isopropyl-β-D-thiogalactopyranoside (IPTG) to a final concentration of 0.2 mM followed by further growth at 37 °C for 5 h. Cells were harvested at 9000 x g for 30 min at 4 °C and disrupted either immediately or stored at -20 °C until further processing. For disruption, cells were suspended (2 mL buffer per 1 g cells) in TEA buffer, 100 mM, pH 6.5, with 1 mM $MgCl_2$, and twice the amount of glass beads ($\varnothing$ 0.5–0.7 mm) was added. Small scale disruption was carried out by using a mixer mill from Retsch (Haan, Germany; 3 x 5 min passages), whereas large volumes of yeast cell suspensions were processed through the Cell-Disintegrator-S from Innomed-Konsult, AB (Stockholm, Sweden). Cell debris was removed by centrifugation at 27 000 x g at 4 °C. Recombinant Gre2p was precipitated with 1.5 M ammonium sulfate and purified at Butyl Sepharose[TM] 4 Fast Flow and Macro-Prep® Ceramic Hydroxyapatite Typ I (40 mm) resin. Purified recGre2p was used

either immediately or stored at 4 °C until further processing.

Determination of native molecular mass

Size-exclusion chromatography was performed using a Superdex[TM] 200 prep grade column (total volume V_t = 120.6 mL ($\varnothing$ 1.6 cm)), equilibrated with 10 CV potassium phosphate buffer (Kpi) (100 mM, pH 6.5, with 150 mM NaCl, 1 mM MgCl$_2$), and two-fold purified recombinant Gre2p. The coefficient of available volume (K_{av} = (V_e - V_0)/(V_t - V_0), V_e: elution volume of the respective protein, V_0: elution volume of thyroglobulin) for Gre2p and the calibration proteins were determined twice. The average K_{av} coefficients for the calibration proteins were; chymotrypsinogen A (20.3 kD, K_{av} = 0.56), ovalbumin (46.7 kD; K_{av} = 0.42), albumin (62.9 kD, K_{av} = 0.36), aldolase (158 kD, K_{av} = 0.29), catalase (232 kD, K_{av} = 0.21), ferritin (440 kD, K_{av} = 0.09). The K_{av} coefficient of Gre2p was determined as 0.44. Data were plotted as log M_r/K_{av}, resulting in a linear correlation with R^2 = 0.9882. Flow: 1 mL min^{-1}. Sample: 1 mL Gre2p (0.5 mg mL^{-1}) in 100 mM Kpi buffer, pH 6.5, including 150 mM NaCl and 1 mM MgCl$_2$.

Enzyme activity assay, pH and temperature optima and kinetic Parameters

The assay mixture with a total volume of 1 mL usually contained 0.25 mM NADPH or NADH, 100 mM TEA buffer pH 6.5, and 15 mM substrate. Activity was determined by monitoring the decrease or increase of the reduced and oxidized cofactor's absorbance at 340 nm at 30 °C for 1 min. One unit (1 U) was defined as the amount of enzyme that catalyzes the oxidation of 1 mmol NAD(P)H or reduction of NAD(P)$^+$ per minute. Temperature and pH optima were measured using the enzyme activity assay. Kinetic parameters (K_M, V_{max}) were determined by altering the concentration of the substrate and keeping the cofactor concentration at saturated conditions (0.25 mM for NADPH and 1 mM for NADP$^+$). The values for K_M and V_{max} were obtained through fitting the Michaelis–Menten equation to raw data using non-linear-regression, as implemented in the

software Origin (version 7) (Northampton, MA: OriginLab Corporation).

Protein concentration determination

Protein concentrations were determined as described by Bradford[39] using bovine serum albumin (BSA) as the standard.

SDS-PAGE

Sodium dodecylsulfate polyacrylamide gel (SDS-PAGE) electrophoresis was performed as described by Laemmli[40] using 4–12% Nu-PAGE Novex Bis-Tris gels from Invitrogen. Samples were mixed with 4 x lithium dodecylsulfate (LDS) sample buffer from Invitrogen, and were heated to 95 °C for 10 min under reducing conditions. After electrophoresis, the gel was stained for 1 h with Coomassie blue using SimplyBlue[TM] SafeStain from Invitrogen.

MALDI-TOF mass spectroscopy

Excision of protein bands, in-gel digestion with Trypsin Gold from Promega (Mannheim, Germany), elution of the resulting peptide fragments and their analysis using matrix assisted laser desorption/ionisation time of flight (MALDI-TOF) mass spectrometry was performed according to the method published by Fountoulakis and Langen.[41] Tryptic peptide fragments were analysed using a Voyager-DETM STR BiospectrometryTM Workstation from Applied Biosystems (Foster City, USA) with an accelerating voltage of 20 kV, a grid voltage of 63% and a time lag of 125 ns, controlled by Voyager[TM] Control Panel Software 5.0.Data analysis and processing was carried out with Voyager[TM] Data Explorer® Software 3.5. Database search was performed using the automated MS-Fit database (http://prospector.ucsf.edu/).

Biocatalysis

For biotransformation reactions, purified recombinant Gre2p (after hydrophobic interaction chromatography) was utilized, coupled with

glucose dehydrogenase (GDH) from *Bacillus subtilis* for cofactor regeneration. Thus, conversions were performed at 1 mL scale at pH 7.5, 30 ℃, under gentle shaking and were monitored by taking samples over time. Volumetric reaction velocities were expressed as space-time yield and calculated as [g L^{-1} d^{-1}]. The reaction mixture was composed of 100 mM TEA, 1 mM MgCl$_2$, 100 mM glucose, 1 mM cofactor (oxidized), 20 mM substrate, GDH and Gre2p or yeast crude extract. For gas chromatography (GC) analysis, samples of 50 mL were mixed with 100 mL ethyl acetate for substrate/product extraction and centrifuged. In order to determine the stereopurity of (2*S*,5*S*)-hexanediol, a sample of 100 mL was mixed with 200 mL chloroform, centrifuged and esterified with 100 mL triflouroacetic acid anhydride (TFAA). After incubation at 60 ℃ for 15 min, the solvent was removed by evaporation. The residue was dissolved by adding 200 mL chloroform and dried over anhydrous magnesium sulfate for 10 min before centrifuging to obtain the organic layer.

Gas-chromatographic procedures

Analysis was performed on a Shimadzu GC-17A (Duisburg, Germany) with a chiral CP-Chirasil-DEX CB (Chrompack (Middelburg, Netherlands), 25 m x 0.25 mm ID) at a helium flow of 3 mL min^{-1}. The temperature program for substrate and product quantification: 60 ℃ (5 min); 80–195 ℃ with 5 ℃ min^{-1}; 195 ℃ (0 min) gave the following retention time: 2,5- hexanedione: 11.70 min; 5-hydroxy-2-hexanone: 15.65 min; 2,5-hexanediol: 20.35 min. The temperature program for separation of the enantiomers: 55 ℃ (30 min) resulted in the following retention time: (2*S*,5*S*)-hexanediol: 20.19 min and (2*R*,5*R*)-hexanediol: 23.43 min and (2*R*,5*S*)-hexanediol, as well as (2*S*,5*R*-hexanediol): 24.67 min.

Acknowledgements

Notes and references

1 K. Goldberg, K. Schroer, S. Lutz and A. Liese, *Appl. Microbiol. Biotechnol.*, 2007, **76**, 237–248.
2 J. Haberland, W. Hummel, T. Daussmann and A. Liese, *Org. Process Res. Dev.*, 2002, **6**, 458–462.
3 M. J. Burk, J. E. Feaster and R. L. Harlow, *Tetrahedron: Asymmetry*, 1991, **2**, 569–592.
4 H. Takada, P. Metzner and C. Philouze, *Chem. Commun.*, 2001, 2350–2351.
5 J. M. Brunel and B. Faure, *J. Mol. Catal. A: Chem.*, 2004, **212**, 61–64.
6 E. Díez, R. Fernández, E. Marqués-López, E. Martin-Zamora and J. M. Lassaletta, *Org. Lett.*, 2004, **6**, 2749–2752.
7 Q. H. Fan, C. H. Yeung and A. S. C. Chan, *Tetrahedron: Asymmetry*, 1997, **8**, 4041–4045.
8 H. Nagai, T. Morimoto and K. Achiwa, *Synlett*, 1994, 289–290.
9   M. J. Burk, J. E. Feaster and R. L. Harlow, *Organometallics*, 1990, **9**, 2653–2655.
10 B. M. Trost, *Angew. Chem., Int. Ed. Engl.*, 1995, **34**, 259–281.
11 R. Machielsen, N. G. H. Leferink, A. Hendriks, S. J. J. Brouns, H. G. Hennemann, T. Daussmann and J. von der Oost, *Extremophiles*, 2008, **12**, 587–594.
12 M. Katzberg, K. Wechler, M. Müller, P. Dünkelmann, J. Stohrer, W. Hummel and M. Bertau, *Org. Biomol. Chem.*, 2009, **7**, 304–314.
13 M. Bertau and M. Bürli, *Chimia*, 2000, **54**, 503–507.
14 J. K. Lieser, *Synth. Commun.*, 1983, **13**, 765–767.
15 H. Engelking, R. Pfaller, G. Wich and D. Weuster-Botz, *Enzyme Microb. Technol.*, 2006, **38**, 536–544.
16 J. C. Moore, D. J. Pollard, B.Kosjek and P.N. Devine, *Acc. Chem. Res.*, 2007, **40**, 1412–1419.
17 G. M.Walker, *Yeast Physiology and Biotechnology*, JohnWiley & Sons, Chichester, New York, 1998, pp. 203.
18 P. Edman and G. Begg, *Eur. J. Biochem.*, 1967, **1**, 80–91.
19 J. L. Brown and W. K. Roberts, *J. Biol. Chem.*, 1976, **251**, 1009–1014.
20 Y. Kawakami and S. Ohmori, *Anal. Biochem.*, 1994, **220**, 66–72.
21 A. Goffeau, B. G. Barrell, H. Bussey, R. W. Davis, B. Dujon, H. Feldmann, F. Galibert, J. D. Hoheisel, C. Jacq, M. Johnston, E. J. Louis, H.W. Mewes, Y. Murakami, P. Philippsen, H. Tettelin and S. G. Oliver, *Science*, 1996, **274**, 546–567.
22 C. N. Chen, L. Porubleva, G. Shearer, M. Svrakic, L. G. Holden, J. L. Dover, M. Johnston, P. R. Chitnis and D. H. Kohl, *Yeast*, 2003, **20**, 545–554.
23 D. J. C. Pappin, P. Hojrup and A. J. Bleasby, *Curr. Biol.*, 1993, **3**, 327–332.
24 I. A. Kaluzna, T. Matsuda, A. K. Sewell and J. D. Stewart, *J. Am. Chem. Soc.*, 2004, **126**, 12827–12832.
25 M. Katz, B. Hahn-Hagerdal and M. F. Gorwa-Grauslund, *Enzyme Microb. Technol.*, 2003, **33**, 163–172.
26 M. Valli, M. Sauer, P. Branduardi, N. Borth, D. Porro and D. Mattanovich, *Appl. Environ. Microbiol.*, 2005, **71**, 1515–1521.
27 B. Persson, Y. Kallberg, J. E. Bray, E. Bruford, S. L. Dellaporta, A. D. Favia, R. G. Duarte, H. Jörnvall, K. L. Kavanagh, N. Kedishvili, M. Kisiela, E. Maser, R. Mindnich, S. Orchard, T. M. Penning, J. M. Thornton, J. Adamski andU. Oppermann, *Chem.-Biol. Interact.*, 2009, **178**, 94–98.
28 H. J örnvall, B. Persson, M. Krook, S. Atrian, R. Gonzalez-Duarte, J. Jeffery and D. Ghosh, *Biochemistry*, 1995, **34**, 6003–6013.
29 C. Filling, K. D. Berndt, J. Benach, S. Knapp, T. Prozorovski, E. Nordling, R. Ladenstein, H. J¨ornvall and U. Oppermann, *J. Biol. Chem.*, 2002, **277**, 25677–25684.
30 S. Kamitori, A. Iguchi, A. Ohtaki, M. Yamada and K. Kita, *J. Mol. Biol.*, 2005, **352**, 551–558.
31 A. J. J. Straathof, S. Panke and A. Schmid, *Curr. Opin. Biotechnol.*, 2002, **13**, 548–556.
32 T. Ema, H. Yagasaki, N. Okita, K. Nishikawa, K. T. and T. Sakai, *Tetrahedron: Asymmetry*, 2005, **16**, 1075–1078.
33 T. Ema, H. Yagasaki, N. Okita, M. Takeda and T. Sakai, *Tetrahedron*, 2006, **62**, 6143–6149.
34 M. Hauser, P. Horn, H. Tournu, N. C. Hauser, J. D. Hoheisel, A. J. P. Brown and J. R. Dickinson, *FEMS Yeast Res.*, 2007, **7**, 84–92.

35 S. Yilmaz and I. Ozer, *Arch. Biochem. Biophys.*, 1990, **279**, 32–36.

36 T. Ema, Y. Sugiyama, M. Fukumoto, H. Moriya, J. N. Cui, T. Sakai and M. Utaka, *J. Org. Chem.*, 1998, **63**, 4996–5000.

37 S. Harju, H. Fedosyuk and K. R. Peterson, *BMC Biotechnol.*, 2004, **4**, 8.

38 C. T. Chung, S. L. Niemela and R. H. Miller, *Proc. Natl. Acad. Sci. U. S. A.*, 1989, **86**, 2172–2175.

39 M. M. Bradford, *Anal. Biochem.*, 1976, **72**, 248–254.

40 U. K. Laemmli, *Nature*, 1970, **227**, 680–685.

41 M. Fountoulakis and H. Langen, *Anal. Biochem.*, 1997, **250**, 153–156.

3

FUNCTIONAL ENZYME PRODUCTION AND BIOCATALYSIS USING ISOLATED ENZYME

3.1

Functional expression of *GRE2* from *Saccharomyces cerevisiae* and application of Gre2p in the asymmetric synthesis of various hydroxy compounds and diols

Marion Müller and Werner Hummel

Functional expression of *GRE2* from *Saccharomyces cerevisiae* and application of Gre2p in the asymmetric synthesis of various hydroxy compounds and diols

Marion Müller and Werner Hummel

Functional recombinant expression of *GRE2* encoding NADPH-dependent alcohol dehydrogenase Gre2p was achieved in *E. coli* and *S. cerevisiae*. Heterologous production led to the formation of highly soluble and active Gre2p when a low-copy number plasmid with a codon-optimised gene was used. The enzyme thus produced revealed a specific activity of 62.5 U mg^{-1} towards 2,5-hexanedione. This was tenfold higher than the activity found after expression of the non-optimised gene from a high-copy number vector. Homologous *GRE2* expression was carried out under control of the *PMA1* promoter and the Gre2p produced showed a specific activity of 14.1 U mg^{-1}. The production of highly active enzyme made *in vitro* synthesis of the valuable chiral building block (2*S*,5*S*)-hexanediol at high concentrations (0.15 and 0.2 M) possible. Starting from 2,5-hexanedione the diol was obtained with a conversion of >99%, an excellent enantiomeric excess of >99% *ee* and high space-time yields (up to 374 g L^{-1} d^{-1}). It was also demonstrated that biotransformations with an excess of the cofactor recycling glucose dehydrogenase were more efficient. The enzyme was also applied in the reduction of aliphatic 2-ketones and *α*- and *β*-diketones yielding the Prelog-configurated alcohols. Results obtained from *α*-diketone reduction can be explained on the basis of promiscuous substrate binding at the active site of the enzyme.

Introduction

Over the past decades, biocatalysts have been increasingly used in synthetic chemistry. They offer many benefits compared to conventional methods such as their high stereo-, regio-, and chemoselectivity which leads to fewer by-products. They are also readily available and sustainable and can be applied at mild reaction conditions (Nestl et al. 2014; Reetz 2013; Turner and O'Reilly 2013).

Nowadays, approximately 40% of all industrially relevant reactions introducing chirality are catalysed by oxidoreductases (EC 1), (Hall and Bommarius 2011; Hollmann et al. 2011). Alcohol dehydrogenases (ADHs) are by far the most frequently employed oxidoreductases in organic synthesis. They have been used successfully in the synthesis of chiral *β*-hydroxy nitriles (Ankati et al. 2009; Kawano et al. 2014; Nowill et al. 2011), hydroxy esters (Bariotaki et al. 2012; Dai et al. 2013; Liu et al. 2014), hydroxy ketones (Goldberg et al. 2007; Hoyos et al. 2010; Müller et al. 2005), and diols (Chen et al. 2012; Jakoblinnert and Rother 2014; Kalaitzakis and Smonou 2010; Kulig et al. 2012). Many of the alcohols thus produced are key building blocks in the production of fine chemicals, active pharmaceutical ingredients and agrochemicals (Fischer and Pietruszka 2010; Muñoz Solano et al. 2012; Patel 2008; Patel 2011; Patel 2013; Tao and Xu 2009; Turner and O'Reilly 2013).

Compounds revealing more than one functional group or stereogenic centre are of pivotal interest, since they can be easily transformed to other functionalities (Adam et al. 1999; Chen et al. 2012; Hoyos et al. 2010). A notable example is the *γ*-diol (2*S*,5*S*)-hexanediol. It is used in the preparation of chiral ligands (Burk et al. 1991), a variety of chiral auxiliaries (Julienne et al. 1998; Short et al. 1989; Takada et al. 2001) and pharmaceutical intermediates (Díez et al. 2004). Therefore, an efficient synthesis route is needed. Chemically, it is synthesised through stereoselective hydrogenation of 2,5-hexanedione using the (*S*)-Ru-BINAP transition metal catalyst producing good yields (86.4%) of highly optically pure diol (>99 *ee*)

Marion Müller, Prof. Dr. Werner Hummel
Institut für Molekulare Enzymtechnologie
Heinrich-Heine Universität Düsseldorf
im Forschungszentrum Jülich
52426 Jülich, Germany

(Fan et al. 1997). The biocatalyitc synthesis consits of the biotransformation of 2,5-hexanedione mediated through baker's yeast providing the (*S*,*S*)-diol in up to 94% yield with >99% *ee* (Bertau and Bürli 2000; Katzberg et al. 2009). However, a major drawback of this synthesis route is the long reaction time due to low quantities of responsible enzyme present in the cells.

In a previous paper we have reported about the identification of the alcohol dehydrogenase Gre2p as the 2,5-hexanedione reducing enzyme in *Saccharomyces cerevisiae*. Addionally, we have successfully synthesised enantiopure (2*S*,5*S*)-hexanediol *in vitro* on a small-scale (20 mM) using recombinant enzyme (Müller et al. 2010). The space-time yield ($g_{product}$ L^{-1} d^{-1}) thus obtained was 17.5-fold higher compared to conventional baker's yeast biotransformation. Nevertheless, this cell-free biocatalysis is not suitable to synthesise the diol on a preparative-scale, since most of the enzyme is produced as insoluble aggregates. Thus, to achieve considerable amounts of recombinant Gre2p, a more efficient recombinant expression system is required.

In this paper we report about the optimisation of the functional expression of *GRE2* in *E. coli* using a codon-optimised gene in combination with a low-copy-number plasmid. The enzyme thus produced is then applied for *in vitro* synthesis of (2*S*,5*S*)-hexanediol at high concentrations. In addition, the asymmetric reduction of various *α*- and *β*-diketones is examined, along with some 2-ketones. In a parallel study, a homologous gene expression system is developed and investigated as well.

Materials and methods

General

All chemicals used were of highest purity and obtained from Sigma-Aldrich (Buchs, Swizerland). Nicotinamide cofactors were purchased from Biomol (Hamburg, Germany) and restriction enzymes and T4 DNA ligase were obtained from Fermentas (St. Leon-Rot, Germany). Glucose dehydrogenase (GDH) from *Bacillus subtilis* was used for NADPH regeneration and was amplified from pAW-3 (Weckbecker and Hummel 2005), re-cloned into pET-11 and then expressed in *E. coli* BL21(DE3). Chiral gas chromatographic analysis was carried out at the Shimadzu GC-17A (Duisburg, Germany), equipped with a Varian CP-Chirasil-Dex CB column (25 m x 0.25 mm).

Strains, plasmids and media

Escherichia coli DH5α [Δ*lacU169*(Φ80*lacZ*ΔM15) *hsdR17 recA1 end A1 gyrA96 thi-1 relA1*] was used for sub-cloning experiments and was obtained from Invitrogen (Karlsruhe, Germany). *E. coli* BL21(DE3) [F⁻ *ompT hsdS$_B$* (r$_B$⁻ m$_B$⁻) *gal dcm rne131* (DE3)] was purchased from Novagen (Darmstadt, Germany). The *Saccharomyces cerevisiae* strain BY4741 [*Mat a his3Δ1 leu2Δ0 met15Δ0 ura3Δ0*], and the plasmid pDR195-sus1 (Römer et al. 2004) were kindly provided by Prof. Dr. Lothar Elling (Department of Biotechnology/Biomaterials Science, RWTH Aachen, Germany). The low-copy number vector pKA1 was designed in our laboratories. *E. coli* strains were cultured in LB-medium (1% NaCl, 1% tryptone, 0.5% yeast extract) supplemented with chloroamphencicol (CM; 34 μg ml⁻¹). *S. cerevisiae*, BY4741, was cultured in yeast extract peptone dextrose complete medium (YPD; 2% tryptone, 1% yeast extract, 2% glucose) or in yeast minimal synthetic defined drop-out medium (SD) containing 0.67% yeast nitrogen base (YNB; ForMedium™, Norfolk, UK), 2% glucose and 0.077%, Ura-DO Supplement (Clontech, Mountain View, CA).

Construction of the expression plasmids

pKA1-GRE2 and pKA1-optiGRE2 (Fig. 1A): *GRE2* and codon-optimised *GRE2*, designed by Geneart (Regensburg, Germany), were amplified with the restriction sites *Nde*I and *Bam*HI, using standard PCR techniques and the primers up-GGAATTC<u>CATATG</u>TCAGTTTTCGTTTCAGGTG down-CGC<u>GGATCC</u>TTATATTCTGCCCTCAAATTTTAAAAand up-GAGGTCGGT<u>CATATG</u>AGCGTGTTTGTGAGCG and down-CGC<u>GGATCC</u>TTATTAGATACGGCCTTCA-AATTTCAG,respectively.

The plasmid pKA1 was digested with the same restriction enzymes.

pDR195-GRE2 (Fig. 1B): *GRE2* was amplified using the primers up-CCG<u>CTCGAG</u>ATGTCAGTTTTCG-TTTCAGGT and down-CGC<u>GGATCC</u>TTATT-ATATTCTGCCCTCAAATTTTAA flanking the restriction sites *Xho*I and *Bam*HI, and was cloned into pDR195, which was digested with the same enzymes to cut off the foreign gene *sus1*. Sequence identity of all constructs was confirmed by Sequiserve (Vaterstetten, Germany).
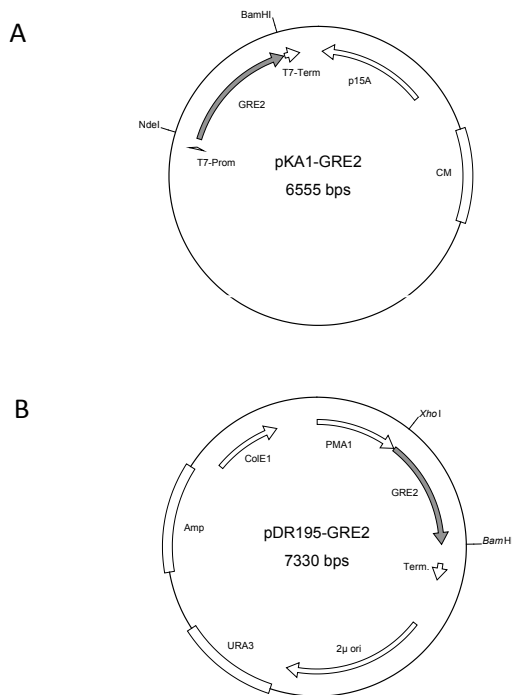
Figure 1: Physical maps of the expression plasmids. (A) pKA1-GRE2 and pKA-optiGRE2. The vector contains a chloroamphenicol (CM) resistance marker and the p15A origin of replication (ori) responsible for the reduction of the copy-number per cell. The gene was cloned downstream from the T7 promoter. (B) pDR195-GRE2. The vector contains a ColE1 ori and an ampicillin resistance marker. The plasmid also contains the *S. cerevisiae* URA3 selection marker and a 2μ ori. The gene was cloned downstream from the proton-ATPase promotor (*PMA1*) for constitutive expression in *S. cerevisiae*.

Codon adaption index (CAI) and relative adaptiveness

The 'codon adaption index' (CAI) represents a mean value that is calculated based on the 'relative adaptiveness' of the codon usage of a gene towards the codon usage of a reference set of genes (Sharp and Li 1987). The relative adaptiveness reflects the frequency of each codon

encoding a specified amino acid. The most frequently used codons are set to 1.0, while less frequently used triplets are scaled down using the rule of proportion.

Heterologous expression experiments and cell harvest

Heterologous gene expression was carried out in *E. coli* BL21(DE3). A colony from a freshly prepared agar plate was used to inoculate LB-medium to prepare the pre-culture. This culture was grown overnight at 37°C and was used to inoculate different amounts of LB-medium containing ampicillin (100 μg ml^{-1}) at a final concentration of 0.05 optical density at 600 nm (OD$_{600}$). The cultures were grown at 37°C. When the OD$_{600}$ reached 0.5 to 0.7 expression was induced by the addition of isopropyl-β-D-thiogalactopyranoside (IPTG) to a final concentration of 0.2 mM. Subsequent cultivation was performed at defined temperatures for different time periods.

The cells were harvested by centrifugation at 2,820g for 30 min or at 27,000g for 1 h and stored at -20°C until further processing. Cells were suspended (33%) in 0.1 M triethanolamine buffer (TEA, pH 7.0) and were disrupted by sonication (3 x 2 min, 37% power) with cooling periods in-between. Cell debris was then removed either at 21,910g for 30 min or at 27,000g for 1 h.

Transformation of *S. cerevisiae* and homologues expression of *GRE2*

Competent cells of *S. cerevisiae* BY4741 were prepared in accordance with Gietz and Woods (Gietz and Woods 2002) using lithium acetate. The cells were subsequently transformed with pDR195-GRE2. To prepare the pre-culture, transformants were cultivated in 20 ml SD glucose medium in a 100 ml flask at 30°C, 120 rpm for 24 h. This culture was then used to inoculate 200 ml SD-medium in a 1 L flask at a final concentration of 0.2 OD$_{600.}$ The culture was incubated at 30°C in an incubator skaker at 120 rpm. After 15 h, 24 h, 40 h and 72 h, 50 ml culture was harvested at 2,820g for 30 min. The cells were suspended (33% (w/v)) in 0.1 M TEA buffer (pH 7.0) containing 1 mM MgCl$_2$ and were homogenized with glass beads (Ø

0.5-0.7 mm) using a mixer mill from Retsch (Haan, Germany; 3 x 5 min passages). Cell-free extract was obtained by centrifugation and was tested for 2,5-hexanedione-reducing activity.

Enzyme assay

The activity assay for the reduction of 2,5-hexanedione was carried out in a total volume of 1 mL using 0.1 M TEA buffer (pH 7.0), containing 20 mM substrate and 0.25 mM NADPH. The mixture was incubated at 30°C and the reaction was started by the addition of 10 µL enzyme solution. Oxidation of D-glucose catalysed by glucose dehydrogenase was carried out in a total volume of 1 mL using 0.1 M TEA buffer (pH 8.0), containing 0.1 M D-glucose and 2 mM $NADP^+$ and was started by the addition of 10 µL enzyme solution. One unit (1 U) was defined as the amount of enzyme that catalyses the oxidation of 1 µmol NADPH or reduction of 1 µmol $NADP^+$, respectively per minute at 340 nm.

Protein analysis

Protein concentrations were determined in accordance with Bradford using BSA as standard (Bradford 1976). SDS-PAGE was performed as described by Laemli (Laemmli 1970) using 4-12% Nu-PAGE Novex Bis-Tris gels from Invitrogen. The SeeBlue® Plus2 Pre-Stained Standard (Invitrogen) was used for molecular weight estimation of proteins.

Cell-free biotransformation reactions and chiral analysis

For cell-free biocatalysis a mixture of substrate (150 or 200 mM 2,5-hexanedione or 50 mM ketone/diketone), D-glucose (375 or 500 mM for 2,5-hexanedione reduction; 125 mM for ketone/diketone reduction), $NADP^+$ (1 mM), Gre2p (cell-free extract, 30-60 U mL^{-1} for 2,5-hexanedione reduction; 1 U mL^{-1} for ketone/diketone reduction) and GDH (cell-free extract; 3:1 or 1:3 ratio of GDH and Gre2p for 2,5-hexanedione reduction, 3:1 ratio of GDH and Gre2p for ketone/diketone reduction) in 15 ml 0.5 M TEA buffer (pH 7.5) was incubated under gentle

shaking at 30°C. To follow product formation, samples of 100 µL were taken periodically and extracted with ethyl acetate. After full conversion the enantiomeric excess *ee* was determined by chiral GC. If necessary the product was derivatised with trifluoroacetic acid anhydride before analysis according to the protocol described previously (Müller et al. 2010). Absolute configuration was identified by comparing the data with commercially available reference compounds. The applied methods used for chiral GC analysis are summarised in Table 1.

Results

Current expression of *GRE2* in *Escherichia coli*

Previously, we have demonstrated that the NADPH-dependent alcohol dehydrogenase Gre2p from *Saccharomyces cerevisiae* reduces the *γ*-diketone 2,5-hexanedione *S*-selectively. Cell-free biotransformation coupled with glucose dehydrogenase (GDH) for cofactor recycling resulted in the synthesis of enantiopure (2*S*,5*S*)-hexanediol (Müller et al. 2010). Unfortunately, the amount of active enzyme produced in *E. coli* BL21(DE3) was not sufficient for commercially viable production of the diol due to the fact that the bulk of the enzyme was produced as inclusion bodies (Figure 2).
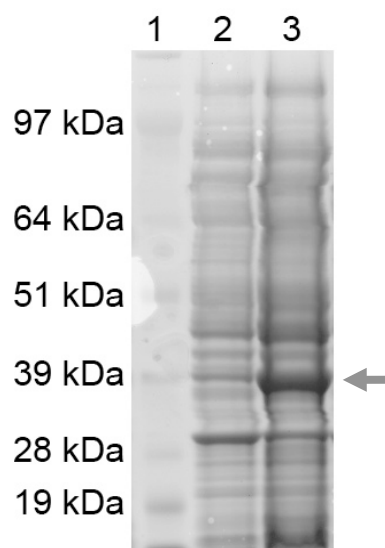
Figure 2: SDS-PAGE analysis of the soluble and insoluble fraction from cultivation of *GRE2* in *E. coli* BL21(DE3) using a pET21 plasmid. Lane 1 protein standard; lane 2 soluble fraction after expression at 37°C for 5 h; lane 3 insoluble fraction after xpression at 37°C for 5 h. 20 µg of total protein was loaded in each lane.

Table 1. Methods for chiral GC analysis.

Products	Temperature programm	Retention time (min)
2,5-hexanediol*	55°C 30 min	20.1 (*S,S*) 23.4 (*R,R*) 24.6 (*S,R* and *R,S*)
2-pentanol (**1a**)	40°C 1.5 min, 5°C/min 66°C, 0.5°C/min 68°C	8.4 (*S*) 8.2 (*R*)
2-hexanol (**2a**)	50°C 5 min, 10°C/min 84°C, 0.5°C/min 86°C	10.6 (*S*) 10.4 (*R*)
2-heptanol (**3a**)*	60°C 5 min, 5°C/min 75°C	7.7 (*S*) 7.9 (*R*)
3-hydroxy-2-butanone (**4a**)	40°C 2 min, 8°C/min 101°C, 0.1°C/min 102°C	7.3 (*S*) 6.9 (*R*)
2,3-butanediol (**4c**)	40°C 2 min, 8°C/min 101°C, 0.1°C/min 102°C	11.7 (*S,S*) 11.9 (*R,R*) 12.6 (*S,R* and *R,S*)
4-hydroxy-2-pentanone (**5a**)	40°C 5 min, 2°C/min 70°C	11.4 (*S*) 11.2 (*R*)
2,4-pentanediol (**5c**)	40°C 5 min, 2°C/min 70°C	17.0 (*S,S*) 16.8 (*R,R*) 16.5 (*S,R* and *R,S*)
2-hydroxy-3-pentanone (**6a**)	60°C 2 min, 5°C/min 195°C	10.3 (*S*) 9.7 (*R*)
2,3-pentanediol (**6c**)	60°C 2 min, 5°C/min 195°C	16.0 (2*S*,3*S*) 16.3 (2*R*,3*R*) 17.0 (2*S*,3*R*) 16.8 (2*R*,3*S*)
2-hydroxy-3-hexanone (**7a**)	60°C 2 min, 5°C/min 195°C	13.1 (*S*) 12.5 (*R*)
2,3-hexanediol (**7c**)	60°C 2 min, 5°C/min 195°C	18.2 (2*S*,3*S*) 18.6 (2*R*,3*R*) 19.2 (2*S*,3*R*) 19.0 (2*R*,3*S*)

*derivatisation was necessary

Because of this, Gre2p generally displayed low specific activities (1.2-6.2 U mg^{-1}) towards 2,5-hexanedione using cell-free extract enzyme samples. Instead of dissolving and refolding the inclusion bodies, which is both difficult and expensive, efforts have been made to find a way of increasing the amount of active Gre2p in *E. coli*. Neither co-expression with chaperone genes (GroEL/ES), which often is an effective method to increase protein solubility due to assisted protein folding (Rosano and Ceccarelli 2014), nor cultivation at low (16°C) or high temperatures (37°C) or varying the incubation times have proven to be successful. Therefore, two alternative approaches were investigated: (i) the use of a low-copy number expression plasmid and (ii) adaption of *GRE2* to the codon usage of *E. coli*.

Expression from a low-copy number plasmid

The plasmid copy-number, controlled by the origin of replication (ori), is an important parameter for optimising recombinant gene expression. An increased average copy-number per cell and thus high recombinant gene dosages may impair cell growth (Betenbaugh et al. 1989; Camps 2010).

This is due to high energy requirements, to maintain the plasmid in cell and to express the foreign DNA, causing stress response machineries in the host strain (Hoffmann and Rinas 2004; Sørensen and Mortensen 2005). Therefore, it was investigated whether and to what extend a reduction of the copy-number per cell influences the formation of active Gre2p in *E. coli*.

For that reason the gene was cloned into the expression plasmid pKA1. In contrast to vectors derived from pBR322 (e.g., the pET-series) reaching 15-60 copies per cell due to the pMB1 ori (closely related to that of ColE1 ori), pKA1 is derived from pACYC184 and has the p15A ori (Chang and Cohen 1978). This is responsible for a more relaxed replication as it results in 10-12 copies per cell (Baneyx 1999; Lee et al. 2006).

The plasmid pKA1-GRE2 (Fig. 1A) was used to transform *E. coli* BL21(DE3) cells. The subsequent gene expression led to significantly higher quantities of Gre2p in the soluble fractions (lanes 6-8 in Fig. 3). Enzyme obtained from cell cultivation at 37°C for 5 h or at 30°C for 16 h displayed the highest specific activities towards the γ-diketone with 42.7 U mg^{-1} and 34.3 U mg^{-1}, respectively. The corresponding protein bands reveal that the enzyme was produced almost in equal amounts in the soluble and insoluble form (lanes 2 and 6 in Fig. 3). Extended incubation times at 37°C consecutivly decreased the activity to 8.4 U mg^{-1} as a consequence of lower quantities of enzyme present in the soluble form (lanes 7 and 8 in comparison with 6). At the same time, an increase of inclusion bodies was observed (lanes 3 and 4).

Codon optimisation to the codon usage of *E. coli*

Because of different codon frequency preferences, heterologous expression of eukaryotic genes in *E. coli* can lead to translational errors and problems during the protein folding formation (Kane 1995). To prevent this, low-usage and rare codons (Chen and Texada 2006) of *GRE2* were optimised and adapted to the codon usage of *E. coli*. This method has been used very often to increase the amounts of recombinant proteins in *E. coli* (Li et al. 2011; Wardenga et al. 2008; Zhang et al. 2010).

As a result, 219 of the original 343 triplets of *GRE2* were changed and the codon adaption index (CAI) was enhanced from 0.61 to 0.98. The re-designed gene shares a homology of 74% to the original template, and all seventeen critical triplets, encoding aginine, leucine or isoleucine, displaying a relative adaptiveness value of approximately 10%, were replaced (Fig. 4).
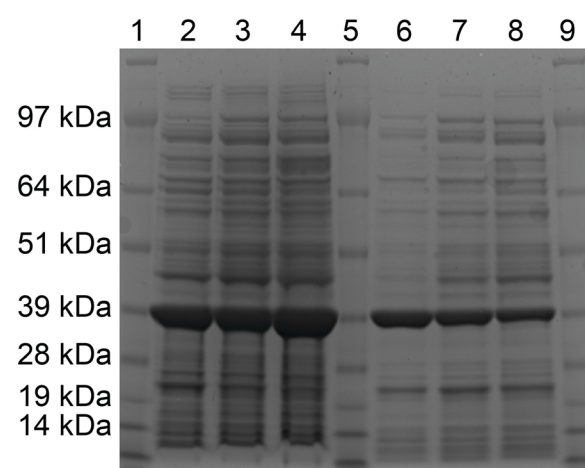
Figure 3: SDS-PAGE analysis of the insoluble and soluble fractions obtained from cultivation from the plasmid pKA1-GRE2. Lane 1, 5 and 9 protein standard; Lane 2-4 insoluble fractions after gene expression at 37°C for 5 h (2), 16 h (3) and 24 h (4); Lane 6-8 soluble fractions from expression at 37°C for 5 h (6), 16 h (7) and 24 h (8).

The optimised gene was cloned into pKA1, resulting in the expression plasmid, pKA1-optiGRE2 (Fig. 1A), which was used to transform *E. coli* BL21(DE3) cells. Cultivation conditions yielding the best results were similar to the production of Gre2p using the low-copy-number plasmid without the codon-optimised gene. The highest specific activity observed was 62.5 U mg^{-1}, which was almost twice as high compared to the pKA1-GRE2 system and ten times higher than the pET-GRE2 system. As shown by SDS-PAGE analysis (Fig. 5) the amounts of soluble Gre2p were significantly increased (lane 5) in comparison to the pET-GRE2 system. Nevertheless, the bulk of enzyme was still produced as inclusion bodies (lane 3).

Homologous expression of *GRE2* in *Saccharomyces cerevisiae*

Homologous expression of *GRE2* in *Saccharomyces cerevisiae* strain BY4741 was carried out under
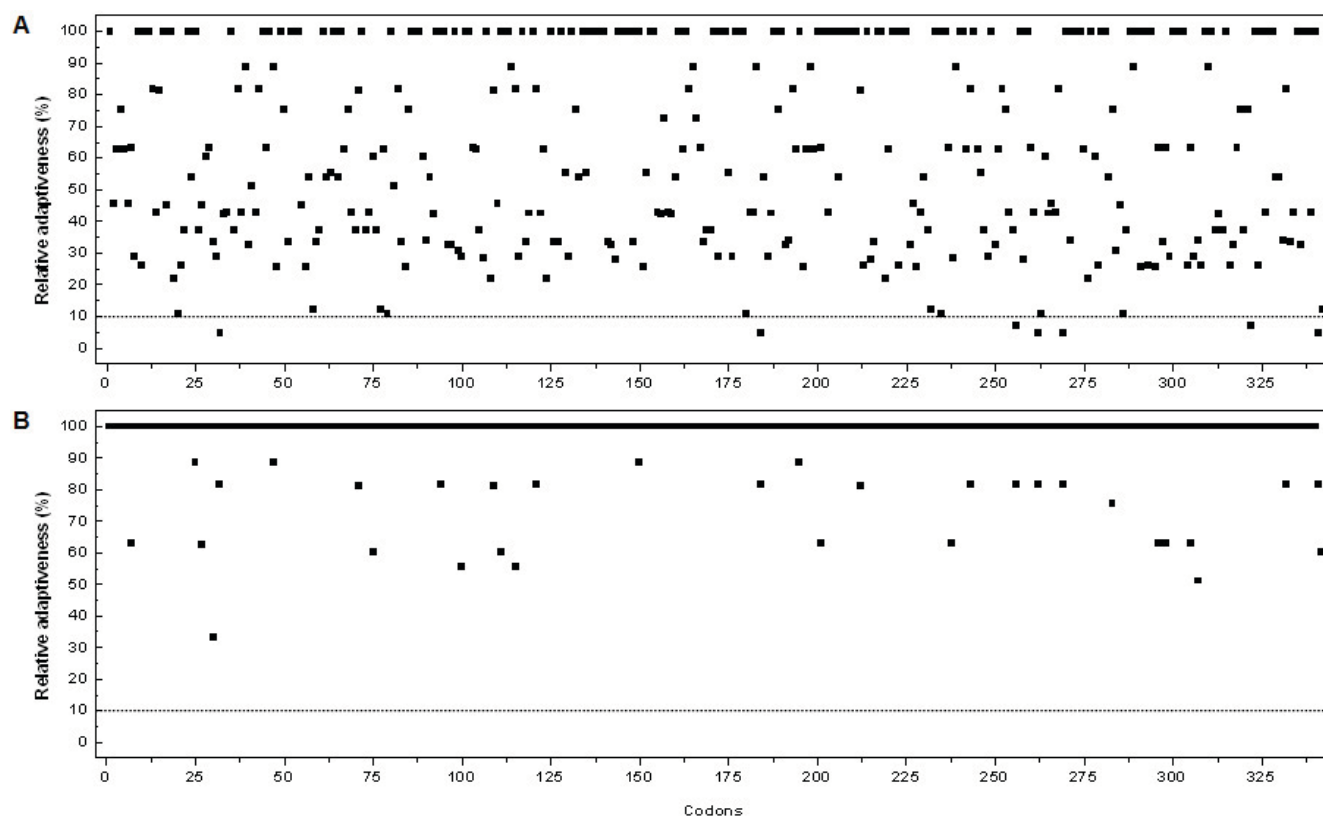
Figure 4: Graphical representation of the relative adaptiveness (%) of the nucleotide sequence of *GRE2* before (A) and after codon optimisation (B). The dashed line represents the threshold of codons which are extremely rare in *E. coli*.

control of the proton-ATPase promotor (*PMA1*) using the plasmid pDR195-GRE2 (Fig. 1B). The gene was constitutively expressed during aerobic cell growth at 30°C. The cell-free extracts of samples taken periodically after 15 and 24 h were analysed for their 2,5-hexanedione-reducing activity. Control experiments were carried with pDR195 which contained no structural gene. As summarised in Table 2, the best activity was obtained when *GRE2* was expressed for 15 h. Nine hours later the enzyme showed less than half of the volumetric activity and the specific activity was reduced by 9%. The SDS-Gel (Fig. 6) shows the proportional decrease in relative band intensity of Gre2p confirming the activity measurements. Further elongation of incubation times resulted in the total loss of activity. The cell-free extract of the strain carrying no structural gene revealed no significant activity at any time and no bands were visible on the SDS-gel (lanes 4 and 5).
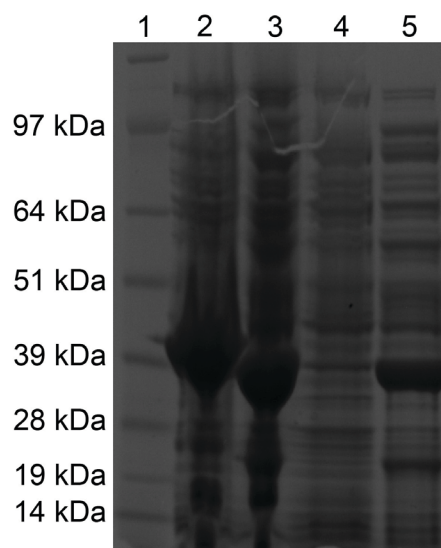
Figure 5: SDS-PAGE analysis of the soluble and insoluble fractions obtained from expression of the the gene from pET-GRE2 and pKA1-optiGRE2. Lane 1 protein standard; Lane 2 insoluble fraction from pET-GRE2 cultivation; Lane 3 insoluble fraction from pKA1-optiGRE2 cultivation; Lane 4 soluble fraction from pET-GRE2 cultivation; Lane 5 soluble fraction from pKA1-optiGRE2.
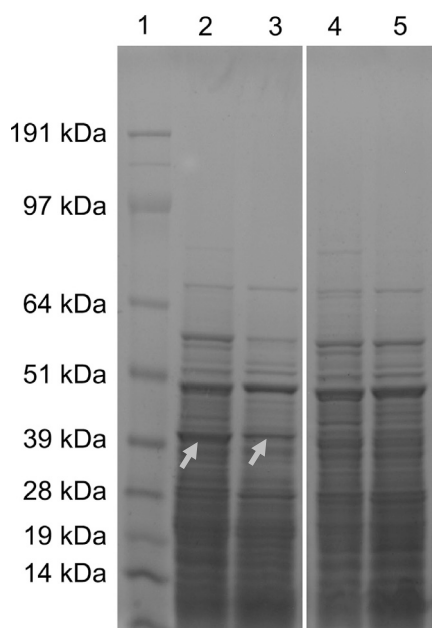
Figure 6: SDS-PAGE analysis of the soluble fractions obtained from homologous Gre2p production in *S. cerevisiae*. 30 μg total protein was loaded in each lane. Lane 1 protein standard; Lane 2 fraction from BY4741-GRE2 15 h; Lane 3 fraction from BY4741-GRE2 24 h; Lane 4 fraction from BY4741 15 h and lane 5 fraction from BY4741 24 h.

Synthesis of (2*S*,5*S*)-hexanediol at high concentrations

Because high amounts of active Gre2p were now available, Gre2p was applied for *in vitro* biotransformations of 0.15 and 0.2 M 2,5-hexanedione. The reaction was coupled to the oxidation of D-glucose catalysed by glucose dehydrogenase (GDH) for *in situ* regeneration of NADPH (Scheme 1). The activity ratio of Gre2p and GDH supplied was either 1:3 or 3:1. The corresponding results are summarised in Table 3. Thus, in each case the *γ*-diketone was reduced to the target diol in high enantiomeric excess at high conversion rates. Biotransformations provided with a ratio of 1:3 of Gre2p and GDH proceeded slightly faster and therefore higher space-time yields (STYs) were achieved.

Reduction of ketones and diketones

Gre2p has been demonstrated to reduce a broad range of substrates, including aldehydes, keto esters, ketones and diketones (Müller et al. 2010). Additionally, the enzyme has been applied in the stereoselective synthesis of a number of hydroxy esters (Ema et al. 2008; Ema et al. 2005; Kaluzna et al. 2004; Padhi et al. 2007). However, reports on the biotransformations of ketones and diketones are rare (Choi et al. 2010; Ema et al. 2005). Therefore, 2-ketones and various *α*- and *β*-diketones (Fig. 7) were used as substrates for Gre2p.
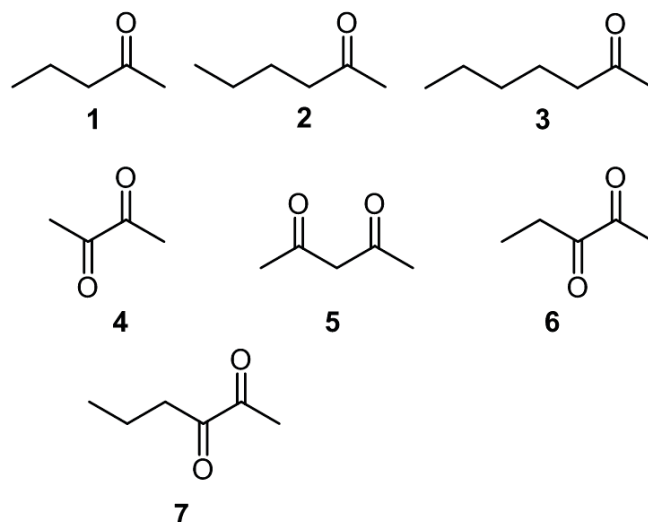
Figure 7: Substrates employed in this study.

As summarised in Table 4, reduction of 2-ketones (Scheme 2) gave the corresponding (*S*)-configured alcohols. The conversion rates increased with the length of the alkyl moiety ($(CH_2)_4CH_3 > (CH_2)_2CH_3$).

Scheme 3 illustrates the biotransformation of various *α*- and *β*-diketones. Accordingly, to produce the corresponding diols, Gre2p must be able to reduce both carbonyl groups.

With respect to *α*-diketones, diol formation (**4**, **6**, **7**) was more likely the longer the alkyl side-chain. Thus, Gre2p synthesised small amounts of 2,3-hexanediol (**7c**), while reduction of 2,3-butanedione stopped at the mono-reduction product (**4a**). In each case, the corresponding *S*-configured hydroxy ketones (**4a**-**7a**) were obtained with an enantioselectivity of ≥94% *ee*. reduction of **6a** and **7a** provided the *anti*-(2*S*,3*R*)-diols in high enantiomeric excess and 47% (**6c**) and 68.5% (**7c**) *de*, respectively.

Biotransformation of the *β*-diketone 2,4-pentanedione (**5**), provided enantiopure (2*S*,4*S*)-pentanediol with a conversion of 68.5%.

Table 2. 2,5-Hexanedione reductase activity in the cell-free extract of BY4741-GRE2 and the control strain BY4741.

Crude extract of strain	Incubation time 15 h		Incubation time 24 h	
	Volumetric activity (U ml^{-1})	Specific activity (U mg^{-1})	Volumetric activity (U ml^{-1})	Specific activity (U mg^{-1})
BY4741-GRE2	82.3	14.1	35.4	12.9
BY4741	0.62	0.063	0.42	0.12
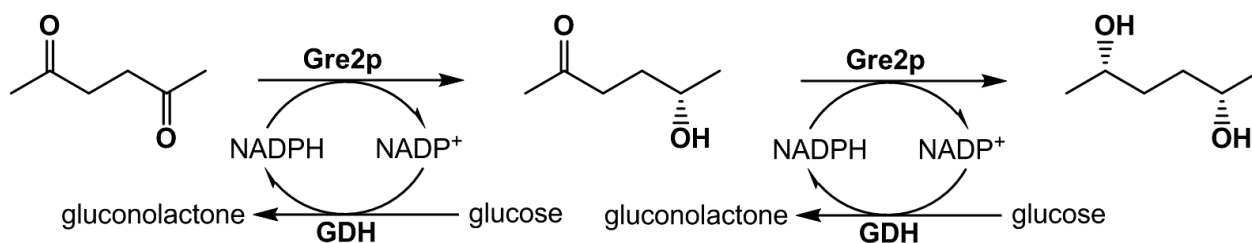
Scheme 1. Two stage-reduction of 2,5-hexanedione via the intermediate (5S)-hydroxy-2-hexanone to (2S,5S)-hexanediol catalysed by Gre2p.

Table 3. Summary of the Gre2-catalysed reduction of 2,5-hexanedione at high concentrations.

2,5-hexanedione (M)	Gre2p:GDH ratio 1:3 (U ml^{-1})	Gre2p:GDH ratio 3:1 (U ml^{-1})	Time (h)	Conversion* (%)	ee# (%)	Space-time yield (g L^{-1} d^{-1})
0.15	20:60	-	1.75	> 99	> 99	240
0.15	-	60:20	2	> 99	> 99	211
0.2	40:120	-	1.5	> 99	> 99	374
0.2	-	80:26.7	2.75	> 99	> 99	204

*measured by GC;
#calculated by chiral GC
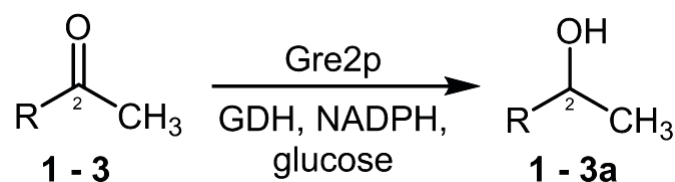
Scheme 2. Reduction of 2-ketones catalysed by Gre2p.

Table 4. Summary of the Gre2p-catalysed reduction of 2-ketones.

Product	Conversion* (%)	Time (h)	ee# (%)
1a	95.7	3	99.1 (*S*)
2a	98.3	3	99.9 (*S*)
3a	99.0	3	99.9 (*S*)

*analysed by chiral GC
#calculated by GC

Discussion

The current lack of an efficient expression system allowing the production of high levels of active Gre2p prevents commercially viable biocatalytic synthesis of (2*S*,5*S*)-hexanediol. Therefore, two optimisation approaches aimed at increasing the amount of active enzyme were carried out.

The first focused on the expression of *GRE2* using a low-copy number plasmid based on pACYC184 instead of pET plasmids. The pKA1-vector was selected since it has been applied successfully in the functional expression of an *adh* gene from *Rhodococcus erythropolis* (RE-ADH) in *E. coli*. RE-ADH activity was increased up to 100-fold compared to the use of a pET expression plasmid (Abokitse 2004). Similarly, activity of Gre2p was enhanced and was seven times higher than with the pET-system. The second approach was the re-design of the gene according to the bias of *E. coli*. This method was chosen because *GRE2* reveals a CAI of 0.61 and contains the extremely rare codons AGA (7x), CUA (6x) and AUA (4x). These occur in all *E. coli* mRNAs at frequencies of 0.21%, 0.29% and 0.39%, respectively (Kane 1995). The presence of such codons in high numbers and clusters in transcripts, can cause translational problems as a consequence of ribosome stalling at positions requiring minor tRNAs (Kurland and Gallant 1996; McNulty et al. 2003). Expression of the codon-optimised gene in combination with the low–copy number plasmid finally led to both the highest amount of soluble protein and highest specific activity in the cell-free extract.

In a comparative study, homologous expression of *GRE2* in *S. cerevisiae* was investigated as well. Using the strain BY4741 and a constitutive expression system, Gre2p activity in cell-free extracts, however, were three and five times lower than obtained by recombinant production using *E. coli* BL21-pKA1-GRE2 and BL21-pKA1-optiGRE2, respectively. Nevertheless, compared to the enzyme activity measured in cell-free extract of wildtype baker's yeast, activity was 120 times higher. Interestingly, the homologous expression system developed here is more efficient than the commercially available expression system developed by Martzen et al (Martzen et al. 1999). Gre2p thus produced was demonstrated to display 0.2 U mg^{-1} (cell-free extract) in the reduction of methylglyoxal (Chen et al. 2003), which is reduced with half the activity of 2,5-hexanedione (Müller et al. 2010). Accordingly, the expected activity for 2,5-hexanedione would be approximately 0.4 U mg^{-1} which would be 35 times lower than the activity revealed with BY4741-GRE2. An explanation for the higher efficiency is probably the more relaxed expression in *S. cerevisiae*, facilitated through the constitutive expression. In contrast, the commercial strain uses Cu^{2+} to immediately induce gene expression which is less relaxing for the cells.

The recombinant expression systems developed here were also more efficient than the one published by Katzberg et al., who achieved a 2,5-hexanedione activity of only 0.14 U mg^{-1} for Gre2p (Katzberg et al. 2010). The reason for this less efficient production could be the use of the non-codon optimised gene in combination with a plasmid containing the same origin of replication like the pET series.

With the good recombinant Gre2p production in hand, it was now feasible to develop a synthesis of (2*S*,5*S*)-hexanediol on a large-scale. Compared to our previously reported *in vitro* diol synthesis, diketone concentration was enhanced from
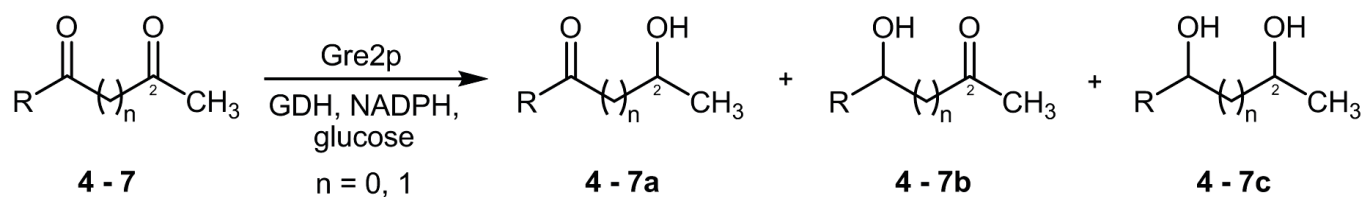
Scheme 3. Reduction of various α- and β-diketones catalysed by Gre2p.

Table 5. Summary of the Gre2p-catalysed reduction of α- and β-diketones.

Substrate	Conversion* a (%)	ee# a (%)	Conversion* b (%)	ee# b (%)	Conversion* c (%)	de# c (%)	ee# c (%)
4	70.2	98.4 (S)	-	-	-	-	-
5	68.5	99.9 (S)	-	-	31.5	> 99	99.0 (2S,4S)
6	95.7	94.3	0.4	n.d.	2.1	47 (2S,3R)	> 99
7	82.2	98.5	1.0	n.d.	13.6	59.1 (2S,3R)	> 99

*measured by GC
#calculated by chiral GC

0.02 M (Müller et al. 2010) to 0.2 M (this study) resulting in a five times higher space-time yield. In comparison to the biotransformation process using baker's yeast, STYs were increased more than 90-fold (Katzberg et al. 2009). Furthermore, biotransformations were more efficient regarding conversion times and STYs when an excess of the cofactor recycling enzyme was supplied.

Reduction of 2-ketones resulted in the corresponding Prelog alcohols (Prelog 1964). Likewise, β-diketone reduction, and the reduction of the α-diketones 2,3-pentanedione and 2,3-hexanedione, to the corresponding hydroxy ketones yielded the (2S,4S)- and (2S)-configurated alcohols, respectively. However, 2,3-pentanedione was reduced to anti-(2S,3R)-pentanediol as the minor product which can be explained by the

promiscuous binding mode of the intermediate in the active site of Gre2p. Thus, one orientation is the same as for 2,3-pentanedione while the second one is the opposite. Because hydride attack often takes place through the same side in ADHs (Schlieben et al. 2005), hydroxy ketone in the first orientation would lead to the Prelog products (anti). However, when the orientation of the mono-reduction product is inverted the corresponding syn-diols (anti-Prelog product) would be achieved.

With respect to the reduction of 2,3-hexanedione the major product was the anti-diol, indicating that Gre2p favoured the same disposition of (2S)-hydroxy-3-hexanone with regard to diketone. Results obtained from the β-diketone reductions also reveal that formation of the Prelog products depends on the substrate structure. Thus, the

larger the distance between the alkanoyl group and the hydroxyethyl moiety the more likely it was that the *anti*-products were formed. A similar binding pattern was also observed for the ADHs from *Rhodococcus ruber* and *Thermoanaerobacter* sp. (Kurina-Sanz et al. 2009).

In summary, optimisation of gene expression led to enhanced production of active Gre2p in *E. coli* and *S. cerevisiae* enabling *in vitro* synthesis of (2*S*,5*S*)-hexanediol at high concentrations. In addition, it was shown that the enzyme can be used in the synthesis of further optically pure hydroxy ketones and diols.

References

Abokitse K (2004) Biochemische und Molekularbiologische Charakterisierung von Alkoholdehydrogenasen und einer Oxygenase aus *Rhodococcus* Spezies PhD thesis, Heinrich-Heine University Düsseldorf

Adam W, Lazarus M, Saha-Möller CR, Schreier P (1999) Biocatalytic synthesis of optically active *α*-oxyfunctionalized carbonyl compounds. Accounts Chem Res 32:837-845

Ankati H, Zhu DN, Yang Y, Biehl ER, Hua L (2009) Asymmetric synthesis of both antipodes of *β*-hydroxy nitriles and *β*-hydroxy carboxylic acids via enzymatic reduction or sequential reduction/hydrolysis. J Org Chem 74:1658-1662

Baneyx F, (1999) Recombinant protein expression in *Escherichia coli*. Curr Opin Biotechnol 10:411-421

Bariotaki A, Kalaitzakis D, Smonou I (2012) Enzymatic reductions for the regio- and stereoselective synthesis of hydroxy-keto esters and dihydroxy esters. Org Lett 14:1792-1795

Bertau M, Bürli M (2000) Enantioselective microbial reduction with baker's yeast on an industrial scale. Chimia 54:503-507

Betenbaugh MJ, Beaty C, Dhurjati P (1989) Effects of plasmid amplification and recombinant gene expression on the growth kinetics of recombinant *E. coli*. Biotechnol Bioeng 33:1425-1436

Bradford MM (1976) Rapid and sensitive method for quantitation of microgram quantities of protein utilizing principle of protein-dye binding. Anal Biochem 72:248-254

Burk MJ, Feaster JE, Harlow RL (1991) New chiral phospholanes; synthesis, characterization, and use in asymmetric hydrogenation reactions. Tetrahedron: Asymmetry 2:569-592

Camps M (2010) Modulation of ColE1-like plasmid replication for recombinant gene expression. Recent Pat DNA Gene Seq 4:58–73

Chang ACY, Cohen SN (1978) Construction and characterization of amplifiable multicopy DNA cloning vehicles derived from P15A cryptic miniplasmid. J Bacteriol 134:1141-1156

Chen CN, Porubleva L, Shearer G, Svrakic M, Holden LG, Dover JL, Johnston M, Chitnis PR, Kohl DH (2003) Associating protein activities with their genes: Rapid identification of a gene encoding a methylglyoxal reductase in the yeast *Saccharomyces cerevisiae*. Yeast 20:545-554

Chen D, Texada DE (2006) Low-usage codons and rare codons of *Escherichia coli*. Gene Ther Mol Biol 10:1-12

Chen Y, Chen C, Wu X (2012) Dicarbonyl reduction by single enzyme for the preparation of chiral diols. Chem Soc Rev 41:1742–1753

Choi YH, Choi HJ, Kim D, Uhm KN, Kim HK (2010) Asymmetric synthesis of (*S*)-3-chloro-1-phenyl-1-propanol using *Saccharomyces cerevisiae* reductase with high enantioselectivity. Appl Microbiol Biotechnol 87:185-193

Dai Z, Guillemette K, Green TK (2013) Stereoselective synthesis of aryl *γ*,*δ*-unsaturated *β*-hydroxyesters by ketoreductases. J Mol Catal B: Enzym 97:264-269

Díez E, Fernández R, Marqués-López E, Martín-Zamora E, Lassaletta JM (2004) Asymmetric synthesis of *trans*-3-amino-4-alkylazetidin-2-ones from chiral *N*,*N*-dialkylhydrazones. Org Lett 6:2749-2752

Ema T, Ide S, Okita N, Sakai T (2008) Highly efficient chemoenzymatic synthesis of methyl (*R*)-*o*-chloromandelate, a key intermediate for clopidogrel, via asymmetric reduction with recombinant *Escherichia coli*. Adv Synth Catal 350:2039-2044

Ema T, Yagasaki H, Okita N, Nishikawa K, Korenaga T, Sakai T (2005) Asymmetric reduction of a variety of ketones with a recombinant carbonyl reductase: Identification of the gene encoding a versatile biocatalyst. Tetrahedron: Asymmetry 16:1075-1078

Fan QH, Yeung CH, Chan ASC (1997) An improved synthesis of chiral diols via the asymmetric catalytic hydrogenation of prochiral diones. Tetrahedron: Asymmetry 8:4041-4045

Fischer T, Pietruszka J (2010) Key building blocks via enzyme-mediated synthesis. In: Piel J (ed) Natural products via enzymatic reactions. Topics in current chemistry. Springer-Verlag, Berlin, Heidelberg, pp 1-43

Gietz RD, Woods RA (2002) Transformation of yeast by lithium acetate/single-stranded carrier DNA/polyethylene glycol method. In: Guthrie C and Fink GR (ed) Guide to yeast genetics and molecular and cell biology: Part B. Methods in enzymology. Academic Press, San Diego, London, pp 87-96

Goldberg K, Schroer K, Lütz S, Liese A (2007) Biocatalytic ketone reduction: A powerful tool for the production of chiral alcohols: Part I: Processes with isolated enzymes. Appl Microbiol Biotechnol 76:237-248

Hall M, Bommarius AS (2011) Enantioenriched compounds via enzyme-catalyzed redox reactions. Chem Rev 111:4088-4110

Hoffmann F, Rinas U (2004) Stress induced by recombinant protein production in *Escherichia coli*. In: Enfors SO (ed) Physiological stress responses in bioprocesses Advances in biochemical engineering/biotechnology. Springer-Verlag, Berlin, Heidelberg, pp 73-92

Hollmann F, Arends IWCE, Holtmann D (2011) Enzymatic reductions for the chemist. Green Chem 13:2285-2314

Hoyos P, Sinisterra JV, Molinari F, Alcántara AR, De María PD (2010) Biocatalytic strategies for the asymmetric synthesis of *α*-hydroxy ketones. Acc Chem Res 43:288-299

Jakoblinnert A, Rother (2014) A two-step biocatalytic cascade in micro-aqueous medium: Using whole cells to obtain high concentrations of a vicinal diol. Green Chem 16:3472-3482

Julienne K, Metzner P, Henryon V, Greiner A (1998) A simple *C*2 symmetrical sulfide for a one-pot asymmetric conversion of aldehydes into oxiranes. J Org Chem 63:4532-4534

Kalaitzakis D, Smonou I (2010) Highly diastereoselective synthesis of 2-substituted-1,3-diols catalyzed by ketoreductases. Tetrahedron 66:9431-9439

Kaluzna IA, Matsuda T, Sewell AK, Stewart JD (2004) Systematic investigation of *Saccharomyces cerevisiae* enzymes catalyzing carbonyl reductions. J Am Chem Soc 126:12827-12832

Kane JF (1995) Effects of rare codon clusters on high-level expression of heterologous proteins in *Escherichia coli*. Curr Opin Biotechnol 6:494-500

Katzberg M, Parachin NS, Gorwa-Grauslund MF, Bertau M (2010) Engineering cofactor preference of ketone reducing biocatalysts: A mutagenesis study on a *γ*-diketone reductase from the yeast *Saccharomyces cerevisiae* serving as an example. International Journal of Molecular Sciences 11:1735-1758

Katzberg M, Wechler K, Müller M, Dünkelmann P, Stohrer J, Hummel W, Bertau M (2009) Biocatalytical production of (5*S*)-hydroxy-2-hexanone. Org Biomol Chem 7:304-314

Kawano S, Hasegawa J, Yasohara Y (2014) Efficient synthesis of (*R*)-3-hydroxypentanenitrile in high enantiomeric excess by enzymatic reduction of 3-oxopentanenitrile. Appl Microbiol Biotechnol 98:5891–5900

Kulig J, Simon RC, Rose CA, Husain SM, Häckh M, Lüdeke S, Zeitler K, Kroutil W, Pohl M, Rother D (2012) Stereoselective synthesis of bulky 1,2-diols with alcohol dehydrogenases. Cat Sci Tec 2:1580-1589

Kurina-Sanz M, Bisogno FR, Lavandera I, Orden AA, Gotor V (2009) Promiscuous substrate binding explains the enzymatic stereo- and regiocontrolled synthesis of enantiopure hydroxy ketones and diols. Adv Synth Catal 351:1842-1848

Kurland C, Gallant J (1996) Errors of heterologous protein expression. Curr Opin Biotechnol 7:489-493

Laemmli UK (1970) Cleavage of structural proteins during assembly of head of bacteriophage T4. Nature 227:680-685

Lee CL, Ow DSW, Oh SKW (2006) Quantitative real-time polymerase chain reaction for determination of plasmid copy number in bacteria. J Microbiol Methods 65:258-267

Li W, Ng IS, Fang B, Yu J, Zhang G (2011) Codon optimization of 1,3-propanediol oxidoreductase expression in *Escherichia coli* and enzymatic properties. Electron J Biotechnol 14:1-9

Liu X, Chen R, Yang Z, Wang J, Lin J, Wei D (2014) Characterization of a putative stereoselective oxidoreductase from *Gluconobacter oxydans* and Its application in producing ethyl (*R*)-4-chloro-3-hydroxybutanoate ester. Mol Biotechnol 56:285–295

Martzen MR, McCraith SM, Spinelli SL, Torres FM, Fields S, Grayhack EJ, Phizicky EM (1999) A biochemical genomics approach for identifying genes by the activity of their products. Science 286:1153-1155

McNulty DE, Claffee BA, Huddleston MJ, Kane JF (2003) Mistranslational errors associated with the rare arginine codon CGG in *Escherichia coli*. Protein Expr Purif 27:365-374

Müller M, Katzberg M, Bertau M, Hummel W (2010) Highly efficient and stereoselective biosynthesis of (2*S*,5*S*)-hexanediol with a dehydrogenase from *Saccharomyces cerevisiae*. Org Biomol Chem 8:1540-1550

Müller M, Wolberg M, Schubert T, Hummel W, Kragl U (2005) Enzyme-catalyzed regio- and enantioselective ketone reductions. Adv Biochem Engin / Biotechnol 92:261-287

Muñoz Solano D, Hoyos P, Hernáiz MJ, Alcántara AR, Sánchez-Montero JM (2012) Industrial biotransformations in the synthesis of building blocks leading to enantiopure drugs. Bioresour Technol 115:196-207

Nestl BM, Hammer SC, Nebel BA, Hauer B (2014) New generation of biocatalysts for organic synthesis. Angew Chem-Int Edit 53:3070-3095

Nowill RW, Patel TJ, Beasley DL, Alvarez JA, Jackson III E, Hizer TJ, Ghiviriga I, Mateer SC, Feske BD (2011) Biocatalytic strategy toward asymmetric *β*-hydroxy nitriles and *γ*-amino alcohols. Tetrahedron Lett 52:2440-2442

Padhi SK, Kaluzna IA, Buisson D, Azerad R, Stewart JD (2007) Reductions of cyclic *β*-keto esters by individual *Saccharomyces cerevisiae* dehydrogenases and a chemo-enzymatic route to (1*R*,2*S*)-2-methyl-1-cyclohexanol. Tetrahedron: Asymmetry 18:2133-2138

Patel RN (2008) Chemoenzymatic-synthesis of chiral pharmaceutical intermediates. Expert Opin Drug Discov 3:187-245

Patel RN (2011) Biocatalysis: Synthesis of key intermediates for development of pharmaceuticals. ACS Catal 1:1056-1074

Patel RN (2013) Biocatalytic synthesis of chiral alcohols and amino acids for development of pharmaceuticals. Biomolecules 3:741-777

Prelog V (1964) Specification of the stereospecificity of some oxido-reductases by diamond lattice sections. Pure Appl Chem 9:119-130

Reetz MT (2013) Biocatalysis in organic chemistry and biotechnology: Past, present, and future. J Am Chem Soc 135:12480-12496

Römer U, Schrader H, Günther N, Nettelstroth N, Frommer WB, Elling L (2004) Expression, purification and characterization of recombinant sucrose synthase 1 from *Solanum tuberosum* L. for carbohydrate engineering. J Biotechnol 107:135-149

Rosano GL, Ceccarelli EA (2014) Recombinant protein expression in *Escherichia coli*: Advances and challenges. Front Microbiol 5:1-17

Schlieben NH, Niefind K, Müller J, Riebel B, Hummel W, Schomburg D (2005) Atomic resolution structures of *R*-specific alcohol dehydrogenase from *Lactobacillus brevis* provide the structural bases of its substrate and cosubstrate specificity. J Mol Biol 349:801-813

Sharp PM, Li WH (1987) The codon adaptation index: A measure of directional synonymous codon usage bias, and its potential applications. Nucleic Acids Res 15:1281-1295

Short RP, Kennedy RM, Masamune S (1989) An improved synthesis of (-)-(2*R*,5*R*)-2,5-dimethylpyrrolidine. J Org Chem 54:1755-1756

Sørensen HP, Mortensen KK (2005) Advanced genetic strategies for recombinant protein expression in *Escherichia coli*. J Biotechnol 115:113-128

Takada H, Metzner P, Philouze C (2001) First chiral selenium ylides used for asymmetric conversion of aldehydes into epoxides. Chem Commun 2350-2351

Tao J, Xu JH (2009) Biocatalysis in development of green pharmaceutical processes. Curr Opin Chem Biol 13:43-50

Turner NJ, O'Reilly E (2013) Biocatalytic retrosynthesis. Nat Chem Biol 9:285-288

Wardenga R, Hollmann F, Thum O, Bornscheuer UT (2008) Functional expression of porcine aminoacylase 1 in *E. coli* using a codon optimized synthetic gene and molecular chaperones. Appl Microbiol Biotechnol 81:721-729

Weckbecker A, Hummel W (2005) Glucose dehydrogenase for the regeneration of NADPH and NADH. In: Barredo JL (ed) Microbial Enzymes and Biotransformations. Meth. in Biotechnology, vol 17. Humana Press Inc., Totowa, N. J., pp 225-237

Zhang R, Xu Y, Geng Y, Wang S, Sun Y, Xiao R (2010) Improved production of (*R*)-1-phenyl-1,2-ethanediol by a codon-optimized *R*-specific carbonyl reductase from *Candida parapsilosis* in *Escherichia coli* Appl Biochem Biotechnol 160:868-878

4

WHOLE-CELL BIOCATALYSIS

4.1

Biocatalytical production of (5*S*)-hydroxy-2-hexanone

Michael Katzberg, Kerstin Wechler, Marion Müller, Pascal Dünkelmann, Jürgen Stohrer, Werner Hummel and Martin Bertau

Biocatalytical production of (5*S*)-hydroxy-2-hexanone

Michael Katzberg[a], Kerstin Wechler[a], Marion Müller[b], Pascal Dünkelmann[c], Jürgen Stohrer[d], Werner Hummel[b] and Martin Bertau[a]*

Biocatalytical approaches have been investigated in order to improve accessibility of the bifunctional chiral building block (5*S*)-hydroxy-2-hexanone (**(*S*)-2**). As a result, a new synthetic route starting from 2,5-hexanedione (**1**) was developed for **(*S*)-2**, which is produced with high enantioselectivity (*ee* >99%). Since **(*S*)-2** can be reduced further to furnish (2*S*,5*S*)-hexanediol (**(2*S*,5*S*)-3**), chemoselectivity is a major issue. Among the tested biocatalysts the whole-cell system *S. cerevisiae* L13 surpasses the bacterial dehydrogenase ADH-T in terms of chemoselectivity. The use of whole-cells of *S. cerevisiae* L13 affords **(*S*)-2** from prochiral **1** with 85% yield, which is 21% more than the value obtained with

ADH-T. This is due to the different reaction rates of monoreduction (**1**→**2**) and consecutive reduction (**2**→**3**) of the respective biocatalysts. In order to optimise the performance of the whole-cell-bioreduction **1**→**2** with *S. cerevisiae*, the system was studied in detail, revealing interactions between cell-physiology and xenobiotic substrate and by-products, respectively. This study compares the whole-cell biocatalytic route with the enzymatic route to enantiopure **(*S*)-2** and investigates factors determining performance and outcome of the bioreductions.

Introduction

(5*S*)-Hydroxy-2-hexanone (**(*S*)-2**) is a valuable bifunctional chiral building block for e. g. pharmaceuticals or aroma compounds. However its poor availability counts against its broad synthetic use. It is for this reason that a new synthetic route was required that allows access to this hydroxy ketone in high selectivity and enantiopurity. Due to their unsurpassed enantio- and chemoselectivity, biocatalytic approaches lend themselves to this purpose.[1] If prochiral diketones are subjected to reduction, two classes of products are accessible. Monoreduction will yield the corresponding bifunctional hydroxyketones, whereas bis-reduction furnishes the corresponding diols. In the case of the γ-diketone 2,5-hexanedione (**1**) reduction affords 5-hydroxy-2-hexanone (**2**) and 2,5-hexanediol (3) (Scheme 1). As enantiopure chiral compounds, both products serve as chiral intermediates. While both enantiomers of **3** are key building blocks of chiral catalysts,[2,3] enantiopure **2** is essential for the synthesis of biodegradable polymers, pharmaceuticals or aroma compounds.[4] Though there is a substantial demand for enantiomers of **2**, previous attempts (both biocatalytic and non-biocatalytic) focused on

the production of enantiopure (**2*R*,5*R*)**- and (**2*S*,5*S*)-3**,[2,4–12] thus underlining the challenge of producing enantiopure **2**. Nevertheless, efforts had been made to selectively obtain **2** enantiomerically pure. In the case of (***R*)-2**, a recently developed route employing whole-cells of *Lactobacillus kefiri* allowed for producing (***R*)-2** with >99% *ee* and 95% selectivity.[13] However enantiomer **(*S*)-2** is not accessible via this route Moreover in order to produce enantiopure **(*S*)-2**, one has to resort to procedures with unsatisfactory cost-efficiency or lower applicability on a larger scale. Non-biocatalytic variants for

[a]   *Michael Katzberg, Kerstin Wechler, Prof. Dr. Martin Bertau*
     Institute of Technical Chemistry
     Freiberg University of Mining and Technology
     09596 Freiberg, Germany

[b]   *Marion Müller, Prof. Dr. Werner Hummel*
     Institute of Molecular Enzyme Technology
     Research Center Juelich
     52426 Juelich, Germany
     Tel: (+49)24641 613790
     E-mail: w.hummel@fz-juelich.de

[c]   *Pascale Dünkelmann*
     Juelich Chiral Solutions GmbH, a Codexis Company
     Juelich, Germany

[d]   *Jürgen Stohrer*
     Wacker AG
     Muenchen, Germany
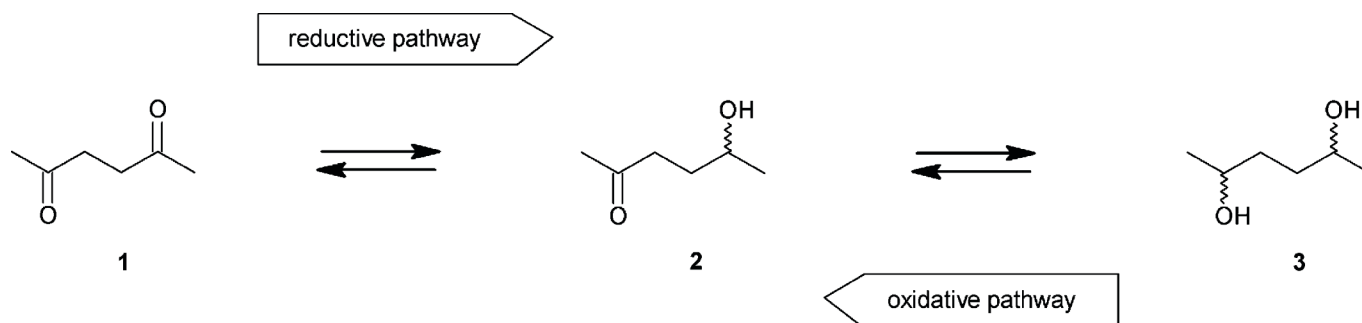
Scheme 1. The prochiral 2,5-hexanedione (**1**) and chiral hexanediol (**3**) are precursors for 5-hydroxy-2-hexanone (**2**); thus **2** can be obtained through either a reductive or an oxidative pathway. Both options are discussed in the text.

production of enantiopure **(S)-2**, such as asymmetric catalytic hydrogenation of **1** with Ru-BINAP[4] and oxidation of **(2S,5S)-3**, have only been successfully applied for production of the respective (R)-enantiomers[4,14] and suffer from harsh reaction conditions or inefficient use of highly valuable reactants.

Among the existing biocatalytical approaches to enantiopure hydroxyketones, lipase-catalysed dynamic kinetic resolution of **rac-2** showed poor enantioselectivity (E-value = 9 for **(R)-2**)[15] and thus is not able to resolve the racemic mixture of **rac-2** satisfactorily.

An alternative dehydrogenase-catalysed route with whole-cells of *Rhodococcus ruber* gave only moderate yields (65% conversion, 38% **(S)-2**, ee>99%)[16]. Another approach consists in the oxidation of **meso-3**, which furnished **(R)-2** in up to 88% yield with >99% ee.[17,16] Via a (R)-selective reductase, e. g. ADH-LK or ADH-LB from *Lactobacillus* sp.,[18] this approach is the only one reported thus far which is applicable for the synthesis of **(S)-2** as well. However, the major drawback of this procedure is that the availability of enantiopure **meso-3** is not given, and it is neither commercially available nor efficiently producible. Furnishing **meso-3** from **rac-3** means laborious multi-step syntheses and low product yields not exceeding 21%[19,20]. Consequently, this strategy must be considered not effective, since it involves considerable expense and suffers from poor substrate availability.

Nevertheless, in view of the rather harsh reaction conditions of the transition metal catalysed variants, and in light of the positive results emerging from the oxidative route that showed **(S)-2** and **meso-3** to be interconvertible by means of dehydrogenase catalysis, we were encouraged to study alternative dehydrogenase-catalysed

approaches to efficiently and cost-effectively produce enantiopure **(S)-2** from **1**, in order to overcome the synthetic bottleneck in the chemistry of **(S)-2**.

Results and discussion

Synthesis of (5S)-hydroxy-2-hexanone (**(S)-2**) through reduction of prochiral 2,5-hexanedione (**1**) is the most efficient approach, not only in terms of atom economy[21] but also in terms of cost and availability of the starting material. Potentially suitable biocatalysts for this process are preferentially those which have been employed for production of (2S,5S)-hexanediol (**(2S,5S)-3**), since the reduction of the two carbonyl groups of **1** proceeds in a consecutive manner, in which an intermediate (in this case **(S)-2**) accumulates transiently. Hence, if the biocatalytic reduction of **1** basically obeys the kinetics of a consecutive reaction, a detailed investigation of the process will allow for identifying conditions permitting the isolation of intermediate product **(S)-2**. In this study two biocatalysts were found potentially suitable for the production of **(S)-2**: on the one hand the cost-effective and easy-to-use whole-cell-biocatalyst *Saccharomyces cerevisiae* known to selectively reduce **1** to **(2S,5S)-3**,[5,6] and on the other an isolated dehydrogenase from *Thermoanaerobacter* sp., which has been employed recently to develop an efficient procedure yielding enantiopure **(2S,5S)-3** through reduction of **1**.[22]

The whole-cell-biocatalyst *Saccharomyces cerevisiae*

Versatility of this whole-cell-biocatalyst has long been recognised,[23–25] but there are no reports in the literature investigating the applicability of this

biocatalyst for the production of enantiopure **(S)-2**.

One reason for disregarding *S. cerevisiae* as a biocatalyst maybe the diversity of yeast strains in use, differing in activity and selectivity, which in turn complicates the portability of developed protocols. Furthermore, at least 49 open-reading-frames coding for dehydrogenases in the *S. cerevisiae* genome[26] are known, which often have counteracting stereoselectivity and thus are the reason for unsatisfactory enantiopurities encountered in a majority of whole-cell biotransformations with *S. cerevisiae*.[26–28] However, the latter fact cannot be generalised, since the stereoselectivity of a given bioreduction not only depends on the kind of the reactant but also on the composition of the reductase-pool in the cell, which in turn is adjusted to the current environmental conditions *via* stress-response pathways in order to maintain cellular homeostasis. In this context, cell-stress is commonly referred to environmental conditions that threaten the survival of a cell, or at least prevent it from performing optimally.[29]

But stress responses of whole-cells can also be used to control stereoselectivity of reductions of xenobiotics by adding a physiologically active substance.[30] Thus expression of reductases may be altered without the need for genetic modification. Hence the use of whole-cells of *S. cerevisiae* should not be ruled out *a priori*. In particular, its use offers important advantages like intracellular cofactor regeneration and a very good availability,[31] allowing for easy up-scaling of a procedure. In the end, every reactant has to be evaluated with regard to whether *S. cerevisiae* is a suitable biocatalyst for an intended biotransformation, and whether the mentioned disadvantages outweigh the advantages of this versatile biocatalyst. Consequently, the applicability of the whole-cell-biocatalyst *S. cerevisiae* for production of **(S)-2** needs to be investigated. In order to study a strain with preferably high activity towards **1**, we compared the commonly used laboratory-yeast strains CEN.PK 113–7D (haploid)[32] with the industrial model-strain CBS8066 (diploid)[33] and the industrially produced strain L13 (polyploid: tetraploid and an euploid).[34] The diversity in activity towards reduction of **1**

among the studied yeast strains is shown in Table 1. The results clearly show that all strains accept **1** as a xenobiotic substrate but that it is advisable to use the industrial strain L13 due to its superior activity. Thus, the intracellular level of 2,5-hexanedione-reductase(s) (in the following abbreviated as HDOR) and hence the activity of the respective whole-cellbiocatalyst varies from strain to strain.

This observation may have its reason in the different ploidy of the strains, which has been found to correlate with protein content of the cells under optimal conditions[35,36] and would thus potentially affect enzyme activity. Furthermore the strains are not isogenic, so expression level or even the structure of the respective HDOR are potentially different,[37] which can result in a different activity of the whole-cell-biocatalyst towards **1**. However extensive elucidation of the reasons for strain-dependent differences in activities of xenobiotica-accepting reductases is too complex to be addressed here in detail. In the light of these results the strain with the highest activity, *S. cerevisiae* L13, was selected for further studies.

Table 1. 2,5-Hexanedione reducing activity varies among yeast strains.

Strain	Relative 2,5-hexanedione reducing activity
S. cerevisiae L13	100%
S. cerevisiae CBS 8066	58%
S. cerevisiae CEN.PK 113-7D	61%

Alcohol-dehydrogenase from *Thermoanaerobacter* sp. (ADH-T)

The second promising biocatalyst, investigated in terms of production of **(S)-2**, is a (S)-selective alcohol-dehydrogenase from a thermophilic bacterium (ADH-T) which has recently been used to develop an efficient procedure to obtain enantiopure **(2S,5S)-3**.[22] ADH-T is available in an isolated form, which results in advantages like high specific activity towards its substrates and a well-defined system. However since the enzyme depends on the cofactor NADPH, which, due to its price, cannot be used in stoichiometric amounts, care has to be taken on efficient regeneration of

the cofactor in order to get a cost-effective system. Often enzyme coupled cofactor regeneration is employed, which necessitates an additional enzyme together with its corresponding substrate, to reduce NADP$^+$, *e.g.* glucose-dehydrogenase/glucose.[38] In this context an important advantage of ADH-T becomes obvious. Since it is capable of catalysing oxidation of secondary alcohols with a sufficient rate even at pH 7, its pH-optimum for reduction,[39] the use of ADH-T allows for a substrate-coupled cofactor regeneration approach, thus abolishing the need for an additional enzyme.

The use of ADH-T permits the use of 2-propanol (**4**) as a hydrogen donor, which is oxidized to acetone (**5**), regenerating the NADPH needed for reduction of **1** (Scheme 2).
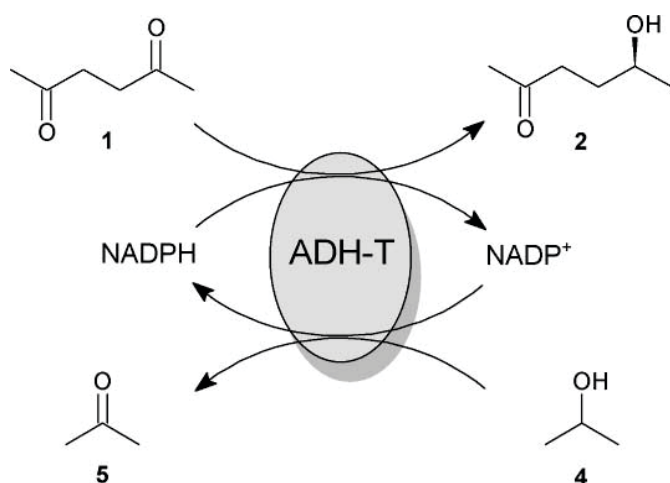
Scheme 2. Substrate-coupled production of (*S*)-**2** employing ADH-T. Cofactor regeneration and reduction of 2,5-hexanedione (**1**) are catalysed by one and the same enzyme.

Due to the laws of mass action, the overall equilibrium of the whole system only depends on the free energies of the two alcohols and the corresponding ketones, in which the equilibrium constant is determined through eqn (1). Hence, if full conversion of **1** is intended the equilibrium can be shifted towards **3** through removal of **3** or acetone as well as the use of **4** in large excess.

$$K_{eq} = \frac{c_{eq}(3) \cdot c^2_{eq}(5)}{c_{eq}(1) \cdot c^2_{eq}(4)} \qquad (1)$$

However since selective removal of **3** is not easily achieved, it is obvious that full conversion can only be obtained through the use of excess **4** and removal of formed **5**. However if full conversion is not intended, as is the case in the investigation of ADH-T catalysed formation of (*S*)-**2**, it was found that acetone removal is not necessary in order to reach the maximal concentration of **2**.

Although the maximal cofactor-regenerating capacity of the system in Scheme 2 is not required to study mono-reduction of **1**, it will be of use in a final process in order to improve efficiency by saving 2-propanol.

Bioreduction of 2,5-hexanedione through ADH-T and *S. cerevisiae* L13

With the aforementioned considerations in mind, bioreduction of **1** was achieved by using either ADH-T with substrate-coupled cofactor-regeneration employing 2-propanol or resting whole-cells of *Saccharomyces cerevisiae* L13 (SCL13), which were supplied with sucrose as the sole carbon source. From the representative time-courses of the respective reductions depicted in Figure 1, it is obvious that both reductions obey the kinetics of a consecutive reduction. That is, intermediate **2** accumulates transiently in the course of the reaction and its maximal concentration is reached under non-equilibrium conditions. Since the desired product **2** forms faster than **3**, it is advisable to control the reaction kinetically rather than thermodynamically (equilibrium-controlled). Investigations into condensation reactions in which the desired product hydrolyzed subsequently (and thus can be understood as an intermediate of a consecutive reaction) showed that a higher product yield could be obtained more rapidly in a kinetically controlled process than in an equilibrium controlled process.[40] These observations and considerations show that production of **2** is possible if the reaction is
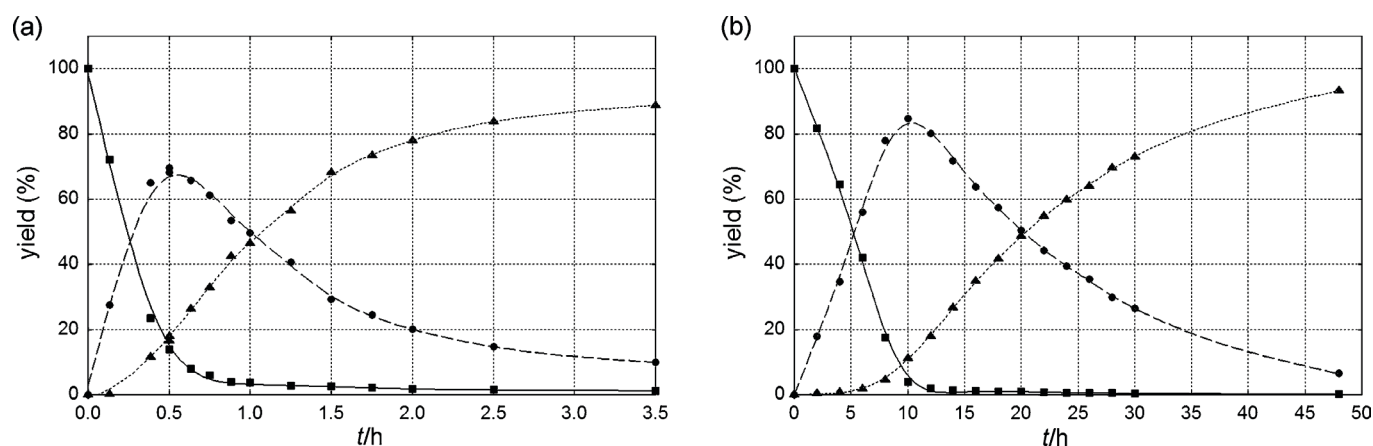
Figure 1. Time course of a bioreduction of 2,5-hexanedione (■) (80 mM): (**a**) with ADH-T, employing substrate-coupled cofactor regeneration *via* 2-propanol (2 M) without removing acetone at pH 7.0; (**b**) with whole-cells of *S. cerevisiae* L13 (SCL13) supplied with sucrose; both at 30 °C (5-hydroxy-2-hexanone (●); 2,5-hexanediol (▲)).

conducted under kinetic control, *i. e.* the reaction is stopped at maximal concentration of **2**, yielding a reaction medium containing the maximum achievable product concentration of **2** under the prevailing reaction conditions.

Determination of product enantiopurities gave that both reactions (**1**→**2** and **1**→**3**) proceed with very high enantioselectivity yielding both (**S**)-**2** and (**2S,5S**)-**3** in >99% *ee*.

This extraordinarily high stereoselectivity indicates that in the case of SCL13 no counteracting reductase reducing **1** with different stereo-selectivity is present in the cell, which furthermore underlines that this whole-cell biocatalyst must not be regarded unselective in general. The observation that conversion of **1**→**2** with ADH-T is achieved in a fraction of time needed by SCL13 has its reason in the concentration of **1**-reducing dehydrogenases in the respective experiment. Application of isolated enzymes like ADH-T allows for higher concentrations of **1**-reducing dehydrogenases since the plethora of enzymes needed to maintain a whole-cell are not present. Thus higher activity per volume unit can be achieved with isolated enzymes. Unfortunately HDOR from SCL13 is not yet available in an isolated form since identification and isolation are part of ongoing studies. However, it has to be stressed here that compared to isolated enzymes, the use of whole-cell-biocatalysts may be less favourable in terms of activity, but this drawback is compensated for by the much lower price and

the ease of handling (*e.g.* no care has to be taken on cofactor regeneration) and thus still renders the use of whole-cell biocatalyst economically attractive.

Besides these considerations, the major advantage of using SCL13 is the high peak concentration of **2**, which is 21% higher than that achieved with ADH-T. Thus SCL13 allows for a more efficient synthesis of (**S**)-**2**, since the amount of remaining reactant **1** and secondary product **3** is reduced, which simplifies downstream processing.

Since the system is kinetically controlled, the kinetic parameters of the biocatalyst determine the maximal peak concentration of **2**. This is also reflected by the apparent kinetic parameters determined in the presence of saturating concentrations of cofactor NADPH (Table 2). From these parameters is evident that the affinity of both biocatalysts for **1** is higher than for **2** (K_M(**2**)/K_M(**1**) = 4.1 for both biocatalysts), which basically is advantageous for accumulation of **2**. However, since the difference and thus the ratio K_M(**1**)/K_M(**2**) is comparable for both biocatalysts, K_M cannot account for the better performance of SCL13. Considering the apparent maximal velocities of both reactions (Table 2) it becomes evident that the difference between v_1(**1**→**2**) and v_2(**2**→**3**) is much more pronounced for HDOR of SCL13 than for ADH-T (v_1(**1**→**2**)/v_2(**2**→**3**): SCL13 = 15.3; ADH-T = 1.8), which results in the superior chemoselectivity of SCL13 in production of **2**. Given that both reactions are reversible in general,

oxidation of **2** and **3** was also investigated.

In the presence of saturating concentrations of NADP$^+$, oxidation of **3** with HDOR of SCL13 will only become effective at a high concentration of **3** due to its high K_M (42.8mM), whereas the kinetic parameters of ADH-T (K_M(**3**) = 1.5 mM) for oxidation of **3** allow for becoming effective at lower concentrations of **3**. However, the subsequent oxidation of **2** through ADH-T will be slower when compared to oxidation of **3** because of the slower apparent maximal velocity (Table 2). Hence oxidation of **3** through ADH-T will also lead to an accumulation of **2**, which is not the case if **3** is oxidised by HDOR of SCL13, because this biocatalyst would catalyse oxidation of **2** at a higher rate, due to K_M(**2**) < K_M(**3**) (Table 2), if c < 10K_M. However, oxidation of substrates **2** and **3** will play a minor role if both biocatalysts are used to produce **2** by reduction of **1**, a process that is more effective than the oxidation of highly valuable enantiopure **(2S,5S)-3**. Under these conditions reduction of **1** will be favoured through an excess of NADPH over NADP$^+$ in the cells, which was found in a number of yeast strains.[33,41] In the case of a system employing ADH-T, oxidation of alcohols is the key to regenerate NADP$^+$. However, the excess of 2-propanol will competitively inhibit oxidation of **2** and **3**, respectively, although the contribution of oxidation of **3** to accumulation of **2** cannot be neglected and thus contributes to accumulation of **2**.

A full characterisation of both biocatalysts in detail requires the pure enzymes for which the assumed ordered bi–bi mechanism has to be validated, followed by determination of the 16 individual rate constants as defined in the rate equation,[42] and thus goes far beyond the scope of this contribution.

Although the kinetic parameters of the biocatalyst determine the maximal yield of **2** and hence the chemoselectivity of the bioprocess, it is also essential to study factors affecting the activity of the whole-cell-biocatalyst in order to identify conditions allowing for its most efficient use.

Factors affecting the activity of 2,5-hexanedione-reductases (HDOR) in *S. cerevisiae* L13

Besides strain-dependent variation, the physio-logical status of the respective whole cell biocatalyst is a potential affector of HDOR-activity. As the expression of dehydrogenases is altered through a number of stress-responses in *S. cerevisiae*,[43–45] expression of HDOR is most likely affected during exposure of yeast cells to stress. Hence, conditions should exist under which the activity of the whole-cell-biocatalyst is improved through stress-exposure. As is evident from Figure 2a, exposing exponentially growing cells to heat shock, osmotic stress or chemical stress increases the activity of HDOR. Furthermore, Figure 2a also shows that HDOR-activity resulting from exposure of *S. cerevisiae* L13 to osmotic stress by far exceeds activities resulting from exposure to other conditions.

The induction of HDOR had no effect on stereo-selectivity of the biocatalyst, which underlines that no dehydrogenases accepting **1** as a substrate with counteracting selectivity were induced through the provoked stress responses.

Comparison of the activity of exponentially growing cells with that of commercial grade SCL13 (compressed yeast) revealed that the latter exhibit an up to fourfold higher HDOR-activity (76mU/mg(protein) vs. 19 mU/mg(protein) in exponentially growing cells). This observation is reasonable since industrially produced compressed yeast cells are exposed to a lack of nutrients at the end of the production process, which constitutes a stressful condition, employed in order to increase robustness of the organisms and shelf-life of the product.[46,47] Hence the increased HDOR-activity of industrial grade SCL13 can be attributed to a stress-response during production and thus under-lines the inducibility of HDOR through cell-stress.

Table 2. Kinetic constants determined for HDOR and ADH-T

	Reaction	K_M[b]	v_{max}[b,c]
S. Cerevisiae L13[a]	**1→2**	2.5 mM	94.7 mU/mg
	2→3	10.2 mM	6.2 mU/mg
	3→2	42.8 mM	23.8 mU/mg
	2→1	3.4 mM	28.0 mU/mg
ADH-T[a]	**1→2**	0.2 mM	27.3 kU/mg
	2→3	0.7 mM	15.0 kU/mg
	3→2	1.5 mM	15.8 kU/mg
	2→1	0.2 mM	3.6 kU/mg

[a] For experimental conditions see experimental section. [b] Apparent values under saturating conditions of cofactor. [c] No k_{cat} given since biocatalysts were not purified to homogeneity.

The induction of HDOR through multiple stresses suggests that the gene encoding for this enzyme is regulated as for the so-called environmental-stress-response genes, a group of genes whose expression is altered by diverse types of stress.[48,49] In this group only 9 genes encoding for biotransformation-relevant putative and confirmed dehydrogenases can be found, and will be good candidates in future investigations concerning identification of HDOR.

So exposing cells to stressful conditions prior to or during the biotransformation is of benefit in terms of HDOR-activity. Due to the fact that commercial grade compressed yeast already has a high basic level of HDOR-activity, its use is more practicable than exposing exponentially growing cells to osmotic shock.

Since biotransformations with commercial grade SCL13 are carried out at high cell-densities under non-growing conditions (resting cells) and nitrogen limitation, it remains to be elucidated whether exposure of non-growing cells to osmotic shock under conditions of a biotransformation will also increase HDOR-activity. Figure 2b shows the results of these experiments. Though induction of HDOR after 1 h and 10 h of exposure to osmotic stress took place, the relative increase of HDOR-activity, related to the control, is much smaller than that observed in exponentially growing cells. This is attributable to the significantly decreased protein biosynthesis in resting, stationary-phase-like cells[50] and the circumstance that expression of every chromosomal encoded protein in a living organism cannot be increased indefinitely, *i.e.* if a maximal HDOR-activity in wild-type yeast-cells is already present, it cannot be increased any further through alteration of biotransformation conditions.

Though osmotic stress induces HDOR in non-growing *S. cerevisiae* L13, it must be noted that prolonged incubation of these cells under biotransformation conditions resulted in a similar increase in HDOR-activity without sorbitol being present (Figure 2b). Hence the conclusion needs to be drawn that there is no further benefit in applying stressful conditions (for instance by additives in whole-cell biotransformations of **1**), since conditions of the biotransformation itself lead to an increase in the already high activity of HDOR in commercial grade *S. cerevisiae* L13. Though the activity of exponentially growing cells exposed to 1 M sorbitol (up to 130 mU/mg(protein)) was not reached with industrially produced compressed *S. cerevisiae* L13 (up to 100 mU/mg(protein) after incubation under conditions of biotransformation), use of the latter is more practical in terms of price and availability. After having identified conditions allowing for a maximal HDOR-activity, a comprehensive study of the intended process should not ignore the limitations of the process. Those limitations may arise from the complexity of a whole-cell biocatalyst and the effects of a xenobiotic compound on cell physiology and the
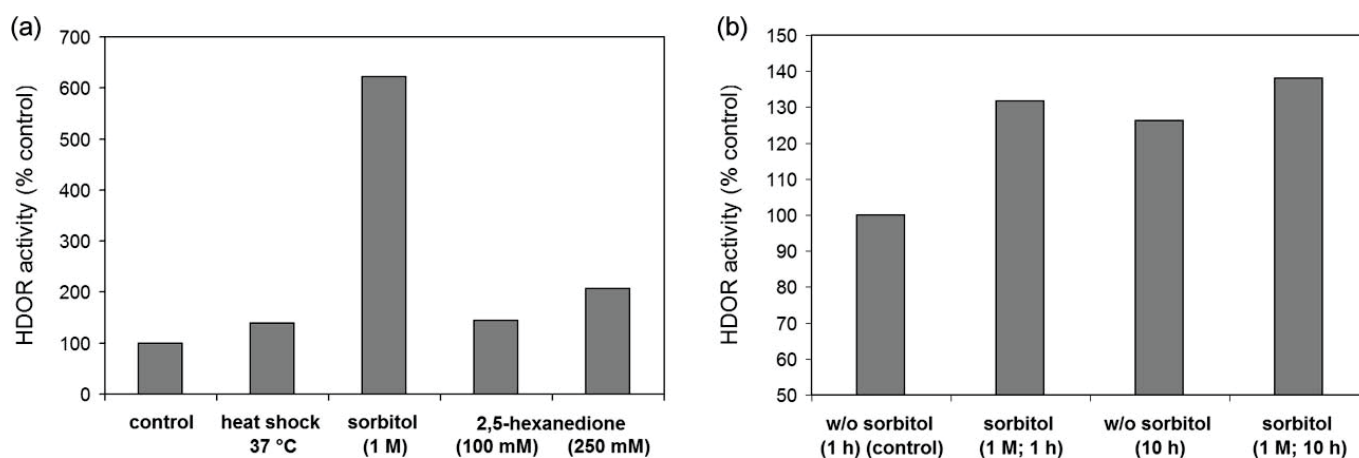
Figure 2. (a) Induction of HDOR in exponentially growing *S. cerevisiae* L13 (SCL13) after exposure to heat-shock (37 °C), osmotic-stress (1 M sorbitol) and chemical-stress (2,5-hexanedione) for 1 h. **(b)** Induction of HDOR-activity in resting *S. cerevisiae* L13 under conditions of a biotransformation and exposure to osmotic stress.

metabolic network. Together with side-reactions, these processes may impair the performance of the bioprocess, and thus need to be investigated in order to assess the potential of the process and to identify optimisation strategies.

Limitations of biocatalytic production of (5S)-hydroxy-2-hexanone with *S. cerevisiae* L13

Since the outcome of a bioreduction with whole-cells not only depends on the functionality of the dehydrogenase catalysing the reduction, but on the whole cellular metabolic network and the integrity of the cell, vitality of the cells is a major issue.

Effects on cell-vitality. 1 does not affect cell-vitality up to a concentration of 5% v/v (440 mM). Additionally 3-methylcyclopentenone (**7**), a reactant impurity-resulting from intramolecular condensation of **1** and a potential fungicide,[51] will not

impair cell-vitality if **1** is used in technical grade (purity>95%) at least. Thus even in batch-biotransformations with 5% **1**, the concentration of **7** will, in the worst case, not exceed 0.25%, a concentration which has been found to be tolerated by *S. cerevisiae* L13. Moreover, *S. cerevisiae* L13 is capable of reducing **7**, forming 3-methylcyclopentanone (**8**).

Formation of by-products and interaction with cell physiology. Though vitality of *S. cerevisiae* is not significantly impaired even at high concentrations of **1**, metabolic processes are affected at lower concentrations. This has its reason in the electrophilic properties of **1**,making it capable of reacting with nucleophiles like protein amino- or thiol-groups. Whereas reaction with the former, furnishes (semi)-thioacetals (**16**) the latter reaction gives rise to the formation of Schiff-bases (**13**, **15** and **9**) and pyrroles (**14**), respectively (Scheme 3), resulting in the modificat-
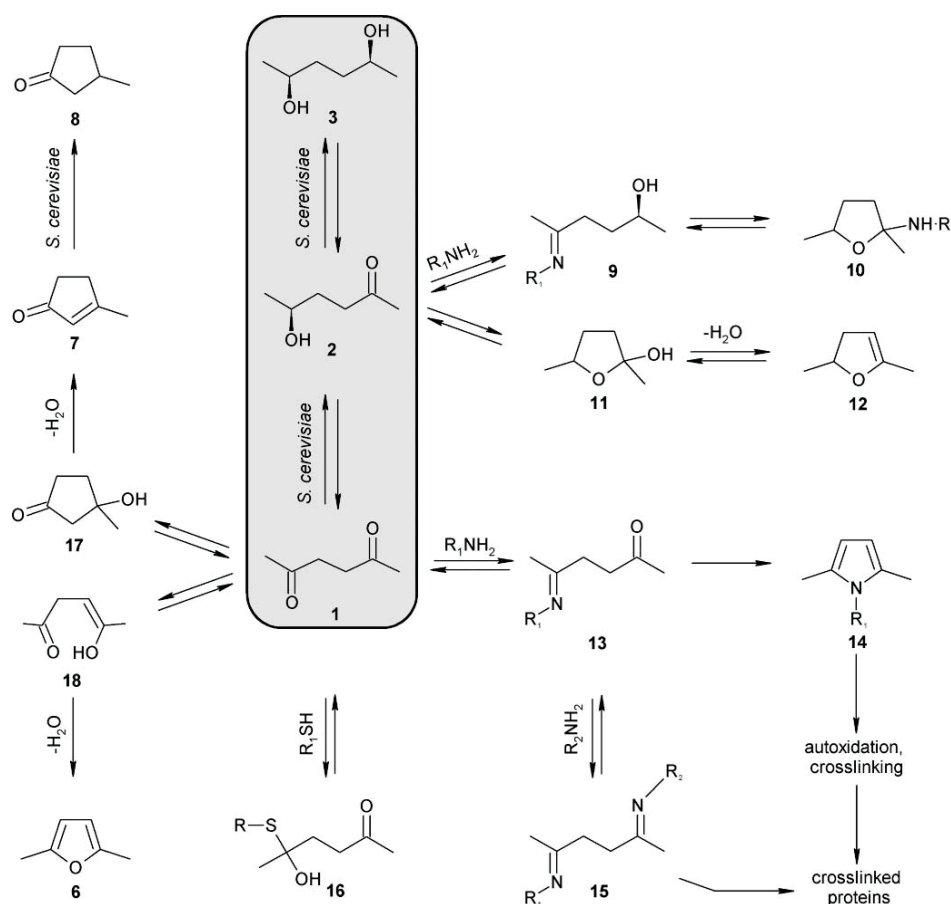
Scheme 3. Overview of side reactions in biotransformations of 2,5-hexanedione.

ion of proteins through **1** and **2**. Furthermore **1** is also capable of crosslinking proteins through pyrroles or reaction with two amino-groups from different proteins (**13**→**15**).

Since thiol- and amino-groups are often essential for catalytic activity of enzymes,[52,53] modification of such residues would inhibit the activity of the effected enzyme. Indeed, inhibition of the key glycolytic enzyme glyceraldehydes-3-phosphate dehydrogenase was found in *S. cerevisiae* L13 exposed to **1** (Figure 3), which is corroborated by studies with rats in which **1** was found to affect the activity of phosphofructokinase and glyceraldehyde-3-phosphate dehydrogenase.[54,55]

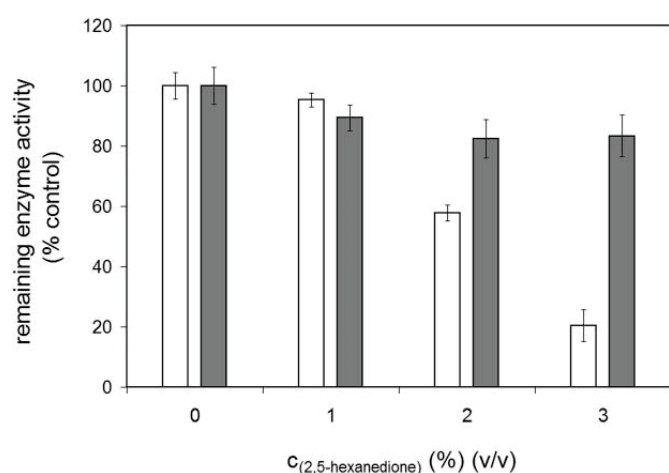**Figure 3.** Remaining activity of glyceraldehydes-3-phosphate dehydrogenase (grey bars; 100% correspond to 10.9 U/mg(protein)) and glucose-6-phosphate dehydrogenase (white bars; 100% correspond to 0.4 U/mg(protein)) in *S. cerervisiae* L13 after exposure to different concentrations of 2,5-hexanedione after 24 h under biotransformation conditions.

However, inhibition of glyceraldehyde-3-phosphate dehydrogenase in *S. cerevisiae* is not fatal for cellular metabolism, since glycolytic enzymes are present in high abundance.[56] However, further investigations showed that **1** also affects the activity of the lower abundant enzyme glucose-6-phosphate dehydrogenase (Zwf1p) (Figure 3), which is especially important in biotransformations, since it is the major NADPH-regenerating enzyme in *S. cerevisiae*.[57]

The reduced activity of Zwf1p after 24 h of bioreduction of **1** has to be attributed to inhibition of this enzyme through **1** since its expression is reported to be essentially constitutive.[58] Thus it can be ruled out that this significant decrease in activity of Zwf1p is due to repression through

stress-responses provoked by **1**. Inhibition of glucose-6-phosphate dehydrogenase may result in a decrease in the velocity of reduction of the prochiral ketones **1** and **2**, which depends on NADPH.

Furthermore, NADPH is required to detoxify reactive oxygen species (ROS) and needed to maintain the level of reduced glutathione, the key determinant of intracellular redox-status.[59,60] Thus the probability of oxidative damage and oxidative stress increases with decreasing intracellular NADPH-levels.

Formation of by-products throughout the bio-reduction not only affects cell physiology but also product yield, since competing reactions consume reactant and product, respectively. The investigated side-reactions were found not to significantly impair product yield and can be assessed to account for a maximal loss of around 1% of starting material.

Much more important is the ability of **2** to undergo intramolecular cyclisation with subsequent dehydration, furnishing 2,3-dihydro-2,5-dimethylfuran. Through this reaction pathway, **2** would be continuously withdrawn from the reaction, thus impairing product yield. Fortunately, acetalisation of **2** is an equilibrium-dependent process[61,62] in which **2** mainly exists in the open chain form as long as water is present.[63–66] This observation can be ascribed to the limited number of stabilising intramolecular hydrogen bonds in hemiacetal **11**. When compared to the most prominent 2-keto-alcohol: D-fructose, it is obvious that the β-D-fructofuranose has more possibilities to stabilize *via* intramolecular hydrogen bonds (Scheme 4) than **11**, and hence it

11   **β-D-fructofuranose**
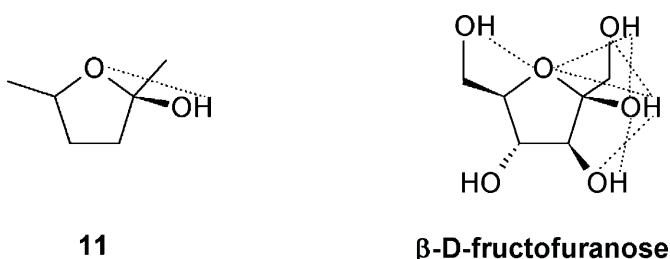
Scheme 4. A network of intramolecular hydrogen bonds (possible H-bonds are represented by dashed lines) stabilizes the hemiacetal of b-D-fructose. Hemiacetal **11** cannot stabilize in the same manner due to the lack of capability to forman intramolecular hydrogen bond network. Data on hydrogen bonds for β-D-fructofuranose is reproduced from quantum mechanics/molecular mechanics studies.[73]

is reasonable that D-fructose exists mainly in the hemiacetal form, whereas **2** mainly exists in the open-chain-conformation.

Hence the possibility of product loss through formation of 2,3-dihydro-2,5-dimethylfuran during the biotransformation in water can be neglected. The situation becomes different if the product is freed from water due to purification or storage as a neat substance. Under these conditions cyclisation and dehydration are favoured, especially if metal ions, catalysing the reaction, are present. Dihydrofurans easily auto-oxidize and crosslink and thus contaminate the product.[67,65] Hence it is advisable to store **2** as an aqueous solution or carry out subsequent reactions in one pot together with the biotransformation. If **2** is needed as a neat substance, substantial losses (>50%) in isolated yield have to be tolerated.

Adsorption and absorption through yeast.
Another limiting issue observed is the capability of yeast cells to bind a proportion of reactant and product, either by absorption and retention in the cells' cytoplasm or adsorption on the outer cell wall. Though this behaviour is of benefit in order to remove (for instance) mycotoxins,[68] it leads to an apparent lower substrate and product concentration in the supernatant of a bioreduction after removal of biomass, and necessitates extraction of the cell pellet if a maximal product yield is desired. After 48 h of bioreduction of **1** (batch with 1% v/v **1**) 20% of the resulting mixture of **1**, **2** and **3** were found to be adsorbed and absorbed by the employed yeast cells. Since adsorption and absorption of substrates and products is also described for ethyl 3-oxobutanoate (20–30% adsorbed and absorbed after 24 h),[31] in general care has to be taken to properly extract the cells during down-stream processing in order to avoid significant product loss.

Cell-free bioreduction

In order to by-pass the aforementioned drawbacks, cell-free approaches could provide a solution. The feasibility of reduction of **1** in a cell-free system using yeast dehydrogenases can be exemplified by employing a crude-extract of *S.*

cerevisiae L13 with regeneration of cofactor NADPH through glucose-dehydrogenase (Fig. 4). By using this system an even higher peak concentration of (*S*)-**2** could be observed (89%). However, the advantages of a cell-free system are accompanied by the disadvantageous demand for an additional cofactor-regenerating enzyme, which results in increased production costs.
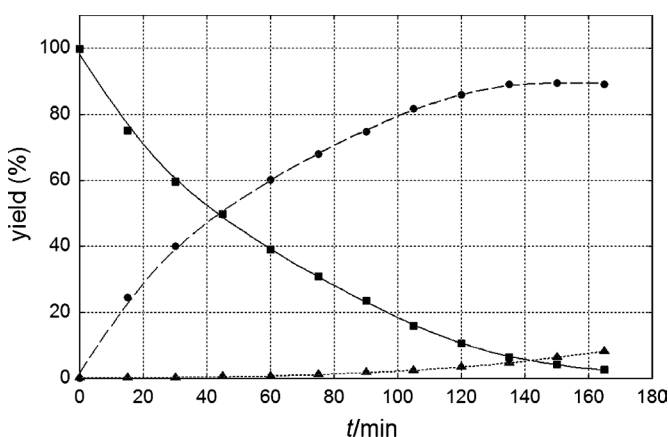
Figure 4. Representative time course of a bioreduction employing *S. cerevisiae* L13 crude extract (0.8U/mL 2,5-hexanedione-reductase; 4.5U/mL glucose-dehydrogenase; 120 mM glucose; 50 mM 2,5-hexanedione; 1 mM NADP⁺).

The productivity of the suggested system could be increased further by isolation, identification and heterologous expression of the reductase responsible for reduction of 2,5-hexanedione in *S. cerevisiae*. These investigations are currently being examined, and are beyond the scope of this contribution.

Further improvement would aim at increasing the selectivity of the biocatalyst by increasing the ratio of the apparent reaction velocities v_1(**1**→**2**)/v_2(**2**→**3**), which determines selectivity and yield of **2**.

One possibility is conducting the reduction with c_0(**1**) < K_M(**2**); however, K_M(**1**) and K_M(**2**) are both in the mM range and thus would limit the concentration of the product to an inefficient level. Improving c_{max}(**2**) through reaction engineering is quite challenging since only the second part of the reaction should be affected. However, both reductions (**1**→**2** and **2**→**3**) are catalysed by the same enzyme and hence any change of reaction parameters will always affect both parts of the reaction. Furthermore, a simplified *in silico* model (implemented in COPASI[69]) of the consecutive reaction (**1**→**2**→**3**)

obeying reversible Michaelis–Menten kinetics predicts that $c_{max}(2)$ for the intermediate only approaches 100% as the ratio of the reaction velocities $v_1:v_2$ approaches infinity (Figure 5). Hence if $c_{max}(2)$ is already high, as is the case in bioreductions of **1** employing *S. cerevisiae* L13, an increase in the difference between $v1$ and $v2$ will have less effect on $c_{max}(2)$.
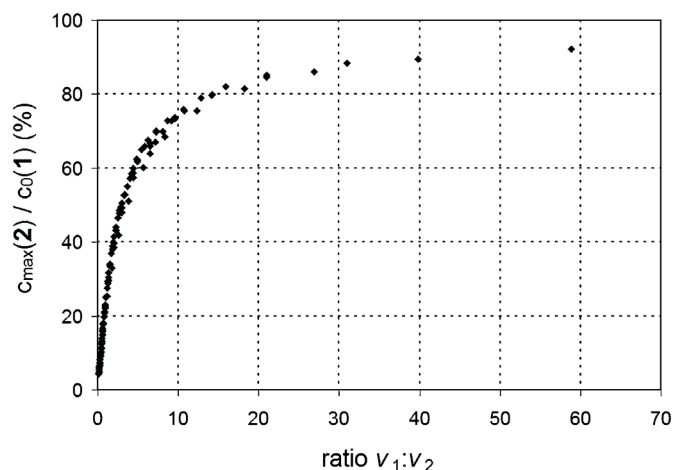
Figure 5. Prediction of cmax(**2**) in dependence of the ratio of the maximal reaction velocities v1:v2. Simulation was carried out with COPASI using a simplified model employing parameters from Table 2 assuming reversible Michaelis–Menten kinetics for the consecutive reduction of **1**.

Another option to increase the yield of **2** is its selective removal from the reaction medium; however, this is quite difficult to achieve since reactant and product are highly similar. A promising alternative would be directed evolution of the enzyme with the aim of decreasing the affinity of the biocatalysts towards **2**, without affecting affinity for **1** and reaction rate for its reduction.

Conclusions

Application of enantiopure hydroxyketones, which are valuable building blocks in organic synthesis, is limited by their poor availability. Hence there is a need to develop strategies for a sustainable and effective production of these building blocks. In this field biocatalytic approaches are most promising due to their unsurpassed selectivity and operation at ambient conditions. In terms of atom economy, the optimal reactant to obtain (5*S*)-hydroxy-2-hexanone (**(S)-2**) is the commercially available diketone 2,5-hexanedione (**1**). Since the reduction proceeds as a consecutive reaction

finally yielding (2*S*,5*S*)-hexanediol (**(2S,5S)-3**), the desired product is an intermediate, which transiently accumulates. Comparison of two biocatalysts already successfully applied in enantioselective synthesis of **(2S,5S)-3** revealed that 2,5-hexanedione-reductase(s) (HDOR) from *S. cerevisiae* L13 are particularly suitable for the production of enantiopure **(S)-2** since the developed procedure yields up to 89% **(S)-2** from **1** with high stereoselectivity (*ee* >99%).

Further investigations outlined the potentials and limitations of using whole-cells and cell-free approaches. Whereas production of **(S)-2** by employing whole-cells of *S. cerevisiae* L13 is costeffective, limitations arise from interactions of the reactants with cell physiology. In order to bypass these limitations, cell-free approaches can be used, although these will be more expensive. However, one has the freedom to select the approach towards **(S)-2** that best meets the required demands.

Taken together, these studies illustrate the possibilities to produce enantiopure (5*S*)-hydroxy 2-hexanone with either whole cells of *S. cerevisiae* or a cell-free approach for the first time, and thus improves availability of a versatile chiral building block. Furthermore, the detailed investigation of the processes taking place during the bioreduction contributes to a deeper understanding and allows for the assessment of potentials and optimisation strategies.

Experimental

Chemicals

2,5-Hexanedione (97%) was obtained from Wacker AG and purified to 99% by distillation before use. Chemicals and enzymes used in enzymatic assays were purchased from Sigma. ADH-T and glucose dehydrogenase (GDH) was kindly provided by Juelich Chiral Solutions GmbH, a Codexis company. All other chemicals were obtained from Fluka and Acros. Sucrose was obtained from a local store.

Yeast strains and growth conditions

The *Saccharomyces cerevisiae* strains used in this study were: CBS8066 (Centraal Bureau voor Schimmelcultures, Delft, The Netherlands); L13 (FALA Societé industrielle de levure, Strasbourg, France) and CEN.PK 113–7D (Euroscarf, Frankfurt, Germany). Strains were grown in YPD medium (2% (w/v) D-glucose; 2% (w/v) peptone; 1% (w/v) yeast extract). If necessary, media was solidified by addition of 1.8% (w/v) agar.
.

Gas-chromatographic procedures

Determination of extent of conversion. After addition of *n*-butanol as an internal standard, extent of conversion was measured by means of GC/FID (HP 6890 GC equipped with an automatic liquid sampler). Separation was achieved on a CS-Carbowax CW 20M (CS-Chromtographie, Langerwehe) capillary column (50 m x 0.32 mm x 0.5 mm). The pressure of the carrier gas H_2 was 0.8 bar; the temperatures of injector and detector were 250 ℃ and 260 ℃, respectively. The temperature program: 80 ℃ (0 min); 80 ℃ to 160 ℃ with 20 K/min; 160 ℃ (4.5 min); 160 ℃ to 180 ℃ with 40 K/min gave the following retention time: **1**: 6.4 min; **2**: 8.0 min; **3**: 11.0 min; *n*-butanol: 3.3 min; **7**: 6.8 min.

Determination of enantiomeric and dia-stereomeric excess. Gaschromatographic separation of all isomers of **2** and **3** on a CS-Cyclodex β/IP (Chromatographie Service Langerwehe) capillary column (50 m \ 0.32 mm) was achieved after derivatisation with methoxylamine and trifluoroacetic anhydride. Cell-free samples were extracted three times with *tert*-butyl methyl ether (TBME), dried with $MgSO_4$ and evaporated to dryness. Methoximes of 5-hydroxy-2-hexanone were obtained after addition of 200 mL of methoxylamine hydrochloride (300 mM in dry pyridine) at 80 ℃ for 30min. Excess pyridine was evaporated in a stream of nitrogen. Purification of methoximes was achieved by adding 500 mL of H_2O, saturated with NaCl and subsequent extraction with TBME. The combined extracts were dried over $MgSO_4$ and concentrated in a stream of nitrogen before 70 mL of trifluoroacetic anhydride were added carefully. After standing for 30 min at room temperature excess of trifluoroacetic acid and its anhydride was evaporated. Prior to injection the residue was diluted with CH_2Cl_2. Analysis was carried out on a HP6890 GC/FID equipped with an HP 5971 autosampler. The pressure of carrier gas H_2 was 0.48 bar; the temperatures of injector and detector were 250 ℃ and 300 ℃, respectively. The temperature program: 50 ℃ (45 min); 50 ℃ to 100 ℃ with 20 K/min; 100 ℃ (15 min); 100 ℃ to 170 ℃ (5 min) resulted in the following retention times: **(2S,5S)-3**: 49.0 min; **(2R,5R)-3**: 49.3min; *meso*-**3**: 50.3min; **(2S)-2**: 52.2 and 52.7min†; **(2R)-2**: 51.5 and 52.4 min‡.

---

†Methoximation of 5-hydroxy-2-hexanone results in two diastereomeric methoximes per enantiomer; hence every enantiomer gives rise to two peaks.

Strain dependence of 2,5-hexandione reducing activity

After incubation of *S. cerevisiae* strains CBS 8066, CEN.PK 113–7D and L13 for 7 d in YPD cells were harvested through centrifugation (5 min, 5000g), washed with ice-cold 0.9% NaCl. Activity of 2,5-hexanedione-dehydrogenases was determined after disruption of the cells.
In order to determine enantioselectivity of the strains under study, 1% v/v 2,5-hexanedione was subjected to biotransformation employing the respective yeast strains. Conditions were equal to experiments with industrially produced compressed yeast as stated below. After complete conversion of **1** to **3**, the enantiopurity of the product was analysed by chiral-capillary GC/FID as stated above.

Stress induction

In order to expose exponentially growing cells to stress an overnight culture (OD_{600} = 5) was diluted to OD_{600} = 0.4 with fresh YPD and incubated for 2.5 h at 30 ℃ so that the culture was in exponential phase and an OD_{600} of 0.8 was reached. Cells were exposed to osmotic shock by addition of an equal volume of YPD containing 2 M sorbitiol (prewarmed to 30 ℃). In order to expose the culture to heat shock, an equal amount of

fresh YPD having a temperature of 44 °C (mixing temperature = 37 °C) was added. Stress induction through 2,5-hexanedione was studied after addition of 1% v/v (85 mM) of 2,5-hexanedione to an exponentially growing culture (OD_{600}=0.8). Cells were exposed to different stresses for 1 h at 30 °C or 37 °C (heat shock cells) with shaking (150 rpm). Subsequently cells were collected by centrifugation (5 min, 5000g) at 4 °C and washed once with cold 0.9% NaCl before being subjected to disruption and determination of enzyme activity. For experiments with resting non-growing cells, commercially supplied yeast cells (L13) were washed and suspended in PBS buffer pH 6.5 with 2% w/v glucose at an OD_{600} of 1.8. After preincubation for 1 h at 30 °C/150 rpm cells were subjected to osmotic stress by adding an equal amount of a prewarmed (30 °C) solution of 2 M sorbitol in PBS buffer pH 6.5 with 2% glucose to the culture. After an incubation period of 1 h and 10 h, respectively, cells were harvested and disrupted as described above in order to determine 2,5-hexanedione-reducing activity.

Enzyme assays

Disruption of yeast cells. Yeast cells were washed with cold 0.9% NaCl and resuspended in 0.1 M sodium phosphate buffer pH 7.0. After disruption according to ref. 70, enzyme activities were determined in cell crude extract. Protein was determined by the method of Bradford.[71]

Activity of dehydrogenases. Activity of dehydrogenases was measured spectrophotometrically by monitoring the decrease in absorbance at 340 nm with a ATI UNICAM UV4 spectrophotometer at 30 °C. The standard assay was carried out in phosphate buffer 0.1 M pH 7.0 containing 0.2 mM NADPH and 0.2 mM $NADP^+$ for reduction and oxidation experiments, respectively. Concentration of substrate was 10 mM. The reaction was started by addition of the substrate. Apparent K_M and v_{max} were determined in a similar manner, whereas substrate concentrations were varied in a concentration range between 0.05 and 80 mM. The apparent Michaelis kinetic parameters were obtained by directly fitting the data to the rate equation of an enzymatic monosubstrate reaction by means of non-linear regression. One unit corresponds to the formation or consumption of 1 mmol NADPH per minute at pH 7.0 at 30 °C.

Glucose-6-phosphate activity. Glucose-6-phosphate assay was based on ref. 72. Enzymatic activity was measured in the presence of 20 mM $MgCl_2$ and 0.7 mM $NADP^+$ in 60 mM TRIS pH 7.6 using 2 mM glucose-6-phosphate as a substrate. The increase in absorbance at 340 nm was monitored spectrophotometrically with a ATI UNICAM UV4 spectrophotometer after the start of the reaction with 20–70 mL of cell extract. One unit catalyses the oxidation of 1 mmol glucose-6-phosphate per min at 30 °C in the presence of $NADP^+$ at pH 7.6.

Glyceraldehyde-3-phosphate activity. Glyceraldehyde-3-phosphate activity was measured in the reverse direction in a coupled system with 3-phosphoglyceric phosphokinase. Activity was assayed in 100 mM TRIS pH7.6 with 6.7 mM 3-phosphoglycerate, 3.3 mM cysteine hydrochloride, 1.7 mM $MgSO_4$, 0.16 mM NADH, 1.1 mM ATP and 3.3 U/mL 3-phosphoglycerat phosphokinase. Decrease in absorbance at 340 nm was monitored with an ATI UNICAM UV4 spectrophotometer after the addition of 20–40 mL of cell extract. One unit catalyses the reduction of 1 mmol 3-phosphoglycerate per min in a coupled system with 3-phosphoglyceric phosphokinase at pH 7.6 at 30 °C.

Biotransformation of 2,5-hexanedione
Whole cell bioreduction. Whole-cell biotransformation of 2,5-hexanedione was carried out by suspending 125 g/L (wet-weight) of industrially produced compressed yeast in tap water containing 10% w/v sucrose. pH was kept constant at pH 6.3 by addition of 1.5% w/v $CaCO_3$. Adequate aeration was achieved by adhering to a maximal air:culture ratio of 5:1. After 30 min of incubation (30 °C/150 rpm) 2,5-hexanedione was added, resulting in the stated concentration (standard concentration 1% v/v). Progress of the biotransformation was monitored by GC. To obtain (5S)-hydroxy-2-hexanone, biotransfor-

mations were stopped after 10 h, whereas (2*S*,5*S*)-hexanediol was obtained after 48 h of reaction.

Cells were removed from the reaction mixture by centrifugation (5 min 5000g) and extracted three times with acetone. The cell free supernatant was concentrated *in vacuo* and subsequently treated with an excess of acetone in order to precipitate remaining cell fragments. After filtration acetone extracts were combined, concentrated *in vacuo* and dried over $MgSO_4$. After evaporation of the remaining acetone 5.2 g (66%) of raw product (containing 87% **2**) was obtained, as a clear, slightly yellow oil. Further purification of (5*S*)-hydroxy-2-hexanone was achieved through column chromatography on silica gel 60 (particle size: 0.045–0.06 mm; filling level: 27 cm; inner diameter of column: 2 cm) with ethyl acetate/n-hexane 1:1 v/v as eluent, resulting in 49% isolated yield.

Cell-free bioreduction with cofactor regeneration. Reduction of **1** with ADH-T employing substrate coupled cofactor regeneration was carried out in 0.1 M phosphate buffer pH 7.0 containing 80 mM 2,5-hexanedione, 2 M 2-propanol, 1 mM $NADP^+$ and 2 U/mL ADH-T. Reduction of **1** with a crude extract from *S. cerevisiae* L13 employing enzyme coupled cofactor regeneration through glucose/glucose dehydrogenase, was carried out in 0.2 M citrate-phosphate buffer pH 7.5 containing 120 mM D-glucose, 1 mM $NADP^+$, 50 mM 2,5-hexanedione, 0.8 U/mL 2,5- hexanedione reductase (added as crude extract) and 4.5 U/mL glucose dehydrogenase. The progress of the bioreduction was monitored by GC. Samples were obtained by withdrawing 100 mL from the reaction mixture and mixing it with 300 mL of ice-cold acetone containing *n*-butanol as an internal standard. After standing on ice for 2 h, samples were centrifuged (30 min, 10000g) and the supernatant analyzed by GC/FID.

Extent of ad- and absorption on cells of *Saccharomyces cerevisiae* L13. 6.25 g wet-weight of industrially produced compressed *S. cerevisiae* L13, 5 g sucrose, 0.75 g CaCO3 and 500 mL 2,5-hexanedione (4.36 mmol) were weighed in a 50mL volumetric flask and filled with tap water to the graduation mark. A solution prepared in the same manner but without yeast, $CaCO_3$ and sucrose served as a control. Concentration of **1**, **2** and **3** was determined in the cell-free-supernatant after 48 h of biotransformation and compared to the control.

Simulations

Simulation was carried out using software COPASI.[69] Reversible Michaelis–Menten kinetics was assumed for both reactions. Kinetic parameters were taken from Table 2. The maximal velocities of both reactions were altered ($v_{max}(\mathbf{1{\rightarrow}2})$ = 1–50 fold $v_{max}(\mathbf{2{\rightarrow}1})$; $v_{max}(\mathbf{2{\rightarrow}1})$ = const.; $v_{max}(\mathbf{2{\rightarrow}3})$ = 1–10 fold $v_{max}(\mathbf{3{\rightarrow}2})$; $v_{max}(\mathbf{3{\rightarrow}2})$ = const.) and the resulting maximal concentration of the intermediate plotted against the ratio of $v_{max}(\mathbf{1{\rightarrow}2})/v_{max}(\mathbf{2{\rightarrow}3})$.

References

1   K. Nakamura, R. Yamanaka, T. Matsuda and T.Harada, *Tetrahedron: Asymmetry*, 2003, **14**, 2659–2681.
2   M. J. Burk, J. E. Feaster and R. L. Harlow, *Tetrahedron: Asymmetry*, 1991, **2**, 569–592.
3   R. P. Short, R. M. Kennedy and S. Masamune, *J. Org. Chem.*, 1989, **54**, 1755–1756.
4   *Eur. Pat.,* EP 0592881B1, 1998.
5   J. K. Lieser, *Synth. Commun.*, 1983, **13**, 765–767.
6   M. Bertau and M. Bürli, *Chimia*, 2000, **54**, 503–507.
7   J. Haberland, A. Kriegesmann, E. Wolfram,W. Hummel and A. Liese, *Appl. Environ. Microbiol.*, 2002, **58**, 595–599.
8   J. K. Whitesell and D. Reynolds, *J. Org. Chem.*, 1983, **48**, 3548–3551.
9   M. Kim, I. S. Lee, N. Jeong and Y. K. Choi, *J. Org. Chem.*, 1993, **58**, 6483–6485.
10 A. Mattson, N. Öhrner, K. Hult and T. Norin, *Tetrahedron:Asymmetry*, 1993, **4**, 925–930.
11 J. Bach, R. Berenguer, J. Garcia, M. López, J. Manzanal and J. Vilarrasa, *Tetrahedron*, 1998, **54**, 14947–14962.
12 G. J. Quallich, *Tetrahedron Lett.*, 1995, **36**, 4729–4732.
13 A. W. I. Tan, M. Fischbach, H. Huebner, R. Buchholz, W. Hummel, T. Daussmann, C. Wandrey and A. Liese, *Appl. Environ. Microbiol.*, 2006, **71**, 289–293.
14 B. R. Davis, G. D. Rewcastle, R. J. Stevenson and P. D. Woodgate, *J. Chem. Soc. Perkin Trans. 1*, 1977, 2148–2154.
15 B. Martin-Matute, M. Edin and J. Bäckvall, *Chem. Eur. J.*, 2006, **12**, 6053–6061.

16 K. Edegger, W. Stampfer, B. Seisser, K. Faber, S. F.Mayer, R. Oehrlein, A. Hafner and W. Kroutil, *Eur. J. Org. Chem.*, 2006, **8**, 1904–1909.

17 K. Edegger, H. Mang, K. Faber, J. Gross and W. Kroutil, *J. Mol. Catal. A: Chem.*, 2006, **251**, 66–70.

18 W. Hummel, *Adv. Biochem. Eng. Biotechnol.*, 1997, **58**, 145–184.

19 A. Molnar, K. Felföldi and M. Bartók, *Tetrahedron*, 1981, **37**, 2149–2151.

20 G. Caron and R. J.Kazlauskas, *Tetrahedron: Asymmetry*, 1994, **5**, 657–664.

21 B. M. Trost, *Angew. Chem., Int. Ed. Engl.*, 1995, **34**, 259–281.

22 M. Katzberg, K. Wechler, M. Müller, T. Daußmann, J. Stohrer, W. Hummel and M. Bertau, unpublished work.

23 T. Johanson, M. Katz and M. F. Gorwa-Grauslund, *FEMS Yeast Res.*, 2005, **5**, 513–525.

24 W. F. H. Sybesma, A. J. J. Straathof, J. A. Jongejan, J. T. Pronk and J. J. Heijnen, *Biocatal. Biotransform.*, 1998, **16**, 95–134.

25 I. A. Kaluzna, T. Matsuda, A. K. Sewell and J. D. Stewart, *J. Am. Chem. Soc.*, 2004, **126**, 12827–12832.

26 J. D. Stewart, S. Rodriguez and M. M. Kayser, *in Enzyme technologies for pharmaceutical and biotechnological applications*, ed. H. A. Kirst, W. Yeh and M. J. Zmijewski, Marcel Dekker, New York, 2001, pp. 175–207.

27 K. Kita, M. Kataoka and S. Shimizu, *J. Biosci. Bioeng.*, 1999, **88**, 591–598.

28 W. Shieh and C. J. Sih, *Tetrahedron: Asymmetry*, 1993, **4**, 1259–1269.

29 S. Hohmann and W. H. Mager, in *in Yeast stress responses*, ed. ed. S. Hohmann and W. H. Mager, Springer-Verlag, Berlin, Heidelberg, 2003, pp. 1–9.

30 M. Bohn, K. Leppchen, M. Katzberg, A. Lang, J. Steingroewer, J. Weber, T. Bley and M. Bertau, *Org. Biomol. Chem.*, 2007, **5**, 3456–3463.

31 I. Chin-Joe, P. M. Nelisse, A. J. J. Straathof, J. A. Jongejan, J. T. Pronk and J. J. Heijnen, *Biotech. Bioeng.*, 2000, **69**, 370–376.

32 J. P. Van Dijken, J. Bauer, L. Brambilla, P. Duboc, J. M. Francois, C. Gancedo, M. L. F. Giuseppin, J. J. Heijnen, M. Hoare, H. C. Lange, E. A. Madden, P. Niederberger, J. Nielsen, J. L. Parrou, T. Petit, D. Porro, M. Reuss, N. Van Riel, M. Rizzi, H. Y. Steensma, C. T. Verrips, J. Vindeløv and J. T. Pronk, *Enzyme Microb. Technol.*, 2000, **26**, 706–714.

33 T. L. Nissen, M. Anderlund, J. Nielsen, J.Villadsen and M.C.Kielland-Brandt, *Yeast*, 2001, **18**, 19–32.

34 A. Teunissen, F. Dumortier, M. Gorwa, J. Bauer, A. Tanghe, A. Loiez, P. Smet, P. Van Dijck and J. M. Thevelein, *Appl. Environ. Microbiol.*, 2002, **68**, 4780–4787.

35 R. L. Weiss, J. R. Kukora and J. Adams, *Proc. Nat. Acad. Sci.*, 1975, **72**, 794–798.

36 E. Schweizer and H. O. Halvorson, *Exp. Cell Res.*, 1969, **56**, 239–244.

37 W. Wei, J. H. McCusker, R. W. Hyman, T. Jones, Y. Ning, Z. Cao, Z. Gu, D. Bruno, M. Miranda, M. Nguyen, J. Wilhelmy, C. Komp, R. Tamse, X. Wang, P. Jia, P. Luedi, P. J. Oefner, L. David, F. S. Dietrich, Y. Li, R. W. Davis and L. M. Steinmetz, *Proc. Nat. Acad. Sci.*, 2007, **104**, 12825–12830.

38 M. Eckstein, T. Daußmann and U. Kragl, *Biocatal. Biotransform.*, 2004, **22**, 89–96.

39 *World Pat.*, WO2005121326, 2005.

40 V. Kasche, *Enzyme Microb. Technol.*, 1986, **8**, 4–16.

41 L. Satrustegui, J. Bautista and A. Machado, *Mol. Cell. Biochem.*, 1983, **51**, 123–127.

42 V. Leskovac, *Comprehensive enzyme kinetics*, Kluwer academic publishers, New York, 2004.

43 A. P. Gasch, P. T. Spellman, C.M. Kao, O. Carmel-Harel, M. B. Eisen, G. Storz, D. Botstein and P. O. Brown, *Mol. Biol. Cell*, 2000, **11**, 4241–4257.

44 Q. Chang, T. M. Harter, L. T. Rikimaru and J.M. Petrash, *Chem. Biol. Interact.*, 2003, **143–144**, 325–332.

45 A. Garay-Arroyo and A. A. Covarrubias, *Yeast*, 1999, **15**, 879–892.

46 F. Randez-Gil, P. Sanz and J. A. Prieto, *Trends Biotechnol.*, 1999, **17**, 237–244.

47 A. Bekatorou, C. Psarianos and A. A. Koutinas, *Food Technol. Biotechnol.*, 2006, **44**, 407–415.

48 A. P. Gasch, *in Yeast stress responses*, ed. S. Hohmann and P. W. H. Mager, Springer-Verlag, Heidelberg, 2003, pp. 11–70.

49 A. P. Gasch, *Yeast*, 2007, **24**, 961–976.

50 E. K. Fuge and M. Werner-Washburne, *in Yeast Stress Responses*, ed. S. Hohmann and P.W. H.Mager, Springer-Verlag, Berlin, Heidelberg, 1997, pp. 51–75.

51 J. A. Miller, A. W. Pugh, G. M. Ullah and G. M. Welsh, *Tetrahedron Lett.*, 2001, **42**, 955–959.

52 G. Foucault, J. M. Bodo and M. Nakano, *Eur. J. Biochem.*, 1981, **119**, 625–632.

53 M. T. Vincenzini, P. Vanni, G. M. Hanozet, P. Parenti and A. Guerritore, *Enzyme*, 1986, **36**, 239–246.

54 M. I. Sabri, *Arch. Toxicol.*, 1984, **55**, 191–194.

55 M. I. Sabri, *Brain Res.*, 1984, **297**, 145–150.

56 S. Ghaemmaghami, W. Huh, K. Bower, R. W. Howson, A. Belle, N. Dephoure, E. K. O'Shea and J. S. Weissman, *Nature*, 2003, **425**, 737–741.

57 D. Grabowska and A. Chelstowska, *J. Biol. Chem.*, 2003, **278**, 13984–13988.

58 K. I. Minard and L. McAlister-Henn, *J. Biol. Chem.*, 2005, **280**, 39890–39896.

59 C. M. Grant, *Mol. Microbiol.*, 2001, **39**, 533–541.

60 S. Izawa, K. Maeda, T. Miki, J. Mano, Y. Inoue and A. Kimura, *Biochem. J.*, 1998, **330**, 811–817.

61 J. Baker, J. Arey and R. Atkinson, *J. Photochem. Photobiol. A*, 2005, **176**, 143–148.

62 G. I. Nikishin, V. G. Glukhovtsev, S. S. Spektor and E. D. Lubuzh, *Russ. Chem. Bull.*, 1973, **22**, 684–686.

63 T. Holt, R. Atkinson and J. Arey, *J. Photochem. Photobiol. A*, 2005, **176**, 231–237.

64 J. E. Whiting and J. T. Wilson, *Can. J. Chem.*, 1971, **49**, 3799–3806.

65 P. Dimroth and H. Pasedach, *Angew. Chem.*, 1960, **22**, 865.

66 D. M. Jones and N. F. Wood, *J. Chem. Soc.*, 1964, 5400–5403.

67 Q. Q. Zhu and W. Schnabel, *Polymer*, 1998, **39**, 897–901.

68 D. Ringot, B. Lerzy, K. Chaplain, J. Bonhoure, E. Auclair and Y. Larondelle, *Bioresour. Technol.*, 2007, **98**, 1812–1821.

69 S. Hoops, R. Gauges, C. Lee, J. Pahle, N. Simus, M. Singhal, L. Xu, P. Mendes and U. Kummer, *Bioinformatics*, 2006, **22**, 3067–3074.

70 W. Hummel and M. R. Kula, *J. Microbiol. Meth.*, 1989, **9**, 201–209.

71 M. M. Bradford, *Anal. Biochem.*, 1976, **72**, 248–254.

72 E. Noltmann, C. Gubler and S. Kuby, *J. Biol. Chem.*, 1961, **236**, 1225–1230.

73 M. T. C. Martins-Costa, *Carbohydr. Res.*, 2005, **340**, 2185–2194.

4.2

Asymmetric synthesis of (2*S*,5*S*)-hexanediol on a preparative-scale using a *Saccharomyces cerevisiae* strain expressing *GRE2* encoding NADPH-dependent alcohol dehydrogenase Gre2p

Marion Müller and Werner Hummel

Asymmetric synthesis of (2*S*,5*S*)-hexanediol on a preparative-scale using a *Saccharomyces cerevisiae* strain expressing *GRE2* encoding NADPH-dependent alcohol dehydrogenase Gre2p

Marion Müller and Werner Hummel*

The *S. cerevisiae* strain BY4741-GRE2 expressing the gene encoding NADPH-dependent alcohol dehydrogenase Gre2p, was applied in the synthesis of optically pure (2*S*,5*S*)-hexanediol starting from 2,5-hexanedione. Prior to its use the catalyst was characterised. Thus, when grown in an aerobic environment for 17 h the catalyst displayed its highest cell activity (5.08 U g^{-1}), while under anaerobic conditions the best activity (8.60 U g^{-1}) was reached after 24 h. In the case of temperature and pH dependency, optimal whole-cell activities were obtained in the pH range of 6.0-8.0 and at 25°C to 30°C. Permeabilisation either with toluene or one freeze-thaw cycle did not increase the activity. The use of the co-substrates D-glucose or D-fructose for internal NADPH regeneration gave the highest cell activities. D-sucrose as sole electron source could only be utilised when an invertase was added to the reaction mixture or when the strain had been grown on D-sucrose-supplemented medium before. No activities were obtained when ethanol was supplied as co-substrate. Based on these results, BY4741-GRE2 has been successfully applied in the highly stereoselective bioreduction of 2,5-hexanedione. Even at a substrate concentration of 150 mM the corresponding *γ*-diol was obtained with a high conversion rate of >93%. Additionally, both the space-time yield (48 g L^{-1} d^{-1}) and the co-substrate yield (196 mg g^{-1}) thus obtained were several times higher compared to existing baker's yeast wild-type biotransformations. Overall, the results achieved here demonstrate the great potential of the whole-cell catalyst in the preparative synthesis of (2*S*,5*S*)-hexanediol.

Introduction

Over the last decades biocatalysis has established itself as a key technology in synthetic chemistry (Bornscheuer et al. 2012; Huisman & Collier 2013; Reetz 2013; Turner & O'Reilly 2013; Choi et al. 2015). The advantages of using enzymes or microorganisms are obvious as they catalyse reactions with high regio-, chemo-, and stereoselectivity mostly under mild reaction conditions and in aqueous solutions. Moreover, in many cases, biocatalysts are readily available, sustainable and easy in their handling so that even non-biologists can apply them for their purposes without difficulties (Faber 2011; Faber et al. 2015). Oxidoreductases are of key interest for the industry due to their ability to generate chiral compounds which are valuable building blocks in the production of active pharmaceutical ingredients (API's), fine- and agrochemicals as well as natural products (Hilterhaus & Liese 2007; Muñoz Solano et al. 2012; Patel 2013; Schrittwieser & Resch 2013; Turner & O'Reilly 2013). The oxidoreductases most often employed in organic synthesis are alcohol dehydrogenases (ADHs, E.C. 1.1.1) (Hall & Bommarius 2011; Hollmann et al. 2011). They have been used to synthesise a lot of optically pure hydroxy esters, hydroxy ketones, *β*-hydroxy nitrils and diols (Hoyos et al. 2010; Huisman et al. 2010; Bariotaki et al. 2012; Chen et al. 2012; Xu et al. 2013). ADHs require a stoichiometric amount of the cofactor NAD(P)H which serves as electron carrier. However, due to the fact that nicotinamide cofactors are very expensive, in particular in the reduced form, their stoichiometric use is not feasible in terms of economical applicability. As a consequence, when using isolated enzymes for reduction reactions the cofactor has to be recycled *in situ*; mainly done by coupling another ADH-catalysed reaction (Weckbecker et al. 2010; Wu et al. 2013).

Marion Müller, Prof. Dr. Werner Hummel
Institute of Molecular Enzyme Technology
Research Center Juelich
52426 Juelich, Germany
Tel: (+49)24641 613790
E-mail: w.hummel@fz-juelich.de

One major advantage of applying microorganisms for red-ox reactions is the internal cofactor regeneration and therefore no addition of expensive cofactor is required. Moreover, instead of isolating and purifying the enzymes after cultivation and separation, application of whole-cells require the last two steps only prior to biotransformation. Another advantage is the protection of the enzymes from the surrounding environment by the intracellular medium (Gröger et al. 2006; Goldberg et al. 2007; Carballeira et al. 2009; Tufvesson et al. 2011; Kratzer et al. 2015). Baker's yeast (*Saccharomyces cerevisiae*) is readily available, non-pathogenic and easy to handle and has therefore been applied in various synthesis reactions. Many efficient stereoselective reductions of carbonyl compounds have been reported in literature, e.g. the reduction of ketones, aldehydes, keto esters or diketones (Lieser 1983; Csuk & Glaenzer 1991; Sybesma et al. 1998; Kayser et al. 1999; Bertau & Bürli 2000; Carballeira et al. 2009; Katzberg et al. 2009).

The biotransformation of the *γ*-diketone 2,5-hexanedione to (2*S*,5*S*)-hexanediol has been synthesised through baker's yeast on a preparative-scale (Bertau & Bürli 2000). The diol is a key building block for the production of a variety of chiral auxiliaries (Short et al. 1989; Takada et al. 2001), transition metal catalysts (Burk et al. 1991), and active pharmaceutical intermediates (Díez et al. 2004). However, because of the low quantities of the responsible enzyme within the cells the productivity of the cells is low resulting in long reaction times (24-144 h) (Lieser 1983; Bertau & Bürli 2000; Katzberg et al. 2009).

In a previous paper we have discovered that the NADPH-dependent ADH Gre2p is primarily responsible for the reduction of 2,5-hexanedione in baker's yeast. We have also successfully synthesised (2*S*,5*S*)-hexanediol on laboratory-scale (20 mM) using a cell-free system and glucose dehydrogenase for cofactor regeneration (Müller et al. 2010). However, because the need to isolate both Gre2p and the NADPH-recycling enzyme and the requirement to add external cofactor is disadvantageous, we were encouraged to transfer the cell-free *γ*-diol synthesis to a baker's yeast-mediated whole-cell system.

Herein, we report about the characterisation of a *S. cerevisiae* strain which homologously expresses the gene encoding Gre2p with regard to different growth conditions, pH, temperature, and other parameters. Results thus obtained are then used to develop an efficient whole-cell synthesis of (2*S*,5*S*)-hexanediol at preparative scale.

Materials and methods

General

Unless stated otherwise, all chemicals were obtained from Sigma-Aldrich (Buchs, Swizerland) at the highest purity available and were used without further purification. Nicotinamide cofactors were purchased from Biomol (Hamburg, Germany). The *Saccharomyces cerevisiae* strain, BY4741-GRE2 and the control strain carrying the pDR195 plasmid (Addgene, Cambridge, USA) without a structural gene were generated in our laboratories.

Cultivation under Standard Conditions

20 mL Synthetic medium (SD) (0.77 g L^{-1} Ura-Drop Out supplement (from Clontech Takara Bio Europe (Saint-Germain-en-Laye, France)), 20 g L^{-1} glucose and 6.7 g L^{-1} Yeast Nitrogen Base) in a 100 ml shaking flask was inoculated with a freshly grown clone of *S. cerevisiae* BY4741-GRE2. The culture was incubated for 24 h at 30°C and 120 rpm and was used to inoculate 200 mL SD medium in a 1 L shaking flask at a final concentration of 0.2 optical density at 600 nm (OD_{600}). After cultivation at 30°C for 17 h at 120 rpm cells were harvested by centrifugation at 2820*g* for 30 min.

Preparation of cell-free extract

The cells were suspended in 100 mM triethanolamine hydrochloride buffer (TEA, pH 7.0) at a ratio of 1 g wet cells to 2 mL buffer. After addition of twice the amount of glass beads (ø 0.5-0.7 mm) disruption was carried out by three mixing runs of 5 min using a mixer mill from Retsch (Haan, Germany) with cooling periods in-between. Cell debris was then removed by

centrifugation at 21,910g for 30 min. Protein concentrations were determined according to the protocol described by Bradford using bovine serum albumin as standard (Bradford 1976).

Spectrophotometric measurements of activity

Enzyme activity was determined spectrophotometrically by monitoring the NADPH concentration at 340 nm over 1 min. One unit (1 U) was defined as the amount of enzyme that catalyses the oxidation of 1 µmol NADPH per minute under standard conditions (pH 7.0, 30°C). The assay mixture contained of 970 µL 2,5-hexanedione (20 mM in 100 mM TEA buffer), 20 µL NADPH (12.5 mM in dionised water) and 10 µL enzyme extract.

Activity measurements using gas chromatography analysis

To determine the initial rates at standard conditions (30°C, 800 rpm), 20 mg mL^{-1} fresh cells (wet weight) were suspended in 100 mM TEA buffer (pH 7.0). 1 mL of this suspension was then mixed with 1 mL substrate solution (40 mM benzaldehyde, 200 mM glucose in dionised water). Benzyl alcohol formation was monitored using the gas chromatograph, GC-17A, from Shimadzu (Duisburg, Germany) equipped with a CP-Chirasil-DEX column (25 m x 0.25 mm ID) from Varian (Santa Clara, USA). Samples of 100 µL were taken periodically and mixed with 800 µL ethyl acetate and 100 µL of 2.5 mM octanol (internal standard). The organic layer was analysed using the following temperature program: 60°C for 2 min, 10°C min^{-1} to 135°C and 5°C min^{-1} to 150°C. Cell activity is expressed as U which means µmol benzyl alcohol formed per minute. Cell-specific activity is expressed as U g^{-1} cell wet weight.

Varying parameters for whole-cell characterisation

Alteration of the growth conditions: For anaerobic growth 200 ml SD medium in a 250 ml flask was inoculated from an aerobically grown pre-culture at a final OD$_{600}$ concentration of 0.2. The flasks were closed with a rubber plug and residual oxygen was removed by degassing with argon for

15-20 min. Under gentle shaking the cultures were incubated at 30°C for different incubation times. *Temperature optimum*: Beside the standard condition (30°C) biotransformations were accomplished at 25°, 37°, 45° and 55°C. *pH optimum*: Beside the standard condition (pH 7.0) biotransformations were carried out using 100 mM buffers of different pHs (5.0-8.8); sodium acetate for pH 5.0 and 5.5, TEA for pH 6.0 and tris (hydroxymethyl) aminomethane hydrochloride (TRIS-HCl) for pH 8.0 and 8.8. *Permeability experiment*: Freshly harvested cells were suspended in 100 mM TEA buffer pH 7.0 and were treated with different amounts of toluene (0.1-10% v/v) following incubation for 0.5-1 h at 4°, 30° and 37°C.

General procedure for the bioreduction of 2,5-hexanedione using whole-cells of BY4741-GRE2

Reduction of 2,5-hexanedione is exemplified for the reaction using a substrate concentration of 150 mM. Thus, 2.25 g fresh cells of BY4741-GRE2, harvested after aerobic expression for 17 h at 30°C, were added to a solution of 2.25 mmol 2,5-hexanedione (265 mg) and 6.75 mmol glucose (1.22 g) in 15 ml of 0.5 M potassium phosphate buffer (Kpi pH 7.5). To determine the conversion, samples of 100 µl were taken periodically and diluted with 1.4 ml ethyl acetate. The organic layer was analysed by gas chromatography as described above. To determine the enantiomeric excess (*ee*) 300 µl was taken from the mixture and diluted with 200 µl diethyl ether. Afterwards, the sample was derivatised for 30 min with trifluoroacetic acid anhydride (TFAA) according to the protocol described earlier (Müller et al. 2010). For determination the *ee* value using the same column the temperature of the gas oven was kept at 55°C for 30 min.

Results

Development of a standard reduction reaction to determine whole-cell activities of BY4741-GRE2
Baker's yeast has been used in the synthesis of optically pure (2*S*,5*S*)-hexanediol (Lieser 1983; Bertau & Bürli 2000; Katzberg et al. 2009). The enzyme responsible for the successive

stereoselective reduction of 2,5-hexanedione was found to be the NADPH-dependent ADH, Gre2p (Müller et al. 2010). However, due to low quantities of Gre2p in wild-type cells, cell productivity is low which leads to low reaction velocities. One way to increase the amount of Gre2p in *S. cerevisiae* is the use of a strain expressing the corresponding gene *GRE2*, homologously. Therefore, we have generated the strain BY4741-GRE2 which constitutively expresses the gene under control of the *PMA1* promoter. As a result, the cell-free extract revealed a 120-times higher activity towards 2,5-hexanedione than observed with cell-free extract from wild-type yeast (to be published).

Before applying the strain in the preparative synthesis of (2*S*,5*S*)-hexanediol, the influence of different parameters on its whole-cell activity was investigated. Therefore, the reduction of benzaldehyde to benzyl alcohol was selected as standard reaction (Fig. 1). The model substrate benzaldehyde was chosen over 2,5-hexanedione, which is reduced via the transient formation of the intermediate (5*S*)-hydroxy-2-hexanone, due to its higher applicability and more reliable GC analysis than. Moreover, cell-free extract of BY4741-GRE2 revealed an activity of 3.8 U mg^{-1} towards the aromatic aldehyde which is one-third of the activity obtained with the *γ*-diketone (12.7 U mg^{-1}) (Müller et al. 2010). Initial rates were obtained by measuring the benzyl alcohol concentration over 90 min at 30°C and pH 7.0 in the presence of 100 mM D-glucose which was used for internal cofactor regeneration. Figure 2 illustrates the typical time course for the determination of the initial rate under standard conditions. The linear slope was used to calculate the specific activity which is expressed as U g^{-1} (μmol$_{(product)}$ min^{-1} g$^{-1}_{(cells)}$). Accordingly, BY4741-GRE2 revealed an activity of 5.08 ± 0.2 U g^{-1}. In contrast, the corresponding control strain without any structural gene displayed an activity of 1.12 ± 0.01 U g^{-1}. The standard conditions were then used to examine the influence of different parameters on the activity of the whole-cell catalyst.
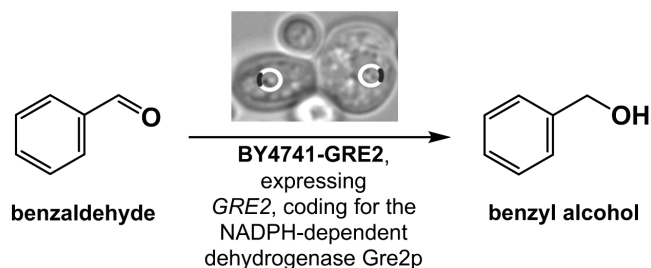

Figure 1. Reaction scheme for the standard reaction catalysed by the yeast strain BY4741-GRE2. Benzaldehyde is reduced into benzyl alcohol by Gre2p. NADPH regeneration is facilitated internally through addition of 100 mM D-glucose.

Effect of cultivation and growth conditions

In order to study the influence of different growth conditions on the cell activity of BY4741-GRE2, the strain was grown under aerobic and anaerobic conditions for 17, 24 and 41 h, respectively. Afterwards, initial rates were determined followed by the calculation of the cell activities. The corresponding results are summarised in Figure 3A. Accordingly, cells obtained after growth in an aerobic environment revealed best cell activities after 17 h (5.08 U g^{-1}, standard) while the highest cell activity (8.60 U g^{-1}) after anaerobic growth was observed after 24 h. Interestingly, with respect to growth at aerobic conditions, activity decreased significantly with longer incubation times with virtually no activity after 41 h. In contrast, cells harvested after an anaerobic growth for 41 h still revealed one-third (2.60 U g^{-1}) of the activity. Furthermore, the wet weight cell biomass per litre was different as well. For example, after 24 h the cell biomass was approximately four-fold higher (4.7 g L^{-1}) when growth was carried out in an aerobic environment than it was after anaerobic growth (1.2 g L^{-1}).

Change of whole-cell activity in dependence of temperature and pH value

Analysis of the pH dependency of the BY4741-GRE2-catalysed biotransformation of benzaldehyde revealed a pH-optimum at 8.0 (5.82 U g^{-1}). At acidic conditions (pH 5.0 and 5.5) a major
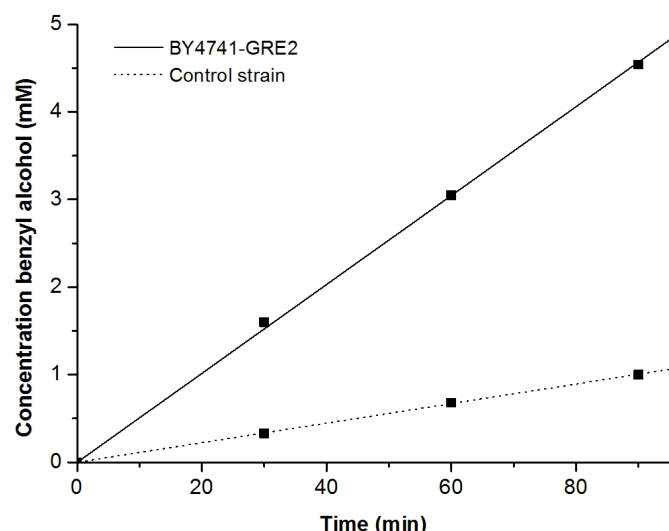
Figure 2. Determination of initial rates for the conversion of 20 mM benzaldehyde over a period of 90 min catalysed either by 10 mg mL^{-1} fresh cells of BY4741-GRE2 or 10 mg mL^{-1} of cells expressing the empty plasmid. Additionally, 100 mM D-glucose was added to the reaction mixture to facilitate internal NADPH regeneration. The standard reaction was carried out at 30°C and pH 7.0. Benzyl alcohol was measured using gas chromatography.

loss of cell activity was observed of 70 and 40%, respectively compared to standard conditions (5.08 U g^{-1}), while at alkaline conditions activity decreased only slightly (3%) up to pH 8.8. In summary, the results show that optimal bioreduction activities are obtained in the pH range of 6.0 to 8.0 (Fig. 3B).

In order to examine the influence of temperature on the catalyst activity, biotransformations were carried out at different temperatures. Hence, BY4741-GRE2 activity was twice as high at 37°C than at 30°C (standard condition). The highest cell activity was observed at 45°C with 12.7 U g^{-1} which is 2.5-fold higher than under standard conditions. Higher temperatures led to a complete loss of activity. Due to the fact that cell activity at 25°C (4.49 U g^{-1}) differs only slightly from that monitored at 30°C, biotransformation can be considered at this temperature as well (Fig 3 B).

Effect of toluene treatment and freezing and thawing on the activity of the catalyst

Toluene treatment is a way to make yeast cells permeable to exogenous substrates (Murakami et al. 1980; Sybesma, Straathof et al. 1998). Therefore, cells of BY4741-GRE2 were treated with different concentrations of toluene before

determination of the initial rates. Surprisingly, as shown in Figure 3C, toluene treatment did not have any effect on increasing the activity of BY4741-GRE2. At concentration above 0.5% (v/v) cell specific activities were even significantly below the activity observed with untreated cells (standard). In comparison, cells subjected to one freeze-thaw cycle exhibited 75% (3.77 U g^{-1}) of the standard activity.

The Influence of the co-substrate on the whole-cell activity

Since Gre2p is NADPH-dependent an optimal recycling system is required to maintain optimal bioreduction activity. In order to investigate the influence of different co-substrates and concentrations thereof on the activity of the catalyst, biotransformations were accomplished at different concentrations of D-glucose and at altering concentrations of the co-substrates D-fructose, D-sucrose, and ethanol.

The corresponding results are illustrated in Figure 4. Accordingly, when D-glucose (10-500 mM) or D-fructose (100-500 mM) were employed as energy source, respectively cell specific activities were either similar to the standard activity (100 mM glucose) or slightly higher (up to ~1.3-fold). In contrast, when D-sucrose (100-500 mM) was used as co-substrate cell specific activities were just 20% of the activity obtained under standard conditions. However, when an invertase was added to the reaction mixture the activity was increased and was as high as the standard activity indicating that the sugar had been digested into D-glucose and D-fructose. Moreover, a cell activity of 2.95 U g^{-1} was achieved when BY4741-GRE2 had been cultivated on medium containing D-sucrose (20 g L^{-1}) in place of D-glucose (data not shown).

Ethanol (100-500 mM) as energy source instead of a carbohydrate was investigated as well. However, specific activities of BY4741-GRE2 were on average 10.5-times (Ø 0.48 U g^{-1}) lower than in comparison to the activity reached under standard conditions. Without co-substrate no activity was observed.
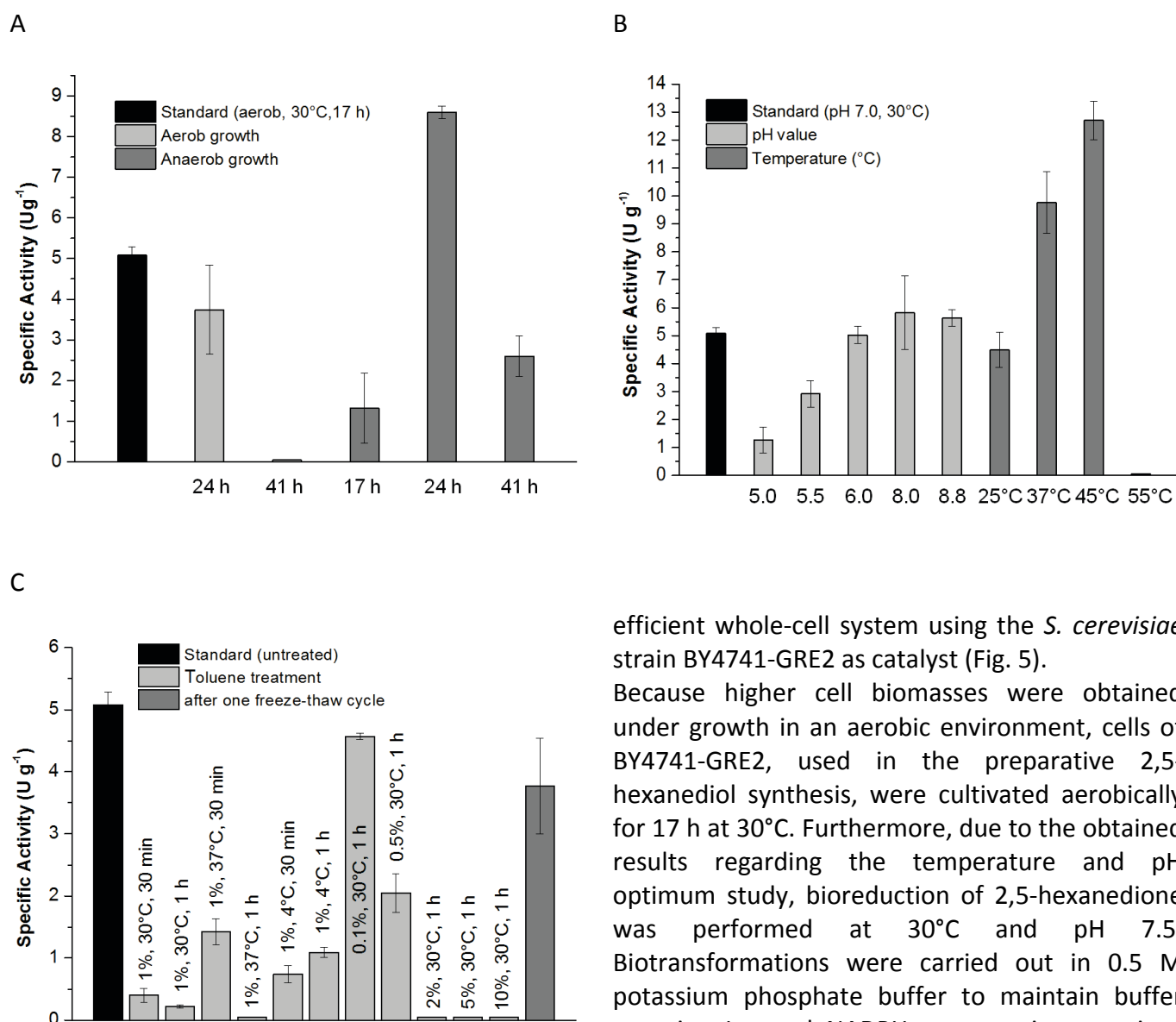
A

B

C

Figure 3. Influence of different parameters on the specific cell activity in the reduction of benzaldehyde. Specific activities at (A) different growth conditions, (B) different pH values and temperatures, and after (C) toluene treatment and one freeze-thaw cycle. The activity obtained under standard conditions is set black. The results were obtained from at least three independent measurements.

Bioreduction of 2,5-hexanedione into enantiomerically pure (2S,5S)-hexanediol

Enantiopure (2S,5S)-hexanediol is a versatile building block in the synthesis of a variety of different chiral auxiliaries, fine chemicals, and pharmaceuticals. Therefore, we were encouraged to transfer the results of the cell-free system to an

efficient whole-cell system using the *S. cerevisiae* strain BY4741-GRE2 as catalyst (Fig. 5).

Because higher cell biomasses were obtained under growth in an aerobic environment, cells of BY4741-GRE2, used in the preparative 2,5-hexanediol synthesis, were cultivated aerobically for 17 h at 30°C. Furthermore, due to the obtained results regarding the temperature and pH optimum study, bioreduction of 2,5-hexanedione was performed at 30°C and pH 7.5. Biotransformations were carried out in 0.5 M potassium phosphate buffer to maintain buffer capacity. Internal NADPH regeneration reactions was achieved by the addition of D-glucose as energy source for all biotransformations.

Table 1 summarises the results of the bioreduction of different concentrations of 2,5-hexanedione catalysed by BY4741-GRE2. Accordingly, at any concentration an almost full conversion (>93%) to (2S,5S)-hexanediol was achieved at excellent enantiomeric purity (*ee*>99%). It is worth mentioning that the reduction ability is reduced at *γ*-diketone concentrations >100 mM as the incubation times were slightly increased. This is also reflected by the space-time yields (STY) which were directly proportional from 20 to 100 mM but increased only marginally up to 120 and 150 mM diketone concentration. Nevertheless, for the reduction of 150 mM of 2,5-hexanedione a STY of
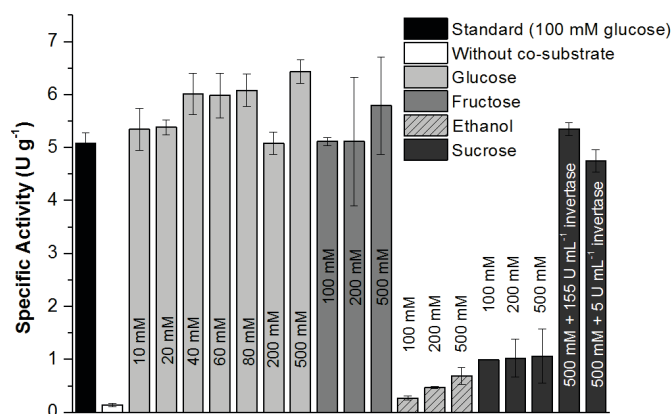
Figure 4. Specific activities of BY4741-GRE2 at altering concentration of D-glucose, D-fructose, ethanol and D-sucrose. The activity obtained under standard conditions is set black. The results were obtained from at least three independent measurements.

Figure 5. Scheme of the two-stage reduction of 2,5-hexanedione to (2S,5S)-hexanediol catalysed by BY4741-GRE2. D-glucose was added as energy source to the reaction mixture for internal NADPH regeneration.

first reduction step, activity diminished gradually, but to a much lower extent than observed for the reduction of 2,5-hexanedione.

Optimisation of the co-substrate yield

The co-substrate yield - the amount of product formed per amount of consumed co-substrate - is of great economic interest for whole-cell biotransformations. The higher this parameter, the lower the production costs due to the fact that less co-substrate is needed. Because of this, we were encouraged to optimise the BY4741-GRE2-mediated biotransformation of 2,5-hexanedione towards a high co-substrate yield.

To meet this objective, the biotransformation of 150 mM γ-diketone (17.6 g L^{-1}) at altering D-glucose concentrations (150, 300, 450, and 600 mM) was investigated. The amount of yeast cells (150 g L^{-1}) applied was kept the same for any reaction. The corresponding results are summarised in Table 2. Thus, the maximum co-substrate yield with 222 mg g^{-1} was achieved when 300 mM D-glucose (54 g L^{-1}) was used. However, as only two-third of the diketone was converted to (2S,5S)-hexanediol this condition would not be economically viable. An increase of the glucose concentration to 450 mM (81.1 g L^{-1} glucose) led to a conversion rate of 89.9% and a co-substrate yield of 196 mg g^{-1}. Due to the fact that at higher D-glucose concentrations only a slight increase in conversion rate (93.1%) was observed 450 mM D-glucose was necessary to yield the best co-substrate yield.

Discussion

In the present study a *Saccharomyces cerevisiae*

49.5 g L^{-1} d^{-1} was achieved which is 5.5-fold higher compared to the reduction of 20 mM diketone.

Calculation of the reduction rates (mM h^{-1}) for both reduction steps reveal in-depth analysis of the biotransformations. The corresponding results are illustrated in Figure 6A. Thus, reduction of 2,5-hexanedione is favoured over the hydroxy ketone. Moreover, as expected, the reduction rate was nearly twice as high at 40 mM diketone concentration than it was at 20 mM. At concentration >40 mM, the reduction rate of the first reduction step was no longer directly proportional to the concentration of 2,5-hexanedione. Likewise, the reduction rate for the second step was two-times higher at 40 mM 2,5-hexanedione than at 20 mM but increased only by a factor of 1.5 and 1.3 up to 60 and 80 mM of γ-diketone, respectively. Up to 150 mM diketone the hydroxy ketone reduction rate raised only slightly.

The activity of the whole-cell catalyst (U g^{-1}) was calculated as well and is shown in Figure 6 B. Thus, cell activities for the first reduction step were significantly higher for any 2,5-hexanedione biotransformation. With respect to the reduction of the diketone the highest cell activity was achieved for bioreduction of 20 mM 2,5-hexanedione. At higher diketone concentrations the activity of BY4741-GRE2 decreased steadily. The highest cell activity for the hydroxy ketone reduction was obtained when 60 mM 2,5-hexanedione was employed. Then, similarly to the
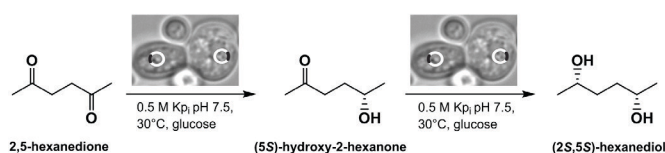
Table 1. Asymmetric reduction of 2,5-hexanedione at increased substrate concentrations catalysed by whole-cells of BY4741-GRE2.

2,5-hexanedione concentration (mM)	Glucose concentration (mM)	Cells (g L^{-1})	Time (h)	Conversion (%)	Space-time yield (g L^{-1} d^{-1})	ee (%)
20	100	20	6	95.4	8.97	>99
40	200	40	6	95	17.9	>99
60	300	60	6	95.5	26.9	>99
80	400	80	6	95.9	35.9	>99
100	500	100	6	95.7	44.8	>99
120	600	120	7	93.7	46.5	>99
150	750	150	8	93.2	49.5	>99

A

B
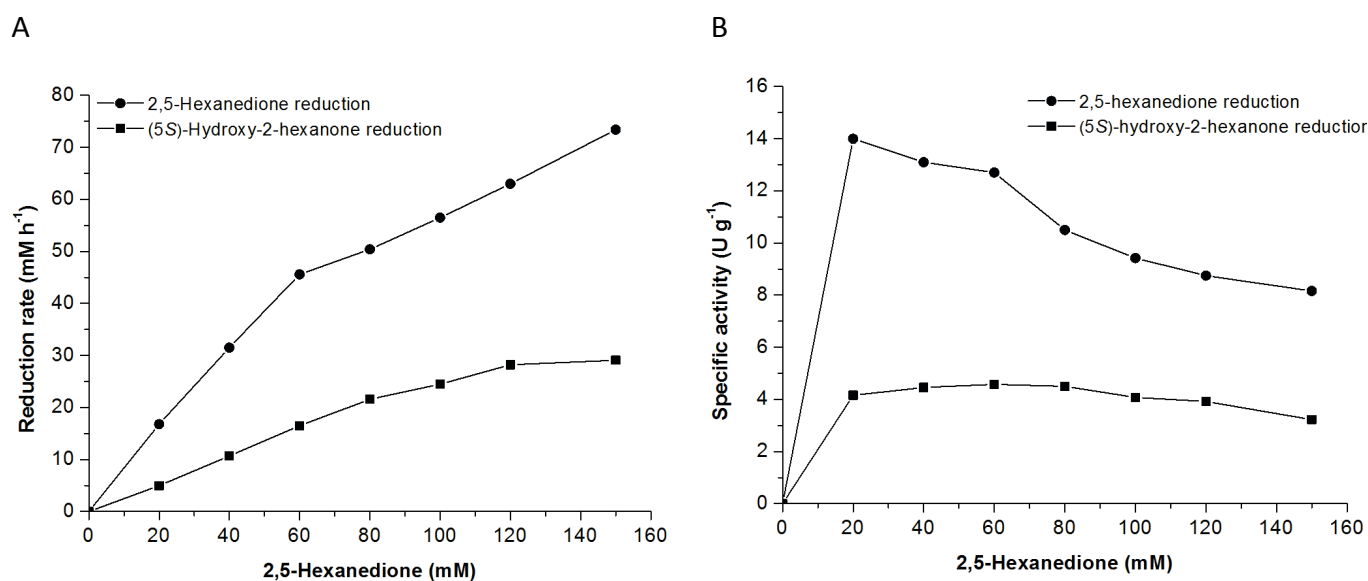
Figure 6. Demonstration of the effect of different 2,5-hexanedione concentrations on the reduction rates (A) and the specific activities (B) calculated for both reduction steps catalysed by BY4741-GRE2. Calculations are derived from the biotransformations summarised in Table 1.

whole-cell catalyst, which homologously expresses the NADPH-dependent alcohol dehydrogease gene *GRE2*, was characterised.

Because pH and temperature are crucial parameters, the dependence of the catalyst on these parameters has been investigated. The catalyst was found to be most active in the pH range of 6.0 to 8.0 which is also the range where isolated Gre2p was demonstrated to display its highest reduction activity. The temperature at which the yeast catalyst reveals its highest specific

Table 2. Whole-cell bioreduction of 150 mM (17.6 g L^{-1}) 2,5-hexanedione catalysed by 150 g L^{-1} BY4741-GRE2 cells. Biotransformation was performed as described above using fresh cells aerobically grown at 30°C for 17 h.

Glucose (mM)	Glucose (g L^{-1})	Conversion (%)	(2S,5S)-hexanediol (mM)	(2S,5S)-hexanediol (g L^{-1})	Co-substrate yield (mg$_{(2S,5S)\text{-hexanediol}}$ g$^{-1}_{glucose}$)
150	27	25.1	37.7	4.44	164
300	54	68	102	12	222
450	81.1	89.8	135	15.9	196
600	108.1	93.1	140	16.5	153

activity was about 10°C lower than the one found for isolated enzyme (Müller et al. 2010), most likely due to the loss of cell viability at higher temperatures.

Regarding the use of different co-substrates as energy source we could show that the use of D-fructose yielded cell activities similar to D-glucose. This is not surprising as following the uptake both sugars are phosphorylated and in case of D-fructose also isomerised, to glucose-6-phoshate (Bisson & Fraenkel 1983; Aguilera & Zimmermann 1986). Glucose-6-phoshate then enters the pentose phosphate pathway which is mainly responsible for NADPH regeneration in *S. cerevisiae* providing two moles of NADPH per one mole of glucose-6-phoshate (Bruinenberg 1986).

The use of D-sucrose as co-substrate led to significantly lower cell activities compared to the use of D-glucose or D-fructose. However, the activities were increased by delivering an invertase to the reaction medium. Another way to boost cell activity was achieved through cell growth in the presence of D-sucrose (20 g L^{-1}) instead of D-glucose. Due to the fact that hydrolysis of D-sucrose occurs very gradually (Wolfenden & Yuan 2008) it can be concluded that an invertase was produced by BY4741-GRE2 when cultivated on medium supplemented with the disaccharide. Despite the fact that the gene encoding the two different forms of invertase (internal and external enzyme) is a constitutive genomic component, invertase activity varies

significantly in different *S. cerevisiae* strains attributed to different transcription levels. Thus, in comparison to other wild-type strains, e.g. L610, NCYC625 the invertase activity of BY4741 was considerably low (Yang et al. 2015). This matter of fact help explain why cell activities with D-sucrose as co-substrate were lower than with either monosaccharide.

When ethanol was supplied as energy source cell activities were significantly below the standard. An explanation could be the formation of acetic acid which might have affected the diol synthesis negatively due to its toxicity (Sybesma et al. 1998). The yeast catalyst has also been successfully applied in the asymmetric synthesis of highly optically pure (2S,5S)-hexanediol, even at substrate concentrations of 150 mM. We have also demonstrated that BY4741-GRE2 catalyses the first reduction step faster than the second one leading to a transient accumulation of the intermediate. This is in agreement with observations made by Katzberg et al. who therefore concluded a higher affinity of Gre2p towards the diketone than the hydroxy ketone (Katzberg et al. 2009). However, calculation of both the reduction rates and specific cell activities revealed that the efficiency of the bioreduction diminished at diketone concentrations >40 mM. As this was not observed with isolated Gre2p (to be published) it can be assumed that the biotransformation is affected by either high concentrations of the substrate, hydroxy ketone

Table 3. Comparison of the parameters obtained for the bioreduction of 2,5-hexanedione catalysed by BY4741-GRE2 with data reported elsewhere.

Strain	2,5-hexanedione (mM)	Cells (g L^{-1})	Carbon source	Carbon source (g L^{-1})	Time (h)	Conversion (%)	ee (%)	(2S,5S)-hexanediol (g L^{-1})	Co-substrate yield (mg g^{-1})	Space-time yield (g (L^{-1} d^{-1})	Productivity (mg$_{(2S,5S)\text{-hexanediol}}$ g$^{-1}_{cells}$)	Ref.
Wild-type Budweiser baker's yeast	50	80	sucrose	215	144	95	≥95	5.61	26.1	0.94	70.1	(Lieser 1983)
Wild-type SCL13	80	125	sucrose	100	48	93	>99	8.78	87.8	4.39	70.2	(Katzberg et al. 2009)
BY4741-GRE2	150	150	glucose	81.1	8	89.8	>99	15.9	196	48	106	this work

or both compounds. Inhibitory effects of the synthesis of (2S,5S)-hexanediol catalysed by baker's yeast was also observed by Meitian et al. They found that at 2,5-hexandione concentrations ≥100 mM not the production of the hydroxy ketone was influenced but the synthesis of the diol was inhibited by excess accumulation (>30 mM) of intermediate (Meitian et al. 2009).

In Table 3, data and parameters obtained from the stereoselective reduction of 2,5-hexanedione carried out with conventional baker's yeast (Lieser 1983; Katzberg et al. 2009) are summarised and compared with the results from our study. Thus, using BY4741-GRE2 the conversion time was considerably lower in comparison to the biotransformations performed with wild-type yeast cells. Additionally, the obtained space-time yield was 11- and 51-fold higher than it was with SCL13 and Budweiser yeast, respectively. Furthermore, the co-substrate yield was improved by 2.2- and 7.5-times respectively. Finally, the cell productivity was 1.5-fold higher in comparison to both, SCL13 and Budweiser yeast due to higher quantities of Gre2p produced by BY4741-GRE2.

Conclusion

In this study we have demonstrated the successful development of an efficient biocatalytic synthesis route to the chiral building block (2S,5S)-hexanediol. Using a *S. cerevisiae* catalyst, homologously expressing the gene encoding NADPH-dependent alcohol dehydrogenase Gre2p, the diol was synthesised with excellent conversion yields and enantiomeric excess, even on a preparative-scale. Additionally, the space-time

yield, co-substrate yield and cell productivity thus obtained were higher compared to existing wild-type baker's yeast-mediated 2,5-hexanedione biotransformations.

Acknowledgement

References

Aguilera A, Zimmermann FK. 1986. Isolation and molecular analysis of the phosphoglucose isomerase structural gene of *Saccharomyces cerevisiae*. Mol. Gen. Genet. 202:83 89.

Bariotaki A, Kalaitzakis D, Smonou I. 2012. Enzymatic reductions for the regio- and stereoselective synthesis of hydroxy-keto esters and dihydroxy esters. Org. Lett. 14:1792-1795.

Bertau M, Bürli M. 2000. Enantioselective microbial reduction with baker's yeast on an industrial scale. Chimia 54:503-507.

Bisson LF, Fraenkel DG. 1983. Involvement of kinases in glucose and fructose uptake by *Saccharomyces cerevisiae*. Proc. NatL Acad. Sci. U.S.A. 80:1730-1734.

Bornscheuer UT, Huisman GW, Kazlauskas RJ, Lutz S, Moore JC, Robins K. 2012. Engineering the third wave of biocatalysis. Nature 485:185-194.

Bradford MM. 1976. Rapid and sensitive method for quantitation of microgram quantities of protein utilizing principle of protein-dye binding. Anal. Biochem. 72:248-254.

Bruinenberg PM. 1986. The NADP(H) redox couple in yeast metabolism. Antonie van Leeuwenhoek 52:411-429.

Burk MJ, Feaster JE, Harlow RL. 1991. New chiral phospholanes: Synthesis, characterization, and use in asymmetric hydrogenation reactions. Tetrahedron: Asymmetry 2:569-592.

Carballeira JD, Quezada MA, Hoyos P, Simeó Y, Hernaiz MJ, Alcantara AR, Sinisterra JV. 2009. Microbial cells as catalysts for stereoselective red-ox reactions. Biotechnol. Adv. 27:686-714.

Chen Y, Chen C, Wu X. 2012. Dicarbonyl reduction by single enzyme for the preparation of chiral diols. Chem. Soc. Rev. 41:1742-1753.

Choi JM, Hamn SS, Kim HS. 2015. Industrial applications of enzyme biocatalysis: Current status and future aspects. Biotechnol. Adv. 33:1443–1454.

Csuk R, Glaenzer BI. 1991. Baker's yeast mediated transformations in organic chemistry. Chem. Rev. 91:49-97.

Díez E, Fernández R, Marqués-López E, Martín-Zamora E, Lassaletta JM. 2004. Asymmetric synthesis of *trans*-3-amino-4-alkylazetidin-2-ones from chiral *N,N*-dialkylhydrazones. Org. Lett. 6:2749-2752.

Faber K. 2011. Biotransformations in organic chemistry. Berlin: Springer-Verlag.
Faber K, Fessner WD, Turner NJ. 2015. Biocatalysis in Organic Synthesis (3 volumes). Stuttgart: Thieme Verlag.

Goldberg K, Schroer K, Lütz S, Liese A. 2007. Biocatalytic ketone reduction: A powerful tool for the production of chiral alcohols - part II: Whole-cell reductions. Appl. Microbiol. Biotechnol. 76:249-255.

Gröger H, May O, Werner H, Menzel A, Altenbuchner J. 2006. A "second-generation process" for the synthesis of L-neopentylglycine: Asymmetric reductive amination using a recombinant whole cell catalyst. Org. Process Res. Dev. 10:666-669.

Hall M, Bommarius AS. 2011. Enantioenriched compounds *via* enzyme-catalyzed redox reactions. Chem. Rev. 111:4088-4110.

Hilterhaus L, Liese A. 2007. Building Blocks. In: Ulber R, Sell D, Editors. White Biotechnology. Berlin: Springer-Verlag. pp. 133-173.

Hollmann F, Arends IWCE, Holtmann D. 2011. Enzymatic reductions for the chemist. Green Chem. 13:2285-2314.

Hoyos P, Sinisterra JV, Molinari F, Alcántara AR, De María PD. 2010. Biocatalytic strategies for the asymmetric synthesis of *α*-hydroxy ketones. Accounts Chem. Res. 43:288-299.

Huisman GW, Collier SJ. 2013. On the development of new biocatalytic processes for practical pharmaceutical synthesis. Curr. Opin. Chem. Biol. 17:284-292.

Huisman GW, Liang J, Krebber A. 2010. Practical chiral alcohol manufacture using ketoreductases. Curr. Opin. Chem. Biol. 14:122-129.

Katzberg M, Wechler K, Müller M, Dünkelmann P, Stohrer J, Hummel W, Bertau M. 2009. Biocatalytical production of (5*S*)-hydroxy-2-hexanone. Org Biomol Chem. 7:304-314.

Kayser MM, Mihovilovic MD, Kearns J, Feicht A, Stewart JD. 1999. Baker's yeast-mediated reductions of *α*-keto esters and an *α*-keto-*β*-lactam: Two routes to the paclitaxel side chain. J. Org. Chem. 64:6603-6608.

Kratzer R, Woodley JM, Nidetzky B. 2015. Rules for biocatalyst and reaction engineering to implement effective, NAD(P)H-dependent, whole cell bioreductions. Biotechnol. Adv. 33:1641-1652.

Lieser JK. 1983. A Simple Synthesis of (*S,S*)-2,5-hexanediol. Synth. Commun. 13:765-767.

Meitian X, Jing Y, Yawu Z, Yayan H. 2009. Reaction characteristics of asymmetric synthesis of (2*S*,5*S*)-2,5-hexanediol catalyzed with baker's yeast number 6. Chin. J. Chem. Eng. 17:493-499.

Müller M, Katzberg M, Bertau M, Hummel W. 2010. Highly efficient and stereoselective biosynthesis of (2*S*,5*S*)-hexanediol with a dehydrogenase from *Saccharomyces cerevisiae*. Org. Biomol. Chem. 8:1540-1550.

Muñoz Solano D, Hoyos P, Hernáiz MJ, Alcántara AR, Sánchez-Montero JM. 2012. Industrial biotransformations in the synthesis of building blocks leading to enantiopure drugs. Bioresour. Technol. 115:196-207.

Murakami K, Nagura H, Yoshino M. 1980. Permeabilization of yeast cells: Application to study on the regulation of AMP deaminase activity in situ. Anal. Biochem. 105:407-413.

Patel RN. 2013. Biocatalytic synthesis of chiral alcohols and amino acids for development of pharmaceuticals. Biomolecules 3:741-777.

Reetz MT. 2013. Biocatalysis in organic chemistry and biotechnology: Past, present, and future. J. Am. Chem. Soc. 135:12480-12496.

Schrittwieser JH, Resch V. 2013. The role of biocatalysis in the asymmetric synthesis of alkaloids. RSC Advances 3:17602-17632.

Short RP, Kennedy RM, Masamune S. 1989. An improved synthesis of (-)-(2*R*,5*R*)-2,5-dimethylpyrrolidine. J. Org. Chem. 54:1755-1756.

Skorupa Parachin N, Carlquist M, Gorwa-Grauslund MF. 2009. Comparison of engineered *Saccharomyces cerevisiae* and engineered *Escherichia coli* for the production of an optically pure keto alcohol. Appl. Microbiol. Biotechnol. 84:487-497.

Sybesma WFH, Straathof AJJ, Jongejan JA, Pronk JT, Heijnen JJ. 1998. Reductions of 3-oxo esters by baker's yeast: Current status. Biocatal. Biotransform. 16:95-134.

Takada H, Metzner P, Philouze C. 2001. First chiral selenium ylides used for asymmetric conversion of aldehydes into epoxides. Chem. Commun.:2350-2351.

Tufvesson P, Lima-Ramos J, Nordblad M, Woodley JM. 2011. Guidelines and cost analysis for catalyst production in biocatalytic processes. Org. Process Res. Dev. 15:266-274.

Turner NJ, O'Reilly E. 2013. Biocatalytic retrosynthesis. Nat. Chem. Biol. 9:285-288.

Weckbecker A, Gröger H, Hummel W. 2010. Regeneration of nicotinamide coenzymes: Principles and applications for the synthesis of chiral compounds. Adv. Biochem. Eng./Biotechnol. 120:195-242.

Wolfenden R, Yuan Y. 2008. Rates of spontaneous cleavage of glucose, fructose, sucrose, and trehalose in water, and the catalytic proficiencies of invertase and trehalas. J. Am. Chem. Soc. 130:7548–7549.

Wu H, Tian C, Song X, Liu C, Yang D, Jiang Z. 2013. Methods for the regeneration of nicotinamide coenzymes. Green Chem. 15:1773-1789.

Xu GC, Yu HL, Zhang ZJ, Xu JH. 2013. Stereocomplementary bioreduction of *β*-ketonitrile without ethylated byproduct. Org. Lett. 15:5408–5411.

Yang F, Liu ZC, Wang X, Li LL, Yang L, Tang WZ, Yu ZM, Li X. 2015. Invertase Suc2-mediated inulin catabolism is regulated at the transcript level in *Saccharomyces cerevisiae*. Microb. Cell. Fact. 14:1-10.

4.3

Construction and characterisation of *Escherichia coli* whole-cell catalysts co-producing *Saccharomyces cerevisiae* alcohol dehydrogenase Gre2p and glucose dehydrogenase and their application in the synthesis of (2*S*,5*S*)-hexanediol

Marion Müller and Werner Hummel

Manuscript in preparation

Construction and characterisation of *Escherichia coli* whole-cell catalysts co-producing *Saccharomyces cerevisiae* alcohol dehydrogenase Gre2p and glucose dehydrogenase and their application in the synthesis of (2*S*,5*S*)-hexanediol.

Marion Müller and Werner Hummel*

Two *E. coli* whole-cell catalysts co-expressing the NADPH-dependent alcohol dehydrogenase Gre2p from *Saccharomyces cerevisiae* and the glucose dehydrogenase (GDH) from *Bacillus subtilis* were designed. Because two different plasmids were constructed with the genes in reverse order, the strains BL21-GRE2-gdh and BL21-gdh-GRE2 differ from each other, leading to reversed Gre2p : GDH activity ratios. Best cell activities (18.4 and 21.1 U/g) were observed after cultivation in LB medium at 37°C for 5 h and in autoinduction medium (AI) at 37°C for 24 h, respectively. A characterisation study revealed an optimal temperature and pH range of 25°-37°C and 6.0-8.0. In addition, an increase of cell activity by a factor of three was observed when the cells were permeabilised. A 7-fold increase in activity was observed when NADP$^+$ (≥0.5 mM) was added to these cells. Both catalysts were successfully applied in the synthesis of optically pure (2*S*,5*S*)-hexanediol (≥95%, *ee*>99%). Using BL21-gdh-GRE2, up-scaling of this process was feasible. Thus, 0.5 and 1M diketone was reduced to the corresponding (*S*,*S*)-diol, resulting in excellent space-time yields (361 and 572 g/(L·d)) and cell productivities (467 and 451 $mg_{(2S,5S)\text{-hexanediol}}/g_{cells}$).

1. Introduction

The past two decades have seen a steadily increasing use of enzymatic processes in organic synthesis, especially for the production of chiral compounds [1-6]. In contrast to conventional chemical synthesis routes, enzymes carry out reactions with higher regio-, chemo- and stereoselectivity, limiting the number of reaction steps as well as the occurrence of unwanted products and side reactions. Additionally, they are able to work under mild conditions and are mostly readily available, cheap, health friendly, renewable and easy to handle [7, 8].

Oxidoreductases are of great industrial interest because of their applicability in asymmetric synthesis. The chiral compounds thus produced can act as valuable building blocks for the manufacture of fine chemicals, agrochemicals, natural products and pharmaceuticals [9-15]. Alcohol dehydrogenases (ADHs, E.C. 1.1.1) are the most commonly applied oxidoreductases [16-18]. They have been used to synthesise a broad spectrum of chiral hydroxy esters, numerous hydroxy ketones, alcohols, and diols [19-24].

To maintain reductive catalytic activity, ADHs depend on stoichiometric amounts of the cofactor NAD(P)H. However, as nicotinamide cofactors are very expensive, especially in their reduced form, a stoichiometric use is not economically feasible. Therefore, much effort has been made to develop efficient *in situ* recycling methods. As a consequence, a number of chemical, electrochemical, photochemical and enzymatic recycling methods have been established [25-27]. The latter have proven the most efficient due to their high selectivity for the active cofactor form and high compatibility with other enzymes and reagents [26]. Because glucose dehydrogenase (GDH) is able to regenerate both NADH and NADPH with high specific activities it has been

Marion Müller, Prof. Dr. Werner Hummel
Institute of Molecular Enzyme Technology
Research Center Juelich
52426 Juelich, Germany
Tel: (+49)24641 613790
E-mail: w.hummel@fz-juelich.de

preferentially coupled to many enantioselective reduction reactions as demonstrated by the many examples found in the literature [28-32]. The γ-diol (2S,5S)-hexanediol is a valuable building block as it serves as starting material for the preparation of a variety of chiral auxiliaries and chiral phosphorus (III) ligands [33-37]. It is also a precursor in the production of β-lactam antibiotics [38]. It has been synthesised chemically through either hydrogenation or hydrosilylation of the corresponding diketone 2,5-hexanedione or chemoenzymatically through enzymatic acylation of rac-2,5-hexanediol using lipases [39-41]. Despite the high enantioselectivities achieved in most cases, the moderate yields, low atom economies, numerous side reactions, and the use of toxic reagents as well as organic solvents are however not favourable for industrial applications. The preparative synthesis of (2S,5S)-hexanediol is, nowadays, carried out via baker's yeast biotransformation of 2,5-hexanedione [42, 43]. However, despite its benefits, such as the high stereoselectivity, yield, and atom economy, the drawbacks are the long reaction time, the accumulation of the mono reduction product and the use of only low diketone concentrations [44]. Because these are the result of low quantities of diketone reducing enzyme present in the cells a recombinant production system was aspired.

In a previous paper we reported on the identification and recombinant production of the NADPH-dependent alcohol dehydrogenase Gre2p from S. cerevisiae and were able to show its successful application in the synthesis of optically pure (2S,5S)-hexanediol by a cell-free system [45]. However, because of the need for isolated enzymes and the addition of the expensive cofactor NADP$^+$, up-scaling of the process is inappropriate for economic reasons.

A very cost-efficient way to overcome the problem of cofactor regeneration and to improve and simplify the process is the use of a whole-cell catalyst which co-expresses a cofactor recycling gene along with the alcohol dehydrogenase gene in a single cell [26]. The benefits are clear, as isolation and purification of the enzymes is not required. Additionally, external cofactor addition is not essential [46, 47]. Therefore, it is no wonder that such "designer" catalysts have been frequently used for asymmetric synthesis reactions [30-32, 48-51].

Following our cell-free synthesis of (2S,5S)-hexanediol using Gre2p and GDH, in this study we constructed two E. coli whole cell catalysts which produce both enzymes simultaneously. The catalysts have different plasmids, because the order of the corresponding genes was reversed. We carried out a characterisation study to find the optimal conditions for the catalysts. Both catalysts were then applied in the synthesis of (2S,5S)-hexanediol.

2. Experimentals

2.1. Chemicals, materials and equipments

If not stated otherwise, all chemicals were obtained from Sigma-Aldrich (Buchs, Swizerland) at the highest purity available and were used without further purification. The nicotinamide cofactors, NADPH and NADP$^+$ were purchased from Biomol (Hamburg, Germany) and restriction enzymes and T4-DNA ligase were obtained from Fermentas (St. Leon-Rot, Germany). The plasmid pACYCDuet-1 and the Escherichia coli expression strain BL21(DE3) were purchased from Novagen (Madison, USA).

2.2. Construction of the E. coli whole-cell catalysts

For construction of pACYCDuet-GRE2-gdh, an E. coli codon-optimised GRE2 gene (not yet published) was amplified, flanking the restriction sites BsaI and HindIII. The commercially available pACYCDuet-1 was digested with NotI and HindIII. It is important to mention that using BsaI causes the loss of the plasmid's NcoI site after insertion of the gene. The glucose dehydrogenase gene, gdh, from Bacillus subtilis was amplified from pAW-3 [52] and was cloned into pACYCDuet-GRE2 using NdeI and XhoI restriction sites.

The plasmid pACYCDuet-gdh-GRE2 contains the genes in reverse order. Accordingly, the gdh gene was amplified flanking the restriction sites BsaI and HindIII, and GRE2 was amplified, introducing the sites NdeI and XhoI. The sequences of the primers utilised for PCR are summarised in Table1.

Table 1. Primers utilised for the construction of the expression plasmids, pACYCDuet-GRE2-gdh and pACYCDuet-gdh-GRE2. Restrictions sites are in bold.

5'-upstream-3'	5'-downstream-3'	Fragment	Construct
TGCC**GGTCTCGC**ATGAGCGTGTTTGT	CCC**AAGCTT**TTATTAGATACGGC CTTCAAATTTCAG	*Bsa*I-GRE2-*Hind*III for MCSI	pACYCDuet-GRE2-gdh
GGGAATTC**CATATG**TATCCGG ATTTAAAAGGAAAAG	CCG**CTCGAG**TTATTAACCGCGGCCT	*Nde*I-gdh-*Xho*I for MCSII	
GGGAATTC**CATATG**AGCGTGTTT GTGAGC	CCG**CTCGAG**TTATTAGATACGGC CTTCAAATT	*Nde*I-GRE2-*Xho*I for MCSII	pACYCDuet-gdh-GRE2
TGCC**GGTCTCGC**ATGTATCCG GATTTAAAA	CCC**AAGCTT**TTATTAACC GCG GCC TGC	*Bsa*I-gdh-*Hind*III for MCSI	

2.3. Cell cultivation at standard conditions

A fresh clone of *E. coli* BL21(DE3) cells carrying either pACYCDuet-GRE2-gdh or pACYCDuet-gdh-GRE2 was utilised to inoculated 10 mL LB medium (10 g/L NaCl, 10 g/L tryptone and 5 g/L yeast extract) supplemented with 34 µg/mL chloroamphenicol (CM). The culture was incubated overnight at 37°C and 120 rpm and was used to inoculate 100 mL LB medium (containing 34 µg/mL CM) at a final concentration of 0.05 optical density at 600 nm (OD_{600}). This culture was then grown at 37°C and 120 rpm. When the OD_{600} reached a value between 0.5 and 0.7, gene expression was started by the addition of isopropyl thio-β-D-galactoside (IPTG) to a finalconcentration of 0.2 mM. After 5 h cultivation at 37°C and 120 rpm, the cells were harvested by centrifugation at 2,820*g* for 30 min. Unless stated otherwise, only fresh cells were used for the characterisation.

2.4. Preparation of cell-free extract

The cells were suspended in 100 mM triethanolamine hydrochloride buffer (TEA, pH 7.0) at a ratio of 1 g (wet weight) to 4 mL buffer. Cell disruption was carried out via three sonification cycles of 2 min at 36-37% power output (Bandelin electronic, Berlin, Germany) with cooling periods in-between. Cell debris was removed by centrifugation at 21,910*g* for 30 min. Protein concentration was determined according to Bradford, using bovine serum albumin (BSA) as

standard [53]. SDS-PAGE electrophoresis was performed as described by Laemmli [54], using a 4–12% Nu-PAGE Novex Bis-Tris gel from Invitrogen (Karlsruhe, Germany).

2.5. Spectrophotometric measurements of activity

Enzyme activity was determined spectrophotometrically by monitoring the NADPH concentration at 340 nm over 1 min during reduction or oxidation catalysed by Gre2p or GDH, respectively. One unit (1 U) was defined as the amount of enzyme that catalyses the oxidation of 1 µmol NADPH (Gre2p) or reduction of 1 µmol $NADP^+$ (GDH) per minute under standard conditions (pH 7.0; 30°C). The assay mixture for Gre2p contained 970 µL 2,5-hexanedione (20 mM in 100 mM TEA buffer), 20 µL NADPH (12.5 mM in deionised water) and 10 µL enzyme extract. The assay mixture for GDH contained 970 µL D-glucose (100 mM in 100 mM TEA buffer), 20 µL $NADP^+$ (100 mM in deionised water) and 10 µL enzyme solution.

2.6. Activity measurements using gas chromatography analysis

For the determination of initial reaction rates of the whole-cell catalysts, benzaldehyde was used as standard substrate. Thus, 6 mg/mL cells (wet weight) were suspended in 200 mM TEA buffer (pH 7.0) and then mixed with 1 mL substrate solution (40 mM benzaldehyde, 200 mM glucose in 200 mM TEA buffer pH 7.0). Biotransformation

was then carried out at 30°C and 800 rpm. Samples of 100 μL were taken periodically and were diluted with 800 μL ethyl acetate and 100 μL 2.5 mM octanol (internal standard). The organic phase was analysed via GC using the following temperature protocol: 2 min at 60°C, 10°C/min to 135°C and 5°C/min to 150°C which gave the following retention times: benzaldehyde, 8.0 min; benzyl alcohol, 11.2 min; octanol, 10.0 min. The activity is expressed as U, which corresponds to the production of 1 μmol benzyl alcohol per minute. Cell-specific activity is stated as U/g cell wet weight.

2.7. Characterisation of the whole-cell catalysts

To investigate the effect of different growth conditions on the activities of Gre2p and GDH, both strains were grown in LB medium, TB medium (24 g/L yeast extract, 12 g/L casein hydrolysate and 5 g/L glycerol in 100 mM Kpi buffer pH 7.0) and autoinduction (AI) medium (TB medium containing 2 g/L lactose and 0.5 g/L glucose) which were supplemented with 34 μg/mL CM. The cultures were incubated at different temperatures (25°C, 30°C, and 37°C) and were harvested after 5 h, 16 h and 24 h by centrifugation followed by the determination of the Gre2p and GDH activity using the spectrophotometric assay.

For the characterisation studies the pH, temperature, cofactor concentration, or toluene concentration were varied followed by the determination of the initial rates using the standard conditions.

2.8. Whole-cell bioreduction of 2,5-hexanedione

Whole-cell reduction of 2,5-hexanedione is exemplified for the reaction with a substrate concentration of 150 mM and 375 mM glucose. Thus permeabilised cells were added to a solution of 2.25 mmol 2,5-hexanedione (257 mg), 5.63 mmol glucose (1.01 g) and 7.5 μmol NADP$^+$ (5.9 mg) in 15 mL of 0.5 M potassium phosphate buffer (Kpi pH 7.5). To determine conversion, samples of 100 μL were taken periodically and diluted with 1.4 ml ethyl acetate. The organic layer was then analysed via GC, using the temperature programme mentioned in 2.6, yielding the following retention times: 2,5-hexanedione 7.2 min, 5-hydroxy-2-hexanone 9.0 min and 2,5-hexanediol 11.4 min. To determine the enantiomeric excess (ee), 300 μl of the reaction mixture was taken and diluted with 200 μl diethyl ether. The organic phase was then evaporated and 10 μl of trifluoroacetic acid anhydride (TFAA) was added to derivatise the sample at 30°C for 30 min under gentle shaking. Afterwards, 300 μl from a saturated potassium hydrogen carbonate solution and 200 μl ethyl acetate were added. The organic layer was separated by centrifugation and analysed via GC. The oven temperature was kept at 55°C for 30 min which resulted in the following retention times: (2S,5S)-hexanediol, 20.1 min; (2R,5R)-hexanediol, 23.4 min; and *meso*-2,5-hexanediol, 24.6 min.

For biotransformations performed in the autotitrator, the starting reaction volume was 10 mL. To keep the pH value neutral, 6 N NaOH was successively added.

3. Results and discussion

3.1. Construction of the expression plasmids

For co-expression of *GRE2*, encoding for the 2,5-hexanedione reductase and *gdh*, encoding the NADPH-recycling glucose dehydrogenase in *E. coli* BL21(DE3), the plasmids pACYCDuet-GRE2-gdh (Fig. 1A) and pACYCDuet-gdh-GRE2 (Fig. 1B) were constructed. The genes were either cloned into the first or second multiple-cloning site (MCS) of the commercially available pACYCDuet-1. As a result, the plasmids have different gene orders. Each MCS has its own ribosome binding site and T7 promoter with no transcription terminator between them, allowing the genes to be expressed consecutively. Additionally, the plasmid contains the p15A origin which reduces the copy number per cell, guaranteeing an efficient gene expression.

Transformation of the *E. coli* expression strain BL21(DE3) with either of the two expression plasmids resulted in two different *E. coli* strains, producing Gre2p and GDH simultaneously.
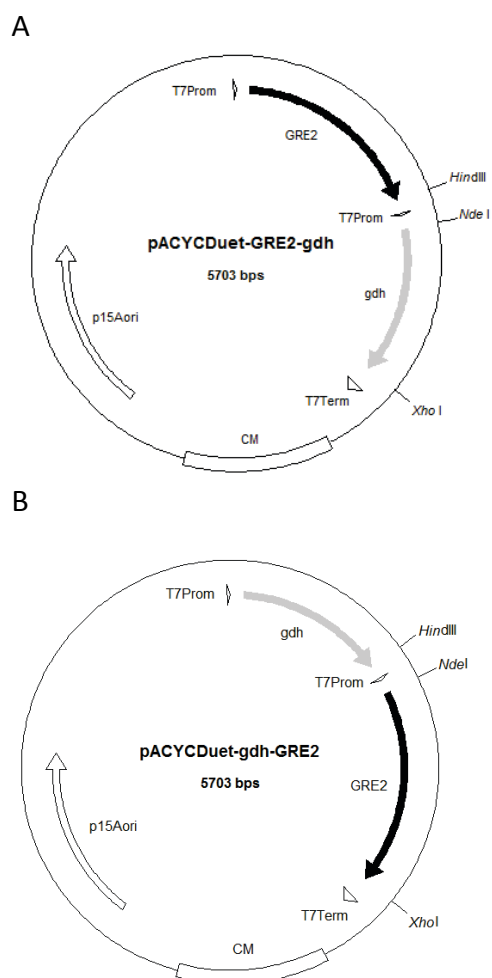
A

B

Figure 1. Plasmid card for (A) pACYCDuet-GRE2-gdh and (B) and pACYCDuet-gdh-GRE2. Both expression plasmids are derived from the commercially available pACYCDuet-1 and contain the p15A origin, a chloramphenicol (CM) resistance marker, two T7 promoters and one T7 terminator downstream from the second multiple cloning site.

3.2. Functional co-expression of GRE2 and gdh

The next step was to investigate how the different arrangements of the genes in the plasmids influence the functional co-expression in the *E. coli* BL21(DE3) strain. To meet this objective, specific activities of both Gre2p and GDH in the cell-free extracts were determined spectrophotometrically. As can be seen in Figure 2, both strains produce active Gre2p and GDH. However, for each cultivation and growth condition tested, specific activity of Gre2p was always lower than that of GDH in the cell-free extracts of BL21-GRE2-gdh (Fig 2A), while the ratios were inverted for the BL21-gdh-GRE2 expression system (Fig. 2B). This observation was confirmed via SDS-PAGE analysis, where the band intensity for Gre2p was decreased compared to

GDH when produced by BL21-GRE2-gdh (lanes 2-5 in Fig. 3) and vice versa when the BL21(DE3) strain expressed the genes from pACYCDuet-gdh-GRE2 (lanes 6-9 in Fig. 3). The fact that the gene located in the second MCS resulted in much higher enzyme activities is most likely due to the formation of two transcripts of this gene. Hence, the first is produced along with the transcript of the first gene when expression starts at the T7 promoter at the first MCS. Due to the lack of a terminator upstream of the second MCS the second transcript is formed when the gene in the second MCS is expressed, because of the presence of another T7 promoter.
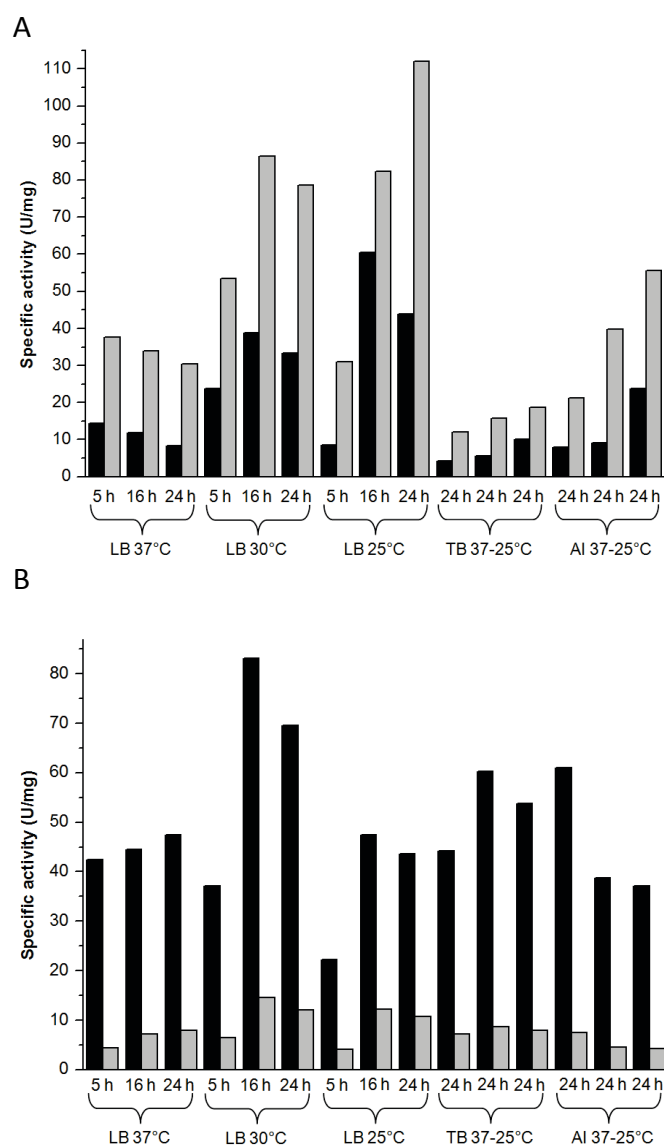
A

B

Figure 2. Effect of growth conditions and media on the expression levels of Gre2p (black) and GDH (grey). (A) BL21-GRE2-gdh and (B) BL21-gdh-GRE2. The temperature order for expression in TB and AI media is as follows: 37°C, 30°C and 25°C.

Variation of growth conditions and media is a way to influence the production levels of the corresponding enzymes. Therefore, a series of experiments, aiming to investigate the effect of altering cultivation and growth conditions on functional co-expression were performed (Figure 2). Accordingly, when cultivated for long enough (16, 24 h) in LB medium at 30°C and 25°C, the BL21-GRE2-gdh system produced the highest specific activities for Gre2p and GDH. In contrast, activities were rather low when the cells were grown in TB or AI media. In general, decreasing the temperature led to a rise in activity. For example, specific activities for Gre2p and GDH were four- (60.5 U/mg) and three-times (112 U/mg) higher when BL21-GRE2-gdh was cultivated in LB medium at 25°C than for the incubation at 37°C (Gre2p: 14.4 U/mg, GDH: 37.6 U/mg). In an appropriate SDS-gel, band intensities for Gre2p and GDH are slightly increased. It also shows that approximately 40% of the total amount of either enzyme was produced in a soluble fashion.
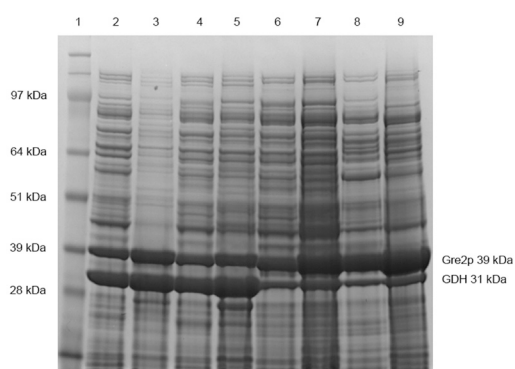

Figure 3. SDS-PAGE analysis of soluble and insoluble fractions of BL21-GRE2-gdh (lanes 2-5) and BL21-gdh-GRE2 (lanes 6-9). Lane 1 molecular weight marker (SeeBlue® Plus2, Invitrogen); Lane 2 soluble fraction of LB, 37°C, 5 h; Lane 3 insoluble fraction of LB, 37°C, 5 h; Lane 4 soluble fraction of LB, 25°C, 16 h; Lane 5 insoluble fraction of LB, 25°C, 16 h; Lane 6 soluble fraction of LB, 30°C, 16 h; Lane 7 insoluble fraction of LB, 30°C, 16 h; Lane 8 soluble fraction of AI, 37°C, 24 h; Lane 9 insoluble fraction of AI, 37°C, 24 h; Equal amounts of 25 µg total protein were loaded.

In case of the BL21-gdh-GRE2 system, altering the growth and cultivation conditions had little influence on the specific enzyme activities of GDH, which were not higher than 15 U/mg. In contrast, Gre2p activity could be increased significantly by varying the media, temperature and incubation time. The highest specific activities were obtained

when the cells were grown in LB medium at 30°C for 16 h (83.1 U/mg). This condition also led to the highest specific activities of GDH at 14.6 U/mg. Another condition which produced high Gre2p activity was 24 h cultivation in AI medium at 37°C, although activity of the NADPH-recycling GDH was only half as high as after growth in LB medium at 30°C for 16 h. Similarly to the BL21-GRE2-gdh system, SDS-PAGE analysis of all these samples revealed that approximately 70% of both Gre2p and GDH were produced as insoluble aggregates.

3.3. The effects of altering cultivation and growth conditions on the whole-cell activity

In order to examine the influence of altering cultivation and growth conditions on the activity of the whole-cell catalysts, the reduction of benzaldehyde to benzyl alcohol was selected as model reaction (Fig. 4). Benzaldehyde was chosen as standard substrate over 2,5-hexanedione because of its higher applicability and more reliable GC analysis. Additionally, Gre2p reveals good activity towards benzaldehyde (one-third of γ-diketone activity) [45] and is therefore appropriate to determine the whole-cell activities of both *E. coli* strains. Initial rates were obtained by measuring the production of benzyl alcohol by GC over a period of 90 min at 30°C and neutral pH value without the addition of an external cofactor. After plotting the concentration of alcohol versus time, the linear slope was used to calculate the whole-cell activity.
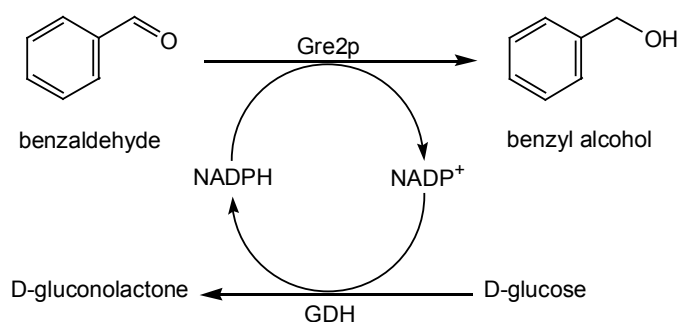

Figure 4. Figure 4. Reaction scheme for the standard reaction. Gre2p reduces benzaldehyde into benzyl alcohol, while GDH simultaneously regenerates NADPH by catalysing the oxidation of glucose.

Figure 5 summarises the whole cell activities of both catalysts obtained after varying the growth and cultivation conditions. Remarkably, the conditions which led to the best cell activities of either strain were not identical with those leading to the highest specific Gre2p and GDH activities. For the GRE2-gdh system, the highest cell activity (18.4 U/g) was observed when growth was carried out in LB medium at 37°C for 5 h. Similarly, cultivation in LB media at 30°C for 16 and 24 h as well as long incubations in TB media at any temperature investigated led to high cell activities. The latter is quite interesting, as under these conditions Gre2p and GDH reveal only low activities.

Best whole-cell activities for BL21-gdh-GRE2 were achieved when the cells were either grown in AI medium at 37°C for 24 h (21.1 U/g) or in LB medium at 37°C for 16 and 24 h (16.8 and 16.2 U/g).

The fact that the cell activities under certain conditions were lower than the measured specific activities for Gre2p and GDH may be due to a substantial limitation of the reactions. This could be caused by the low sum of the intracellular concentration of $NADP^+$/NADPH. Accordingly, neither Gre2p nor GDH reached optimal enzyme activity, ultimately leading to lower cell activity. This issue is examined in more detail in section 3.6.

3.4. The influence of temperature and pH on whole-cell activity

Temperature and pH value are both crucial parameters for technical applications of biocatalysts. Therefore, studies regarding the dependency of temperature and pH on the whole-cell catalyst were performed. To achieve this, biotransformations of benzaldehyde at four different pH values (pH 5.0, 6.0, 8.0 and 9.0) and four different temperatures (25°, 37°, 45° and 50°C) were carried out and compared with the standard conditions at pH 7.0 and 30° C (Fig. 6). For these experiments the catalyst BL21-GRE2-gdh was used which had been grown in LB medium at 37°C for 5 h and gave a cell activity of 18.4 U/g (see Fig. 5).

Regarding temperature dependency the catalyst revealed the highest activity (22.1 U/g) at 37°C which was 17% higher than under standard conditions. Increasing the temperature to 45°C still kept 69% (15.3 U/g) of the cell activity. Interestingly, an increase of another 5°C resulted in the total loss of activity. Whole-cell activity observed 5°C below the standard conditions was decreased to 73% (13.2 U/g) residual activity.
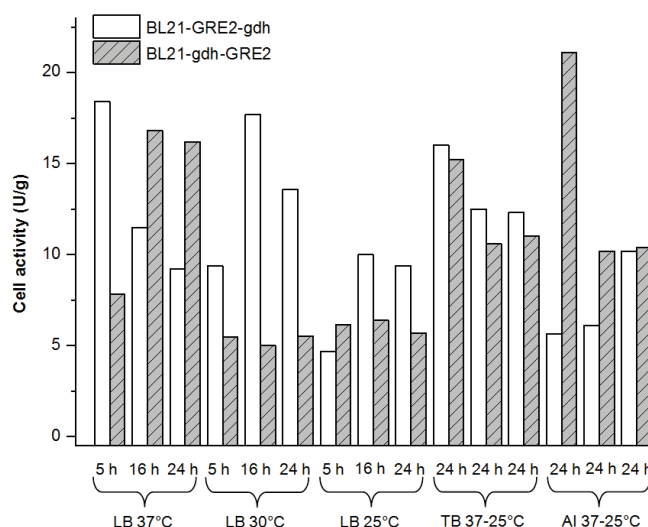

Figure 5. Effect of different growth and cultivation conditions on the cell activities (U/g) of BL21-GRE2-gdh (white) and BL21-gdh-GRE2 (dashed). The temperature order for expression in TB and AI media is as follows: 37°C, 30°C and 25°C.

With respect to pH dependency, cell activity was 3-times lower (6.1 U/g) at slightly acidic conditions (pH 5.0) but increased by a factor of 2.3 at pH 6.0 (13.8 U/g). At pH 8.0 the catalyst displayed optimal activity (19.5 U/g); however, under more alkaline conditions (pH 9.0) a complete loss of activity was observed. The fact that the catalyst displayed high cell activities between pH 6.0-8.0 is not unexpected, because isolated Gre2p and GDH display optimal activities in the pH ranges of 6.5-7.5 and 8.0-8.5, respectively. Also, both enzymes were demonstrated to lose the majority of their activity at pH 9.0, which could explain why no cell activity was observed at this pH value [45, 56].

3.5. The effect of permeability by toluene treatment or by one freeze-thaw cycle

Cells can be permeabilised without lysis or disruption of their inner structure. This allows low-molecular weight molecules to freely enter and leave the cell [57, 58]. This is advantageous when using permeabilised cells in organic synthesis, due to an easier uptake of both substrate and co-substrate and product release [59, 60]. To investigate whether cell permeabilisation has an effect on the activity of the catalyst, toluene (1% (v/v)) was added to the cells of BL21-GRE2-gdh following an incubation at 37°C for 30 min. Alternatively, cells were frozen and thawed before determination of the initial rates. Figure 6 shows that treatment with toluene resulted in a three-fold enhancement of activity (53.9 U/g), while one freeze-thaw cycle only increased activity by a factor of 2.3 (41.1 U/g). When toluene was added to cells that had already been frozen, no further significant enhancement of activity was observed. These experiments confirm that the increase of activity is due to improved access of benzaldehyde into the cells.

However, from the literature it is known that the permeabilisation of *E. coli* by toluene results in a protein loss of approximately 25%; these proteins are released into the surrounding media. Parameters such as the amount of toluene, temperature, the molecular weight of the proteins ($\leq$70 kDa) as well as their charge and location play a pivotal role in this process [57, 61, 62]. Because of its low molecular weight of 38 kDa [45], Gre2p could have been released into the environment. In contrast, GDH, which has a molecular weight of 120 kDa [63], would have remained within the cells. To study whether Gre2p could have been released, cells were washed with suspension buffer before the determination of initial rates. The cells now revealed an activity of 35.5 U/g, a 1.5-fold decrease compared to the activity obtained with unwashed cells. Additionally, the supernatant was tested for enzyme activity. Accordingly, a specific activity of 2.7 U/mg and 3.7 U/mg was obtained for Gre2p and GDH, respectively. Considering that the cell crude extract of BL21-GRE2-GDH displays 14.4 U/mg Gre2p and 37.6 U/mg GDH activity (see Fig. 2a), a release of approximately 19% and 10% of the total protein of Gre2p and GDH was demonstrated.
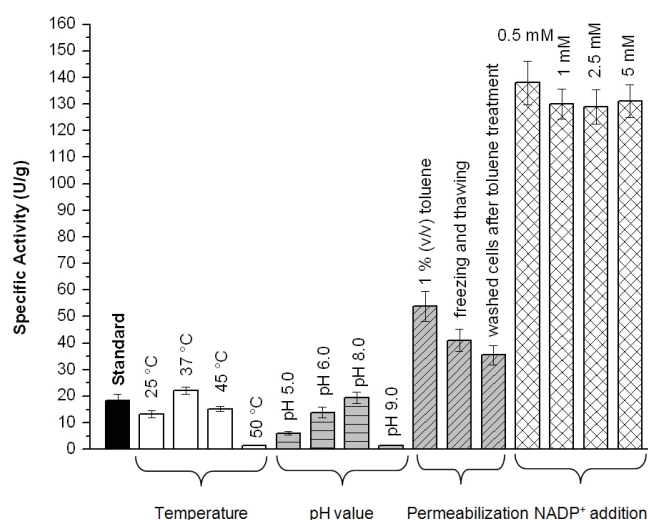

Figure 6. Illustration of the influence of different parameters on the initial rate in the conversion of benzaldehyde by the whole-cell catalyst. The initial rate under standard conditions was 18.4 U/mg (black) and was obtained with BL21-GRE2-gdh at 30°C and pH 7.0 without addition of external cofactor. All the data shown are the results of three independent measurements.

3.6. The impact of external cofactor addition

The availability of nicotinamide cofactors is often limiting and crucial for the efficiency of redox reactions catalysed by whole cells. In recombinant *E. coli* cells, the initial intracellular concentrations of the four nicotinamide cofactors NAD^+, $NADP^+$, NADH, and NADPH is as follows: 566 μM, 47.8 μM, 3.14 μM and 0.59 μM [64]. That is, the sum of the intracellular NADPH and $NADP^+$ concentration is approximately 0.05 mM. However, the investigated enzymes show K_m values of 0.11 mM for NADPH (Gre2p, [65]) and 0.03 mM for $NADP^+$ (GDH, [66]). Accordingly, optimal cell activity would not be feasible by either enzyme. In addition, the cofactor concentration has to be increased, because the good over-expression leads to notably higher quantities of enzymes. Therefore, experiments referencing the influence of the addition of different amounts of $NADP^+$ (0.5-5 mM) on the initial rates were studied. Prior to cofactor addition, cells of BL21-GRE2-gdh were treated with toluene to facilitate its uptake, as an intact cell membrane remains impermeable for pyridine nucleotides [59, 61]. As can be seen in Figure 6, whole-cell activity increased on average by a factor of 7 at any $NADP^+$ concentration tested

in comparison to the standard reaction (without cofactor addition). In a comparative study, cofactor was added to non-permeabilised cells, resulting in no enhancement of activity. Accordingly, the experiments reveal that addition of cofactor leads to a considerable increase in activity due to a faster conversion of benzaldehyde but also showed that cell permeabilization is required to facilitate the uptake of NADP$^+$.

### 3.7. Application of both E. coli strains in the synthesis of enantiopure (2S,5S)-hexanediol

(2S,5S)-hexanediol is an important chiral building block which can be used in the synthesis of a variety of different fine chemicals, chiral auxiliaries and pharmaceuticals. Thus, an efficient synthesis route is required. Because of this, we were encouraged to transfer the results of the previously developed cell-free system into a whole-cell system using both constructed *E. coli* strains. Based on the outcomes of the characterisation studies, BL21-GRE2-gdh and BL21-gdh-GRE2 were cultivated in LB medium at 37°C for 5 h and in AI medium at 37°C for 24 h, respectively, as these conditions produced the highest cell activities (see Fig. 5). Additionally, biotransformations were carried out in the presence of 0.5 mM NADP$^+$ at pH 7.5 using permeabilised cells.

The corresponding results are summarised in Table 2, and reveal that both catalysts are able to reduce 2,5-hexanedione almost completely into highly optically pure (2S,5S)-hexanediol (*ee*>99 %). In comparison to BL21-GRE2-gdh, biotransformation of 200 mM diketone catalysed by BL21-gdh-GRE2 was slightly improved because a lower conversion time was observed. This ultimately led to a higher space-time yield of 350 g/(L·d) (entries 2 and 5). Reactions catalysed by BL21-gdh-GRE2 were also accomplished at 25°C, which matched the results obtained at 30°C when 100 mM 2,5-hexanedione was reduced (entries 3 and 4). However, 200 mM diketone reduction gave a higher space-time yield when performed at 30°C (entries 5 and 6). The cell productivity (mg of formed product per 1 g of cells) was increased

significantly in comparison to the existing synthesis routes catalyzed by baker's yeast [43, 44]. Thus, up to eight-times less cell material is needed to generate 1 g of the diol. This increase is a result of the good recombinant enzyme production and demonstrates the efficiency of both recombinant *E. coli* strains.

3.8. Optimisation of the co-substrate yield

Entries 1-6 (Tab. 2) were accomplished with a five time excess of glucose over the diketone to guarantee a high NADPH:NADP$^+$ ratio, which favours the reduction reaction. The co substrate yield expresses the amount of product formed per amount of co-substrate consumed. The higher this parameter, the lower the production costs, because less co substrate is required. Because this is of primary economic interest we tried to optimise the reaction towards a high co-substrate yield. To achieve this, biotransformations of 150 mM diketone catalysed by BL21-gdh-GRE2 (30 g/L) were carried out with various amounts of glucose (300-675 mM), to find the amount that is needed to attain complete conversion to the diol. As a result, 375 mM glucose (67.6 g) was found to be the quantity of co-substrate needed to drive the reduction reaction into completion (>99% (2S,5S)-hexanediol, in 2.5 h). This corresponds to a co-substrate yield of 259 mg$_{(2S,5S)\text{-hexanediol}}$/g$_{glucose}$ which, in turn, means that 2.5 moles of glucose are required to form 1 mol of diol. However, theoretically, one would expect that two moles of glucose are necessary to drive the diketone reduction into completion. An explanation for the need of super-stoichiometric amounts of glucose might be the presence of other enzymes in the cells consuming NADP$^+$/NADPH too. Nevertheless, after all, 80% of the theoretical yield was achieved. Moreover, the co-substrate yield is 10- and 3-times higher, respectively compared to reported yeast wildtype *γ*-diketone biotransformations [43, 44]. This enhancement is undoubtedly due to the production of large quantities of both the NADPH-dependent Gre2p and the NADPH-recycling GDH, as well as the simultaneous cofactor recycling.

Table 2. Asymmetric 2,5-hexanedione reduction catalysed by the two recombinant *E. coli* strains.
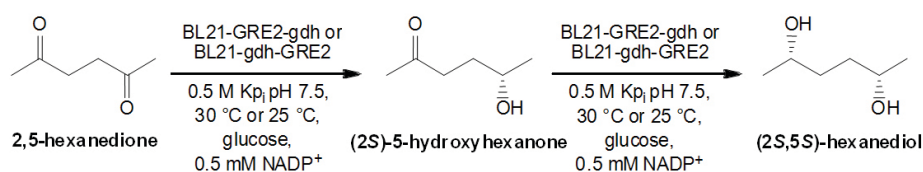
Entry	2,5-hexanedione concentration (mM)	Glucose concentration (mM)	BL21-GRE2-gdh cells (g/L)	BL21-gdh-GRE2 cells (g/L)	Temperature (%)	Time (h)	Conversion (%)	Space-time-yield (g/L·d)	Cell productivity (mg/g)	ee (%)
1	100	500	20	-	30	3	>98	86.5	578	>99
2	200	1000	50	-	30	2.5	>99	175	467	>99
3	100	500	-	20	30	3	>98	86.5	578	>99
4	100	500	-	20	25	3.5	>98	86.5	578	>99
5	200	1000	-	50	30	2	>99	350	467	>99
6	200	1000	-	50	25	3	>99	175	467	>99
7[*]	500	1250	-	125	30	3	>99	572[#]	467	>99
8[*]	1000	2500	-	250	30	8	95.5	361[#]	451	>99

[*] Biotransformation was carried out in an autotitrator at a total volume of 10 mL

[#] Calculated in reference to the added NaOH volume

[+] Conversion was determined via gas chromatography

3.9. Up-scaling the synthesis of (2S,5S)-hexanediol

Basic requirements for economically feasible biotransformations are isolated yields >78% (conversions >95%), space-time yields >300 g/(L·d), and substrate concentrations of at least 5-10% (w/v) (50-100 g/L) [16, 22, 67]. To the best of our knowledge, no reports have been published on the preparative synthesis of the (*S*,*S*)-*γ*-diol using a recombinant whole-cell catalyst. That gave us the confidence to investigate the biotransformations of 0.5 (58 g/L) and 1 M (113 g/L) 2,5-hexanedione catalysed by BL21-gdh-GRE2. This catalyst was chosen as it performed the reduction of 200 mM diketone slightly better than BL21-GRE2-gdh.

Reactions were carried out in 0.1 M potassium phosphate buffer (Kpi) and in an autotitrator, which allowed the successive addition of 6 N NaOH to keep the pH neutral. We also tried to use a more concentrated Kpi buffer, but a reaction inhibition was observed when the buffer had a concentration >0.5 M (data not shown).

As can be seen in Table 2 and Figure 7, reduction of both diketone concentrations gave optically pure diol. However, biotransformation of 0.5 M (entry 7, Fig 7A) proceeded quicker than the reduction of 1 M (entry 8, Fig 7B), although the substrate to catalyst ratio was equal. Also, the conversion was slightly higher. As a consequence, a 1.6-fold higher space-time yield was achieved. In comparison to the wildtype bioreductions [43, 44], the STY was increased up to 609-times. Moreover, because of the good conversion rates, high product concentrations and high STYs, the two biotransformations meet the criteria of an industrial relevant process.

To get a better knowledge of why the two biotransformations proceeded differently, cell activities for both reduction steps as well as for the formation of hydroxy hexanone and (2*S*,5*S*)-hexanediol were calculated. The results are summarised in Table 3. Accordingly, when 0.5 M diketone was reduced, the cell activity was almost four-times higher than for the reduction of 1 M substrate. Likewise, formation of the hydroxy ketone was enhanced by a factor of 3.1. The second reduction step and the formation of the diol, in general, proceeded approximately three

Table 3. Cell activities of the individual steps of the preparative synthesis of (2*S*,5*S*)-hexanediol catalysed by BL21-gdh-GRE2.

Reaction step	Cell activity at 500 mM 2,5-hexanedione (U/g)	Cell activity at 1 M 2,5-hexanedione (U/g)
Reduction of 2,5-hexanedione	90.4	24.2
Formation of (*S*)-5-hydroxy-2-hexanone	80.8	26.0
Reduction of (*S*)-5-hydroxy-2-hexanone	32.3	10.4
Formation of (2*S*,5*S*)-hexanediol	47.2	17.0

A

B

Figure 7. Synthesis of (2S,5S)-hexanediol from 2.5-hexanedione at preparative scale catalysed by BL21-gdh-GRE2. (A) 0.5 M and (B) 1 M 2,5-hexanedione. 2,5-Hexanedione (hell grey squares); (2*S*)-5-hydroxyhexanone (dark grey squares); (2*S*,5*S*)-hexanediol (black triangles).
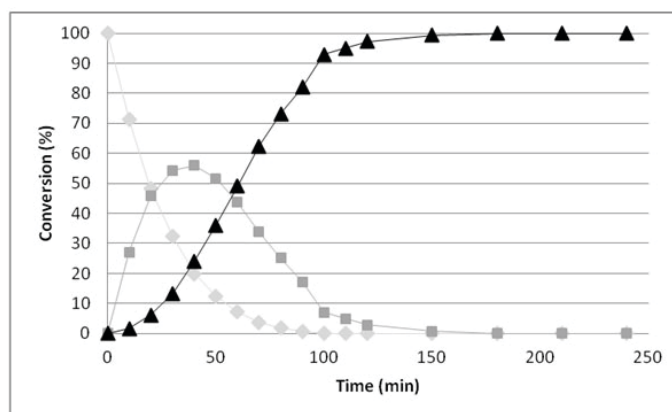
times faster in the biotransformation of 0.5 M 2,5-hexanedione. Hence, the results reveal that a substrate-excess inhibition occurs in the biotransformation of 1 M diketone. Either one or both enzymes are inhibited by their substrates.

4. Conclusion

To sum up, we have successfully constructed two *E. coli* whole-cell catalysts which co express the gene coding for the NADPH-dependent alcohol dehydrogenase from *S. cerevisiae* and the gene encoding the NADPH-recycling glucose dehydrogenase from *Bacillus subtilis*. Both strains produce soluble Gre2p and GDH to a certain extent, and because they differ by the order of the genes on their plasmid, enzyme activity ratios were inverted. We could also show that altering the growth and medium conditions has an influence on both the specific enzyme activities and cell activities. A characterisation study revealed that cell permeabilisation and addition of cofactor (≥0.5 mM) increases the cell activity further.

Both catalysts were applied in the biotransformation of 2,5-hexanedione and were shown to synthesise the corresponding (2*S*,5*S*)-hexanediol with excellent *ee* values and high conversion yields. Additionally, the catalyst BL21-gdh-GRE2 was used in the preparative synthesis of the diol, and was demonstrated to be able to reduce up to 1 M of diketone almost completely
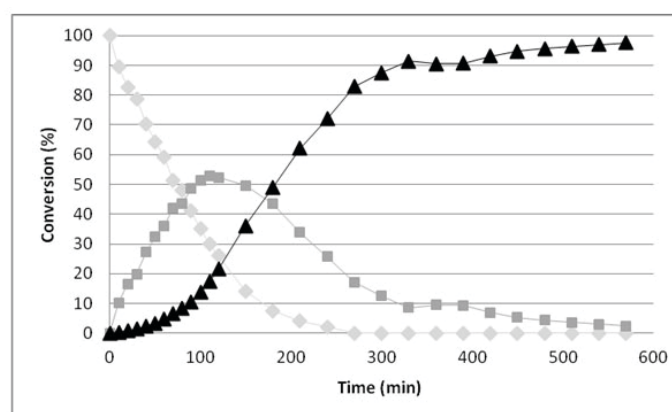
to (2*S*,5*S*)-hexanediol. This proves that an application of the catalyst would be transferable to a commercial-scale. Also, the STYs and cell activities obtained in the synthesis of the (*S*,*S*)-diol were much higher than those obtained via conventional *S. cerevisiae* biotransformation of 2,5-hexanedione. This is the result of the good recombinant production of Gre2p and GDH and strengthens the assertion that the whole-cell catalysts designed in this study can be used efficiently for asymmetric synthesis.

References

[1] B.M. Nestl, S.C. Hammer, B.A. Nebel, B. Hauer, Angew. Chem.-Int. Edit. 53 (2014) 3070-3095.

[2] N.J. Turner, E. O'Reilly, Nat. Chem. Biol. 9 (2013) 285-288.

[3] G.W. Huisman, S.J. Collier, Curr. Opin. Chem. Biol. 17 (2013) 284-292.

[4] M.T. Reetz, J. Am. Chem. Soc. 135 (2013) 12480-12496.

[5] U.T. Bornscheuer, G.W. Huisman, R.J. Kazlauskas, S. Lutz, J.C. Moore, K. Robins, Nature 485 (2012) 185-194.

[6] C.M. Clouthier, J.N. Pelletier, Chem. Soc. Rev. 41 (2012) 1585-1605.

[7] K. Buchholz, V. Kasche, U.T. Bornscheuer, Biocatalysts and Enzyme Technology, Wiley-VCH, Weinheim, 2012.

[8] K. Faber, Biotransformations in organic chemistry, Springer-Verlag, Berlin, 2011.

[9] R.N. Patel, Biomolecules 3 (2013) 741-777.

[10] R.N. Patel, ACS Catal. 1 (2011) 1056-1074.

[11] R.N. Patel, Curr. Org. Chem. 10 (2006) 1289-1321.

[12] J. Tao, J.H. Xu, Curr. Opin. Chem. Biol. 13 (2009) 43-50.

[13] L. Hilterhaus, A. Liese, Building Blocks, in: R. Ulber, D. Sell (Eds.) White Biotechnology, Springer-Verlag, Berlin, 2007, pp. 133-173.

[14] D. Muñoz Solano, P. Hoyos, M.J. Hernáiz, A.R. Alcántara, J.M. Sánchez-Montero, Bioresour. Technol. 115 (2012) 196-207.

[15] Y. Huang, N. Liu, X. Wu, Y. Chen, Curr. Org. Chem. 14 (2010) 1447-1460.

[16] F. Hollmann, I.W.C.E. Arends, D. Holtmann, Green Chem. 13 (2011) 2285-2314.

[17] M. Hall, A.S. Bommarius, Chem. Rev. 111 (2011) 4088-4110.

[18] Y. Ni, J.H. Xu, Biotechnol. Adv. 30 (2012) 1279-1288.

[19] Y. Chen, C. Chen, X. Wu, Chem. Soc. Rev. 41 (2012) 1742-1753.

[20] A. Bariotaki, D. Kalaitzakis, I. Smonou, Org. Lett. 14 (2012) 1792-1795.

[21] P. Hoyos, J.V. Sinisterra, F. Molinari, A.R. Alcántara, P.D. De María, Accounts Chem. Res. 43 (2010) 288-299.

[22] G.W. Huisman, J. Liang, A. Krebber, Curr. Opin. Chem. Biol. 14 (2010) 122-129.

[23] K. Goldberg, K. Schroer, S. Lütz, A. Liese, Appl. Microbiol. Biotechnol. 76 (2007) 249-255.

[24] J.C. Moore, D.J. Pollard, B. Kosjek, P.N. Devine, Accounts Chem. Res. 40 (2007) 1412-1419.

[25] H. Wu, C. Tian, X. Song, C. Liu, D. Yang, Z. Jiang, Green Chem. 15 (2013) 1773-1789.

[26] A. Weckbecker, H. Gröger, W. Hummel, Adv. Biochem. Eng./Biotechnol. 120 (2010) 195-242.

[27] A. Berenguer-Murcia, R. Fernandez-Lafuente, Curr. Org. Chem. 14 (2010) 1000-1021.

[28] Z. Li, W. Liu, X. Chen, S. Jia, Q. Wu, D. Zhu, Y. Ma, Tetrahedron 69 (2013) 3561-3564.

[29] H. Ma, L. Yang, Y. Ni, J. Zhang, C.X. Li, G.W. Zheng, H. Yang, J.H. Xu, Adv. Synth. Catal. 354 (2012) 1765 – 1772.

[30] X. Wu, J. Jiang, Y. Chen, ACS Catal. 1 (2011) 1661-1664.

[31] K. Schroer, U. Mackfeld, I.A.W. Tana, C. Wandrey, F. Heuser, S. Bringer-Meyer, A. Weckbecker, W. Hummel, T. Daußmann, R. Pfaller, A. Liese, S. Lütz, J. Biotechnol. 132 (2007) 438-444.

[32] H. Gröger, F. Chamouleau, N. Orologas, C. Rollmann, K. Drauz, W. Hummel, A. Weckbecker, O. May, Angew. Chem. Int. Ed. 45 (2006) 5677-5681.

[33] H. Takada, P. Metzner, C. Philouze, Chem. Commun. (2001) 2350-2351.

[34] K. Julienne, P. Metzner, V. Henryon, A. Greiner, J. Org. Chem. 63 (1998) 4532-4534.

[35] R.P. Short, R.M. Kennedy, S. Masamune, J. Org. Chem. 54 (1989) 1755-1756.

[36] M.J. Burk, J.E. Feaster, R.L. Harlow, Tetrahedron: Asymmetry 2 (1991) 569-592.

[37] J.M. Brunel, B. Faure, J. Mol. Catal. A: Chem. 212 (2004) 61-64.

[38] E. Díez, R. Fernández, E. Marqués-López, E. Martín-Zamora, J.M. Lassaletta, Org. Lett. 6 (2004) 2749-2752.

[39] Q.H. Fan, C.H. Yeung, A.S.C. Chan, Tetrahedron: Asymmetry 8 (1997) 4041-4045.

[40] R. Kuwano, M. Sawamura, J. Shirai, M. Takahashi, Y. Ito, Tetrahedron Lett. 36 (1995) 5239-5242.

[41] H. Nagai, T. Morimoto, K. Achiwa, Synlett (1994) 289-290.

[42] M. Bertau, M. Bürli, Chimia 54 (2000) 503-507.

[43] J.K. Lieser, Synth. Commun. 13 (1983) 765-767.

[44] M. Katzberg, K. Wechler, M. Müller, P. Dünkelmann, J. Stohrer, W. Hummel, M. Bertau, Org Biomol Chem. 7 (2009) 304-314.

[45] M. Müller, M. Katzberg, M. Bertau, W. Hummel, Org. Biomol. Chem. 8 (2010) 1540-1550.

[46] P. Tufvesson, J. Lima-Ramos, M. Nordblad, J.M. Woodley, Org. Process Res. Dev. 15 (2011) 266-274.

[47] H. Gröger, O. May, H. Werner, A. Menzel, J. Altenbuchner, Org. Process Res. Dev. 10 (2006) 666-669.

[48] S.A. Yoon, H.K. Kim, J. Microbiol. Biotechnol., 23 (2013) 1395-1402.

[49] K. Mädje, K. Schmölzer, B. Nidetzky, R. Kratzer, Microb. Cell Fact. 11 (2012) 1-8.

[50] Y. Ni, C.X. Li, J. Zhang, N.D. Shen, U.T. Bornscheuer, J.H. Xu, Adv. Synth. Catal. 353 (2011) 1213-1217.

[51] M. Kataoka, T. Ishige, N. Urano, Y. Nakamura, E. Sakuradani, S. Fukui, S. Kita, K. Sakamoto, S. Shimizu, Appl. Microbiol. Biotechnol. 80 (2008) 597-604.

[52] A. Weckbecker, W. Hummel, Glucose dehydrogenase for the regeneration of NADPH and NADH, in: J.L. Barredo (Ed.) Microbial Enzymes and Biotransformations, Humana Press Inc., Totowa, N. J., 2005, pp. 225-237.

[53] M.M. Bradford, Anal. Biochem. 72 (1976) 248-254.

[54] U.K. Laemmli, Nature 227 (1970) 680-685.

[55] A. Menzel, H. Werner, J. Altenbuchner, H. Gröger, Eng. Life Sci. 4 (2004) 573-576.

[56] A. Weckbecker, W. Hummel, Biocatal. Biotransform. 24 (2006) 380-389.

[57] H. Felix, Anal. Biochem. 120 (1982) 211-234.

[58] R.W. Jackson, J.A. DeMoss, J. Bacteriol. 90 (1965) 1420-1425.

[59] W. Zhang, K. O'Connor, D.I.C. Wang, Z. Li, Appl. Environ. Microbiol. 75 (2009) 687-694.

[60] M. Cánovas, T. Torroglosa, J.L. Iborra, Enzyme Microb. Technol. 37 (2005) 300-308.

[61] M.J. de Smet, J. Kingma, B. Witholt, BBA Biomembranes 506 (1978) 64-80.

[62] M.P. Deutscher, J. Bacteriol. 118 (1974) 633-639.

[63] A. Karmali, L. Serralheiro, Biochimie 70 (1988) 1401-1409.

[64] K. Schroer, B. Zelic, M. Oldiges, S. Lütz, Biotechnol. Bioeng. 104 (2009) 251-260.

[65] Y.H. Choi, H.J. Choi, D. Kim, K.N. Uhm, H.K. Kim, Appl. Microbiol. Biotechnol. 87 (2010) 185-193.

[66] A. Weckbecker, PhD thesis, Heinrich-Heine-Universität, Düsseldorf 2005.

[67] A.J.J. Straathof, S. Panke, A. Schmid, Curr. Opin. Biotechnol. 13 (2002) 548-556.

5

CRYSTALLISATION OF Gre2p

5.1

Crystallization and preliminary crystallographic analysis of Gre2p, a NADP$^+$-dependent alcohol dehydrogenase from *Saccharomyces cerevisiae*

Klaus Breicha, Marion Müller, Werner Hummel and Karsten Niefind

Crystallization and preliminary crystallographic analysis of Gre2p, a NADP⁺-dependent alcohol dehydrogenase, from *Saccharomyces cerevisiae*

Klaus Breicha[a]#, Marion Müller[b]#, Werner Hummel[b]* and Karsten Niefind[a]*

#the authors contribute equally to this work

Gre2p [Genes de Respuesta a Estres (stress-response gene)] from *Saccharomyces cerevisiae* is a monomeric enzyme of 342 amino acids with a molecular weight of 38.1 kDa. The enzyme catalyses both the stereospecific reduction of keto compounds and the oxidation of various hydroxy compounds and alcohols by the simultaneous consumption of the cofactor NADPH and the formation of NADP⁺, respectively. Crystals of a Gre2p complex with NADP⁺ were grown with PEG 8000 as a precipitant. They belong to the monoclinic space group P2₁. The current diffraction limit is 3.2 Å. In spite of the monomeric nature of Gre2p in solution, packing and selfrotation calculations revealed the existence of two Gre2p protomers per asymmetric connected by a two-fold non-crystallographic axis.

1. Introduction

The alcohol dehydrogenase Gre2p from *Saccharomyces cerevisiae* has been shown to be a versatile biocatalyst for the synthesis of enantiopure hydroxy compounds, which serve as valuable building blocks for the production of a variety of pharmaceuticals and fine chemicals (Müller *et al*., 2010; Choi *et al*., 2010; Ema *et al*., 2008). The enzyme has a monomeric structure and is predominately NADPH-dependent. Its substrate spectrum is very comprehensive, since Gre2p catalyses the reduction of various diketones, *α*- and *β*-keto esters, aliphatic and aromatic aldehydes as well as some aliphatic ketones and hydroxy ketones (Müller *et al*., 2010; Kaluzna *et al*., 2002; Ema *et al*., 2001).

Although the enzyme has been characterised well in terms of its applicability for the stereo- and enantioselective asymmetric synthesis, only scarce information is known about its physiological function. Analysis of the *S. cerevisiae* proteins induced by several stress stimuli revealed that the transcription level of the Gre2p encoding gene is increased, suggesting a role of the enzyme in the stress-response system (Hauser *et al*., 2007; Vido *et al*., 2001; Garay-Arroyo & Covarrubias, 1999). This finding led to the designation "**G**enes de **R**espuesta a **E**stres' (stress-responsive gene).

Further studies proposed Gre2p to be part in detoxification of methylglyoxal from cell, naming the *GRE2* gene product as a methylglyoxal reductase (EC 1.1.1.283; Chen *et al*., 2003), and to be a suppressor of isoamyl alcohol-induced filament formation, suggesting that *GRE2* to an isovaleraldehyde reductase (EC 1.1.1.265; Hauser *et al*., 2007), respectively. Apart from this, Warringer & Blomberg (2006) demonstrated Gre2p to be involved in yeast ergosterol biosynthesis, as *gre2-Δ* deletion strains displayed several growth defects during environmental stress, e.g. to the Ca²⁺ chelator, EGTA (ethylene glycol tetraacetic acid) which decreases the intracellular Ca²⁺ concentration. Additionally, those strains revealed sensitivity to ergosterol-

[a]   *Klaus Breicha , Prof. Dr. Karsten Niefind*
       Institut für Biochemie, Department für Chemie
       Universität zu Köln
       Zülpicher Strasse 47
       50674 Köln, Germany
       Tel: (+49)221 470 6444
       E-mail: karsten.niefind@uni-koeln.de
[b]   *Marion Müller, Prof. Dr. Werner Hummel*
       Institut für Molekulare Enzymtechnologie
       Heinrich-Heine Universität Düsseldorf
       im Forschungszentrum Jülich
       52426 Jülich, Germany
       Tel: (+49)24641 613790
       E-mail: w.hummel@fz-juelich.de

inhibiting enzymes.

The enzyme's primary sequence comprises of 342 amino acids, possesses the typical cofactor-binding motif (Rossmann fold) at the *N*-terminus and exhibits the indispensable catalytic triad (Filling *et al.*, 2002), composed of Ser_{126}–Tyr_{165}–Lys_{169}. Thus, Gre2p can be grouped according to Persson *et al.* (2009) and Jörnvall *et al.* (1995) into the extended short-chain dehydrogenase/reductase superfamily. Moreover, Gre2p has sequence similarity to dihydroflavonol reductases from higher plants (Casamayor *et al.*, 1995), e.g. from *Vitis vinifera*, and is a distant homologue of mammalian 3-*β*-hydroxysteroid dehydrogenases (Warringer & Blomberg, 2006), e.g. from mouse and rat. The highest homology to a protein with solved three-dimensional structure shares the enzyme to the aldehyde reductase II from the red yeast *Sporobolomyces salmonicolor* with 30% identity (Kamitori *et al.*, 2005).

Taken together all the information of Gre2p, a three-dimensional structures could provide useful insights into the differences of the enzyme's substrate specificities,helpful for application of Gre2p as a biocatalyst and and to get more information about its biological function in *S. cerevisiae*. Therefore we were encouraged to crystallize the enzyme as the first step of solving its structure.

2. Materials and Methods

2.1. Protein preparation

The codon-optimized gene, *GRE2* was cloned, over-expressed in *Escherichia coli* BL21(DE3) and purified to homogeneity by three chromatographic separation steps (Müller *et al.*, 2010). According to this, harvested cells (approx. 6–7 g) were resuspended in 100 mM triethanolamine buffer (TEA) pH 7.0 containing 1 mM $MgCl_2$ in a ratio of 1 g cells (wet weight) to 2 ml buffer and were disrupted by three sonification cycles for 2 min (37% power output). Debris was removed by centrifuging under cooling at 45000 x g for 30 min.

To the crude extract 1.5 M ammonium sulphate was added and the suspension was incubated on ice for 2 h, before precipitated protein was removed by centrifuging at 45 000 x g for 30 min at 4 °C. The clear supernatant was loaded onto a Butyl Sepharose 4FF column (height 15 cm, diameter 1.6 cm; GE Healthcare) which previously had been equilibrated with 10 column volumes (CV) 100 mM TEA buffer pH 7.0 containing 1 mM $MgCl_2$ and 1.5 M ammonium sulphate. After sample application the column was washed for 2 h with the buffer at a flow rate of 1 ml·min^{-1}. Elution of Gre2p was accomplished using the same buffer containing no ammonium sulfphate with a linear gradient from 1.5 to 0 M.

Fractions were tested the ability to reduce 2,5-hexanedione using the standard assay as described by Müller *et al.* (2010), and active ones were pooled and loaded onto a Macro-Prep® Ceramic Hydroxyapatite^{TM} column (height 15 cm, diameter 1.6 cm; GE Healthcare), which had been equilibrated with 10 CV 5 mM potassium phosphate buffer (Kp_i) pH 7.0 containing 1 mM $MgCl_2$. The enzyme was eluted with Kp_i, pH 7.0 containing 1 mM $MgCl_2$ using a linear gradient from 5 to 45 mM. The purification was carried out at a flow rate of 1 ml·min^{-1}. Active fractions were pooled and loaded onto a HiLoad^{TM} 16/60 Superdex 75 prep-grade column (GE Healthcare). This column was equilibrated with 10 CV of 10 mM TEA buffer pH 6.8 and purification was accomplished at a flow rate of 1 ml·min^{-1}. Samples gained from this purification procedure had a purity of >95 %, as judged by SDS–PAGE analysis, performed according to the method described by Laemmli (1970).

Prior to crystallisation, the enzyme was concentrated using a Vivaspin 20 (MW 30 kDa, Sartorius Stedim Biotech). The protein mass concentration of Gre2p was determined according to Bradford using BSA as a standard (Bradford, 1976). The final Gre2p mass concentration in the stock solution was 12 mg/ml.

2.2. Crystallization

We attempted to grow Gre2p crystals of both the apo-enzyme and together with the the cosubstrate NADP$^+$. All crystallization experiments were performed at 293 K with the sitting-drop variant of the vapour-diffusion method. For initial screening we used various sparse-matrix and grid

screens from Hampton Research and from JenaBioscience GmbH. Initial hits were optimized with additive screens purchased also from Hampton Research. The crystallization drops were pipetted on 96-well plates using a nanoliter dispenser (Hydra-II from Matrix Technologies).

2.3. Diffraction data collection and analysis

Crystals were prepared for diffraction experiments under cryo conditions by increasing the concentration of the precipitant (PEG 8000) in the mother liquor in two steps. At first,, half of the original reservoir solution (composition: 0.1 M 2-(N-morpholino)ethanesulfonic acid buffer (MES), pH 6.35, 15% w/v PEG 8000) was exchanged with 0.1 M MES buffer, pH 6.35, 40% w/v PEG 8000; after mixing of the new reservoir solution re-equilibration occurred for 24 h. Afterwards, the reservoir solution was completely exchanged with 0.1 M MES buffer, pH 6.35, 40% w/v PEG 8000. After a new re-equilibration for at least 24 h the Gre2p crystals were flash-frozen in liquid nitrogen. X-ray diffraction data were collected on beamline BL14.2 of BESSY, Berlin. A MAR224 CCD detector was mounted. The data-collection temperature was 100 K. The raw diffraction data were processed with XDS (Kabsch, 2010) and finally transferred to structure factor amplitudes using TRUNCATE from the CCP4 program collection (Collaborative Computational Project, Number 4, 1994).

2.4. Crystal-packing, Patterson and self rotation function calculation

The Matthew parameter (Matthews, 1968) together with the solvent was calculated with the program MATTHEWS_COEF (Collaborative Computational Project, number 4). To look for possible pseudo-origin peaks a native Patterson function was computed using the program FFT from the CCP4 program suite (Collaborative Computational Project, number 4). For a systematic search for noncrystallographic symmetry we used the program GLRF from the REPLACE package (Tong & Rossmann, 1997).

3. Results and discussion

After various crystal screening and optimization efforts the best crystals - judged according to the outer habitus (Fig. 1) - grew to dimensions of up to 1.0 X 0.3 X 0.3 mm (Fig. 1) within two weeks.

Figure 1. Co-crystals of Gre2p and $NADP^+$ grown with PEG 8000 as a precipitant.

They were obtained from a Gre2p/$NADP^+$ solution prepared by mixing nine parts of Gre2p stock solution and 1 part of 30 mM $NADP^+$ solution prior to crystallization. The reservoir solution consisted of 1 ml 0.1 M MES, pH 6.35, 15% w/v PEG 8000. In the crystallization drop 5 µl of the Gre2p/$NADP^+$ mixture was added to 4 µl reservoir solution. The resulting solution was finally mixed with 0.5 µl 0.1 M cobalt chloride as an additive.

The Gre2p/$NADP^+$-crystals (Fig. 1) showed X-ray diffraction to a maximum resolution of 2.7 Å , yet with a strongly anisotropic distribution (Fig. 2). A complete X-ray diffraction data set up to 3.2 Å resolution was collected and processed (Tab. 1). The Scaling and inspection of systematic absences revealed that the crystals belong to space group $P2_1$. The overall quality of the diffraction data set is low and requires further optimization in order to solve the structure and to refine it to a satisfactory level.

We performed crystal packing and noncrystallo-graphic symmetry calculations based on the low-resolution data set documented in Tab. 1. On the basis of the cell parameters, the crystal symmetry and the sequence length (342 amino acids) the program MATTHEWS_COEF (Collaborative Computational Project, Number 4) reported as most probable packing (probability 0.93) two Gre2p protomers per asymmetric unit corresponding to a V_M-value of 2.1 ($Å^{3*}$mole)/g Da^{-1} and a solvent content of 41.4%. The alternative solution with a

probabiliiy of 0.06 and one protomer per asymmetric unit leads to a relatively high V_M-value [4.2 (Å^{3*}mole)(g); however, the low diffraction quality of the crystals might be consistent with this.
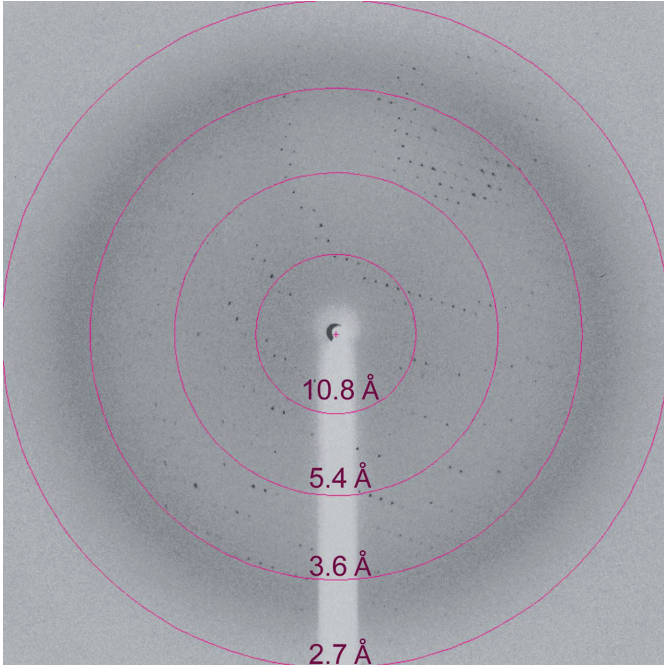

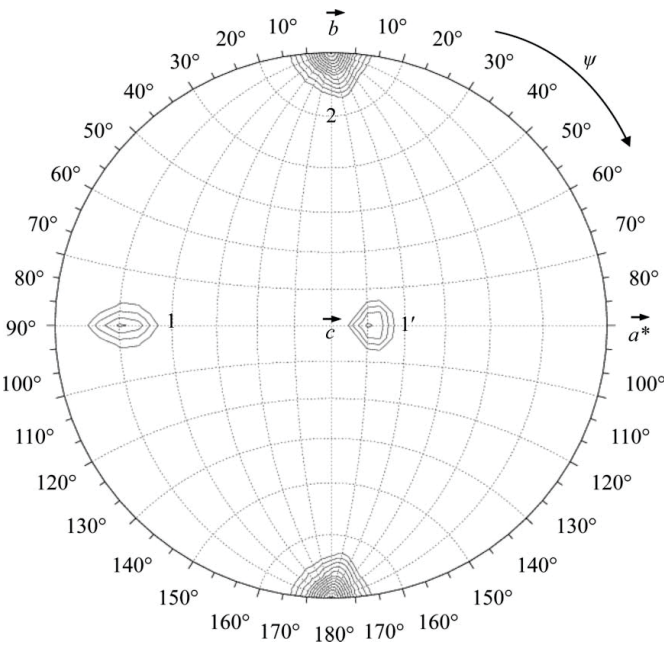**Figure 2.** X-ray diffraction pattern of a monoclinic Gre2p/NADP$^+$ crystal with resolution rings.

Figure 3. Section of the self rotation function with κ = 180°. The self rotation function was calculated with GLRF (Tong & Rossmann, 1997) using diffraction data between 15 and 3.5 Å resolution. Contour lines are drawn starting from 5 RMS. (root means quare) deviations above the mean in intervals of 0.5 RMS. deviations. The two peaks originating from the crystallographic two-fold axis are labelled "2" and "2'" , whereas the non-crystallographic peaks are designated "1" and "1'".

For further clarification clarification we performed Patterson search calculations. A native Patterson function was inconspicuous, i.e. no pseudo-origin peak could be detected. However, in a selfrotation calculation over the full rotation space (0° ≤ φ ≤ 180°; 0° ≤ ψ ≤ 180°; 0° ≤ κ ≤ 180°) and reflections from 15 to 3.5 Å resolution the highest non-crystallographic peaks were found on the κ = 180°-level (peaks 1 and 1' in Fig. 3). These two peaks have a signal-two-noise ratio of 6.5 which is 57.7 % of that of the crystallographic twofold peak (peak 2 in Fig. 3), i.e. they are quite significant and consistent with the existence of two Gre2p protomers per asymmetric unit. Either peak 1 or peak 1' shows the rotation that maps the two protomers on each other while the other is a Klug peak, originating from the fact that the non-crystallographic dyad is perpendicular to the crystallographic one (peak 2 in Figure 3).

The two-fold symmetry between the two Gre2p protomers in the asymmetric unit is somewhat surprising since in solution a dimeric quarternary structure of Gre2p was never observed. The structure solution which is under way while reveal the location and character of the dimerization interface.

Table 1. Statistics of an X-ray data set from a Gre2p/NADP$^+$ crystal.

Wavelength of data collection (Å)	0.91841
Resolution range (Å)	35.0–3.20 (3.28–3.20)
Space group	P21
Unit-cell parameters (Å, °)	a = 60.54, b = 71.54,
	α = γ = 90, β = 104.49
No. of measured reflections	55409
No. of unique reflections	10530
Unit-cell volume (Å^3)	3.23 x 10^5
Completeness (%)	97.5 (92.9)
⟨I/σ(I)⟩	10.4 (2.4)
R$_{merge}$† (%)	17.0 (63.7)

† R$_{merge}$ = $\Sigma_{hkl}\Sigma_i |I_i(hkl) - \langle I(hkl)\rangle|/\Sigma_{hkl}\Sigma_i I_i(hkl)$.

References

Bradford, M. M. (1976). *Anal. Biochem.* **72**, 248–254.

Casamayor, A., Aldea, M., Casas, C., Herrero, E., Gamo, F. J., Lafuente, M. J., Gancedo, C. & Arino, J. (1995). *Yeast*, **11**, 1281–1288.

Chen, C. N., Porubleva, L., Shearer, G., Svrakic,M., Holden, L. G., Dover, J. L., Johnston, M., Chitnis, P. R. & Kohl, D. H. (2003). *Yeast*, **20**, 545–554.

Choi, Y., Choi, H., Kim, D., Uhm, K.-N. & Kim, H.-K. (2010). *Appl. Microbiol. Biotechnol.* **87**, 185–193.

Collaborative Computational Project, Number 4 (1994). *Acta Cryst.* **D50**, 760–763.

Ema, T., Ide, S., Okita, N. & Sakai, T. (2008). *Adv. Synth. Catal.* **350**, 2039–2044.

Ema, T.,Moriya, H., Kofukuda, T., Ishida, T.,Maehara, K., Utaka, M. & Sakai, T. (2001). *J. Org. Chem.* **66**, 8682–8684.

Filling, C., Berndt, K. D., Benach, J., Knapp, S., Prozorovski, T., Nordling, E., Ladenstein, R., Jornvall, H. & Oppermann, U. (2002). *J. Biol. Chem.* **277**, 25677–25684.

Garay-Arroyo, A. & Covarrubias, A. A. (1999). *Yeast*, **15**, 879–892.

Hauser, M., Horn, P., Tournu, H., Hauser, N. C., Hoheisel, J. D., Brown, A. J. P. & Dickinson, J. R. (2007). *FEMS Yeast Res.* **7**, 84–92.

Jörnvall, H., Persson, B., Krook, M., Atrian, S., Gonzalez-Duarte, R., Jeffery, J. & Ghosh, D. (1995). *Biochemistry*, **34**, 6003–6013.

Kabsch, W. (2010). *Acta Cryst.* **D66**, 125–132.

Kaluzna, I., Andrew, A. A., Bonilla, M., Martzen, M. R. & Stewart, J. D. (2002). *J. Mol. Catal. B Enzym.* **17**, 101–105.

Kamitori, S., Iguchi, A., Ohtaki, A., Yamada, M. & Kita, K. (2005). *J. Mol. Biol.* **352**, 551–558.

Laemmli, U. K. (1970). Nature (London), 227, 680–685.
Matthews, B. W. (1968). *J. Mol. Biol.* **33**, 491–497.

Müller, M., Katzberg, M., Bertau, M. & Hummel, W. (2010). *Org. Biomol. Chem.* **8**, 1540–1550.

Persson, B. et al. (2009). *Chem. Biol. Interact.* **178**, 94–98.
Tong, L. & Rossmann, M. (1997). *Methods Enzymol.* **276**, 594–611.

Vido, K., Spector, D., Lagniel, G., Lopez, S., Toledano, M. B. & Labarre, J. (2001). *J. Biol. Chem.* **276**, 8469–8474.

Warringer, J. & Blomberg, A. (2006). *Yeast*, **23**, 389–398.

6

EXPANDING THE BIOCATALYTIC

TOOLBOX

6.1

A novel alcohol dehydrogenase from *Kluyveromyces polysporus* DSM 70294 revealing a broad range of carbonyl compounds and its application in asymmetric synthesis

Marion Müller and Werner Hummel

A novel alcohol dehydrogenase from *Kluyveromyces polysporus* DSM 70294 revealing a broad range of carbonyl compounds and its application in asymmetric synthesis

Marion Müller and Werner Hummel*

A novel NADPH-dependent alcohol dehydrogenase from *Kluyveromyces polyspora* DSM 70294 (KpADH) was identified, cloned and successfully produced by *Escherichia coli*. Enzyme characterisation revealed that a broad range of carbonyl compounds such as diketones, ketones, α- and β-keto esters and aldehydes are converted with high activity. In cell-free asymmetric reactions KpADH revealed its potential to synthesise the corresponding alcohols with high enantioselectivities. The products displayed Prelog configuration, except ethyl 3-methyl-2-hydroxy-butanoate (**10a**) and ethyl mandelate (**11a**) which were obtained with *R*-configuration. Some of the products obtained are key building blocks in the preparation of therapeutically active compounds or ligands. Because of this, KpADH is a promising biocatalyst for industrial applications.

Introduction

Over the past two decades biocatalysis has increasingly become an alternative to traditional metallo- and organocatalysis in synthetic chemistry.[1] The application of enzymes or microbial cells provides many advantages, such as the high chemo-, regio- and stereoselectivity and the use of mild reaction conditions. Biocatalysts are also, in general, readily available, mostly cost-effective, easy in their handling and sustainable.[2] Redox reactions are catalysed by oxidoreductases which are cofactor-dependent enzymes that are ubiquitously distributed. Because of their applicability to produce optically active compounds, integration of redox biocatalysis in organic chemistry has increased substantially over the last couple of years.[3] Alcohol dehydrogenases (ADHs, EC 1.1.1.x.), a subgroup of oxidoreductases, are employed in the stereoselective reduction of carbonyl compounds.[4] Many of the resulting chiral hydroxy compounds serve as key building blocks in the synthesis of several pharmaceuticals, natural compounds, fine- or agrochemicals and are thus of particular industrial interest.[5] For example, the chiral hydroxy ester ethyl (*S*)-4-chloro-3-hydroxy butanoate serves as an important synthon in the process of the chiral statin side chain of the cholesterol-lowering drug atorvastatin.[6] Another example is the chiral phenyl-substituted 1,2-diol (*S*,*S*)-hydrobenzoin which is used in the preparation of phosphite-type ligands.[7]

Because chiral alcohols are in high demand, expansion of the biocatalytic toolbox by novel ADHs is desirable. In this study, we report about the identification, cloning and recombinant production of a novel alcohol dehydrogenase from the yeast *Kluyveromyces polysporus* and its exploitation in the asymmetric synthesis of a variety of hydroxy compounds.

Marion Müller, Prof. Dr. Werner Hummel, Institute of Molecular Enzyme Technology, Research Center Juelich, 52426 Juelich, Germany, Tel: (+49)24641 613790 E-mail: w.hummel@fz-juelich.de

Results and Discussion

Identification of the alcohol dehydrogenase from *K. polysporus* and homology modelling

Bioinformatic analysis based on amino acid sequence-similarity with the ADH Gre2p from *S. cerevisiae*, revealed a homologous open reading-frame (ORF) in the yeast genome of *Kluyveromyces polysporus*. This ORF contains no introns, comprises 1032 bp and encodes the hypothetical annotated protein, Kpol_1057p21 (abbr. KpADH) of unknown function with a polypeptide of 343 amino acids and a calculated molecular mass of 38 kDa. A pair wise amino acid sequence alignment (Figure 1) showed that both enzymes share an identity of 59% and a homology of 76%. Because of the length of the primary sequence, the glycine-rich motif (Gly7-Ala8-Thr9-Gly10-Phe11-Ile12-Ala13) at the *N*-terminus, the primary structure element of the Rossmann-fold, and the presence of the catalytic triad, comprising of Ser, Tyr, and Lys, KpADH can be grouped into the 'extended' short-chain dehydrogenases subfamily.[8]
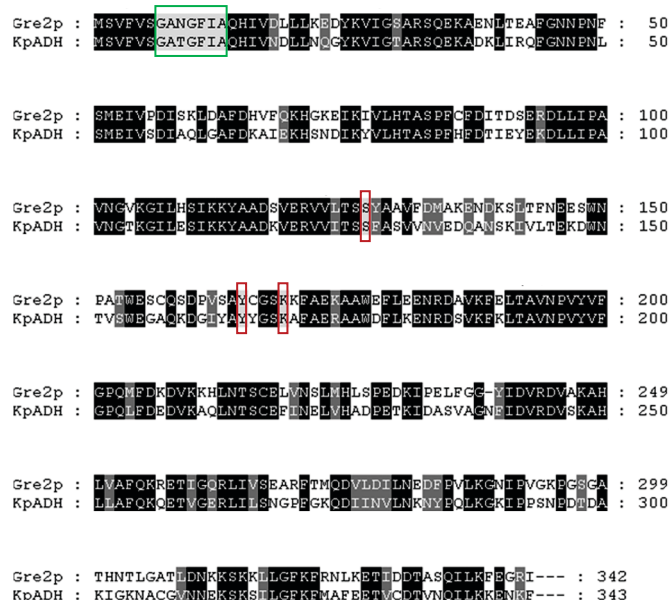
The X-ray structures of Gre2p in its apo-form (PDB ID: 4PVC) and in complex with NADPH (PDB ID: 4PVD) have been solved recently.[9] Because of this, the 3D-structure of Gre2p was used as template to build a homologous model of KpADH (Fig. 2A). Accordingly, likewise Gre2p, the cofactor-binding domain adopts the Rossmann fold consisting of seven parallel-stranded β-sheets which are sandwiched by six α-helices. The glycine-rich motif responsible for binding the adenosine diphosphate (ADP) portion of NAD(P)H is located between β1 and α1. The region between Pro84-His86 (Pro84-Cys86 in Gre2p) is presumably the flexible loop which is meant to bend towards the diphosphate group upon NADPH binding. The smaller substrate-binding domain located in the *C*-terminal region consists of four α-helices and one twisted β-sheet, formed by β1', β2', and β3' which covers the bound cofactor.

A superimposition of the cofactor-binding pocket of the NADPH-complexed Gre2p with the homology model (Fig. 2B) reveals that the residues involved in binding the cofactor in Gre2p match with the residues of the model, except Asn9 which is replaced by a Thr residue in KpADH. The residues Gly7–Ala13 are responsible for binding the ADP portion of the nicotinamide cofactor via five hydrogen bonds in Gre2p (Gly7-O and Gly10-N with hydroxy group of adenosine ribose, Asn9-Nδ2, with phosphate moiety of adenosine, Phe11-N and Ile12-N with diphosphate). However, because Asn9 is replaced by Thr in KpADH a hydrogen bond with the phosphate moiety of adenosine cannot be formed. The hydrogen bonds between the basic amino acids Arg32 (Arg32-Nη) and Lys36 (Lys36-Nζ) and the phosphate moiety of adenosine give Gre2p a stronger affinity for the phosphorylated nicotinamide cofactor. Both amino acids are identical in KpADH and thus it can be deduced by this structural analysis that the enzyme is most likely NADPH-dependent. The adenine ring of NADPH is embedded between Ser83 and Pro84 and the side chains of Arg32 and Ile58 via van der Waal's contacts. Additionally, a hydrogen bond is formed between Asp57 (Asp57-Oδ2) and the amino group of the adenine moiety. Further hydrogen bonds are observed between the nicotinamide ribose and Tyr165 (Tyr165-Oη) and Lys169 (Lys169-Nζ) as well as between the


```
Gre2p : MSVFVSGANGFIAQHIVDLLLKEDYKVIGSARSQEKAENLTEAFGNNPNF : 50
KpADH : MSVFVSGATGFIAQHIVNDLLNQGYKVIGTARSQEKADKLIRQFGNNPNL : 50

Gre2p : SMEIVPDISKLDAFDHVFQKHGKEIKIVLHTASPFCFDITDSERDLLIPA : 100
KpADH : SMEIVSDIAQLGAFDKAIEKHSNDIKYVLHTASPPHFDTIEYEKDLLIPA : 100

Gre2p : VNGVKGILHSIKKYAADSVERVVLTSSYAAVFDMAKENDKSLTFNEESWN : 150
KpADH : VNGTKGILESIKKYAADKVERVVITSSEASVVNVEDQANSKIVLTEKDWN : 150

Gre2p : PATWESCQSDPVSAYCGSKKFAEKAAWEFLEENRDAVKFELTAVNPVYVF : 200
KpADH : TVSWEGAQKDGIYAYYGSKAFAERAAWDFLKENRDSVKFKLTAVNPVYVF : 200

Gre2p : GPQMFDKDVKKHLNTSCBLVNSLMHLSPEDKIPELFGG-YIDVRDVAKAH : 249
KpADH : GPQLFDEDVKAQLNTSCEFINELVHADPETKIDASVAGNEIDVRDVSKAH : 250

Gre2p : LVAFQKRETIGQRLIVSEAREMQDVLDILNEDEPVLKGNIPVGKPGSGA : 299
KpADH : LLAFQKQETVGERLILSNGPEGKQDIINVLNKNYEQLKGKIPPSNEDLDA : 300

Gre2p : THNTLGATLDNKKSKKLLGFKPRNLKETIDDTASQILKFEGRI--- : 342
KpADH : KIGKNACGVNNEKSKSILGFKPMAFEETVCDTVNQILKKENKF--- : 343
```

Figure 1. Figure 1: CLUSTAL W pair wise amino acid sequence alignment of Gre2p and KpADH from *K. polysporus*. Black shaded regions are identical to both sequences, grey shaded regions are homologous. The glycine-rich motif at the *N*-terminus is highlihted in green and the amino acid Ser-Tyr-Lys of the catalytic triad are highlighted in red.

nicotinamide moiety and Val199 (Val199-N) and Ser216 (Ser216-Oγ).

Furthermore, the conformational change of KpADH upon binding the cofactor seems to follow a similar pattern as observed for Gre2p. Thus, the distances of the amino acids in Gre2p, known to shift towards the accommodation cleft, to the homologous residues in KpADH are short. Hence, the side chains of Arg32, Asp57 and Ile58 in KpADH would shift 3.2, 1.7, and 0.6 Å, respectively toward the adenosine ring of NADPH (apoGre2p:Gre2p-NADPH-complex: 2.0, 1.5 and 1.2 Å). Ser83 and Pro84 would shift by 0.9, and 2.5 Å (apoGre2p:Gre2p-NADPH-complex: 0.9 and 4.1 Å) toward the diphosphate group to leave space for the accommodation of the NADPH adenine moiety. The side chains of Tyr165, Lys169 and Ser216 would stabilise the nicotinamide moiety of NADPH by shifting 2.4, 1.9 and 3.1 Å (apoGre2p:Gre2p-NADPH-complex: 2.2, 1.8 and 3.4 Å).

Cloning and recombinant production

The corresponding gene was amplified from genomic DNA by PCR on the basis of sequence information, and was cloned into a medium-copy-number vector to permit efficient over-expression of the gene. This recombinant plasmid was expressed in *E. coli* BL21(DE3), and the highest activity was obtained after an overnight incubation (16h) at 25°C. Towards reduction of the γ-diketone, 2,5-hexanedione, a specific activity of 46.4 U mg^{-1} was obtained. An appropriate SDS-PAGE analysis confirmed the good production of recombinant enzyme since a large amount of enzyme was found in the soluble fraction (Fig. 3, lane 2).

Purification and molecular characteristics of KpADH

KpADH was purified to homogeneity within a three-step procedure, starting with an ammonium sulphate precipitation, followed by hydrophobic interaction chromatography and purification using hydroxyapatite. As illustrated in Figure 3 and summarised in Table 1, nearly pure enzyme

(≥95%) was obtained which revealed a specific activity of 96.8 U mg^{-1} towards 2,5-hexanedione; twice as much as the initial activity. Moreover, because a distinct, single band with an evident molecular size of 39 kDa is visible in the SDS-gel (Fig. 3) the calculated molecular mass of 38 kDa derived from the amino acid sequence could be confirmed.
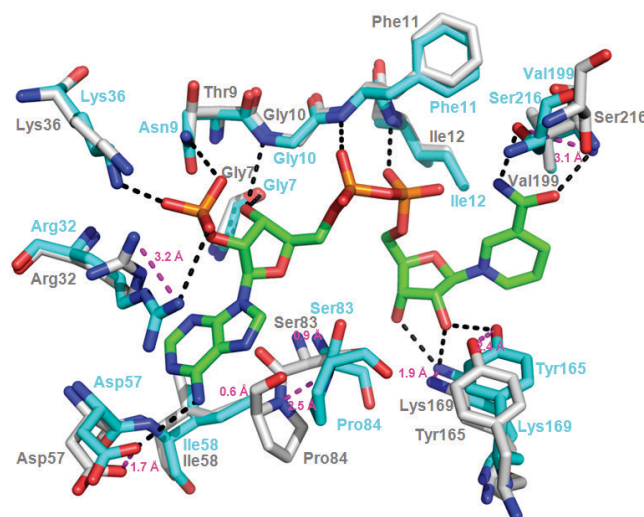
A
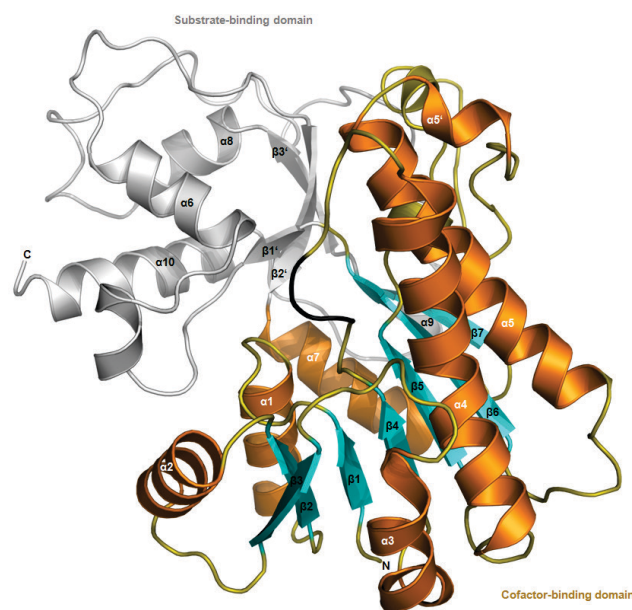
B

Figure 2. Figure 2: (A) Cartoon representation of the overall homology structure model of KpADH based on the X-ray structure of apo-Gre2p (PDB ID: 4PVC). Cyan: β-sheet; orange: α-helix; olive: *N*-terminal cofactor-binding domain; black: flexible loop; grey: *C*-terminal substrate-binding domain. (B) Superimposition of the cofactor-binding pocket of NADPH-complexed Gre2p with the KpADH homology model. Turquoise residues belong to Gre2p; grey residues to KpADH; NADPH in green; black dashed lines indicate the interaction of NADPH with surrounding Gre2p residues; magenta dashed lines show the distance between Gre2p and KpADH residues.

Nevertheless, it was also tried to estimate the native molecular mass by size-exclusion chromatography revealing a mass of about 28 kDa by comparison with standard proteins suggesting a monomeric structure. However, crystallisation of Gre2p confirmed a structure composed of two subunits[9-10] whilst size-exclusion chromatography analysis demonstrated the enzyme to be monomeric either.[11]

Spectrophotometric measurements using cell-free extract and purified enzyme revealed that both NADPH and NADH are accepted as cofactor. However, in both cases the majority of activity (97%) was reached when the phosphorylated cofactor was used confirming the NADPH-dependency concluded from the superimposition. When stored at -20°C and without adding any additives, the purified enzyme was stable for up to three month without losing any activity.
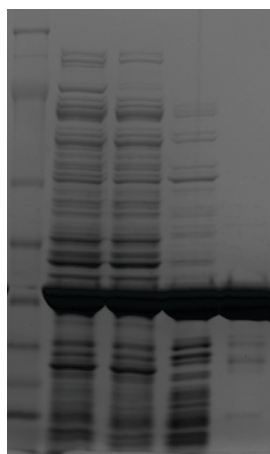
Figure 3. SDS-PAGE analysis of the purification of recombinant KpADH. Lane 1 molecular mass standard; Lane 2 crude extract of soluble protein; Lane 3 crude extract after precipitation wit ammonium sulphate; Lane 4 purified enzyme after butyl sepharose chromatography and Lane 5 purified enzyme after hydroxyapatite chromatography.

Table 1. Summary of the purification of recombinant KpADH

Purification Step	Units (U)	Protein (mg)	Specific activity (U mg^{-1})	Yield (%)	Purification fold
Crude extract*	38605	832	46	100	1.0
Crude extract#	30853	647	48	80	1.03
Butyl Sepharose	7848	110	71	20	1.5
Hydroxyapatite	3678	38	96.8	9.5	2.1

*before precipitation with $(NH_4)_2SO_4$, #after precipitation with $(NH_4)_2SO_4$

Synthesis of (2*S*,5*S*)-hexanediol

The C_2-symmetric *γ*-diol (2*S*,5*S*)-hexanediol is a highly valuable building block since it is used in the preparation of a variety of chiral auxiliaries,[12] ligands[13] and APIs.[14] For efficient synthesis purified recombinant KpADH was employed in the bioreduction of 20 mM 2,5-hexanedione (Figure 4). *In situ* NADPH regeneration was accomplished by coupling the reaction to the oxidation of glucose catalysed by glucose dehydrogenase (GDH). As shown in Figure 5, the diketone was completely (>99%) reduced to the corresponding diol within 7.5 h. Stereochemical analysis revealed that the (*S*,*S*)-diastereomer was formed with ≥99% *de* and *ee* underlining the absolute stereoselectivity of the enzyme.
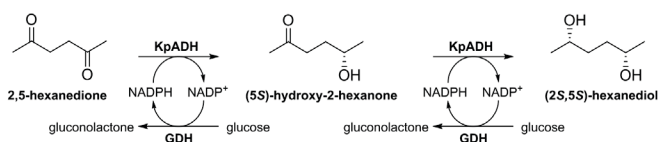

Figure 4. Cell-free reduction of 2,5-hexanedione catalysed by recombinant KpADH. NADPH was regenerated *in situ* by coupling the reaction to the oxidation of glucose catalysed by glucose dehydrogenase from *Bacillus subtilis* (GDH).

The kinetic characterisation of recombinant KpADH towards the reduction reaction is summarised in Table 2. Accordingly, compared to Gre2p[11] the K_M value for 2,5-hexanedione is twice as high suggesting that KpADH reveals a lower affinity towards this substrate. The K_M value for NADPH lies in the range (0.01-0.2 mM) usually found for nicotinamide coenzyme of other dehydrogenases. Because the hydroxy intermediate (5*S*)-hydroxy-2-hexanone is commercially not available and difficult to synthesise no kinetic data could be achieved for this compound. However, since the reaction proceeded via the transient accumulation of the intermediate (Fig. 5) it is evident that the affinity of the enzyme towards the hydroxy ketone is lower than it is towards the diketone. This is in accordance with the data found for the *γ*-diketone reduction catalysed by Gre2p.[11]

Besides Gre2p from *Saccharomyces cerevisiae*[11] and an ADH from *Candida parapsilosis*,[15] KpADH

is the third ADH of yeast origin and in total the sixth ADH, along with an ADH from *Thermoanaerobacter* sp.,[16] *Rodococcus ruber*[17] and *Pyrococcus furiosus*,[18] possesing the ability of reducing both carbonyl groups of 2,5-hexanedione *S*-enantioselectively to the corresponding diol.
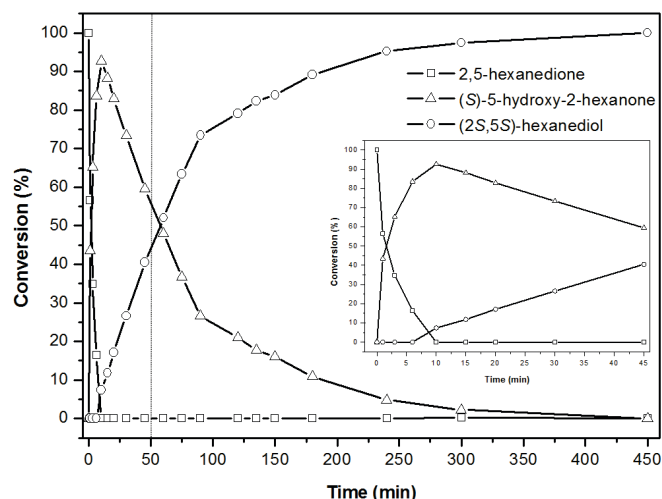

Figure 5. Time course of the synthesis of (2*S*,5*S*)-hexanediol. The reaction mixture consisted of 20 mM substrate, 50 mM glucose, 0.5 mM NADP+, 15 U mL^{-1} glucose dehydrogenase and 5 U mL^{-1} KpADH in a total volume of 15 mL Kpi buffer (0.1 M, pH 7.5). After a transient accumulation of the hydroxy ketone the diketone was fully converted to the diol.

Table 2. Kinetic parameters of purified recombinant KpADH

Substrate	K_M (mM)	V_{max} (U mg^{-1})	k_{cat} (s^{-1})	k_{cat}/K_M (s^{-1} mM^{-1})
2,5-Hexanedione	9.28 ± 0.36	164.2 ± 1.5	105	11.3
NADPH	0.05 ± 0.02	447.1 ± 14.3	287	5740

Substrate specificity of KpADH

To examine the substrate spectrum of KpADH a variety of different carbonyl compounds were employed as substrates and a spectrophotometric assay was carried out following the determination of specific activities. The activities thus obtained were referenced to the 2,5-hexanedione activity (**1**, 96.8 U mg^{-1}). The corresponding results are summarised in Table 3.

With respect to diketone reduction, KpADH accepts several *α*-and *β*-diketones but with lower activities than 2,5-hexanedione. It is also revealed that the enzyme favours the reduction of *α*-diketones over *β*-diketones. For example, activity obtained towards the *α*-diketone 2,3-pentanedione (**6**) was three-fold higher than with 2,4-pentanedione (**2**). Moreover, the tendency to catalyse the reduction of *α*-diketones depends on the position of the carbonyl groups. For instance, KpADH reveals lower activities towards ethyl ketones like 3,4-hexanedione (**5**) than towards methyl ketones like 2,3-hexanedione (**4**). Furthermore, *α*-diketones revealing a C2 carbonyl group are more likely to be reduced the longer the adjacent alkyl chain is. Hence, activity for 2,3-hexanedione (**4**) was nearly twice as much as for 2,3-butanedione (**7**). However, this trend did not continue for the reduction of 2,3-heptanedione (**3**) as the activity was slightly lower (9%) than the activity achieved with **4**.

Regarding the reduction of ethyl *α*-keto esters, catalytic activity increases with the size and bulkiness of the side chain. Accordingly, activity towards ethyl 2-oxo-4-phenylbutanoate (**13**) was over 26-times higher than with the short-chained keto ester ethyl pyruvate (**9**). Methyl *α*-keto esters, in contrast, were shown to be poor substrates and activity decreases with the size of the side chain. Accordingly, methyl 2-oxobutanoate (**10**) revealed a lower activity than methyl pyruvate (**8**).

Catalytic activity towards *β*-keto esters is decreased in comparison to *α*-keto esters. However, substitution at C2 and C4 by the electron withdrawing chlorine atom increases activity. Hence, activities towards ethyl 4-chloro-3-oxobutanoate (**19**) and ethyl 2-chloro-3-oxobutanoate (**18**) were enhanced by factors of seven and 2.4, respectively, compared to ethyl 3-oxobutanoate (**14**). Also, a three-fold enhanced activity was observed when the ester moiety contained an aromatic residue (**16**) instead of the ethyl group (**14**). Among all keto esters tested KpADH displayed the lowest activities towards *tert*-butyl 3-oxobutanoate (**15**) and the cyclic keto ester ethyl 2-oxocyclopentanecarboxylate (**17**).

Aliphatic, aromatic and unsaturated ketones were demonstrated to be poor substrates while 3-ketones were not reduced at all (data not shown). Activity towards aliphatic 2-ketones first increased from 2-butanone (**20**) to 2-pentanone (**21**) before dropping from 2-hexanone (**22**) to 2,3-octanone

(**24**). In contrast, the keto-aldehyde, methylglyoxal (**25**), and hydroxyacetone (**26**), were catalysed with approximately 50% and 9.4% of the 2,5-hexanedione activity, respectively. The high methyglyoxal activity is consistent with the activity found for Gre2p[11] and suggests that KpADH, like demonstrated for Gre2p,[19] plays a role in the *in vivo* detoxification of this compound. Methylglyoxal was put into the group of ketones as Gre2p was demonstrated to catalyse the reduction of the keto group to form (*S*)-lactaldehyde. The very low activity towards ketones, in particular towards 2-ketones, indicates that efficient substrate binding may only be possible if a second keto group or hydrophilic moiety is present in the molecule.

Although aldehydes are less import for biotechnological applications they were investigated as well and the high activities reveal that KpADH favors the reduction of representatives of this substrate class. For example, the enzyme displayed the highest specific activity towards isovaleraldehyde (**34**) which was nearly three-times higher than the activity obtained with 2,5-hexanedione. This was also observed for Gre2p[11] which was considered to play a role in the *in vivo* reduction of isovaleraldehyde as well.[20] The enzymes' catalytic activity for the reduction of aliphatic aldehydes increased significantly from propanal (**30**) to butanal (**31**) and decreased with longer chain length from pentanal (**33**) to hexanal (**35**). While the aromatic aldehyde, benzaldehyde was well accepted by the enzyme, unsaturated *trans*-2-hexenal (**35**) was reduced with half of the activity achieved with hexanal (**35**).

Table 3. Specific activities of purified KpADH towards the reduction of various carbonyl compounds. If not indicated otherwise, all substrates were applied at a concentration of 20 mM.
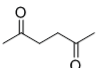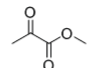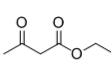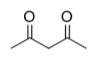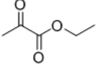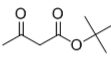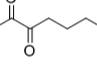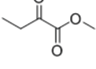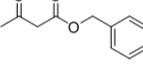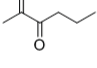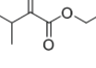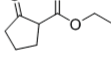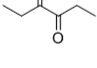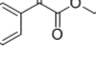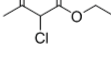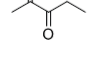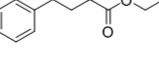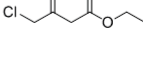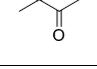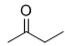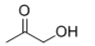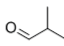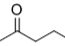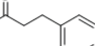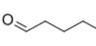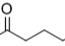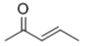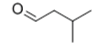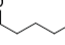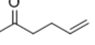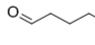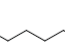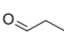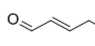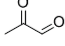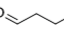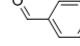
Entry	Substrate	Specific activity (U mg^{-1})	Entry	Substrate	Specific activity (U mg^{-1})	Entry	Substrate	Specific activity (U mg^{-1})
	α, β-diketones			**α-keto esters**				
1		96.8	8		1.8	14		1.6
2		2.9	9		1.5	15		0.3
3		11.6	10		1.0	16		4.8
4		14.3	11		7.9	17		0.2
5		2.1	12*		25.7	18		3.9
6		8.6	13		39.6	19		11.2
7		7.6		**β-keto esters**			**ketones**	

Table 3 (continued).

Entry	Substrate	Specific activity (U mg⁻¹)	Entry	Substrate	Specific activity (U mg⁻¹)	Entry	Substrate	Specific activity (U mg⁻¹)
20		0.1	26		9.1	32		204
21		1.6	27		0.5	33		170
22		1.3	28		0.1	34		275
23		0.4	29		2.4	35		47.2
				aldehydes				
24		0.2	30		1.0	36		23.2
25		52.4	31		233	37		116

* Due to its low solubility 10 mM was applied

Application of KpADH in asymmetric synthesis

Because of the broad substrate spectrum KpADH was applied in cell-free asymmetric syntheses reactions using the oxidation of glucose catalysed by GDH for *in situ* regeneration of NADPH. The corresponding results are summarised in Table 4.

Table 4. Results of the enantioselective reduction of various carbonyl compounds catalysed by KpADH
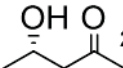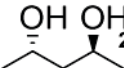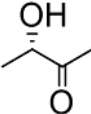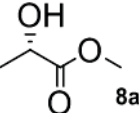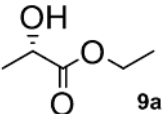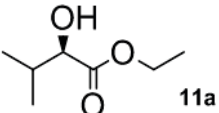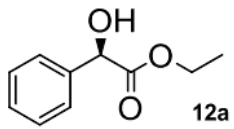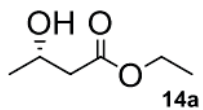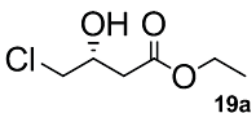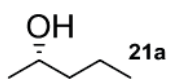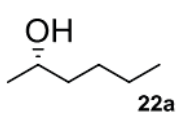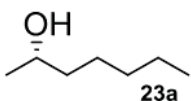
Entry	Product(s)	Time (h)	Conversion (%)	ee (%)	Configuration R/S
2	2a / 2b	1 (a), 24 (b)	99.4 (a) 28.4 (b)	99.0 99.0 (*de*>99.0 %)	S S,S
7	7a	2	82.3	99.0	S
8	8a	1.75	63	97.7	S
9	9a	1.75	98	94.5	S
11	11a	0.4	>99	99.5	R

Table 4 (continued).

12*	OH / ethyl mandelate **12a**	0.3	>99	99.6	R
14	OH O / **14a**	1	>99	99.1	S
19	Cl / OH O / **19a**	3	83.6	95.4	R
21	OH / **21a**	1.25	>99	99.9	S
22	OH / **22a**	1	>99	99.9	S
23	OH / **23a**	1.25	>99	99.9	S

*10 mM was used for *in vitro* biocatalysis

Accordingly, KpADH catalysed the reduction of 2,3-butanedione and 2,4-pentanedione to the corresponding hydroxy ketones (**2a** and **7a**) with excellent enantioselectivities (>99%) and high (99.4%, **2a**) to reasonable (82.3%, **7a**) conversion yields. Regarding the reduction of 2,3-butanedione the reaction stopped with the formation of the hydroxy ketone since no diol (**7b**) was detected after 24 h. In contrast, reduction of the β-diketone yielded minor amount of diol (28.4%, **2b**). In any case KpADH showed a perfect Prelog selectivity,[21] producing the corresponding alcohols with S-configuration. The chiral products are of great industrial interest. For instance, (S)-4-hydroxy-2-pentanone (**2a**) is a building block in the total synthesis of the antifungal macrolide antibiotic (+)-roxaticin[22] and (2S,4S)-pentanediol (**2b**) is used in the synthesis of the novel spiroketal pyrrolidine GSK2336805 which potently inhibits key hepatitis C virus genotype 1b mutants.[23]

α-Hydroxy esters were synthesised with either >99% ee (**11a**, **12a**) or with a slightly decreased enantioselectivity (94-97% ee; **8a** and **9a**). Interestingly, synthesis of methyl and ethyl lactate followed the Prelog rule whereas the absolute configuration of ethyl mandelate and ethyl 2-hydroxy-3-methylbutanoate were opposite to the stereochemical trend as the anti-Prelog products were observed. Optically pure ethyl 2-hydroxy-3-methylbutanoate (**11a**) is useful in the caspase inhibitor synthesis[24] and (R)-ethyl mandelate (**12a**) is a key compound in the preparation of the anti-tumor macrolides cryptophycins 1 and 8.[25] Although reduction of ethyl 3-oxobutanoate revealed a low specific activity, KpADH was able to synthesise the corresponding (S)-hydroxy ester (**14a**) with an ee and a conversion of >99 % within 1 h. Surprisingly, biotransformation of ethyl 4-chloro-3-oxobutanoate which was demonstrated to give a higher activity than its un-substituted keto ester (see Table 3), resulted in a conversion of only 83.6% with a slightly diminished enantioselectivity (95.4% ee, **19a**). Ethyl (R)-4-chloro-3-hydroxybutonoate is used for the

production of the natural compound L-carnitine and the naturally occurring (*R*)-4-hydroxy-2-pyrrolidone.[26]

Although the enzyme displays much lower activities towards aliphatic 2-ketones compared to aldehydes, diketones and keto esters, reduction of 2-pentanone, 2-hexanone and 2-heptanone led to the corresponding Prelog-alcohols (**21a-23a**) with high conversion yields (>99%) and excellent enantioselectivities (*ee*>99.9%). (*S*)-2-pentanol (**21a**) is an intermediate in the synthesis of several potential anti-Alzheimer's drugs inhibiting *β*-amyloid peptide release.[27] It is also the active component of the alarm pheromone in the venom of the giant hornet *Vespa mandarinia*.[28] (*S*)-2-Hexanol (**22a**) is used in the total synthesis of the antivirally active glycolipid cycloviracin B$_1$.[29]

Conclusion

In conclusion, the newly identified alcohol dehydrogenase from *K. polysporus* has been demonstrated to be a valuable biocatalyst as it displays a broad substrate spectrum and reduces carbonyl compounds at high enantiomeric purity. The enzyme showed perfect Prelog selectivity, except for the reduction of ethyl-3-methyl-2-oxobutanoate and ethyl benzoylformate forming the corresponding *R*-alcohols. Many hydroxy compounds produced in this work are potential chiral synthons in the synthesis of pharmaceutical active compounds, ligands and auxiliaries.

Experimental section

General

If not stated otherwise all chemicals were purchased from Sigma-Aldrich (Buchs, Switzerland) and were of highest purity. Nicotinamide cofactors were obtained from Biomol (Hamburg, Germany) and restriction enzymes and T4 DNA ligase were purchased from Fermentas (St. Leon-Rot, Germany). The plasmid pKA1 was constructed in our laboratories. *Kluyveromyces polysporus* (*Vanderwaltozyma polyspora*) DSM 70294 was obtained from the

Deutsche Sammlung von Mikroorganismen und Zellkulturen, DSMZ (Braunschweig, Germany) and was grown as recommended on Yeast extract-Peptone-Dextrose medium (YPD, 10g/L yeast extract, 20 g/L peptone and 20 g/L glucose; pH 6.5) at 25 °C. Glucose dehydrogenase (GDH) from *Bacillus subtilis* was used for NADPH recycling and was amplified from pAW-3,[30] re-cloned into pET-11 and expressed in *E. coli* BL21(DE3). The non-purified enzyme was then applied in asymmetric synthesis reactions.

Chiral GC and HPLC analysis were carried out using the Shimadzu GC-17A (Duisburg, Germany) equipped with a Varian CP-Chirasil-Dex CB column (25 m x 0.25 mm) and the Gynkotec HPLC (Techlab, Erkerode, Germany) equipped with a P580 pump, a UVD320S detector and a Chirapak IC column (25 cm x 0.46 cm, Macherey Nagel, Düren, Germany). An infrared spectrum was obtained from neat sample on a Perkin Elmer FTIR instrument (Waltham, USA). Mass spectroscopy analysis was carried out on the HP 5973 GC/MS System (Hewlett-Packard, Palo Alto, USA). NMR spectra were recorded at 300 K using the Bruker DRX 600 MHz spectrometer (Billerica, USA). Optical rotation was measured with the 341 Perkin-Elmer polarimeter at *λ*=589 nm (sodium-D-line) and 22°C in a cell of 1 dm length.

Molecular cloning and recombinant expression

Genomic DNA was isolated according to the protocol described by Harju[31] and subsequently used as template for PCR. The following primers were used, introducing the restriction sites, *Nde*I and *Bam*HI: 5'-GAGGTCGGT<u>CATATG</u>TCTGTT-TTTGTTTCT-3' and 5'-CGC<u>GGATCC</u>TTATTAAAATT-TATTTTCTTTCTTCAAG-3'. The PCR product was cloned into pKA1 and the resulting expression plasmid pKA1-KpADH was used to transform *E. coli* BL21(DE3) cells. Recombinant protein production was accomplished overnight at 25°C in LB medium (10 g L^{-1} NaCl, 10 g L^{-1} tryptone and 5 g L^{-1} yeast extract), containing 34 µg mL^{-1} chloroamphenicol. Expression was started by the addition of isopropyl thio-*β*-D-galactoside (IPTG) to a final concentration of 0.2 mM when the optical density (OD) at 600 nm reached a value of 0.5-0.7. The

cells were harvested by centrifugation at 27,000*g* for 1 h and were stored at -20°C prior to their use.

Enzyme purification and molecular mass determination

The cell pellet was suspended at a ratio of 1 g cells (wet weight) to 2 mL 0.1 M triethanolamine hydrochloride buffer (TEA, pH 7.0). Cell lysis was done via sonication using three cycles of 2 min at 37% power output with 2 min cooling periods in-between. Cell debris was removed by centrifugation at 27,000*g* at 4°C for 30 min. To the resulting cell-free extract 1.5 M ammonium sulphate was added followed by incubation on ice for 2 h. The pre-cleaned extract was now applied onto a Butyl Sepharose™ 4 Fast Flow (Bio-Rad; Munich, Germany) column which had been equilibrated with 10 column volumes (CVs) of TEA buffer (0.1 M, pH 7.0). Enzyme elution was accomplished using the same buffer without ammonium sulphate in a linear gradient of 1.5-0 M. Active fractions were pooled and applied onto a Macro-Prep® Ceramic Hydroxyapatite (Bio-Rad) column which had been equilibrated with 10 CVs of 5 mM potassium phosphate buffer (pH 7.0) containing 150 mM NaCl. The enzyme was eluted from the column with a linear gradient of 5-45 mM potassium phosphate buffer.

Size-exclusion chromatography was performed using a HiLoad™ 16/60 Superdex™ 200 prep grade column from GE Healthcare (Amersham, UK) and sodium phosphate buffer (50mM, pH 7.2) including 150 mM NaCl.

Activity measurements and protein analysis

Enzyme activity was determined photometrically by monitoring the decrease of NAD(P)H over 1 min at 340 nm and 30°C. KpADH activity is expressed in Unit (U) and one unit is defined as the amount of KpADH catalysing the oxidation of 1 µmol NAD(P)H per minute. If not stated otherwise the assay mixture contained of 20 mM substrate in TEA buffer (0.1M, pH 7.0) and 0.25 mM cofactor in a total volume of 1 mL. The assay was started by the addition of 10 µL enzyme solution. The assay mixture for GDH contained 970 µL D-glucose (100 mM in 100 mM TEA buffer) and 20 µL NADP$^+$ (100 mM in deionised water). The reaction was initiated by adding 10 µL of enzyme solution.

Determination of protein concentrations were carried out according to the protocol described by Bradford using bovine serum albumin (BSA) as standard.[32] As described by Laemmli,[33] SDS-PAGE analysis was performed using a 4-12 % Nu-PAGE Novex Bis-Tris gel from Invitrogen (Darmstadt, Germany).

General procedure for cell-free biotransformation and chiral analytic

To a solution of 0.75 mol D-glucose (135 mg), 7.5 mmol NADP$^+$ (5.6 mg), substrate (20 mM) and 45 U *Bacillus subtilis* GDH (225 U for biotransformation of 2,5-hexanedione) in potassium phosphate buffer (0.1 M Kpi, pH 7.5; 15 mL), 15 U of KpADH in reference to the compound (75 U for biotransformation of 2,5-hexanedione) was added. The mixture was incubated at 30°C under gentle shaking. To follow the reaction course samples were taken periodically and analysed by gas chromatography (GC). After completion of the reaction, the mixture was extracted with ethyl acetate and the organic layer was subjected to chiral GC or HPLC analysis for determination of the enantiomeric excess. Except for ethyl 2-hydroxy-3-methylbutanoate, absolute configuration was assigned in reference to both enantiomers of the corresponding alcohol which were obtained commercially. If required, flash column chromatography was performed using silica gel 0.040-0.063 mm (400-230 mesh, Macherey & Nagel) before analysis. The applied methods and retention times for each product are summarised in Table 5. For a more efficient analysis of 2,5-hexanediol, ethyl-2-hydroxy-3-methylbutanoate, 4-chloro-3-hydroxybutonoate and 2-heptanol derivatisation of the hydroxy group with triflouroacetic acid anhydride was necessary and was performed according to the protocol described previously.[11]

Table 5. Instruments and methods for chiral analytic.

Chiral Products	Instrument/ method	Retention time (min)
2,5-Hexanediol*	GC, 55 °C 30 min	**(S,S): 20.1** (R,R): 23.4 (meso): 24.6
2a	GC, 40 °C 5 min, 2 °C/ min 70 °C	**(S): 11.4** (R): 11.2
2b	GC, 40 °C 5 min, 2 °C/ min 70 °C	**(S,S): 17.0** (R,R): 16.8 (meso): 16.5
7a	GC, 40 °C 2 min, 8 °C/ min 101 °C, 0.1 °C/ min 102 °C	**(S): 7.3** (R): 6.9
8a	GC, 40°C 3 min, 5 °C/ min 90°C	**(S): 10.0** (R): 10.7
9a	GC, 40°C 3 min, 5 °C/ min 90°C	**(S): 12.0** (R): 12.5
11a*	GC, 60 °C 2 min, 1 °C/ min 90 °C	(S): 12.2 **(R): 10.6**
12a	HPLC, flow rate 0.5 ml/ min, heptane-isopropanol = 90:10, 225 nm	(S): 20.2 **(R): 18.5**
14a*	GC, 70 °C, 5 °C/ min 86 °C, 0.1 °C/ min 87°C	**(S): 6.9** (R): 6.7
19a*	GC, 100 °C, 1 °C/ min 113 °C	(S): 9.0 **(R): 9.3**
21a	40 °C 1.5 min, 5 °C/ min 66 °C, 0.5 °C/ min 68 °C	**(S): 8.4** (R): 8.2
22a	50 °C 5 min, 10 °C/ min 84 °C, 0.5 °C/ min 86 °C	**(S): 10.6** (R): 10.4
23a*	60 °C 5 min, 5 °C/ min 75 °C	**(S): 7.7** (R): 7.9

*derivatisation was necessary

Preparation of racemic reference compound, ethyl 2-hydroxy-3-methylbutanoate

Ethyl 2-hydroxy-3-methylbutanoate (**10a**) was synthesised through reduction of ethyl 3-methyl-2-oxobutyrate (**10**) according to a standard Luche-procedure.[34] The reaction was carried out using *Schlenk* technique under an atmosphere of dry nitrogen. Glass-ware was oven-dried at 120°C overnight prior to use. Dichloromethane (CH_2Cl_2) was dried in a solvent purification system from MBRAUN (Garching, Germany). Solvent evaporation under reduced pressure was performed on a rotary evaporator at 40°C (water bath). A 20 mL Schlenk flask was charged with keto ester (500 mg, 3.5 mmol, 1 eq.), $CeCl_3$ (855 mg, 3.5 mmol, 1 eq.) and ethanol (5 mL) and cooled to -78°C. After the addition of $NaBH_4$ (197 mg, 5.2 mmol, 1.5 eq.) stirring was continued for 5 h at -78°C and then the reaction mixture was allowed to warm up to 0°C; TLC indicated complete conversion into hydroxy ester. The remaining $NaBH_4$ was hydrolysed with 2 M aq. HCl (2 mL). After extraction with CH_2Cl_2 (3x15 mL) the combined organic layer was washed with brine (3x20 mL) and dried over $MgSO_4$. After removal of the solvent under reduced pressure, the desired product (**10a**) was obtained containing traces of

the corresponding diol, 3-methylbutane-1,2-diol. Column chromatography with petroleum ether/ethyl acetate (90:10) yielded the pure compound (340 mg, 2.3 mmol, 67%) as colorless liquid. The analytical data are in agreement with those reported in literature.[35] R_f (80% petroleum ether/ethyl acetate) 0.32; ν_{max} (liquid film): 3502 (br, O-H-ν), 2964, 2935, 2877 (aliph. C-H-ν), 1727 (C=O-ν), 1468, 1388, 1369, 1256, 1209, 1178, 1137, 1098, 1070, 1030, 971, 930, 911, 866, 755 cm^{-1}; ^{1}H NMR (CDCl$_3$, 600 MHz) 0.87 [3 H, d, ^3J 6.9, CH(C**H**$_3$)$_2$], 1.03 [3 H, d, ^3J 6.9, CH(C**H**$_3$)$_2$], 1.31 (3 H, t, ^3J 7.1 Hz, CH$_2$C**H**$_3$), 2.08 [1 H, dqq, ^3J 6.9 Hz, ^3J 6.9 Hz, ^3J = 3.5 Hz, C**H**(CH$_3$)$_2$], 2.71 (1 H, d, ^3J 6.1 Hz, O**H**), 4.03 (1 H, dd, ^3J 3.5 Hz, J 6.1 Hz, C**H**OH), 4.31 - 4.21 (2 H, m, OC**H$_2$**); ^{13}C NMR (CDCl$_3$, 151 MHz) 14.3 (CH$_2$**C**H$_3$), 16.0 [CH(**C**H$_3$)$_2$], 18.8 [CH(**C**H$_3$)$_2$], 32.2 [**C**H(CH$_3$)$_2$], 61.6 (O**C**H$_2$), 75.0 (**C**HOH), 175.0 (**C**=O); GC/MS (EI, 70 eV, H$_2$): t_{ret} 4.1 min, m/z 147 (<1) [(M+H)$^+$], 104 (17) [(M-C$_3$H$_6$)$^+$], 103 (11) [(M-C$_3$H$_7$)$^+$], 76 (47) [(M-C$_5$H$_{11}$)$^+$], 75 (11) [(M-C$_5$H$_{12}$)$^+$], 73 (100) [(M-C$_3$H$_5$O$_2$)$^+$]. $[\alpha]_D^{22}$ = -8.7 (c 1, CHCl$_3$, (**R**)-**10a** {$[\alpha]_D^{22}$ = -9.5 (c 1, CHCl$_3$)}.[36]

Acknowledgment

References

[1]   (a) B. M. Nestl, S. C. Hammer, B. A. Nebel, B. Hauer, *Angew. Chem.-Int. Edit.* **2014**, *53*, 3070-3095; (b) M. T. Reetz, *J. Am. Chem. Soc.* **2013**, *135*, 12480-12496; (c) N. J. Turner, E. O'Reilly, *Nat. Chem. Biol.* **2013**, *9*, 285-288.

[2]   (a) K. Buchholz, V. Kasche, U. T. Bornscheuer, *Biocatalysts and Enzyme Technology, Vol. 2nd Edn.*, Wiley-VCH, Weinheim, **2012**; (b) K. Faber, *Biotransformations in organic chemistry, Vol. 6th Edn.*, Springer-Verlag, Berlin, **2011**.

[3]   (a) M. Hall, A. S. Bommarius, *Chem. Rev.* **2011**, *111*, 4088-4110; (b) F. Hollmann, I. W. C. E. Arends, D. Holtmann, *Green Chem.* **2011**, *13*, 2285-2314.

[4]   (a) Y. Ni, J. H. Xu, *Biotechnol. Adv.* **2012**, *30*, 1279-1288; (b) H. Gröger, W. Hummel, R. Metzner, in *Comprehensive Chirality, Vol. 7* (Eds.: E. M. Carreira, H. Yamamoto), Elsevier, Amsterdam, **2012**, 181-215; (c) H. Gröger, S. Borchert, M. Kraußer, W. Hummel, in *Enzyme catalysis in organic synthesis, Vol. 3* (Eds.: K. Drauz, H. Gröger, O. May), Wiley-VCH Weinheim, **2012**, 1037-1110; (d) H. Gröger, S. Borchert, M. Kraußer, W. Hummel, in *Encyclopdia of industrial biotechnology: Bioprocess,*

bioseparation and cell technology Vol. 3 (Ed.: M. C. Flickinger), John Wiley & Sons, Hoboken, New Jersey, **2010**, 2094-2110.

[5]   (a) R. N. Patel, *Biomolecules* **2013**, *3*, 741-777; (b) D. Muñoz Solano, P. Hoyos, M. J. Hernáiz, A. R. Alcántara, J. M. Sánchez-Montero, *Bioresour. Technol.* **2012**, *115*, 196-207; (c) T. Fischer, J. Pietruszka, in *Natural Products via Enzymatic Reactions, Vol. 297* (Ed.: J. Piel), Springer Berlin Heidelberg, **2010**, 1-43; (d) J. Tao, J. H. Xu, *Curr. Opin. Chem. Biol.* **2009**, *13*, 43-50.

[6]   (a) A. Liljeblad, A. Kallinen, L. T. Kanerva, *Curr. Org. Synth.* **2009**, *6*, 362-379; (b) M. Müller, *Angew. Chem.-Int. Edit.* **2005**, *44*, 362-365.

[7]   K. N. Gavrilov, S. V. Zheglov, M. N. Gavrilova, I. V. Chuchelkin, N. N. Groshkin, E. A. Rastorguev, V. A. Davankov, *Tetrahedron Lett.* **2011**, *52*, 5706-5710.

[8]   K. Kavanagh, H. Jörnvall, B. Persson, U. Oppermann, *Cell. Mol. Life Sci.* **2008**, *65*, 3895-3906.

[9]   P. C. Guo, Z. Z. Bao, X. X. Ma, Q. Xia, W. F. Li, *Biochim. Biophys. Acta* **2014**, *1844*, 1486–1492.

[10]   K. Breicha, M. Müller, W. Hummel, K. Niefind, *Acta Crystallogr. F-Struct. Biol. Cryst. Commun.* **2010**, *66*, 838-841.

[11]   M. Müller, M. Katzberg, M. Bertau, W. Hummel, *Org. Biomol. Chem.* **2010**, *8*, 1540-1550.

[12]   (a) H. Takada, P. Metzner, C. Philouze, *Chem. Commun.* **2001**, 2350-2351; (b) K. Julienne, P. Metzner, V. Henryon, A. Greiner, *J. Org. Chem.* **1998**, *63*, 4532-4534; (c) R. P. Short, R. M. Kennedy, S. Masamune, *J. Org. Chem.* **1989**, *54*, 1755-1756.

[13]   M. J. Burk, J. E. Feaster, R. L. Harlow, *Tetrahedron: Asymmetry* **1991**, *2*, 569-592.

[14]   E. Díez, R. Fernández, E. Marqués-López, E. Martín-Zamora, J. M. Lassaletta, *Org. Lett.* **2004**, *6*, 2749-2752.

[15]   A. Gupta, A. Tschentscher, M. Bobkova, WO2006EP07425, 2008.

[16]   M. Katzberg, K. Wechler, M. Müller, P. Dünkelmann, J. Stohrer, W. Hummel, M. Bertau, *Org. Biomol. Chem.* **2009**, *7*, 304-314.

[17]   K. Edegger, W. Stampfer, B. Seisser, K. Faber, S. F. Mayer, R. Oehrlein, A. Hafner, W. Kroutil, *Eur. J. Org. Chem.* **2006**, 1904-1909.

[18]   R. Machielsen, N. G. H. Leferink, A. Hendriks, S. J. J. Brouns, H. G. Hennemann, T. Daußmann, J. van der Oost, *Extremophiles* **2008**, *12*, 587-594.

[19]   C. N. Chen, L. Porubleva, G. Shearer, M. Svrakic, L. G. Holden, J. L. Dover, M. Johnston, P. R. Chitnis, D. H. Kohl, *Yeast* **2003**, *20*, 545-554.

[20]   M. Hauser, P. Horn, H. Tournu, N. C. Hauser, J. D. Hoheisel, A. J. P. Brown, J. R. Dickinson, *FEMS Yeast Res.* **2007**, *7*, 84-92.

[21]   V. Prelog, *Pure Appl. Chem.* **1964**, *9*, 119-130.

[22]   D. A. Evans, B. T. Connell, *J. Am. Chem. Soc.* **2003**, *125*, 10899-10905.

[23]   W. M. Kazmierski, A. Maynard, M. Duan, S. Baskaran, J. Botyanszki, R. Crosby, S. Dickerson, M. Tallant, R. Grimes, R. Hamatake, M. Leivers, C. D. Roberts, J. Walker, *J. Med. Chem.* **2014**, *57*, 2058-2073.

[24]   C. Mellon, R. Aspiotis, C. W. Black, C. I. Bayly, E. L. Grimm, A. Giroux, Y. X. Han, E. Isabel, D. J. McKay, D. W. Nicholson, D. M. Rasper, S. Roy, J. Tam, N. A. Thornberry, J. P. Vaillancourt, S. Xanthoudakis, R. Zamboni, Bioorg. *Med. Chem. Lett.* **2005**, *15*, 3886-3890.

[25]   K. M. Gardinier, J. W. Leahy, *J. Org. Chem.* **1998**, *62*, 7098–7099.

[26]   (a) A. Matsuyama, H. Yamamoto, Y. Kobayashi, *Org. Process Res. Dev.* **2002**, *6*, 558-561; (b) B. N. Zhou, A. S. Gopalan, F. VanMiddlesworth, W. R. Shieh, C. J. Sih, *J. Am. Chem. Soc.* **1983**, *105*, 5925-5926.

[27]   R. N. Patel, Expert. Opin. Drug Discov. 2008, 3, 187-245.

[28]   M. Ono, H. Terabe, H. Hori, M. Sasaki, *Nature* **2003**, *424*, 637-638.

[29]   A. Fürstner, M. Albert, J. Mlynarski, M. Matheu, E. DeClercq, *J. Am. Chem. Soc.* **2003**, *125*, 13132-13142.

[30]   A. Weckbecker, W. Hummel, in *Microbial Enzymes and Biotransformations, Vol. 17* (Ed.: J. L. Barredo), Humana Press Inc., Totowa, N. J., **2005**, 225-237.

[31]   S. Harju, H. Fedosyuk, K. R. Peterson, *BMC Biotechnol.* **2004**, *4*, 1-6.

[32]   M. M. Bradford, *Anal. Biochem.* **1976**, *72*, 248-254.

[33]   U. K. Laemmli, *Nature* **1970**, *227*, 680-685.
[34]   A. L. Gemal, J. L. Luche, *J. Am. Chem. Soc.* **1981**, *103*, 5454-5459.
[35]   (a) J. Kim, K. A. De Castro, M. Lim, H. Rhee, *Tetrahedron* **2010**, *66*, 3995-4001; (b) K. Inoue, Y. Makino, N. Itoh, *Tetrahedron: Asymmetry* **2005**, *16*, 2539-2549.
[36]   D. Zhu, Y. Yang, L. Hua, *J. Org. Chem.* **2006**, *71*, 4202-4205.

7

DISCUSSION

As previously outlined, (2*S*,5*S*)-hexanediol is in high demand as it serves as a valuable building block for the synthesis of fine chemicals, chiral auxiliaries and pharmaceutical active compounds. Therefore, proficient synthesis routes are required. A major focus of the present thesis was the development of efficient biocatalytic approaches.

This section deals with the identification of the 2,5-hexanedione reducing enzyme in *S. cerevisiae*, which was necessary to establish recombinant expression systems to produce the enzyme in large quantities. The various constructed biocatalytic synthesis routes will be summarised following their evaluation and comparison to existing routes.

Because chiral hydroxy ketones and diols have more than one functional group which can easily be transformed into other functionalities, they are of particular interest in synthetic chemistry. They are versatile building blocks and are also used in the production of pharmaceuticals and fine chemicals. Therefore, another task was to investigate the substrate scope of the 2,5-hexandione reductase, particularly its ability to synthesise chiral hydroxy ketones and diols. The following discusses whether and to what extent the enzyme is capable of synthesising these compounds and gives an explanation for the enzyme's stereoselectivity.

Finally, this chapter discusses the expansion of the biocatalytic toolbox by a novel ADH from *Kluyveromyces polysporus.* Its ability to synthesise chiral hydroxy compounds is investigated and compared with the 2,5-hexanedione reducing enzyme.

7.1 IDENTIFICATION OF THE 2,5-HEXANEDIONE REDUCING ENZYME

Section 1.6. described different approaches to identifying natural enzymes, which in principle can be divided into sequence- and activity-based methods. By applying the activity-based approach, Gre2p was identified as the 2,5-hexanedione reducing enzyme which will be discussed in more detail in the following section.

7.1.1 Identification of Gre2p as the 2,5-hexanedione-reducing enzyme from *S. cerevisiae*

On a commercial-scale, (2*S*,5*S*)-hexanediol is produced by baker's yeast. However, because of the small quantities of the responsible enzyme in the cells, this process technology suffers from low reaction velocities and poor usable substrate concentrations. Therefore, a more efficient synthesis route must be developed. To meet this objective, the gene responsible for

2,5-hexanedione reduction first had to be identified. Various strategies were viable for this: (i) purification of the enzyme from cell-free extract of baker's yeast towards the reduction of 2,5-hexanedione or (ii) *in vivo* or *in vitro* diketone activity screening of cells or extracts, which can be obtained from either *S. cerevisiae* deletion strains [305] or *S. cerevisiae* or *E. coli* over-expression strains, respectively [306].

Regarding protein purification (also called "wild-type purification"), a major challenge, aside from choosing the right column material, is the low enzyme activity due to the non-physiological character of the substrate. This, in turn, requires several time-consuming and laborious steps of enzyme sample concentrations. A further drawback is the parallel purification of two or more enzymes displaying similar properties, such as molecular weight, isoelectric point, substrate specificity or stereoselectivity [307, 308]. Such mixtures of "purified" enzyme solutions would make it difficult to determine the sequence of the target protein. However, knowledge of using this technique would help to avoid or at least minimise these obstacles. By this means, enzyme identification via purification remains useful, as seen in recent successful applications of this technique [108, 160, 309-311].

For *in vitro* or *in vivo* activity screening, relevant clones are either commercially available or must be constructed. With respect to the latter, sequence information of any open-reading frame (ORF) can be obtained from several databases, such as the *Saccharomyces* Genome Database (SGD http://www.yeastgenome.org) or the MIPS *Saccharomyces cerevisiae* Genome Database (http://mips.helmholtz-muenchen.de/genre/proj/yeast), as the genome has been completely sequenced [312].

While this methodology may seem relatively simple in its application, it is no less laborious or time-intensive than purifying the target protein from an organism. Approximately 50 oxidoreductases are present in *S. cerevisiae,* of which at least half must be assayed, as they have been found to be most promising in the reduction of various carbonyl compounds [313, 314]. Moreover, prior to screening, cells must be cultivated and, if cell-free extract is analysed for activity, also disrupted. When using *S. cerevisiae* as expression host, enzyme purification is also necessary due to the presence of competing reductase activities.

Many examples of yeast ORF identification through *S. cerevisiae* deletion or over-expression strains are found in the literature [104, 119, 122, 172, 307]. Unfortunately, these methods only produce very low amounts of recombinant protein [106, 313]. For example, Chen *et al.* identified Gre2p as a methylglyoxal reductase. In order to demonstrate that the enzyme is

responsible for methylglyoxal reduction, they tested cell-free extract from the corresponding over-expression clone, which revealed a specific activity of 0.2 U·mg^{-1} [311]. Considering that this substrate is reduced with half of the activity observed for the γ-diketone, displaying 0.1 U·mg^{-1} in wild-type cell-free extract [160], specific activity was only enhanced by a factor of four.

Because of the low enzyme activities obtained from *S. cerevisiae* over-expression strains, researchers were forced to substantiate their results by combining the use of yeast over-expression strains with yeast deletion strains [119, 307].

There are also reports of using recombinant *E. coli* cells to identify yeast reductases [105, 120]. Although enzymes produced in this manner revealed higher specific activities than the ones obtained from yeast over-expression clones, the amount was only 10% of the total protein [313]. Additionally, when using *E. coli* as the expression host, one must be aware that expression of eukaryotic genes can lead to the formation of insoluble aggregates [315].

Generally, commercially available strains produce reductases with an additional fusion tag, like hexa-histidine (His$_6$-tag) or glutathione *S*-transferase (GST) to allow for easier protein purification. However, it has been demonstrated that a tag can have an impact on the catalytic properties of enzymes, facilitates protein dimer formation, and can be responsible for incorrectly folded proteins [316-318]. For instance, Katz *et al*. supposed that the GST-tag might be responsible for the unsuccessful identification of membrane-bound yeast reductases. They assumed that the tag would lead to incorrectly-folded reductases being unable to insert into the membranes [239]. González *et al*. observed that a tag can decrease the enzyme's activity; they obtained different activities when they produced a dehydrogenase with (1.6 U·mg^{-1}) and without a His$_6$-tag fusion (25 U·mg^{-1}) [319].

By weighting the *pros* and *cons* of each identification tool, purification of the 2,5-hexanedione reductase from baker's yeast cell-free extract seemed to be the most promising one and was therefore chosen in this work.

After each purification step, fractions were assayed towards their ability to reduce 2,5-hexanedione. However, since (2*S*,5*S*)-hexanediol is synthesised through a two-stage reduction from the diketone, spectrophotometrical measurements were insufficient, as only the decrease of NADPH at 340 nm was monitored. Therefore, *in vitro* biotransformation of 2,5-hexanedione using purified enzyme as catalyst and GDH, for cofactor recycling, was

performed following gas chromatographic product analysis. This showed that Gre2p catalyses both reduction steps.

Because of the great number of oxidoreductases in *S. cerevisiae*, the question raised if there are further ADHs which are capable to reduce 2,5-hexanedione. To answer this, a *GRE2*-deficient mutant was investigated. As this strain revealed very little diketone activity it can, indeed, be concluded that there are additional 2,5-hexanedione reducing enzymes present but Gre2p remains responsible for the majority of the diketone activity [160]. Moreover, since the *γ*-diketone was reduced to (2*S*,5*S*)-hexanediol in excellent enantiomeric excess (>99% *ee*) using wild-type baker's yeast cells it is evident that these additional reductases display no opposite stereoselectivity [225].

With today's knowledge, the activity-based identification method using *E. coli* as expression host would not have easily led to the identification of Gre2p because of the formation of inclusion bodies (section 7.2.1).

7.2 EFFICIENT PRODUCTION OF BAKER'S YEAST 2,5-HEXANEDIONE REDUCTASE

Whether isolated enzymes or whole cells are used as biocatalysts in organic synthesis, a large-scale production of the target enzyme is essential. This is facilitated through over-expression of the particular gene in a suitable expression host. In the present thesis, the gram-negative bacterium *E. coli* and *S. cerevisiae* were employed to enhance the production of Gre2p.

2.2.1 Heterologous expression in *Escherichia coli*

The expression host *E. coli* was chosen because it allows for production of large quantities of the enzyme of interest while being easy to transform, fast-growing in simple media and inexpensive in terms of growth and storage equipment [320]. In addition, it reveals a low reductase level [105] and is thus ideal for recombinant production of dehydrogenases. However, disadvantageous is its lack in post-translational and splicing mechanisms [321] which, fortunately, was not an issue for the production of Gre2p, as the gene *GRE2* reveals no introns or post-translational modifications.

To enhance the Gre2p level, three different heterologous expression systems were constructed (Table 7.1). In each case, the *E. coli* strain BL21(DE3) was utilised. The lowest

specific activity was observed when the gene was expressed from a commercially available pET plasmid, because the majority of Gre2p was produced as insoluble aggregates. In contrast, replacement of the plasmid by the pACYC184-derived pKA1 [322, 323] yielded a sevenfold increase in enzyme activity owing to higher amounts of soluble Gre2p (BL21-pKA-1-GRE2). This is most likely the result of a more relaxed plasmid replication. A high copy-number per cell, which is provided by the vector's origin of replication (ori), generally, leads to high levels of the target gene. However, high energy is required to maintain the plasmid in the cells which can inhibit cell growth, finally leading to a less efficient protein production [324-327]. The pET plasmids are derivatives of the pBR322 vector which possess a ColE1-type ori [328], and are known to replicate with 15-20 copies in *E. coli* cells [329, 330]. In contrast, plasmids carrying the p15A ori, like pKA1, have a copy-number no higher than 12, leading to a more relaxed replication that is less taxing on the expression host [315]. The plasmid pKA1 was selected because of its successful application in enhancing the expression efficiency of an *adh* gene from *Rhodococcus erythropolis*. The RE-ADH thus obtained displayed a 60-fold increase in reduction activity compared to RE-ADH produced by expression from a pET-plasmid [322].

Table 7.1. Comparison of the different *E. coli* BL21(DE3) expression systems constructed in this work.

Expression system	BL21-pET-GRE2	BL21-pKA1-GRE2	BL21-pKA1-optiGRE2
Plasmid	pET-11, pET-21	pKA1	pKA1
Copy-number per cell*	15-20	10-12	10-12
Gene	wild-type	wild-type	codon-optimised
Ratio soluble:insoluble Gre2p#	10:90	30:70	50:50
Highest specific Gre2p activity (U·mg^{-1})+	6.2	42.7	62.5

*as described in literature
#estimated from comparison of the Gre2p band intensity of the soluble and insoluble fraction
+determined from cell-free extract

Although Gre2p activity was increased, the majority of protein was still formed as inclusion bodies. Therefore a third expression system was developed, which produced the 2,5-hexanedione reductase from the pKA1 plasmid carrying a codon-optimised gene. *GRE2* was adapted to the bias of *E. coli* because of its low codon adaption index (CAI) [331] of 0.61 and the existence of 17 extremely rare *E. coli* sense codons (Table 7.2). These triplets, encoding the amino acids arginine, leucine and isoleucine, were found to have a usage frequency of less than 0.5% in *E. coli* [332]. Thus, when present in large quantities or in clusters in transcripts, heterologous protein production can be affected negatively as a consequence of ribosome stalling at positions requiring minor tRNAs, which ultimately leads to translational errors [333-335]. Because of this, both the rare and the low-usage codons were replaced by synonymous ones with higher usage frequencies. The newly synthesised *GRE2* ("optiGRE2") displayed a CAI of 0.98 and its application yielded a 1.5-fold increase in enzyme activity compared to BL21-pKA1-GRE2. Even the solubility of Gre2p was increased further, although a large quantity of enzyme (about 50%) was still produced as inclusion bodies. Notably, the specific activity was 625-times higher compared to the activity obtained in cell-free extract of wild-type yeast (0.1 U·mg^{-1} [160]).

Table 7.2. Rare codons in *GRE2* and their replacement.

Rare codon	AGA	AGG	CUA	AUA
Amino acid	arginine	arginine	leucine	isoleucine
Position	32, 184, 262, 269, 341	256, 322	20, 79, 180, 235, 263, 286	58, 77, 232, 342
E. coli usage frequency*	0.21	0.13	0.29	0.39
Synonymous codon	CGU	CGU, CGC	CUG	AUU, AUC (Pos. 342)
E. coli usage frequency*	2.47	2.47, 2.15	5.41	2.72, 2.70

*obtained from Chen and Texada, 2006 [332]

7.2.2 Homologous expression in *Saccharomyces cerevisiae*

In a parallel study it was investigated to what extent gene expression in the natural habitat influences the production of Gre2p. For this purpose, *GRE2* was expressed constitutively under the *PMA1* promoter in the *S. cerevisiae* strain BY4741 (BY4741-GRE2). The enzyme thus produced displayed a maximum activity of 12.6 U·mg^{-1} (cell-free extract). Thus, homologous production was less efficient than heterologous production but, without doubt, more efficient than the wild-type, as the 2,5-hexanedione reducing activity was 120-times higher.

In comparison with the commercially available strain [306], Gre2p produced by the over-expression strain developed here revealed a much higher activity. As mentioned in section 7.1.1, only 0.2 U·mg^{-1} (cell-free extract) was observed for methylglyoxal reduction using the purchased over-expression strain. Even after purification, activity could only be enhanced by a factor of 2.5 [311]. Taking into account that methylglyoxal is reduced with half of the activity of 2,5-hexanedione [160], it can be assumed that cell-free extract of BY4741-GRE2 would produce approximately 6 U·mg^{-1}, which is 30-times higher. One reason for the inefficient enzyme production using commercial strain's is probably associated with the *N*-terminal GST-tag. As described earlier, the tag could have had affected protein conformation, diminishing enzyme activity. This is substantiated by another *GRE2* expression system: Katzberg *et al.*, who used the plasmid pRSET B to express the gene with an *N*-

terminal His$_6$-tag in *E. coli*, were only able to achieve an activity of 0.14 U·mg^{-1} in the cell-free extract [336].

Another reason could be the expression plasmid itself. The one used in this work allowed for a constitutive gene expression due to the *PMA1* promoter, probably resulting in a more relaxed Gre2p production. In contrast, gene expression in the commercially available over-expression strain is started immediately by the addition of Cu^{2+}.

To sum up, both the homologous and the heterologous expression systems resulted in much higher amounts of functional Gre2p, which is required for an efficient biocatalytic application.
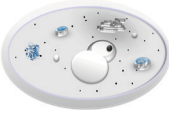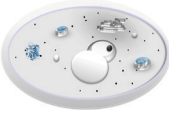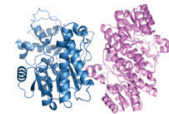
7.3 SYNTHESIS OF (2*S*,5*S*)-HEXANEDIOL

As (2*S*,5*S*)-Hexanediol is a valuable chiral building block, the main focus of the present thesis was developing efficient biocatalytic synthesis routes. To meet this objective, a cell-free (chapter 2.1, 3.1) and three different whole-cell systems were developed. With respect to whole-cell biocatalysis, a *S. cerevisiae* strain producing Gre2p (chapter 4.2) and two *E.coli* strains co-producing Gre2p and GDH (BL21-GRE2-gdh and BL21-gdh-GRE2, Chapter 4.3) were applied.

7.3.1 Overview of (2*S*,5*S*)-hexanediol synthesis

In order to evaluate each catalyst regarding its synthesis of (2*S*,5*S*)-hexanediol from 2,5-hexanedione, various process parameters were calculated. The results are summarised in Table 7.3 and are compared with baker's yeast-mediated 2,5-hexanedione biotransformations using Budweiser yeast [229] and *S. cerevisiae* L13 [225], respectively.

Table 7.3. Summary of the process parameters of the different biocatalytic routes to (2S,5S)-hexanediol.

Chapter/Reference	[229]	4.1 [225]	4.2	4.3	3.1
Biocatalyst	Wild-type* S. cerevisiae (Budweiser)	Wild-type# S. cerevisiae (L13)	BY4741-GRE2+	BL21-gdh-GRE2+	Gre2p/GDH+ (1:3)
Specific enzyme activity (U·mg^{-1})	-	0.1	Gre2p: 12.7	Gre2p: 83.1 GDH: 14.6	Gre2p: 62.5
Conversion (%)	95	93	90	>99	>99
Enantiomeric excess (%)	>99	>99	>99	>99	>99
Reaction time (h)	144	48	8	2.75	1.75
Co-substrate yield (mg$_{2,5\text{-hexanediol}}$/g$_{glucose}$)	26	88	196	259	259
Space-time yield (g·L^{-1}·d^{-1})	0.9	4	48	132	210
Cell productivity (mg$_{2,5\text{-hexanediol}}$/g$_{cells}$)°	70	70	106	583	1530

* 50 mM 2,5-hexanedione; # 80 mM 2,5-hexanedione; + 150 mM 2,5-hexanedione; ° g$_{cells}$ are gram wet cells

Accordingly, every biocatalyst was able to reduce 2,5-hexanedione to the desired (S,S)-diol with an excellent enantioselectivity. With respect to whole-cell catalysis, this also means, that no counteracting reductases with different stereoselectivities were present.

The highest conversion rates were obtained with both the cell-free and the *E. coli* system. As a consequence, and because of their fast reaction times , the resulting space-times yields (STYs) were much higher than those obtained by wild-type and recombinant yeast biotransformation. However, since high STYs can easily be achieved through higher catalyst supplementations, this parameter is often insufficient for evaluating biotransformations. In contrast, cell productivity (gram product produced per gram cells) allows for a more clearly

defined conclusion. Thus, all biocatalytic synthesis routes developed here led to higher cell productivities compared to wildtype baker's yeast-mediated biotransformation. This was the result of the recombinant production of Gre2p leading to higher quantities of active Gre2p. Thus, specific enzyme activities were increased significantly.

Comparing the cell productivities achieved by whole-cell biocatalysis using the recombinant *S. cerevisiae* strain and *E. coli*, respectively, one may assume that this parameter is higher when using *E. coli* as catalyst because of its 6.5-fold enhanced Gre2p activity. However, this hypothesis has to be reconsidered, since a second *E. coli* catalyst (BL21-GRE2-gdh) expressing the plasmid with the revised order of *GRE2* and *gdh*, produced a Gre2p activity of 14.4 U·mg^{-1}, which is similar to that of BL21-gdh-GRE2. Nevertheless, when this strain was applied for the reduction of 150 mM 2,5-hexanedione, cell productivity thus obtained was in the same range as observed with BL21-gdh-GRE2 (see chapter 4.3). This result reveals that there are existing effects which slow-down the productivity of the yeast biocatalyst.

An explanation might be the non-saturating NADPH concentration, ranging approximately from 0.01-0.06 mM [337], in the cytosol of *S. cerevisiae*. The majority of intracellular NADPH is generated by the oxidative part of the pentose-phosphate pathway (PPP) by the action of glucose-6P dehydrogenase (G6PDH) and 6-phosphogluconate dehydrogenase (6-PDH). By this means, at least two moles of NADPH are produced per one mole of glucose-6-phosphate (G6P) entering the PPP [338]. In addition to this path, further enzymes such as the NADP$^+$-dependent isocitrate dehydrogenase [339] or –acetaldehyde dehydrogenase [340], are capable of cytosolic NADPH regeneration, but play only a minor role.

Unlike yeast biotransformation, BL21-gdh-GRE2-mediated reduction was performed in the presence of 0.5 mM NADP$^+$, added externally. Assimilation was facilitated through cell permeabilisation, which was necessary since, generally, membranes remain impermeable for nicotinamide cofactors [206, 341]. As a result, the cofactor concentration in the *E. coli* cell was higher than the observed K_M value for NADPH (0.11 mM) and NADP$^+$ (0.03 mM) for the reactions catalysed by Gre2p [150] and GDH [342], respectively. Thus, optimal cell activities were achieved leading to a higher cell productivity.

The fact that yeast's cytosolic NADP$^+$/NADPH concentration is crucial in asymmetric ketone reduction reactions was also observed by other researchers, and has led to attempts to enhance the cofactor pool through metabolic (Fig. 7.1) or medium (Fig. 7.2) engineering.

In *S. cerevisiae*, the majority of the total glucose flux is metabolised through glycolysis, while only 10-30% occurs through the PPP [343]. Forcing glucose into the PPP can be achieved through metabolic engineering. Some researchers have developed strains that over-express NADPH-dependent reductases alongside a reduced or deleted phosphoglucose isomerase (PGI) activity [169, 239, 240, 344]. For example, the combination of PGI-deletion and over-expression of the gene coding for G6PDH resulted in a fourfold increase in STY relative to strains without altered glucose metabolism [169].
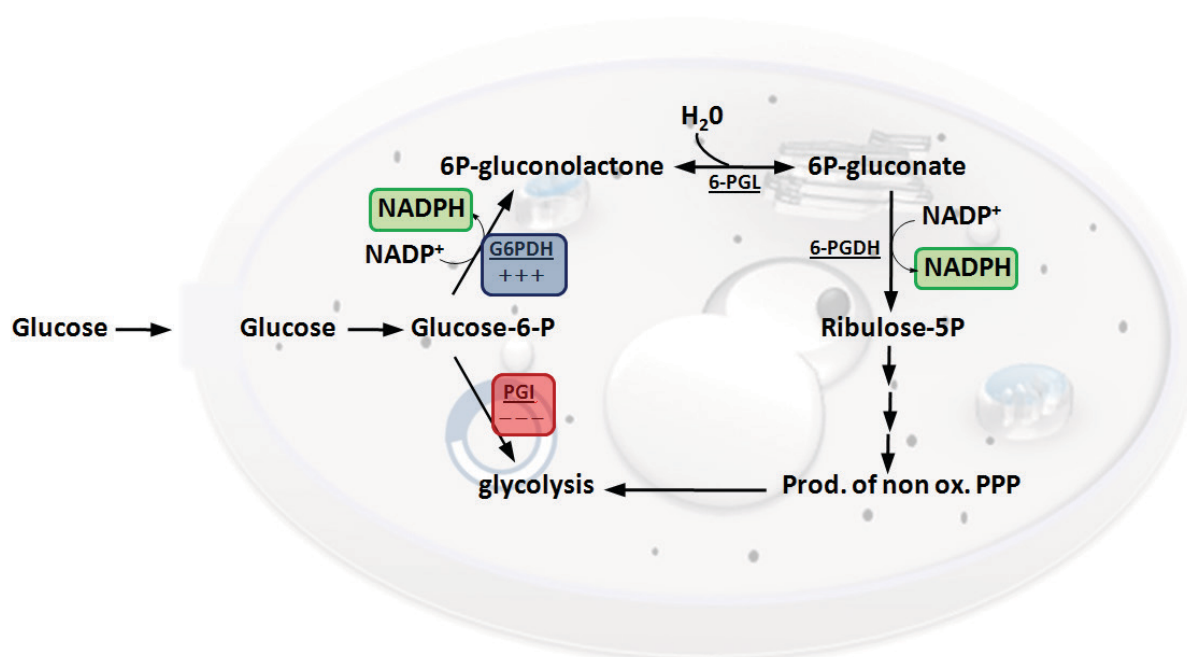
Figure 7.1. Metabolic engineering to increase the intracellular NADPH-pool in *S. cerevisiae*. To avoid or to reduce the flux of glucose through glycolysis, PGI activity is either deactivated or reduced which causes a greater flux through the PPP, whose oxidative part (G6PDH and 6-PGDH) is primarily responsible for NADPH production. Regeneration of NADPH can also be enhanced by G6PDH over-expression. **PGI** phosphoglucose isomerase, **G6PDH** glucose-6-phosphate dehydrogenase, **6-PGL** 6-phosphogluconate lactonase, **6-PGDH** 6-phosphogluconate dehydrogenase. This figure was modified according to Skorupa-Parachin *et al*. [169].

Medium engineering acts on *de novo* NADH/NADPH biosynthesis, and is achieved through adenine supplementation to the medium. The nucleobase is thought to enter the metabolism, as it is the precursor in the ATP biosynthesis [345, 346]. Since there are many enzymes requiring ATP in the biosynthesis of NAD(P)H, addition of adenine would enhance the intracellular NADPH pool. This engineering method was successfully applied to a *S. cerevisiae* strain expressing the *β*-subunit of the NADPH-dependent fatty acid synthase. The

concentration of intracellular NADPH was increased by a factor of four to up to 0.25 mM. When this strain was subsequently applied to asymmetric synthesis of (*S*)-4-chloro-3-hydroxybutanoate, specific cell productivity was also increased [237, 337].

The higher cell productivity achieved with the cell-free system in comparison to *E. coli* whole-cell catalysis was most likely due to a more efficient cofactor regeneration. While cell-free biotransformation was accomplished at a ratio of 1:3 with respect to Gre2p and GDH, specific activities of BL21-gdh-GRE2 revealed a ratio of 8:1. Similar results were obtained by cell-free experiments in which Gre2p was used in excess (three times) of GDH. All biotransformations were slightly less efficient than those where the cofactor-recycling enzyme was applied in excess (chapter 3.1).

The last parameter to be considered is the co-substrate yield which expresses how much product is synthesised by one gram of co-substrate. The higher this value, the lower the production costs, since less co-substrate is required. This has economic benefits when a process is scaled-up [174]. The best co-substrate yield was identified by finding the minimum amount of glucose needed to drive the reaction fully to the diol. As a result, the highest co-substrate yield of 259 $mg_{2,5\text{-hexanediol}}/g_{glucose}$ was achieved with both the cell-free and the *E. coli* systems, requiring 2.5 moles of glucose per 1 mole of diketone. Biotransformation using the recombinant *S. cerevisiae* strain resulted in a lower co-substrate yield (169 $mg_{2,5\text{-hexanediol}}/g_{glucose}$). This might be due to both the low intracellular cofactor pool and cofactor limitation as a consequence of a competition for NADPH occurring between the reduction of 2,5-hexanedione and reductive processes of the cell metabolism and anabolism [347]. The even lower co-substrate yield obtained with wild-type biotransformations can be explained by the fact that no effort was made to optimise this parameter. The co-substrate yield of yeast biotransformations can be improved using the previously mentioned genetic manipulation strategies to enhance the cofactor pool. This, for instance, was successfully demonstrated for the reduction of bicyclo[2.2.2]octane-2,6-dione using a *S. cerevisiae* strain displaying reduced PGI activity [239, 344].
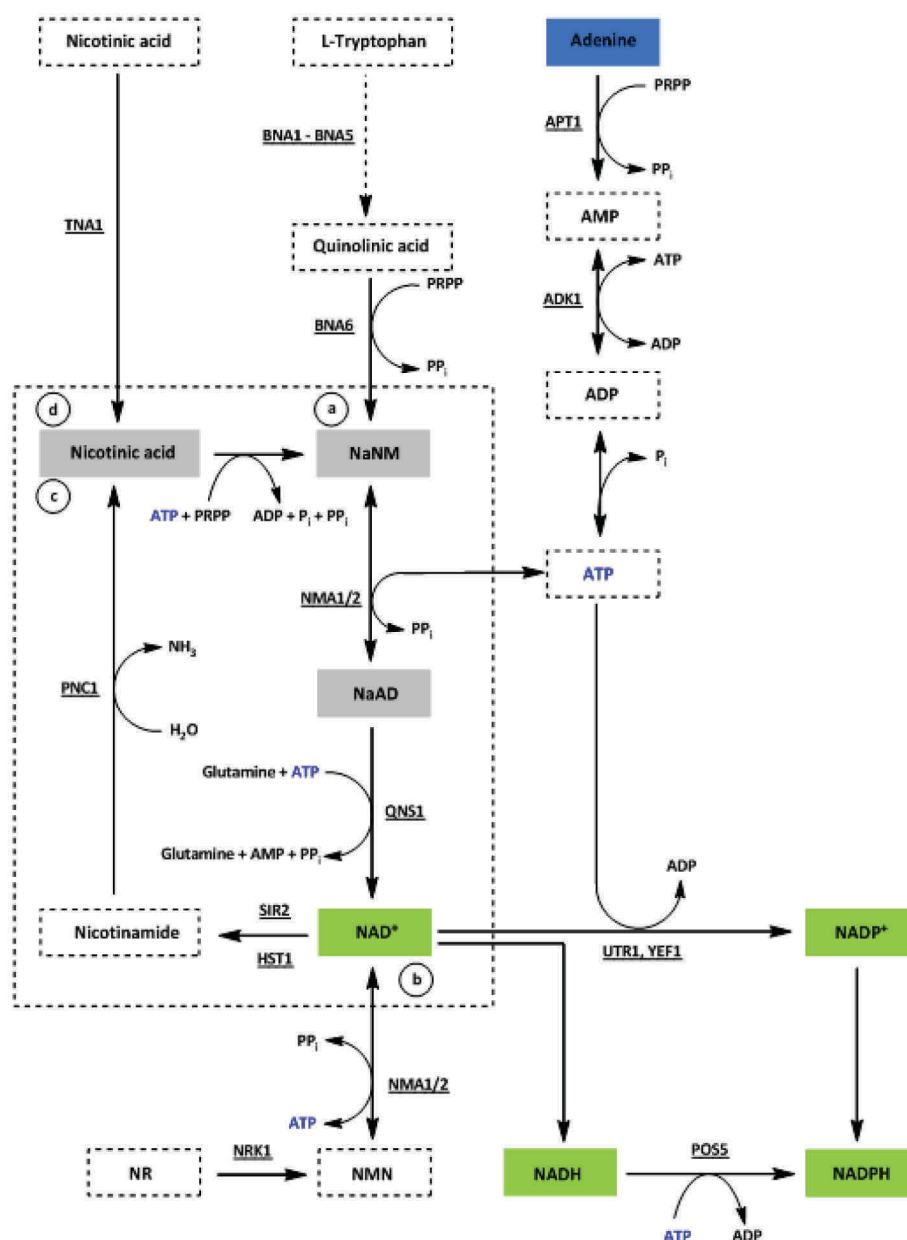
Figure 7.2. Medium engineering to enhancing the intracellular NADPH-pool in *S. cerevisiae*. Adenine supplementation increases the NADH and NADPH concentration, as it is a precursor in the ATP-synthesis. ATP is required in the *de novo* biosynthesis of NAD(H)/NAD(P)H. Participating enzymes are underlined; bold and thin arrows indicate major biosynthetic and associated conversions, respectively; the dashed arrow from L-tryptophan to quinolinic acid represents the five enzymatic and one non-enzymatic reactions within the *de novo* pathway; the dashed box expresses the cycle of NAD$^+$; the grey boxes, including also NAD$^+$, are intermediates of the Preiss-Handler pathway, which comprises the three steps from nicotinic acid via nicotinic acid mononucleotide (**NaMN**) and nicotinic acid adenine dinucleotide (**NaAD**) to nicotinamide adenine dinucleotide (**NAD$^+$**). The last two steps from NaMN to NAD$^+$ are identical with the *de novo* biosynthetic pathway (**a**) which starts from L-tryptophan. An alternative route to NAD$^+$ starts from nicotinamide riboside (**NR**) via nicotinamide mononucleotide (**NMN**) (**b**). NAD$^+$ can also be synthesized from NR via NaMN. Thereby, nicotinamide enters the Preiss-Handler pathway as nicotinic acid (**c**). *S. cerevisiae* is also capable to take nicotinic acid up from the environment (**d**). **NADP$^+$** nicotinamide adenine dinucleotide phosphate; **AMP** adenosine monophosphate; **ADP** adenosine diphosphate; **ATP** adenosine triphosphate; **P$_i$** inorganic phosphate; **PP$_i$** inorganic diphosphate; **PRPP** phosphoribosyl pyrophosphate; The figure was modified according to Knepper *et al.* [337].

7.3.2 Up-scaling of the reduction process

Reduction of 2,5-hexanedione at concentrations of ≥0.2 M was possible with both the cell-free and the *E. coli* whole-cell system (chapters 3.1 and 4.3). In contrast, a slow-down in the synthesis of (2*S*,5*S*)-hexanediol was observed with the recombinant *S. cerevisiae* strain at diketone concentrations of ≥0.1 M (chapter 4.2). This was due to the lower reduction velocity ($mol·L^{-1}·h^{-1}$) of the second reaction step, which resulted in an interim accumulation of the intermediate. Meitian *et al*. also observed this when using conventional baker's yeast to synthesise (2*S*,5*S*)-hexanediol. They encountered inhibition of diol synthesis at 5*S*-hydroxy-2-hexanone cocentrations of ≥30 mM [348]. This leads to the assumption that high substrate concentrations may cause stress reactions in *S. cerevisiae* [230].

Although both the cell-free and the *E. coli* whole-cell system can be applied for synthesising (2*S*,5*S*)-hexanediol at high concentrations, designer cell catalysis will be favoured in industrial applications, because only one fermentation step and one cell separation step is required prior to biotransformation [235]. In contrast, for cell-free application two fermentation steps are necessary for the production of Gre2p and GDH, significantly increasing process costs. Moreover, the cells have to be disrupted following enzyme concentration. Thus, the general rule-of-thumb applies: the crudest possible form of enzyme which maintains product quality is acceptable [234, 349]. Therefore, engineered *E. coli* cells were employed for diketone biotransformation at concentrations higher than 0.2 M.

A relevant biocatalytic process should have an average product yield of 78% and a STY of >300 $g·L^{-1}·d^{-1}$ [26]. Until today, only a few examples of microbial reduction systems have been demonstrated which are able to achieve this range of STY [91, 112, 113, 116, 194, 213]. Application of BL21-gdh-GRE2 for the biotransformation of 0.5 and 1 M 2,5-hexanedione yielded STYs of 572 and 371 $g·L^{-1}·d^{-1}$, respectively, demonstrating that this process would be transferable to a commercial-scale.

The lower STY and slower reaction time (six hours instead of three) obtained for reduction of 1 M diketone might be the result of a substrate-excess inhibition of Gre2p or GDH, since 2.5 M glucose was employed. Substrate-excess inhibition can be minimised through a continuously operating reduction process by feeding the reaction medium continuously with substrate [350]. Such a continuous production process was successfully applied in the synthesis of (2*R*,5*R*)-hexanediol, employing recombinant *E. coli* cells expressing the alcohol

dehydrogenase from *Lactobacillus brevis*. After feeding the medium successively with varying diketone concentrations (0.1-0.3 M) for a period of 16 days, 287 g diol and a STY of 172 $g·L^{-1}·d^{-1}$ could be achieved. Moreover, due to high catalyst stability, an extremely high cell productivity of 17.9 $g_P/g_{wet\ cell\ weight}$ was obtained [304].

7.3.3 Alternative enzymes for the synthesis of (2*S*,5*S*)-hexanediol

Other enzymes capable of reducing 2,5-hexanedione *S*-selectively into (2*S*,5*S*)-hexanediol have been found. Three are of bacterial origin (ADH-A from *Rhodococcus ruber* [136], ADH-T from *Thermoanaerobacter* sp. [225] and Pf-ADH from the hyperthermophilic archaeon *Pyrococcus furiosus*) [162], whereas the carbonyl reductase S-ADH was identified from the yeast *Candida parapsilosis* [351]. A comparison of the reaction parameters is provided in Table 7.4.

With the exception of ADH-A and S-ADH, the enzymes are NADPH-dependent and, in contrast to Gre2p-mediated biotransformation, continuous production of the reduced cofactor was realised via substrate-coupled regeneration. Thus, 2-propanol (ADH-T, ADH-A, Pf-ADH) or 4-methyl-2-propanol (S-ADH) were used as a co-substrate, respectively. In terms of enantioselectivity, all enzymes were capable of synthesising optically pure (*S*,*S*)-diol. The highest STYs of 58.2 and 68.8 $g·L^{-1}·d^{-1}$ were observed with ADH-T and S-ADH, respectively. A significantly lower STY was observed for both recombinant ADH-A and *E. coli* cells producing this ADH. Diketone reduction processes catalysed by ADH-A or S-ADH were performed in hexane or in a biphasic system (4-methyl-2-pentanol/water), demonstrating the stability of these enzymes even in non-aqueous reaction media. This could be advantageous when they are used for biotransformation of 2,5-hexanedione at concentrations ≥1 M, as the solubility of the diketone in water is limited to ≤100 $g·L^{-1}$.

Table 7.4. Overview of enzymes producing (2*S*,5*S*)-hexanediol.

Enzyme	ADH-T	ADH-A	Pf-ADH	S-ADH	Gre2p
Chapter/Reference	4.1 [225]	[136]	[162]	[351]	3.1, 4.3
Source	*Thermo-anaerobacter* sp.	*Rhodococcus ruber*	*Pyrococcus furiosus*	*Candida parapsilosis*	*Saccharomyces cerevisiae*
Catalyst	recombinant enzyme	recombinant enzyme[*]; recombinant *E. coli* cells[+]	recombinant enzyme	recombinant enzyme	recombinant enzyme
System	aqueous	micro-aqueous hexane, 99% v v^{-1}	aqueous	biphasic	aqueous
Cofactor	NADPH	NADH	NADPH	NADH	NADPH
Cofactor regeneration	substrate-coupled with 2-propanol	substrate-coupled with 2-propanol	substrate-coupled with 2-propanol	substrate-coupled with 4-methyl-2-pentanol	GDH-coupled
Diketone concentration (M)	0.08	0.28	0.13	0.87	0.2 (isolated enzyme)[*], 1 (*E. coli* designer cells)
Temperature (°C)	30	30	30	RT	30[*], 25
pH	7.0	7.5	7.0	7.5	7.5
Time (h)	3.5	42[*]; 24[+]	[#]	24	2.75[*], 8
Conversion (%)	90	74.1[*]; 76.4[+]	[#]	67	>99[*], 95.5
Enantiomeric excess (%)	>99	>99	[#]	>99	>99[*], >99
Space-time yield (g·L^{-1}·d^{-1})	58.2	13.5[*]; 24.4[+]	not calculable	68.8	204[*], 371

[*] recombinant ADH-A; [+] *E. coli* cells expressing ADH-A; [#] no data available

The ADH from *Pyrococcus furiosus* has not been applied in 2,5-hexanedione biotransformation. It was demonstrated that the enzyme is well adapted to high

temperatures, with 90°C being the optimum. At 30°C, a preferred temperature for industrial-scale production, only 5% of the catalytic activity was measured. In an attempt to adapt the enzyme to this temperature, various Pf-ADH mutants have been developed and investigated. The most compelling variant exhibited a 20-fold higher reducing activity in comparison to the wild-type [162].

In summary, among all biocatalytic (2*S*,5*S*)-hexanediol synthesis routes, Gre2p-mediated catalysis, using either isolated enzyme or engineered *E. coli* cells, is the most promising in terms of conversion, incubation time and STY. Even at high diketone concentrations efficient diol production is achievable (see 7.3.2).

7.3.4 Chemical versus biocatalytic synthesis of (2*S*,5*S*)-hexanediol

A comparison of the chemical routes to (2*S*,5*S*)-hexanediol (see **1.7.2.1**) with the biocatalytic approaches developed here reveals that the latter are much more efficient in terms of stereoselectivity and conversion yields. Thus, in all cases the diol was obtained with a conversion of ≥90% and an enantioselectivity of >99% *ee*. Additionally, the biocatalytic approaches require fewer reaction steps than the chemical ones, with the exception of the hydrogenation of 2,5-hexanedione using the (*S*)-Ru-BINAP catalyst (reaction **1** in **Fig. 1.13**). A reduction in the number of reaction steps makes a process more economical and easier to handle, as fewer purification and work-up steps are required [352-354]. It also minimises the production of waste [355]. The enzymatic approaches are also more cost effective and attractive from an environmental perspective, since the enzymatic reactions were carried out in aqueous solutions (buffer) under mild conditions (30°C, neutral pH) and used readily available, biodegradable, renewable and cheap catalysts and reagents (glucose, Gre2p, GDH, *E. coli* and *S. cerevisiae*, respectively). In contrast, the chemical routes use toxic and expensive catalysts (reaction **1-4**), are performed mostly under harsh conditions (reactions **1-4**), require organic solvents, like methanol (**1**), tetrahydrofuran (**3**), or dimethoxyethane (**4**) or additional reagents, e.g. bases (**2**) or acids (**1**).

In summary, the biocatalytic routes to (2*S*,5*S*)-hexanediol developed here meet the criteria of a "green" process [356], under which a product is synthesised from preferably renewable raw materials, prioritising the elimination of waste and avoiding the use of toxic and hazardous reagents and solvents.

7.4 SUBSTRATE SPECTRUM

The current work (chapters 2.1, 3.1) and numerous other publications found in literature have demonstrated that Gre2p reduces an extremely broad spectrum of carbonyl compounds. Therefore, the enzyme can be applied in the stereoselective synthesis of further valuable chiral building blocks. The following sections provide an overview of the substrates which can be reduced by Gre2p.

7.4.1 Reduction of *α*- and *β*-diketones and hydroxy ketones

Because chiral hydroxy ketones and diols are in high demand as they are used for the production of pharmaceutical active compounds or fine chemicals, the present work has also focused on the reduction of other diketones.

7.4.1.1 Gre2p-catalysed reduction of *α*- and *β*-diketones

Various *α*- and *β*-diketones were tested as substrates revealing that Gre2p's activity was consistently lower than with 2,5-hexanedione. The second highest activity was observed with 2,3-hexanedione while the *β*-diketone, 2,4-pentanedione was the poorest substrate (chapter 2.1). It is also noteworthy that in case of *α*-diketones, Gre2p preferred the reduction of methyl (such as 2,3-hexanedione) over ethyl ketones (e.g., 3,4-hexanedione) indicating that the first were possibly easily accessible for hydrogen transfer through the enzyme.

Cell-free biotransformation (chapter 3.1) of 2,3-butanedione ended with the formation of the intermediate, whereas reduction of 2,3-pentanedione and 2,3-hexanedione resulted in trace amounts of the corresponding diols. It was also observed that the ability to produce diols depends on the size of the alkyl chain. Thus, reduction of 2,3-hexanedione resulted in a six times higher conversion rate (13.6%) than the reduction of 2,3-pentanedione.

With respect to stereoselectivity, Gre2p-mediated diketone reduction resulted in the Prelog products [357]. This was also true for the first reduction step of 2,3-pentanedione and 2,3-hexanedione, as the appropriate (2*S*)-hydroxy-3-ketones were formed with a high enantioselectivity (94-98% *ee*). These were the main products, however, minor amounts of the corresponding 3-hydroxy-2-ketones were also detected. This was unlikely to be due to

enzymatic synthesis but rather a rearrangement caused by intramolecular hydrogen bond interactions between the hydroxy group and the oxygen atom, as illustrated in Figure 7.3. This phenomenon is common and was reported for hydroxy compounds revealing an electronegative group or atom [146].
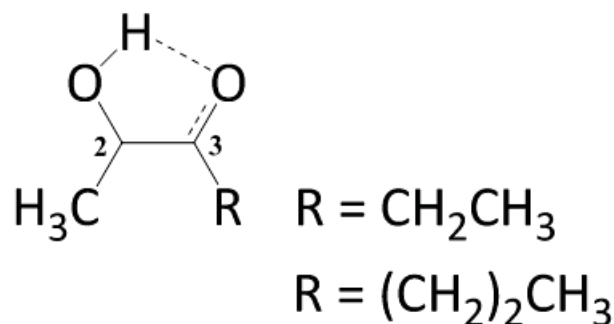
Figure 7.3. H-bond formation between the hydroxy group and the electronegative oxygen atom.

As shown in Fig. 7.4 the hydroxy ketones can have two different orientations within the active site of Gre2p. Since H$^-$ attack always takes place through the same side due to the well-defined nicotinamide cofactor location in the active sites of ADHs [358], *anti-* or *syn-* diols are possible. If the orientation is the same as for the diketones, the Prelog products, the *anti-*(2*S*,3*R*)-diols, will be obtained while an opposite orientation provides the *syn-* (2*S*,3*S*)-diols.

With respect to (2*S*)-hydroxy-3-pentanone, no binding-mode is preferred , as both the *anti-* and the *syn*-product were produced to equal amounts. On the contrary, the ADH provided a higher amount of *anti*-diol from 2,3-hexanedione indicating that Gre2p favours the same disposition of the hydroxy ketone with regard to the diketone. Furthermore, the results reveal that formation of the Prelog products is influenced by the substrate structure. Thus, the larger the distance between the alkanoyl group and the hydroxyethyl moiety the more likely it is that the *anti*-products were provided. A similar pattern was also observed for ADH-A and ADH-T which revealed the same regioselectivity and stereoselectivity towards the previously described substrates [163, 359].
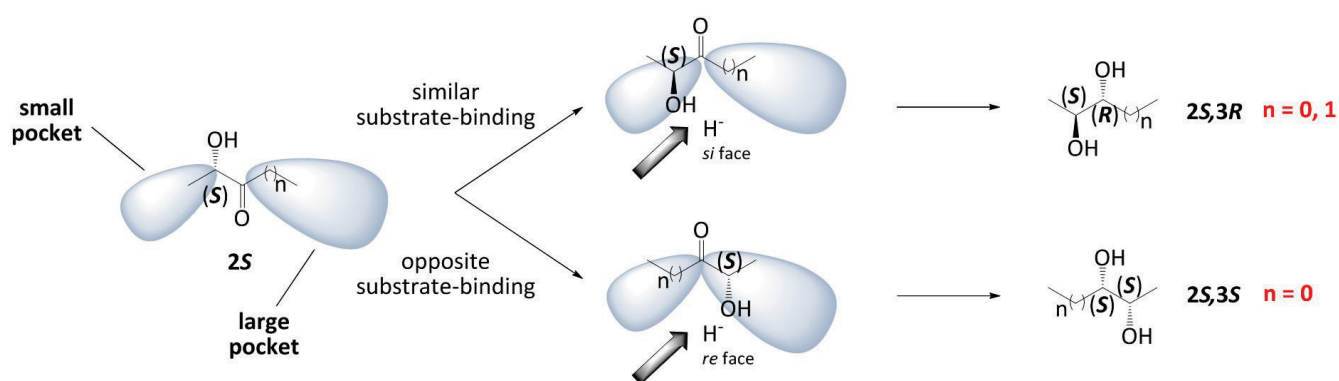
Figure 7.4. Promiscuous binding modes of the 2-hydroxy ketones in the active site of Gre2p. 2,3-pentanedione (n=0) and 2,3-hexanedione (n=1). The figure was modified according to Kurina-Sanz *et al*. [359]

Although reduction of 2,4-pentanedione resulted in the lowest Gre2p activity, the diketone was reduced to optically pure *S,S*-diol with a conversion rate of 31.5%. From the literature it is also known that the enzyme is able to accept 2,4-hexanedione and 2,4-octanedione as substrates. They are reduced to the corresponding (2*S*)-hydroxy-4-ketones at a conversion rate of approximately 70% [101]. Unfortunately, no information is available as to whether the diol was also produced.

Furthermore, the results reveal that the likelihood of Gre2p to produce diol depends on the distance between the two carbonyl groups. That is, the greater the distance the more likely diol was formed. Thus, when 2,4-pentanedione was the substrate a conversion rate of 31.5% was reached while only 2.1% diol was obtained when 2,3-pentanedione was reduced. A similar pattern was observed for the hexanedione biotransformations (2,5-hexanediol >99% and 2,3-hexanediol 13.6%).

7.4.2 Stereoselective reduction of ketones

While diketones are well-accepted by Gre2p, only low activities were observed with ketones. For example, activity towards 2-hexanone was about 29-times lower than with 2,5-hexanedione and with 3-hexanone no activity was observed. Therefore, ketone biotransformations were not investigated further, with the exception of the reduction of 2-pentanone, 2-hexanone and 2-heptanone, respectively. In each case the corresponding Prelog alcohol (S-form) was synthesised with excellent enantiopurity and high conversion rates (chapter 3.1). Nevertheless, due to very low enzyme activity it is not possible to

synthesise these products on a preparative-scale. Moreover, existing routes are much more powerful. For example, 1.06 kg of enantiopure (*S*)-2-pentanol is obtained through *Gluconobacter oxydans*-mediated reduction [360]. An alternative approach is the synthesis on a preparative-scale (about 50 g·L^{-1}) through enzymatic resolution of *rac*-2-pentanol catalysed by the lipase B from *Candida antarctica*. The catalyst is also able to synthesise (*S*)-2-heptanol from *rac*-2-heptanone [361].

Gre2p was also shown to reduce several chlorine-substituted and *α*-acetoxy ketones. In general, biotransformations proceeded with high enantioselectivity but the isolated yields of the products were low to moderate. Depending on the *α*-substituent (Cl or OAc), reduction resulted in either (*R*) or (*S*)-alcohols [100, 101, 170, 171]. It has recently been demonstrated that 3-chloro-1-phenyl-1-propanone is also accepted by Gre2p as substrate. Although low enzyme activities were obtained (0.99 U·mg^{-1} using purified and recombinant Gre2p), complete conversion to the corresponding optically pure (*S*)-alcohol was achieved [150].

7.4.3 Stereoselective reduction of ketoesters

The activity measurements carried out in this thesis (chapter 2.1), in combination with the huge number of publications dealing with chiral hydroxy ester synthesis mediated by Gre2p, demonstrate that the enzyme is able to reduce an extraordinarily broad spectrum of *α*- and *β*-ketoesters. The following sections explains the reduction of these substrates in more detail.

7.4.3.1 In principle, Gre2p reduces keto esters following Prelog's rule

Figure 7.5 summarises the reduction of various aliphatic *α*-, *β*- and *α*-substituted-*β*-keto esters catalysed by Gre2p. The enzyme synthesised the corresponding hydroxy esters following Prelog's rule (*S*-alcohols). That is, the bulkier moiety (ester group) is located on the right-hand side, while the smaller one is located on the left side of the carbonyl group. If the smaller substituent reveals a higher Cahn–Ingold–Prelog priority than the larger one, the molecule is assigned the *R*-configuration, e.g. ethyl (*R*)-4-chloro-3-hydroxy-butanoate (**5**). With the exception of the hydroxy eters **2** and **11-13**, all aliphatic hydroxy esters were obtained with excellent optical purities [100, 101, 105, 138, 170, 171].
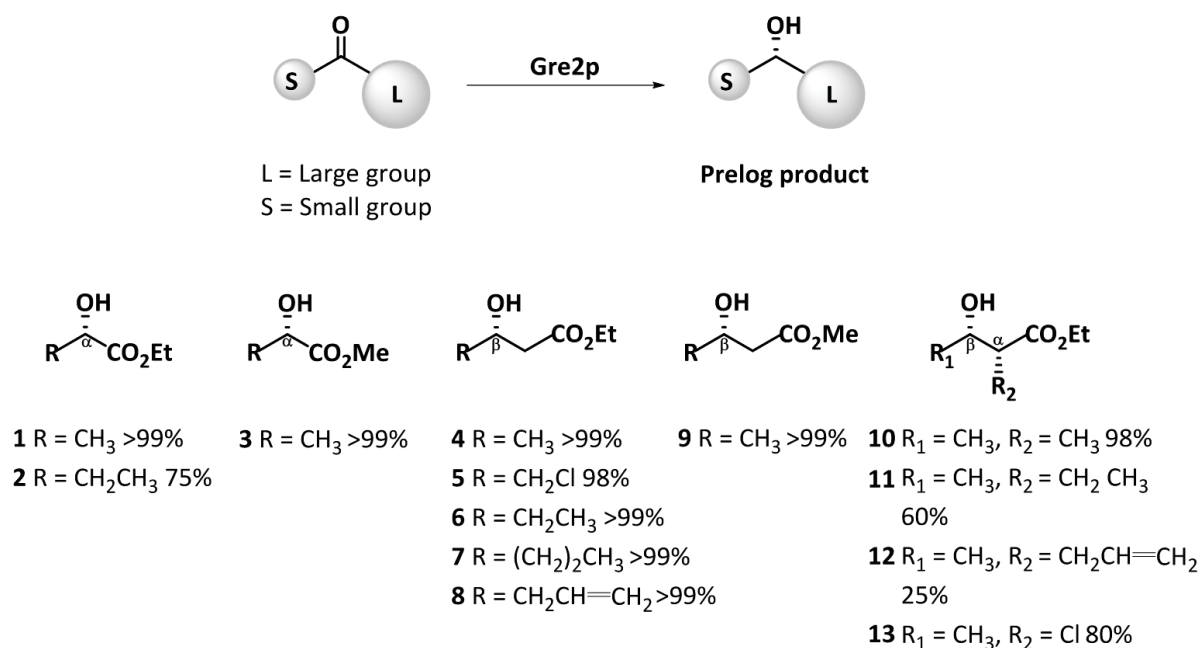
Figure 7.5. In principal, the reduction of α- and β-keto esters catalysed by Gre2p follows the Prelog fashion. The resulting hydroxy esters reveal a larger moiety at the right-hand site. Also given is the enantiomeric excess in %.

Reduction of α-substituted-β-ketoesters resulted in two of the four possible diastereomeric alcohols, the *syn*-2R,3S and *anti*-2R,3R-diastereomer. The *syn*-diastereomer was the major product when the α-substituent was less bulkier (e.g. -CH$_3$ **10**, -Cl **13**), while the opposite product was predominant when a bulkier resin was present at this position (-CH$_2$CH=CH$_2$ **12**). Notably, α-substituted-β-ketoesters were reduced with a lower stereoselectivity than the corresponding β-ketoesters. In addition, the optical purity of the products decreased the bigger the α-substituent (compare *ee* values of **10**-**12** in Fig. 7.5).

Moreover, it was demonstrated that Gre2p catalysed the highly enantioselective reduction of the γ-keto ester methyl 4-oxo-pentanoate following Prelog's rule providing the corresponding S-alcohol [105, 170].

Gre2p is also able to reduce cyclic keto esters. Both ethyl 2-oxo-cyclopentanecarboxylate and ethyl 2-oxo-cyclohexanecarboxylate are accepted as substrates, whereas activity decreases with the size of the ring [160]. Biotransformation of the first compound failed to produce just one of the four possible diastereomers. Instead, a diastereomeric mixture of *trans*-(1R,2R)- and *cis*-(1R,2S)-alcohol was observed, of which the latter was predominant. In

contrast, the six-membered cyclic keto ester was converted to *cis*-(1*R*,2*S*)-hydroxy ester with a *de* and *ee* of >98% and >98%, respectively [122].

7.4.3.2 Exception to the rule

Although Gre2p was demonstrated to contribute strictly to Prelog's rule, the enzyme also produced the anti-Prelog-type hydroxy esters **14**-**17** (Figure 7.6) [106, 170]. That is, the left-hand moiety of the products is bulkier than the right-hand moiety.
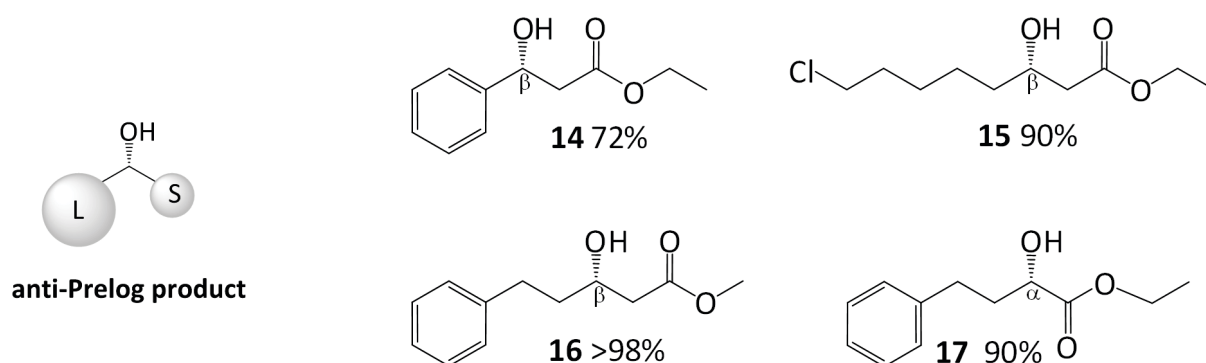
Figure 7.6. Anti-Prelog-type hydroxy esters obtained with Gre2p. The left-hand moiety is larger than the substituent at the right-hand side. Given is also the enantiomeric excess in %.

According to Ema *et al.* this can be explained by assuming that Gre2p possesses a binding pocket that can accomodate in order of affinity, either an ester group or a hydrophobic substituent. Because the substrates reveal both an ester moiety and a bulkier resin an ambiguous recognition of the enantioface of the carbonyl group occurs as a consequence of the competitive binding of both substituents. However, they supposed that the ester group was primarily accomodated over that of the bulkier resin due to the fact that the enantioselectivities were increasing the more unbalanced the two substituents are, flanking the carbonyl group (compare **14** with **15-17** in Fig. 7.6) [170].

The theory also explains why the hydroxy ketones **18-22** (Fig. 7.7), obtained from the reduction of benzoylformate esters, their chlorine-substituted analogues and of ethyl 2-oxopentanonate, revealed an opposite absolute configuration [100, 105, 112, 113]. Thus, binding of the aromatic or alkyl residue was predominant over that of the ester moiety while the H⁻ attack took place from the same side.
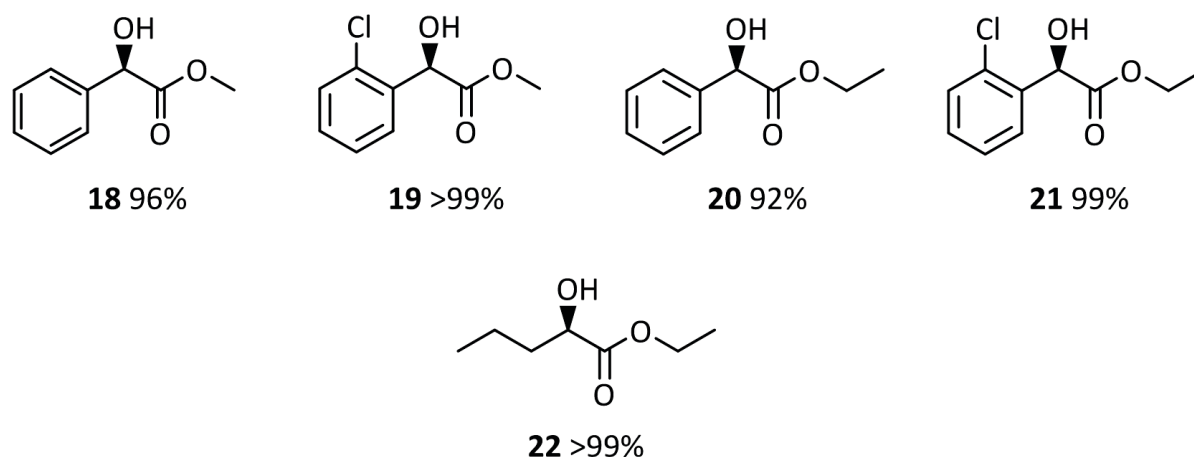
Figure 7.7. Opposite absolute product configuration. The absolute configuration of these products was opposite to the stereochemical trend described in section 7.4.3.1 and illustrated in Fig. 7.5 and 7.6, respectively. Given is also the enantiomeric excess in %.

With respect to the reduction of benzoylformate ester, enantioselectivity increased with the presence of the electron-withdrawing chlorine atom in *ortho* position.

When comparing the reduction of ethyl 2-oxo-butanoate and ethyl 2-oxo-pentanoate, it is evident that the corresponding products, ethyl 2-hydroxy-butanoate **2** (Fig. 7.5) and ethyl 2-hydroxy-pentanoate **22** (Fig. 7.7), display opposite configurations. This is astonishing, as the only difference is an additional methylene group in the alkyl moiety. It appears that, chain elongation led to a preferred accomodation of the alkyl moiety.

7.4.4 Reduction of aldehydes

Because it is assumed that Gre2p works *in vivo* as both an isovaleraldehyde and methythylglyoxal reductase [311, 362], several aldehydes were also tested as substrates (chapter 2.1). Indeed, towards the first compound the enzyme displayed the highest activity, which was almost twice as much as with 2,5-hexanedione. This result corroborates the hypothesis where Gre2p functions as a suppressor of filament formation by virtue of catalysing the reduction of isovaleraldehyde to isoamyl alcohol [362]. Additionally, as expected, aldehydes similar to isovaleraldehyde, like butanal or 2-methylpropanal, were also accepted by Gre2p leading to similar activities. In contrast, reduction activity for methylglyoxal was only half as high as with the γ-diketone suggesting that Gre2p acts *in vivo* as isovaleraldehyde rather than a methylglyoxal reductase. This hypothesis is substantiated by the fact that *gre2Δ* mutants were shown to reveal no sensitivity towards methylglyoxal

[363]. Thus, the initial assumption that Gre2p plays a role in methylglyoxal detoxification needs to be reconsidered.

Aside from aliphatic aldehydes, Gre2p also catalysed the reduction of aromatic aldehydes, e.g. benzaldehyde. Moreover, it was shown that the enzyme exhibits reduction activity towards the heteroaryl aldehydes, furfural and 5-hydroxymethylfurfural (HMF) [364]. Both compounds are mainly produced from microbial degradation of lignocellulosic feedstocks [365]. However, they are toxic and are considered to inhibit cell growth. As a consequence, cells need to have a resistance mechanism. In *S. cerevisiae*, resistance to high concentrations of furfural is based on the reduction of the aldehydes to the less-toxic furfuryl alcohols, catalysed by reductases [364, 366].

In summary, Gre2p displays an extraordinary substrate scope towards a variety of carbonyl compounds. The tendency to reduce a substrate increases with the presence of an electron-withdrawing group. Additionally, the enzyme catalyses the reduction of compounds, revealing large hydrophobic moieties adjacent to the carbonyl carbon atom. Generally, reduction catalysed by Gre2p results in the corresponding Prelog products. The fact that there are few exceptions to this rule will hopefully be explained in near future, since the three-dimensional structure has been solved very recently [379].

7.5 STRUCTURE-FUNCTION RELATIONSHIP

Oxidoreductases are grouped into various protein super-families. Short- and medium-chain dehydrogenases reveal a sequence length of typically 250 (SDRs) and 350 amino acids (MDRs), respectively [367]. The long-chain forms of SDRs, also called "extended SDRs", possess the same length as MDRs, as they have an additional 100 aa residue at the *C*-terminus [368-370]. SDRs and MDRs have distinct domain architectures. Most SDRs, with some exceptions for extended ones, usually display one-domain architecture, with the substrate binding site located in the highly variable *C*-terminal region [371, 372]. Their active site is formed by a triad (or tetrad) with the residues Tyrosine (Tyr), Lysine (Lys), Serine (Ser) (and Asparagine (Asn)) [373]. In contrast, MDRs typically have two-domain subunits where the cofactor-binding domain very often covers the *C*-terminal half, while the catalytic domain comprises half of the *N*-terminus and a segment of the *C*-terminus. Moreover, the

catalytic mechanism is either Zn-dependent or Tyr-based [367, 372]. Common to both families is the Rossmann-fold, which contains of six to seven central, twisted parallel β-sheets flanked by three to four α-helices on each side. This structural motif displays a highly variable glycine-rich sequence pattern which is responsible for cofactor binding [371, 374].

Members of the aldo-keto reductases (AKRs) are mainly monomeric proteins consisting of approximately 320 amino acids. In comparison to both SDRs and MDRs, they do not possess a Rossmann-fold. A typical feature of their ternary structure is the $(\alpha/\beta)_8$-barrel motif [375].

7.5.1 Gre2p is a SDR member and is homologous to SSCR from *S. salmonicolor*

Gre2p consists of 342 amino acids and displays the typical α/β-Rossmann-structure with the glycine-rich pattern (Gly7-Ala8-Asn9-Gly10-Phe11-Ile12-Ala13) at the *N*-terminus. In addition, the sequence displays the catalytically important triad, consisting of Ser127, Tyr165 and Lys169. Accordingly, the enzyme can be grouped into the extended short-chain dehydrogenase family. The primary sequence of Gre2p shows significant levels of identity with both the plant dihydroflavonol-4-reductases (24-27%), which catalyse reactions involved in the detoxification of flavonoid compounds [376], and the mammalian 3-β-hydroxysteroid dehydrogenases (26-30%), which take part in the interconversion of steroid precursors in the steroid biosynthesis [377].

A comparison of the crystal structure of the NADPH-dependent carbonyl reductase from *Sporobolomyces salmonicolor* (SSCR) [378] with the recently solved 3D-structure of Gre2p in complex with NADPH [379] reveals that the cofactor-binding site is highly conserved which suggests a similar NADPH binding pattern. In SSCR the glycine-rich motif (Gly19-Ala20-Ala21-Gly22-Phe23-Val24-Ala25) binds the cofactor through formation of hydrogen bonds with the diphosphate moiety and through a water-mediated hydrogen bond with the ribose of AMP. Additionally, the basic residues Arg44 and Lys48 were found to form strong salt-bridges with the negatively charged phosphate moiety at the 2'-position of AMP [378]. In Gre2p the equivalent residues are Arg32 and Lys36 alongside Asn9. They are responsible to form hydrogen bonds with the phosphate moiety giving the enzyme a stronger affinity for NADPH. In SSCR, the residue Arg44 also interacts with an adenine ring of AMP, which helps to anchor the AMP moiety [378]. The importance of the equivalent residue in Gre2p in binding the cofactor was demonstrated by Katzberg *et al.* Replacement of Arg32 with the negatively charged glutamic acid (Glu) or aspartic acid (Asp) significantly decreased activities towards

NADPH. In addition, the activity towards NADH was reduced as well compared to the wild-type enzyme [336]. In an attempt to exchange the cofactor specificity of Gre2p, it was discovered that replacing Asn9 with either Glu or Asp increased the activity for NADH while the NADPH activity was decreased [128, 336] due to the loss of the hydrogen bond with the phosphate moiety. It was also supposed that binding of NADPH was hampered by electrostatic repulsion and, in terms of Glu9, steric hindrance. On the other hand, it was assumed that an extra hydrogen bond between the side chain carboxyl group of Glu9 and NADH improved stabilisation of the cofactor [128, 336].

In comparison with the cofactor-binding domain, no homology is shared with the substrate-binding domain, even though both enzymes display a similar substrate scope [115]. According to docking models established by Kamitori *et al.* the active site of SSCR forms a hydrophobic channel with the binding of NADPH. This may possibly help a substrate to access the catalytic site and plays a role in recognising a substrate [378]. It is proposed that this is also the case for Gre2p explaining why the enzyme accepts such a broad range of substrates [379].

7.6. EXPANDING THE BIOCATALYTIC TOOLBOX BY A NOVEL ADH FROM *KLUYVEROMYCES POLYSPORUS*

Because of the steadily increasing demand for novel biocatalysts, expansion of the biocatalytic toolbox by a novel ADH was also part of the present thesis. Because of its broad substrate spectrum and its ability to synthesise the valuable chiral synthon (2*S*,5*S*)-hexanediol with high conversion rate and excellent enantiomeric excess, *in silico* screening based on the amino acid sequence of Gre2p was performed. This approach uncovered several putative oxidoreductases, mainly of yeast origin, with a sequence identity of up to 59%. Two putative annotated oxidoreductases with unknown function in the genomes of *Kluyveromyces polysporus* (59%) and *Pichia guilliermondii* (50%) revealed the highest identities. Subsequently, the corresponding genes were cloned and over-expressed in *E. coli*, followed by an assay to test the ability to reduce 2,5-hexanedione. Hence, the ADH from *K. polysporus* (Kp-ADH) revealed a specific activity of 46.4 U·mg^{-1}, while no activity was observed with the reductase from *P. guilliermondii,* which was therefore not considered further.

Because of the high relation to Gre2p, it is no wonder that Kp-ADH displayed the same cofactor preference (NADPH) and revealed a similar substrate spectrum. Accordingly, diketones were well-accepted by Kp-ADH and were reduced to the corresponding Prelog products. In addition, the preference for reducing the proximal keto group of asymmetrical diketones was identical. Nevertheless, slight differences were noticeable. Thus, Kp-ADH revealed a higher K_M value (9.28 ± 0.36 mM) for the reduction of 2,5-hexanedione than Gre2p (4.33 ± 0.28 mM), indicating that the affinity towards the dicarbonyl compound was diminished by a factor of two. This might have affected the synthesis of (2S,5S)-hexanediol. Although less enzyme (5 U·mL^{-1}) was applied in cell-free bioreduction of 20 mM diketone compared to Gre2p (20 U·mL^{-1}), conversion to the diol proceeded significantly slower. While Gre2p completed the reaction after 45 min, completion took 450 min when Kp-ADH was applied. Considering that the amount of Kp-ADH in the reaction mixture was four times lower, one would expect completion after about 180 min. As a consequence, a ten times lower STY (7.6 g L^{-1} d^{-1}) was achieved than by Gre2p-mediated reduction (70 g·L^{-1}·d^{-1}) (Chapter 2.1).

What is more, reducing activity towards 2,3-diketones was on average approximately half as high as with Gre2p, except the reduction of 2,3-pentanedione. Hence, 2,3-hexanedione, which is reduced by Gre2p with 32% of the activity obtained for 2,5-hexanedione, was reduced by Kp-ADH with only 15% of the activity. Both Gre2p and Kp-ADH displayed the second highest diketone activity towards 2,3-hexanedione.

While α-keto esters were well accepted by Kp-ADH, however, activity towards β-keto esters was poor compared with Gre2p. Hence, ethyl 3-oxo-butanote was reduced with a ten times lower activity (1.6 U·mg^{-1}) than did Gre2p (16.3 U·mg^{-1}). Similar to Gre2p, the electron-withdrawing substituent chlorine increased reduction activity, however, activities towards ethyl 2-chloro-3-oxo butanoate and ethyl 4-chloro-3-oxo butanoate were still significantly lower than the ones observed with Gre2p. The stereochemical trend was the same as observed for Gre2p.

Small-scale conversions revealed the great biotechnological potential of the enzyme, as various carbonyl compounds were reduced to the corresponding hydroxy ketones, diols, alcohols, and α-, and β-hydroxy esters in high enantiomeric excess at high conversion rates.

8 CONCLUSION

In this thesis, Gre2p from *S. cerevisiae* was identified of catalysing the reduction of 2,5-hexanedione to (2*S*,5*S*)-hexanediol. The diol serves as a versatile chiral building block in the production of various chiral auxiliaries, ligands and pharmaceutical active compounds. Subsequent (2*S*,5*S*)-hexanediol production was successfully achieved using a cell-free system, *E. coli* whole-cell systems and a *S. cerevisiae* strain expressing the 2,5-hexandione reductase gene. Comparison with existing routes revealed that the biocatalytic approaches developed here were much more efficient in terms of conversion rate, STYs, cell productivity and co-substrate yield. Using the *E. coli* catalyst, it was even possible to scale-up the diol synthesis indicating that the process would be transferable to a commercial-scale.

It was also shown for the first time that Gre2p displays reducing activity towards other diketones, such as *α*- and *β*-diketones. The enzyme was able to convert them to the corresponding chiral hydroxy ketones following Prelog's rule. In some cases, even the corresponding diol was achieved. The fact that the enzyme also accepts various diketones in addition to keto esters and some ketones widens its biocatalytic application in the synthesis of chiral alcohols.

Though crystals could be produced in preliminary crystallisation experiments, it was not possible to solve the 3D structure of Gre2p in this thesis. However, recently the structures of the apo enzyme and in complex with NADPH have been solved [379] and thus it will be possible to gain profound knowledge about the catalytic mechanism in the future.

Furthermore, a novel ADH based on the amino acid sequence of Gre2p was identified, and small-scale conversions revealed that it is an excellent biocatalyst for the synthesis of chiral hydroxy ester, in particular, of *α*-hydroxy ester.

Overall, the scope of developing efficient biocatalytic routes to (2*S*,5*S*)-hexanediol was achieved. Moreover, the biocatalytic toolbox was expanded by the identification of a novel ADH. Finally, it was shown that the ADHs are highly useful in the production of chiral building blocks.

9 REFERENCES

[1] **Patel R.N.** Biocatalytic synthesis of chiral alcohols and amino acids for development of pharmaceuticals. *Biomolecules* **2013**; 3:741-777.

[2] **Patel R.N.** Biocatalysis: Synthesis of key intermediates for development of pharmaceuticals. *ACS Catal.* **2011**; 1:1056-1074.

[3] **Patel R.N.** Chemo-enzymatic synthesis of chiral pharmaceutical intermediates. *Expert. Opin. Drug Discov.* **2008**; 3:187-245.

[4] **Patel R.N.** Biocatalysis: Synthesis of chiral intermediates for pharmaceuticals. *Curr. Org. Chem.* **2006**; 10:1289-1321.

[5] **Muñoz Solano D., Hoyos P., Hernáiz M.J., Alcántara A.R., Sánchez-Montero J.M.** Industrial biotransformations in the synthesis of building blocks leading to enantiopure drugs. *Bioresour. Technol.* **2012**; 115:196-207.

[6] **Hilterhaus L., Liese A.** *Building Blocks*. In: White Biotechnology. Edited by: Ulber R, Sell D. Springer-Verlag Berlin; **2007**. pp. 133-173.

[7] **Tao J., Xu J.H.** Biocatalysis in development of green pharmaceutical processes. *Curr. Opin. Chem. Biol.* **2009**; 13:43-50.

[8] **Mori K.** Organic synthesis in pheromone science. *Molecules* **2005**; 10:1023-1047.

[9] **Meyer H.P., Turner N.J.** Biotechnological manufacturing options for organic chemistry. *Mini-Rev. Org. Chem.* **2009**; 6:300-306.

[10] **Lin G.Q., You Q.D., Cheng J.F.** *Chiral drugs*. Hoboken, John Wiley & Sons, Inc., New Jersey; **2011**.

[11] *Global Markets for Chiral Technology*. **2012**. http://www.bccresearch.com/market-research/biotechnology/chiral-products-technology-global-markets-bio012f.html

[12] FDA's policy statement for the development of new stereoisomeric drugs. *Chirality* **1992**; 4:338-340.

[13] **Faber K.** *Biotransformations in organic chemistry*. Springer-Verlag Berlin; **2011**.

[14] **Faber K., Patel R.** Chemical biotechnology - A happy marriage between chemistry and biotechnology: Asymmetric synthesis *via* green chemistry *Curr. Opin. Biotechnol.* **2000**; 11:517-519.

[15] **Brooks W.H., Guida W.C., Daniel K.G.** The Significance of chirality in drug design and development. *Curr. Top. Med. Chem.* **2011**; 11:760-770.

[16] **Breuer M., Ditrich K., Habicher T., Hauer B., Keβeler M., Stürmer R., Zelinski T.** Industrial methods for the production of optically active intermediates. *Angew. Chem. Int. Ed.* **2004**; 43:788-824.

[17] **Agranat I., Caner H., Caldwell A.** Putting chirality to work: The strategy of chiral switches. *Nat. Rev. Drug Discov.* **2002**; 1:753-768.

[18] **Rouhi A.M.** Chirality at work. *Chem. Eng. News* **2003**; 81:45-55.

[19] **Huisman G.W., Collier S.J.** On the development of new biocatalytic processes for practical pharmaceutical synthesis. *Curr. Opin. Chem. Biol.* **2013**; 17:284-292.

[20] **Hollmann F., Arends I.W.C.E., Holtmann D.** Enzymatic reductions for the chemist. *Green Chem.* **2011**; 13:2285-2314.

[21] **Fischer T., Pietruszka J.** *Key building blocks via enzyme-mediated synthesis*. In: Natural Products via Enzymatic Reactions. Edited by: Piel J. Springer Berlin Heidelberg; **2010**. pp. 1-43.

[22] **Wohlgemuth R.** Asymmetric biocatalysis with microbial enzymes and cells. *Curr. Opin. Microbiol.* **2010**; 13:283-292.

[23] **Ghanem A., Aboul-Enein H.Y.** Application of lipases in kinetic resolution of racemates. *Chirality* **2005**; 17:1-15.

[24] **Hudlicky T., Reed J.W.** Applications of biotransformations and biocatalysis to complexity generation in organic synthesis. *Chem. Soc. Rev.* **2009**; 38:3117-3132.

[25] **Nguyen L.A., He H., Pham-Huy C.** Chiral drugs: An overview. *Int. J. Biomed. Sci.* **2006**; 2:85-100.

[26] **Straathof A.J.J., Panke S., Schmid A.** The production of fine chemicals by biotransformations. *Curr. Opin. Biotechnol.* **2002**; 13:548-556.

[27] **Trost B.M.** Asymmetric catalysis: An enabling science. *Proc. Natl. Acad. Sci. USA* **2004**; 101:5348-5355.

[28] **Knowles W.S., Noyori R.** Pioneering perspectives on asymmetric hydrogenation. *Accounts Chem. Res.* **2007**; 40:1238–1239.

[29] **Kolb H.C., VanNieuwenhze M.S., Sharpless K.B.** Catalytic asymmetric dihydroxylation. *Chem. Rev.* **1994**; 94:2483-2547.

[30] **Hall M., Bommarius A.S.** Enantioenriched compounds *via* enzyme-catalyzed redox reactions. *Chem. Rev.* **2011**; 111:4088-4110.

[31] **Matsuda T., Yamanaka R., Nakamura K.** Recent progress in biocatalysis for asymmetric oxidation and reduction. *Tetrahedron: Asymmetry* **2009**; 20:513-557.

[32] **Nakamura K., Matsuda T.** Biocatalytic reduction of carbonyl groups. *Curr. Org. Chem.* **2006**; 10:1217-1246.

[33] **Stewart J.D.** Dehydrogenases and transaminases in asymmetric synthesis. *Curr. Opin. Chem. Biol.* **2001**; 5:120-129.

[34] **Reetz M.T**. Biocatalysis in organic chemistry and biotechnology: Past, present, and future. *J. Am. Chem. Soc.* **2013**; 135:12480-12496.

[35] **Buchholz K., Kasche V., Bornscheuer U.T.** *Biocatalysts and Enzyme Technology*. Wiley-VCH Weinheim; **2012**.

[36] **Pollard D.J., Woodley J.M.** Biocatalysis for pharmaceutical intermediates: The future is now. *Trends Biotechnol.* **2007**; 25:66-73.

[37] **Rosenthaler L.** Enzyme effected asymmetrical synthesis. *Biochem. Z.* **1908**; 14:238-253.

[38] **Schrittwieser J.H., Resch V.** The role of biocatalysis in the asymmetric synthesis of alkaloids. *RSC Advances* **2013**; 3:17602-17632.

[39] **Jegannathan K.R., Nielsen P.H.** Environmental assessment of enzyme use in industrial production: A literature review. *J. Clean. Prod.* **2013**; 42:228-240.

[40] **Turner N.J., O'Reilly E.** Biocatalytic retrosynthesis. *Nat. Chem. Biol.* **2013**; 9:285-288.

[41] **Clouthier C.M., Pelletier J.N.** Expanding the organic toolbox: a guide to integrating biocatalysis in synthesis. *Chem. Soc. Rev.* **2012**; 41:1585-1605.

[42] **Wenda S., Illner S., Mell A., Kragl U.** Industrial biotechnology: The future of green chemistry? *Green Chem.* **2011**; 13:3007-3047.

[43] **Zheng G.W., Xu J.H.** New opportunities for biocatalysis: Driving the synthesis of chiral chemicals. *Curr. Opin. Biotechnol.* **2011**; 22:784-792.

[44] **Wohlgemuth R.** Biocatalysis: Key to sustainable industrial chemistry. *Curr. Opin. Biotechnol.* **2010**; 21:713-724.

[45] **Liljeblad A., Kallinen A., Kanerva L.T.** Biocatalysis in the preparation of the statin side chain. *Curr. Org. Synth.* **2009**; 6:362-379.

[46] **Bornscheuer U.T., Buchholz K.** Highlights in biocatalysis: Historical landmarks and current trends. *Eng. Life Sci.* **2005**; 5:309-323.

[47] **Wandrey C., Liese A., Kihumbu D.** Industrial biocatalysis: Past, present, and future. *Org. Process Res. Dev.* **2000**; 4:286-290.

[48] **Schulze B., Wubbolts M.G.** Biocatalysis for industrial production of fine chemicals. *Curr. Opin. Biotechnol.* **1999**; 10:609-615.

[49] **Arnold F.H.** Combinatorial and computational challenges for biocatalyst design. *Nature* **2001**; 409:253-257.

[50] **Arnold F.H.** Directed evolution: Creating biocatalysts for the future. *Chem. Eng. Sci.* **1996**; 51:5091-5102.

[51] **Stemmer W.P.C.** Rapid evolution of a protein *in vitro* by DNA shuffling. *Nature* **1994**; 370:389-391.

[52] **Damborsky J., Brezovsky J.** Computational tools for designing and engineering enzymes. *Curr. Opin. Chem. Biol.* **2014**; 19:8-16.

[53] **Kries H., Blomberg R., Hilvert D.** *De novo* enzymes by computational design. *Curr. Opin. Chem. Biol.* **2013**; 17:221–228.

[54] **Kiss G., Çelebi-Ölçüm N., Moretti R., Baker D., Houk K.N.** Computational enzyme design. *Angew. Chem. Int. Ed.* **2013**; 52:5700-5725.

[55] **Wijma H.J., Janssen D.B.** Computational design gains momentum in enzyme catalysis engineering. *FEBS J.* **2013**; 280:2948-2960.

[56] **Verma R., Schwaneberg U., Roccatano D.** Computer-aided protein directed evolution: A review of web servers, databases and other computational tools for protein engineering. *Comput. Struct. Biotechnol. J.* **2012**; 2:1-12.

[57] **Barrozo A., Borstnar R., Marloie G., Kamerlin S.C.L.** Computational protein engineering: Bridging the gap between rational design and laboratory evolution. *Int. J. Mol. Sci.* **2012**; 13:12428-12460.

[58] **Lutz S.** Beyond directed evolution: Semi-rational protein engineering and design. *Curr. Opin. Biotechnol.* **2010**; 21:734–743.

[59] **Bornscheuer U.T., Pohl M.** Improved biocatalysts by directed evolution and rational protein design. *Curr. Opin. Chem. Biol.* **2001**; 5:137-143.

[60] **Voigt C.A., Mayo S.L., Arnold F.H., Wang Z.G.** Computationally focusing the directed evolution of proteins. *J. Cell Biochem. Suppl.* **2001**; 37:58-63.

[61] **Bommarius A.S., Paye M.F.** Stabilizing biocatalysts. *Chem. Soc. Rev.* **2013**; 42:6534-6565.

[62] **Reetz M.T.** *Directed evolution of enzymes*. In: Enzyme catalysis in organic synthesis. Edited by: Drauz K, Gröger H, May O. Wiley-VCH Weinheim; **2012**.

[63] **Brustad E.M., Arnold F.H.** Optimizing non-natural protein function with directed evolution. *Curr. Opin. Chem. Biol.* **2011**; 15:201-210.

[64] **Bloom J.D., Meyer M.M., Meinhold P., Otey C.R., MacMillan D., Arnold F.H.** Evolving strategies for enzyme engineering. *Curr. Opin. Struct. Biol.* **2005**; 15:447-452.

[65] **Farinas E.T., Bulter T., Arnold F.H.** Directed enzyme evolution. *Curr. Opin. Biotechnol.* **2001**; 12:545-551.

[66] **Woodley J.M.** Protein engineering of enzymes for process applications. *Curr. Opin. Chem. Biol.* **2013**; 17:310-316.

[67] **Bornscheuer U.T., Huisman G.W., Kazlauskas R.J., Lutz S., Moore J.C., Robins K.** Engineering the third wave of biocatalysis. *Nature* **2012**; 485:185-194.

[68] **Ni Y., Xu J.H.** Biocatalytic ketone reduction: A green and efficient access to enantiopure alcohols. *Biotechnol. Adv.* **2012**; 30:1279-1288.

[69] **Gröger H., Asano Y.** *Principles and historical landmarks of enzyme catalysis in organic synthesis* In: Enzyme catalysis in organic synthesis*.* Edited by: Drauz K, Gröger H, May O. Weinheim: Wiley-VCH Weinheim; **2012**.

[70] **Menger F.M.** Enzyme reactivity from an organic perspective. *Accounts Chem. Res.* **1993**; 26:206-212.

[71] **Ciriminna R., Pagliaro M.** Green chemistry in the fine chemicals and pharmaceutical industries. *Org. Process Res. Dev.* **2013**; 17:1479-1484.

[72] **Woodley J.M.** New opportunities for biocatalysis: Making pharmaceutical processes greener. *Trends Biotechnol.* **2008**; 26:321-327.

[73] **Festel G., Knöll J., Götz H., Zinke H.** Impact of biotechnology production processes in the chemical industry. *Chem. Ing. Tech.* **2004**; 76:307-312.

[74] *Merck announces full-year and fourth-quarter 2012 financial results*. **2013**. http://www.mercknewsroom.com/press-release/corporate-news/merck-announces-full-year-and-fourth-quarter-2012-financial-results

[75] **Desai A.A.** Sitagliptin manufacture: A compelling tale of green chemistry, process intensification, and industrial asymmetric catalysis. *Angew. Chem. Int. Ed.* **2011**; 50:1974-1976.

[76] **Savile C.K., Janey J.M., Mundorff E.C., Moore J.C., Tam S., Jarvis W.R., Colbeck J.C., Krebber A., Fleitz F.J., Brands J., Devine P.N., Huisman G.W., Hughes G.J.** Biocatalytic asymmetric synthesis of chiral amines from ketones applied to sitagliptin manufacture. *Science* **2010**; 329:305-309.

[77] **Xie X., Tang Y.** Efficient synthesis of simvastatin by use of whole-cell biocatalysis. *Appl. Environ. Microbiol.* **2007**; 73:2054–2060. .

[78] **Xie X., Watanabe K., Wojcicki W.A., Wang C.C.C., Tang Y.** Biosynthesis of lovastatin analogs with a broadly specific acyltransferase. *Chem. Biol.* **2006**; 13:1161-1169.

[79] **Gilson L., Collier S.J., Sukumaran J., Yeo W.L., Alviso O., Teo E.L., Wilson R.J., Xu J.** *Variant LovD polypeptides and their uses*. **2011**. WO 2011/041231 A1

[80] **Collier S.J., Teo E.L., Sukumaran J., Wilson R.J., Xu J.** *Improved LovD acyltransferase*. **2011**. WO 2011/041233 A1

[81] **Moore J.C., Pollard D.J., Kosjek B., Devine P.N.** Advances in the enzymatic reduction of ketones. *Accounts Chem. Res.* **2007**; 40:1412-1419.

[82] **Kroutil W., Mang H., Edegger K., Faber K.** Recent advances in the biocatalytic reduction of ketones and oxidation of *sec*-alcohols. *Curr. Opin. Chem. Biol.* **2004**; 8:120-126.

[83] **Nakamura K., Yamanaka R., Matsuda T., Harada T.** Recent developments in asymmetric reduction of ketones with biocatalysts. *Tetrahedron: Asymmetry* **2003**; 14:2659-2681.

[84] **Huisman G.W., Liang J., Krebber A.** Practical chiral alcohol manufacture using ketoreductases. *Curr. Opin. Chem. Biol.* **2010**; 14:122-129.

[85] **Huang Y., Liu N., Wu X., Chen Y.** Dehydrogenases/reductases for the synthesis of chiral pharmaceutical intermediates. *Curr. Org. Chem.* **2010**; 14:1447-1460.

[86] **Ma S.K., Gruber J., Davis C., Newman L., Gray D., Wang A., Grate J.** A green-by-design biocatalytic process for atorvastatin intermediate. *Green Chem.* **2010**; 12:81–86.

[87] **Wolberg M., Filho M.V., Bode S., Geilenkirchen P., Feldmann R., Liese A., Hummel W., Müller M.** Chemoenzymatic synthesis of the chiral side-chain of statins: Application of an alcohol dehydrogenase catalysed ketone reduction on a large scale. *Bioprocess Biosyst. Eng.* **2008**; 31:183-191.

[88] **Daußmann T., Hennemann H.G., Rosen T.C., Dünkelmann P.** Enzymatische Technologien zur Synthese chiraler Alkohol-Derivate. *Chem. Ing. Tech.* **2006**; 78:249-255.

[89] **Chen X.H., Wei P., Wang X.T., Zong M.H., Lou W.Y.** A novel carbonyl reductase with anti-prelog stereospecificity from *Acetobacter* sp. CCTCC M209061: Purification and Characterization. *PLoS One* **2014**; 9:e94543.

[90] **Li Z., Liu W., Chen X., Jia S., Wu Q., Zhu D., Ma Y.** Highly enantioselective double reduction of phenylglyoxal to (*R*)-1-phenyl-1,2-ethanediol by one NADPH-dependent yeast carbonyl reductase with a broad substrate profile. *Tetrahedron* **2013**; 69:3561-3564.

[91] **Ma H., Yang L., Ni Y., Zhang J., Li C.X., Zheng G.W., Yang H., Xu J.H.** Stereospecific reduction of methyl *o*-chlorobenzoylformate at 300 g·L^{-1} without additional cofactor using a carbonyl reductase mined from *Candida glabrata*. *Adv. Synth. Catal.* **2012**; 354:1765 – 1772.

[92] **Ni Y., Li C.X., Ma H.M., Zhang J., Xu J.H.** Biocatalytic properties of a recombinant aldo-keto reductase with broad substrate spectrum and excellent stereoselectivity. *Appl. Microbiol. Biotechnol.* **2011**; 89:1111-1118.

[93] **Ni Y., Li C.X., Wang L.J., Zhang J., Xu J.H.** Highly stereoselective reduction of prochiral ketones by a bacterial reductase coupled with cofactor regeneration. *Org. Biomol. Chem.* **2011**; 9:5463-5468.

[94] **Ni Y., Li C.X., Zhang J., Shen N.D., Bornscheuer U.T., Xu J.H.** Efficient reduction of ethyl 2-oxo-4-phenylbutyrate at 620 g·L^{-1} by a bacterial reductase with broad substrate spectrum. *Adv. Synth. Catal.* **2011**; 353:1213-1217.

[95] **Nie Y., Xiao R., Xu Y., Montelione G.T.** Novel anti-Prelog stereospecific carbonyl reductases from *Candida parapsilosis* for asymmetric reduction of prochiral ketones. *Org. Biomol. Chem.* **2011**; 9:4070-4078.

[96] **Richter N., Hummel W.** Biochemical characterisation of a NADPH-dependent carbonyl reductase from *Neurospora crassa* reducing α- and β-keto esters. *Enzyme Microb. Technol.* **2011**; 48:472-479.

[97] **Wang L.J., Li C.X., Ni Y., Zhang J., Liu X., Xu J.H.** Highly efficient synthesis of chiral alcohols with a novel NADH-dependent reductase from *Streptomyces coelicolor*. *Bioresour. Technol.* **2011**; 102:7023-7028.

[98] **Asako H., Shimizu M., Itoh N.** Biocatalytic production of (*S*)-4-bromo-3-hydroxybutyrate and structurally related chemicals and their applications. *Appl. Microbiol. Biotechnol.* **2009**; 84:397-405.

[99] **Sorgedrager M.J., van Rantwijk F., Huisman G.W., Sheldon R.A.** Asymmetric carbonyl reductions with microbial ketoreductases. *Adv. Synth. Catal.* **2008**; 350:2322-2328.

[100] **Ema T., Yagasaki H., Okita N., Takeda M., Sakai T.** Asymmetric reduction of ketones using recombinant *E coli* cells that produce a versatile carbonyl reductase with high enantioselectivity and broad substrate specificity. *Tetrahedron* **2006**; 62:6143-6149.

[101] **Ema T., Yagasaki H., Okita N., Nishikawa K., Korenaga T., Sakai T.** Asymmetric reduction of a variety of ketones with a recombinant carbonyl reductase: Identification of the gene encoding a versatile biocatalyst. *Tetrahedron: Asymmetry* **2005**; 16:1075-1078.

[102] **Weckbecker A., Hummel W.** Cloning, expression, and characterization of an (*R*)-specific alcohol dehydrogenase from *Lactobacillus kefir*. *Biocatal. Biotransform.* **2006**; 24:380-389.

[103] **Inoue K., Makino Y., Itoh N.** Production of (*R*)-chiral alcohols by a hydrogen-transfer bioreduction with NADH-dependent *Leifsonia* alcohol dehydrogenase (LSADH). *Tetrahedron: Asymmetry* **2005**; 16:2539-2549.

[104] **Kaluzna I.A., David R. J., Kambourakis S.** Ketoreductases: Stereoselective catalysts for the facile synthesis of chiral alcohols. *Tetrahedron: Asymmetry* **2005**; 16:3682-3689.

[105] **Kaluzna I.A., Matsuda T., Sewell A.K., Stewart J.D.** Systematic investigation of *Saccharomyces cerevisiae* enzymes catalyzing carbonyl reductions. *J. Am. Chem. Soc.* **2004**; 126:12827-12832.

[106] **Kaluzna I., Andrew A.A., Bonilla M., Martzen M.R., Stewart J.D.** Enantioselective reductions of ethyl 2-oxo-4-phenylbutyrate by *Saccharomyces cerevisiae* dehydrogenases. *J. Mol. Catal. B: Enzym.* **2002**; 17:101-105.

[107] **Wu X., Wang Y., Ju J., Chen C., Liu N., Chen Y.** Enantioselective synthesis of ethyl (*S*)-2-hydroxy-4-phenylbutyrate by recombinant diketoreductase. *Tetrahedron: Asymmetry* **2009**; 20:2504-2509.

[108] **Parkot J., Gröger H., Hummel W.** Purification, cloning, and overexpression of an alcohol dehydrogenase from *Nocardia globerula* reducing aliphatic ketones and bulky ketoesters. *Appl. Microbiol. Biotechnol.* **2010**; 86:1813-1820.

[109] **Pennacchio A., Giordano A., Rossi M., Raia C.A.** Asymmetric reduction of α-keto esters with *Thermus thermophilus* NADH-dependent carbonyl reductase using glucose dehydrogenase and alcohol dehydrogenase for cofactor regeneration. *Eur. J. Org. Chem.* **2011**; 2011:4361-4366.

[110] **Pennacchio A., Giordano A., Pucci B., Rossi M., Raia C.A.** Biochemical characterization of a recombinant short-chain NAD(H)-dependent dehydrogenase/reductase from *Sulfolobus acidocaldarius*. *Extremophiles* **2010**; 14:193-204.

[111] **Pennacchio A., Pucci B., Secundo F., La Cara F., Rossi M., Raia C.A.** Purification and characterization of a novel recombinant highly enantioselective short-chain NAD(H)-dependent alcohol dehydrogenase from *Thermus thermophilus*. *Appl. Environ. Microbiol.* **2008**; 74:3949-3958.

[112] **Ema T., Ide S., Okita N., Sakai T.** Highly efficient chemoenzymatic synthesis of methyl (*R*)-*o*-chloromandelate, a key intermediate for clopidogrel, *via* asymmetric reduction with recombinant *Escherichia coli*. *Adv. Synth. Catal.* **2008**; 350:2039-2044.

[113] **Ema T., Okita N., Ide S., Sakai T.** Highly enantioselective and efficient synthesis of methyl (*R*)-*o*-chloromandelate with recombinant *E coli*: Toward practical and green access to clopidogrel. *Org. Biomol. Chem.* **2007**; 5:1175-1176.

[114] **Zhu D., Mukherjee C., Rozzell J.D., Kambourakis S., Hua L.** A recombinant ketoreductase tool-box: Assessing the substrate selectivity and stereoselectivity toward the reduction of *β*-ketoesters. *Tetrahedron* **2006**; 62:901-905.

[115] **Zhu D., Yang Y., Buynak J.D., Hua L.** Stereoselective ketone reduction by a carbonyl reductase from *Sporobolomyces salmonicolor*. Substrate specificity, enantioselectivity and enzyme-substrate docking studies. *Org. Biomol. Chem.* **2006**; 4:2690-2695.

[116] **Gröger H., Chamouleau F., Orologas N., Rollmann C., Drauz K., Hummel W., Weckbecker A., May O.** Enantioselective reduction of ketones with "Designer cells" at high substrate concentrations: Highly efficient access to functionalized optically active alcohols". *Angew. Chem. Int. Ed.* **2006**; 45:5677-5681.

[117] **Gröger H., Hummel W., Rollmann C., Chamouleau F., Hüsken H., Werner H., Wunderlich C., Abokitse K., Drauz K., Buchholz S.** Preparative asymmetric reduction of ketones in a biphasic medium with an (*S*)-alcohol dehydrogenase under in situ-cofactor-recycling with a formate dehydrogenase. *Tetrahedron* **2004**; 60:633-640.

[118] **Zhang J., Duetz W.A., Witholt B., Li Z.** Rapid identification of new bacterial alcohol dehydrogenases for (*R*)- and (*S*)-enantioselective reduction of *β*-ketoesters. *Chem. Commun.* **2004**:2120-2121.

[119] **Rodríguez S., Kayser M.M., Stewart J.D.** Highly stereoselective reagents for *β*-keto ester reductions by genetic engineering of baker's yeast. *J. Am. Chem. Soc.* **2001**; 123:1547-1555.

[120] **Rodríguez S., Schroeder K.T., Kayser M.M., Stewart J.D.** Asymmetric synthesis of *β*-hydroxy esters and *α*-alkyl-*β*-hydroxy esters by recombinant *Escherichia coli* expressing enzymes from baker's yeast. *J. Org. Chem.* **2000**; 65:2586-2587.

[121] **Agudo R., Roiban G.D., Reetz M.T.** Induced axial chirality in biocatalytic asymmetric ketone reduction. *J. Am. Chem. Soc.* **2013**; 135:1665-1668.

[122] **Padhi S.K., Kaluzna I.A., Buisson D., Azerad R., Stewart J.D.** Reductions of cyclic β-keto esters by individual *Saccharomyces cerevisiae* dehydrogenases and a chemo-enzymatic route to (1*R*,2*S*)-2-methyl-1-cyclohexanol. *Tetrahedron: Asymmetry* **2007**; 18:2133-2138.

[123] **Dai Z., Guillemette K., Green T.K.** Stereoselective synthesis of aryl γ,δ-unsaturated β-hydroxyesters by ketoreductases. *J. Mol. Catal. B: Enzym.* **2013**; 97:264-269.

[124] **Bhuniya R., Mahapatra T., Nanda S.** *Klebsiella pneumoniae* (NBRC 3319) mediated asymmetric reduction of α-substituted β-oxo esters and its application to the enantioiselective synthesis of small-ring carbocycle derivatives. *Eur. J. Org. Chem.* **2012**:1597-1602.

[125] **Bariotaki A., Kalaitzakis D., Smonou I.** Enzymatic reductions for the regio- and stereoselective synthesis of hydroxy-keto esters and dihydroxy esters. *Org. Lett.* **2012**; 14:1792-1795.

[126] **Wu X., Jiang J., Chen Y.** Correlation between intracellular cofactor concentrations and biocatalytic efficiency: Coexpression of diketoreductase and glucose dehydrogenase for the preparation of chiral diol for statin drugs. *ACS Catal.* **2011**; 1:1661-1664.

[127] **Chen S.Y., Yang C.X., Wu J.P., Xu G., Yang L.R.** Multi-enzymatic biosynthesis of chiral β-hydroxy nitriles through co-expression of oxidoreductase and halohydrin dehalogenase. *Adv. Synth. Catal.* **2013**; 355:3179-3190.

[128] **Yoon S.A., Kim H.K.** Development of a bioconversion system using *Saccharomyces cerevisiae* reductase YOR120W and *Bacillus subtilis* glucose dehydrogenase for chiral alcohol synthesis. *J. Microbiol. Biotechnol.* **2013**; 23:1395-1402.

[129] **Liu X., Chen R., Yang Z., Wang J., Lin J., Wei D.** Characterization of a putative stereoselective oxidoreductase from *Gluconobacter oxydans* and Its application in producing ethyl (*R*)-4-chloro-3-hydroxybutanoate ester. *Mol. Biotechnol.* **2014**; 56:285–295.

[130] **Jung J., Park S., Kim H.K.** Synthesis of a chiral alcohol using a rationally designed *Saccharomyces cerevisiae* reductase and a NADH cofactor regeneration system. *J. Mol. Catal. B: Enzym.* **2012**; 84:15-21.

[131] **Jung J., Park H.J., Uhm K.N., Kim D., Kim H.K.** Asymmetric synthesis of (*S*)-ethyl-4-chloro-3-hydroxy butanoate using a *Saccharomyces cerevisiae* reductase: Enantioselectivity and enzyme-substrate docking studies. *BBA-Proteins Proteomics* **2010**; 1804:1841-1849.

[132] **Cao H., Mi L., Ye Q., Zang G., Yan M., Wang Y., Zhang Y., Li X., Xu L., Xiong J., Ouyang P., Ying H.** Purification and characterization of a novel NADH-dependent carbonyl reductase

from *Pichia stipitis* involved in biosynthesis of optically pure ethyl (*S*)-4-chloro-3-hydroxybutanoate. *Bioresour. Technol.* **2011**; 102:1733-1739.

[133] **Bisogno F.R., Lavandera I., Kroutil W., Gotor V.** Tandem concurrent processes: One-pot single-catalyst biohydrogen transfer for the simultaneous preparation of enantiopure secondary alcohols. *J. Org. Chem.* **2009**; 74:1730-1732.

[134] **Ye Q., Yan M., Xu L., Cao H., Li Z., Chen Y., Li S., Ying H.** A novel carbonyl reductase from *Pichia stipitis* for the production of ethyl (*S*)-4-chloro-3-hydroxybutanoate. *Biotechnol. Lett.* **2009**; 31:537-542.

[135] **Ye Q., Yan M., Yao Z., Xu L., Cao H., Li Z., Chen Y., Li S., Bai J., Xiong J., Ying H., Ouyang P.** A new member of the short-chain dehydrogenases/reductases superfamily: Purification, characterization and substrate specificity of a recombinant carbonyl reductase from *Pichia stipitis*. *Bioresour. Technol.* **2009**; 100:6022-6027.

[136] **de Gonzalo G., Lavandera I., Faber K., Kroutil W.** Enzymatic reduction of ketones in "micro-aqueous" media catalyzed by ADH-A from *Rhodococcus ruber*. *Org. Lett.* **2007**; 9:2163-2166.

[137] **Zhang J., Witholt B., Li Z.** Coupling of permeabilized microorganisms for efficient enantioselective reduction of ketone with cofactor recycling. *Chem. Commun.* **2006**:398-400.

[138] **Kaluzna I.A., Feske B.D., Wittayanan W., Ghiviriga I., Stewart J.D.** Stereoselective, biocatalytic reductions of α-chloro-β-keto esters. *J. Org. Chem.* **2005**; 70:342-345.

[139] **Yamamoto H., Mitsuhashi K., Mitsuhashi K., Matsuyama A., Esak N., Kobayashi Y.** A novel NADH-dependent carbonyl reductase from *Kluyveromyces aestuarii* and comparison of NADH-regeneration system for the synthesis of ethyl (*S*)-4-chloro-3-hydroxybutanoate. *Biosci., Biotechnol., Biochem.* **2004**; 68:638-649.

[140] **Yamamoto H., Kimoto N., Matsuyama A., Kobayashi Y.** Purification and properties of a carbonyl reductase useful for production of ethyl (*S*)-4-chloro-3-hydroxybutanoate from *Kluyveromyces lactis*. *Biosci., Biotechnol., Biochem.* **2002**; 66:1775-1778.

[141] **Kataoka M., Hoshino-Hasegawa A., Thiwthong R., Higuchi N., Ishige T., Shimizu S.** Gene cloning of an NADPH-dependent menadione reductase from *Candida macedoniensis*, and its application to chiral alcohol production. *Enzyme. Microb. Tech.* **2006**; 38:944-951.

[142] **Kataoka M., Yamamoto K., Kawabata H., Wada M., Kita K., Yanase H., Shimizu S.** Stereoselective reduction of ethyl 4-chloro-3-oxobutanoate by *Escherichia coli* transformant

cells coexpressing the aldehyde reductase and glucose dehydrogenase genes. *Appl. Microbiol. Biotechnol.* **1999**; 51:486-490.

[143] **Kratzer R., Pukl M., Egger S., Nidetzky B.** Whole-cell bioreduction of aromatic α-keto esters using *Candida tenuis* xylose reductase and *Candida boidinii* formate dehydrogenase co-expressed in *Escherichia coli*. *Microb. Cell. Fact.* **2008**; 7:1-12.

[144] **Leuchs S., Na'amnieh S., Greiner L.** Enantioselective reduction of sparingly water-soluble ketones: Continuous process and recycle of the aqueous buffer system. *Green Chem.* **2013**; 15:167-176.

[145] **Yan Z., Nie Y., Xu Y., Liu X., Xiao R.** Biocatalytic reduction of prochiral aromatic ketones to optically pure alcohols by a coupled enzyme system for cofactor regeneration. *Tetrahedron Lett.* **2011**; 52:999-1002.

[146] **Lavandera I., Oberdorfer G., Gross J., de Wildeman S., Kroutil W.** Stereocomplementary asymmetric reduction of bulky–bulky ketones by biocatalytic hydrogen transfer. *Eur. J. Org. Chem.* **2008**:2539–2543.

[147] **Kosjek B., Stampfer W., Pogorevc M., Goessler W., Faber K., Kroutil W.** Purification and characterization of a chemotolerant alcohol dehydrogenase applicable to coupled redox reactions. *Biotechnol. Bioeng.* **2004**; 86:55-62.

[148] **Yang W., Xu J.H., Pan J., Xu Y., Wang Z.L.** Efficient reduction of aromatic ketones with NADPH regeneration by using crude enzyme from *Rhodotorula* cells and mannitol as cosubstrate. *Biochem. Eng. J.* **2008**; 42:1-5.

[149] **Gröger H., Hummel W., Buchholz S., Drauz K., van Nguyen T., Rollmann C., Huesken H., Abokitse K.** Practical asymmetric enzymatic reduction through discovery of a dehydrogenase-compatible biphasic reaction media. *Org. Lett.* **2003**; 5:173-176.

[150] **Choi Y.H., Choi H.J., Kim D., Uhm K.N., Kim H.K.** Asymmetric synthesis of (*S*)-3-chloro-1-phenyl-1-propanol using *Saccharomyces cerevisiae* reductase with high enantioselectivity. *Appl. Microbiol. Biotechnol.* **2010**; 87:185-193.

[151] **Ma Y.H., Lv D.Q., Zhou S., Lai D.Y., Chen Z.M.** Characterization of an aldo–keto reductase from *Thermotoga maritima* with high thermostability and a broad substrate spectrum. *Biotechnol. Lett.* **2013**; 35:757–762.

[152] **Hummel W.** Reduction of acetophenone to *R*-(+)-phenylethanol by a new alcohol dehydrogenase from *Lactobacillus kefir*. *Appl. Microbiol. Biotechnol.* **1990**; 34:15-19.

[153] **Nowill R.W., Patel T.J., Beasley D.L., Alvarez J.A., Jackson II I. E., Hizer T.J., Ghiviriga I., Mateer S.C., Feske B.D.** Biocatalytic strategy toward asymmetric β-hydroxy nitriles and γ-amino alcohols. *Tetrahedron Lett.* **2011**; 52:2440-2442.

[154] **Ankati H., Zhu D., Yang Y., Biehl E.R., Hua L.** Asymmetric synthesis of both antipodes of β-hydroxy nitriles and β-hydroxy carboxylic acids *via* enzymatic reduction or sequential reduction/hydrolysis. *J. Org. Chem.* **2009**; 74:1658-1662.

[155] **Kawano S., Hasegawa J., Yasohara Y.** Efficient synthesis of (*R*)-3-hydroxypentanenitrile in high enantiomeric excess by enzymatic reduction of 3-oxopentanenitrile. *Appl. Microbiol. Biotechnol.* **2014**; 98:5891–5900.

[156] **Spickermann D., Hausmann S., Degering C., Schwaneberg U., Leggewie C.** Engineering of highly selective variants of *Parvibaculum lavamentivorans* alcohol dehydrogenase. *ChemBioChem* **2014**; 15:2050-2052.

[157] **Jakoblinnert A., Rother D.** A two-step biocatalytic cascade in micro-aqueous medium: Using whole cells to obtain high concentrations of a vicinal diol. *Green Chem.* **2014**; 16:3472-3482.

[158] **Kulig J., Simon R.C., Rose C.A., Husain S.M., Häckh M., Lüdeke S., Zeitler K., Kroutil W., Pohl M., Rother D.** Stereoselective synthesis of bulky 1,2-diols with alcohol dehydrogenases. *Catal. Sci. Technol.* **2012**; 2:1580-1589.

[159] **Yan Y., Lee C.C., Liao J.C.** Enantioselective synthesis of pure (*R*,*R*)-2,3-butanediol in *Escherichia coli* with stereospecific secondary alcohol dehydrogenases. *Org. Biomol. Chem.* **2009**; 7:3914-3917.

[160] **Müller M., Katzberg M., Bertau M., Hummel W.** Highly efficient and stereoselective biosynthesis of (2*S*,5*S*)-hexanediol with a dehydrogenase from *Saccharomyces cerevisiae*. *Org. Biomol. Chem.* **2010**; 8:1540-1550.

[161] **Baer K., Kraußer M., Burda E., Hummel W., Berkessel A., Gröger H.** Sequential and modular synthesis of chiral 1,3-diols with two stereogenic centers: Access to all four stereoisomers by combination of organo- and biocatalysis. *Angew. Chem., Int. Ed.* **2009**; 48:9355-9358.

[162] **Machielsen R., Leferink N.G.H., Hendriks A., Brouns .SJ.J., Hennemann H.G., Daußmann T., van der Oost J.** Laboratory evolution of *Pyrococcus furiosus* alcohol dehydrogenase to improve the production of (2*S*,5*S*)-hexanediol at moderate temperatures. *Extremophiles* **2008**; 12:587-594.

[163] **Edegger K., Stampfer W., Seisser B., Faber K., Mayer S.F., Oehrlein R., Hafner A., Kroutil W.** Regio- and stereoselective reduction of diketones and oxidation of diols by biocatalytic hydrogen transfer. *Eur. J. Org. Chem.* **2006**:1904-1909.

[164] **Yamada-Onodera K., Kawahara N., Tani Y., Yamamoto H.** Synthesis of optically active diols by Escherichia coli transformant cells that express the glycerol dehydrogenase gene of *Hansenula polymorpha* DL-1. *Eng. Life Sci.* **2004**; 4:413-417.

[165] **Kihumbu D., Stillger T., Hummel W., Liese A.** Enzymatic synthesis of all stereoisomers of 1-phenylpropane-1,2-diol. *Tetrahedron: Asymmetry* **2002**; 13:1069-1072.

[166] **Kalaitzakis D., Smonou I.** A two-step, one-pot enzymatic synthesis of 2-substituted 1,3-Diols. *J. Org. Chem.* **2010**; 75:8658-8661.

[167] **Kalaitzakis D., Smonou I.** Highly diastereoselective synthesis of 2-substituted-1,3-diols catalyzed by ketoreductases. *Tetrahedron* **2010**; 66:9431-9439.

[168] **Kalaitzakis D., Rozzell J.D., Smonou I., Kambourakis S.** Synthesis of valuable chiral intermediates by isolated ketoreductases: Application in the synthesis of α-alkyl-β-hydroxy ketones and 1,3-diols. *Adv. Synth. Catal.* **2006**; 348:1958-1969.

[169] **Skorupa Parachin N., Carlquist M., Gorwa-Grauslund M.F.** Comparison of engineered *Saccharomyces cerevisiae* and engineered *Escherichia coli* for the production of an optically pure keto alcohol. *Appl. Microbiol. Biotechnol.* **2009**; 84:487-497.

[170] **Ema T., Moriya H., Kofukuda T., Ishida T., Maehara K., Utaka M., Sakai T.** High enantioselectivity and broad substrate specificity of a carbonyl reductase: Toward a versatile biocatalyst. *J. Org. Chem.* **2001**; 66:8682-8684.

[171] **Ema T., Sugiyama Y., Fukumoto M., Moriya H., Cui J.N., Sakai T., Utaka M.** Highly enantioselective reduction of carbonyl compounds using a reductase purified from bakers' yeast. *J. Org. Chem.* **1998**; 63:4996-5000.

[172] **Kayser M.M., Drolet M., Stewart J.D.** Application of newly available bio-reducing agents to the synthesis of chiral hydroxy-β-lactams: Model for aldose reductase selectivity. *Tetrahedron: Asymmetry* **2005**; 16:4004-4009.

[173] **Maruyama R., Nishizawa M., Itoi Y., Ito S., Inoue M.** The enzymes with benzil reductase activity conserved from bacteria to mammals. *J. Biotechnol.* **2002**; 94:157-169.

[174] **Johanson T., Katz M., Gorwa-Grauslund M.F.** Strain engineering for stereoselective bioreduction of dicarbonyl compounds by yeast reductases. *FEMS Yeast Res.* **2005**; 5:513-525.

[175] **Kalaitzakis D., Rozzell J.D., Kambourakis S., Smonou I.** Highly stereoselective reductions of α-alkyl-1,3-diketones and α-alkyl-β-keto esters catalyzed by isolated NADPH-dependent ketoreductases. *Org. Lett.* **2005**; 7:4799-4801.

[176] **Kalaitzakis D., Rozzell J.D., Kambourakis S., Smonou I.** A two-step chemoenzymatic synthesis of the natural pheromone (+)-sitophilure utilizing isolated, NADPH-dependent ketoreductases. *Eur. J. Org. Chem.* **2006**:2309-2313.

[177] *Pfizer reports fourth-quarter and full-year 2012 results: Provides 2013 financial guidance.***2012**.
http://www.pfizer.com/files/investors/presentations/q4performance_012913.pdf

[178] **Patel J.M.** Biocatalytic synthesis of atorvastatin intermediates. *J. Mol. Catal. B: Enzym.* **2009**; 61:123-128.

[179] **Fox R.J., Davis S.C., Mundorff E.C., Newman L.M., Gavrilovic V., Ma S.K., Chung L.M., Ching C., Tam S., Muley S., Grate J., Gruber J., Whitman J.C., Sheldon R.A., Huisman G.W.** Improving catalytic function by ProSAR-driven enzyme evolution. *Nat. Biotechnol.* **2007**; 25:338-344.

[180] **Wu H., Tian C., Song X., Liu C., Yang D., Jiang Z.** Methods for the regeneration of nicotinamide coenzymes. *Green Chem.* **2013**; 15:1773-1789.

[181] **Weckbecker A., Gröger H., Hummel W.** *Regeneration of nicotinamide coenzymes: Principles and applications for the synthesis of chiral compounds*. In: Biosystems Engineering I: Creating Superior Biocatalysts. Edited by: Wittmann C, Krull R. Springer-Verlag Berlin; **2010**. pp. 195-242.

[182] **Berenguer-Murcia A., Fernandez-Lafuente R.** New trends in the recycling of NAD(P)H for the design of sustainable asymmetric reductions catalyzed by dehydrogenases. *Curr. Org. Chem.* **2010**; 14:1000-1021.

[183] **Wagenknecht P.S., Penney J.M., Hembre R.T.** Transition-metal-catalyzed regeneration of nicotinamide coenzymes with hydrogen. *Organometallics* **2003**; 22:1180-1182.

[184] **Bhaduri S., Mathur P., Payra P., Sharma K.** Coupling of catalyses by carbonyl clusters and dehydrogenases: Reduction of pyruvate to L-lactate by dihydrogen. *J. Am. Chem. Soc.* **1998**; 120:12127-12128.

[185] **Nakamura K., Yamanaka R.** Light-mediated regulation of asymmetric reduction of ketones by a cyanobacterium. *Tetrahedron: Asymmetry* **2002**; 13:2529-2533.

[186] **Nakamura K., Yamanaka R.** Light mediated cofactor recycling system in biocatalytic asymmetric reduction of ketone. *Chem. Commun.* **2002**:1782-1783.

[187] **Nakamura K., Yamanaka R., Tohi K., Hamada H.** Cyanobacterium-catalyzed asymmetric reduction of ketones. *Tetrahedron Lett.* **2000**; 41:6799-6802.

[188] **Baik S.H., Kang C., Jeon I.C., Yun S.E.** Direct electrochemical regeneration of NADH from NAD$^+$ using cholesterol-modified gold amalgam electrode. *Biotechnol. Tech.* **1999**; 13:1-5.

[189] **Kim S., Lee G.Y., Lee J., Rajkumar E., Baeg J.O., Kim J.** Efficient electrochemical regeneration of nicotinamide cofactors using a cyclopentadienyl-rhodium complex on functionalized indium tin oxide electrodes. *Electrochim. Acta.* **2013**; 96:141-146.

[190] **Kohlmann C., Märkle W., Lütz S.** Electroenzymatic synthesis. *J. Mol. Catal. B: Enzym.* **2008**; 51:57–72.

[191] **Hildebrand F., Lütz S.** Electroenzymatic synthesis of chiral alcohols in an aqueous-organic two-phase system. *Tetrahedron: Asymmetry* **2007**; 18:1187-1193.

[192] **Götz K., Liese A., Ansorge-Schumacher M., Hilterhaus L.** A chemo-enzymatic route to synthesize (*S*)-γ-valerolactone from levulinic acid. *Appl. Microbiol. Biotechnol.* **2013**; 97:3865-3873.

[193] **Schroer K., Tacha E., Lütz S.** Process intensification for substrate-coupled whole cell ketone reduction by *in situ* acetone removal. *Org. Process Res. Dev.* **2007**; 11:836-841.

[194] **Schroer K., Mackfeld U., Tana I.A.W., Wandrey C., Heuser F., Bringer-Meyer S., Weckbecker A., Hummel W., Daußmann T., Pfaller R., Liese A., Lütz S.** Continuous asymmetric ketone reduction processes with recombinant *Escherichia coli*. *J. Biotechnol.* **2007**; 132:438-444.

[195] **Goldberg K., Edegger K., Kroutil W., Liese A.** Overcoming the thermodynamic limitation in asymmetric hydrogen transfer reactions catalyzed by whole cells. *Biotechnol. Bioeng.* **2006**; 95:192-198.

[196] **Stampfer W., Kosjek B., Kroutil W., Faber K.** On the organic solvent and thermostability of the biocatalytic redox system of *Rhodococcus ruber* DSM 44541. *Biotechnol. Bioeng.* **2003**; 81:865-869.

[197] **Stampfer W., Kosjek B., Faber K., Kroutil W.** Biocatalytic asymmetric hydrogen transfer employing *Rhodococcus ruber* DSM 44541. *J. Org. Chem.* **2003**; 68:402-406.

[198] **Stampfer W., Edegger K., Kosjek B., Faber K., Kroutil W.** Simple biocatalytic access to enantiopure (*S*)-1-heteroarylethanols employing a microbial hydrogen transfer reaction. *Adv. Synth. Catal.* **2004**; 346:57-62.

[199] **Matsuyama A., Yamamoto H., Kobayashi Y.** Practical application of recombinant whole-cell biocatalysts for the manufacturing of pharmaceutical intermediates such as chiral alcohols. *Org. Process Res. Dev.* **2002**; 6:558-561.

[200] **Mädje K., Schmölzer K., Nidetzky B., Kratzer R.** Host cell and expression engineering for development of an *E. coli* ketoreductase catalyst: Enhancement of formate dehydrogenase activity for regeneration of NADH. *Microb. Cell Fact.* **2012**; 11:1-8.

[201] **Kratzer R., Pukl M., Egger S., Vogl M., Brecker L., Nidetzky B.** Enzyme identification and development of a whole-cell biotransformation for asymmetric reduction of *o*-chloroacetophenone. *Biotechnol. Bioeng.* **2011**; 108:797-803.

[202] **Bräutigam S., Bringer-Meyer S., Weuster-Botz D.** Asymmetric whole cell biotransformations in biphasic ionic liquid/water-systems by use of recombinant *Escherichia coli* with intracellular cofactor regeneration. *Tetrahedron: Asymmetry* **2007**; 18:1883-1887.

[203] **Ernst M., Kaup B., Müller M., Bringer-Meyer S., Sahm H.** Enantioselective reduction of carbonyl compounds by whole-cell biotransformation, combining a formate dehydrogenase and a (*R*)-specific alcohol dehydrogenase. *Appl. Microbiol. Biotechnol.* **2005**; 66:629-634.

[204] **Johannes T.W., Woodyer R.D., Zhao H.M.** Efficient regeneration of NADPH using an engineered phosphite dehydrogenase. *Biotechnol. Bioeng.* **2007**; 96:18-26.

[205] **Zhang J., Witholt B., Li Z.** Efficient NADPH recycling in enantioselective bioreduction of a ketone with permeabilized cells of a microorganism containing a ketoreductase and a glucose 6-phosphate dehydrogenase. *Adv. Synth. Catal.* **2006**; 348:429-433.

[206] **Zhang W., O'Connor K., Wang D.I.C., Li Z.** Bioreduction with efficient recycling of NADPH by coupled permeabilized microorganisms. *Appl. Environ. Microbiol.* **2009**; 75:687-694.

[207] **Jin J.Z., Li H., Zhang J.** Improved synthesis of (*S*)-1-phenyl-2-propanol in high concentration with coupled whole cells of *Rhodococcus erythropolis* and *Bacillus subtilis* on preparative scale. *Appl. Microbiol. Biotechnol.* **2010**; 162:2075-2086.

[208] **Park H.J., Jung J., Choi H., Uhm K.N., Kim H.K.** Enantioselective bioconversion using Escherichia coli cells expressing *Saccharomyces cerevisiae* reductase and *Bacillus subtilis* glucose dehydrogenase. *J. Microbiol. Biotechnol.* **2010**; 20:1300-1306.

[209] **Ye Q., Cao H., Yan M., Cao F., Zhang Y., Li X., Xu L., Chen Y., Xiong J., Ouyang P., Ying H.** Construction and co-expression of a polycistronic plasmid encoding carbonyl reductase and glucose dehydrogenase for production of ethyl (*S*)-4-chloro-3-hydroxybutanoate. *Bioresour. Technol.* **2010**; 101:6761-6767.

[210] **Ye Q., Cao H., Zang G., Mi L., Yan M., Wang Y., Zhang Y., Li X., Li J., Xu L., Xiong J., Ouyang P., Ying H.** Biocatalytic synthesis of (*S*)-4-chloro-3-hydroxybutanoate ethyl ester using a recombinant whole-cell catalyst. *Appl. Microbiol. Biotechnol.* **2010**; 88:1277-1285.

[211] **Richter N., Neumann M., Liese A., Wohlgemuth R., Weckbecker A., Eggert T., Hummel W.** Characterization of a whole-cell catalyst co-expressing glycerol dehydrogenase and glucose dehydrogenase and its application in the synthesis of L-glyceraldehyde. *Biotechnol. Bioeng.* **2010**; 106:541-552.

[212] **Richter N., Neumann M., Liese A., Wohlgemuth C., Eggert T., Hummel W.** Characterisation of a recombinant NADP-dependent glycerol dehydrogenase from *Gluconobacter oxydans* and its application in the production of L-glyceraldehyde. *Chembiochem* **2009**; 10:1888-1896.

[213] **Kizaki N., Yasohara Y., Hasegawa J., Wada M., Kataoka M., Shimizu S.** Synthesis of optically pure ethyl (*S*)-4-chloro-3-hydroxybutanoate by *Escherichia coli* transformant cells coexpressing the carbonyl reductase and glucose dehydrogenase genes. *Appl. Microbiol. Biotechnol.* **2001**; 55:590-595.

[214] **Kataoka M., Ishige T., Urano N., Nakamura Y., Sakuradani E., Fukui S., Kita S., Sakamoto K., Shimizu S.** Cloning and expression of the L-1-amino-2-propanol dehydrogenase gene from *Rhodococcus erythropolis*, and its application to double chiral compound production. *Appl. Microbiol. Biotechnol.* **2008**; 80:597-604.

[215] **Goldberg K., Schroer K., Lütz S., Liese A.** Biocatalytic ketone reduction: A powerful tool for the production of chiral alcohols - part II: Whole-cell reductions. *Appl. Microbiol. Biotechnol.* **2007**; 76:249-255.

[216] **Venkataraman S., Roy R.K., Chadha A.** Asymmetric reduction of alkyl-3-oxobutanoates by *Candida parapsilosis* ATCC 7330: Insights into solvent and substrate optimisation of the biocatalytic reaction. *Appl. Biochem. Biotechnol.* **2013**; 171:756-770.

[217] **Csuk R., Glaenzer B.I.** Baker's yeast mediated transformations in organic chemistry. *Chem. Rev.* **1991**; 91:49-97.

[218] **Patel R.N., Goswami A., Chu L., Donovan M.J., Nanduri V., Goldberg S., Johnston R., Siva P.J., Nielsen B., Fan J., He W.X., Shi Z., Wang K.W., Eiring R., Cazzulino D., Singh A., Müller R.** Enantioselective microbial reduction of substituted acetophenones. *Tetrahedron: Asymmetry* **2004**; 15:1247-1258.

[219] **Patel R.N., McNamee C.G., Banerjee A., Howell J.M., Robison R.S., Szarka L.J.** Stereoselective reduction of *β*-keto esters by Geotrichum candidum. *Enzyme Microb. Technol.* **1992**; 14:731-738.

[220] **Egri G., Kolbert A., Bálint J., Fogassy E., Novák L., Poppe L.** Baker's yeast mediated stereoselective biotransformation of 1-acetoxy-3-aryloxypropan-2-ones. *Tetrahedron: Asymmetry* **1998**; 9:271-283.

[221] **Carballeira J.D., Quezada M.A., Hoyos P., Simeó Y., Hernaiz M.J., Alcantara A.R., Sinisterra J.V.** Microbial cells as catalysts for stereoselective red-ox reactions. *Biotechnol. Adv.* **2009**; 27:686-714.

[222] **Fogagnolo M., Giovannini P.P., Guerrini A., Medici A., Pedrini P., Colombi N.** Homochiral (*R*)- and (*S*)-1-heteroaryl- and 1-aryl-2-propanols *via* microbial redox. *Tetrahedron: Asymmetry* **1998**; 9:2317-2327.

[223] **Jeong M., Lee Y.M., Hong S.H., Park S.Y., Yoo I.K., Han M.J.** Optimization of enantioselective synthesis of methyl (*R*)-2-chloromandelate by whole cells of *Saccharomyces cerevisiae*. *Biotechnol. Lett.* **2010**; 32:1529-1531.

[224] **Kaliaperumal T., Kumar S., Gummadi S.N., Chadha A.** Asymmetric synthesis of (*S*)-ethyl-4-chloro-3-hydroxybutanoate using *Candida parapsilosis* ATCC 7330. *J. Ind. Microbiol. Biot.* **2010**; 37:159-165.

[225] **Katzberg M., Wechler K., Müller M., Dünkelmann P., Stohrer J., Hummel W., Bertau M.** Biocatalytical production of (5*S*)-hydroxy-2-hexanone. *Org Biomol Chem* **2009**; 7:304-314.

[226] **Haberland J., Hummel W., Daußmann T., Liese A.** New continuous production process for enantiopure (2*R*,5*R*)-hexanediol. *Org. Process Res. Dev.* **2002**; 6:458-462.

[227] **Nanduri V.B., Hanson R.L., Goswami A., Wasylyk J.M., LaPorte T.L., Katipally K., Chung H.J., Patel R.N.** Biochemical approaches to the synthesis of ethyl 5-(*S*)-hydroxyhexanoate and 5-(*S*)-hydroxyhexanenitrile. *Enzyme Microb. Technol.* **2001**; 28:632-636.

[228] **Kayser M.M., Mihovilovic M.D., Kearns J., Feicht A., Stewart J.D.** Baker's yeast-mediated reductions of α-keto esters and an α-keto-β-lactam: Two routes to the paclitaxel side chain. *J. Org. Chem.* **1999**; 64:6603-6608.

[229] **Lieser J.K.** A Simple Synthesis of (*S,S*)-2,5-hexanediol. *Synth. Commun.* **1983**; 13:765-767.

[230] **Jörg G., Hémery T., Bertau M.** Effects of cell stress protectant glutathione on the whole-cell biotransformation of ethyl 2-chloro-acetoacetate with *Saccharomyces cerevisiae*. *Biocatal. Biotransform.* **2005**; 23:9-17.

[231] **Yang Y., Drolet M., Kayser M.M.** The dynamic kinetic resolution of 3-oxo-4-phenyl-β-lactam by recombinant *E. coli* overexpressing yeast reductase Ara1p. *Tetrahedron: Asymmetry* **2005**; 16:2748-2753.

[232] **Walton A.Z., Stewart J.D.** Understanding and improving NADPH-dependent reactions by nongrowing *Escherichia coli* cells. *Biotechnol. Prog.* **2004**; 20:403-411.

[233] **Menzel A., Werner H., Altenbuchner J., Gröger H.** From enzymes to "designer bugs" in reductive amination: A new process for the synthesis of L-*tert*-leucine using a whole cell-catalyst. *Eng. Life Sci.* **2004**; 4:573-576.

[234] **Tufvesson P., Lima-Ramos J., Nordblad M., Woodley J.M.** Guidelines and cost analysis for catalyst production in biocatalytic processes. *Org. Process Res. Dev.* **2011**; 15:266-274.

[235] **Gröger H., May O., Werner H., Menzel A., Altenbuchner J.** A "second-generation process" for the synthesis of L-neopentylglycine: Asymmetric reductive amination using a recombinant whole cell catalyst. *Org. Process Res. Dev.* **2006**; 10:666-669.

[236] **Weckbecker A., Hummel W.** Glucose dehydrogenase for the regeneration of NADPH and NADH. *Adv. Biochem. Engin. / Biotechnol.* **2005**; 17:225-237.

[237] **Engelking H., Pfaller R., Wich G., Weuster-Botz D.** Reaction engineering studies on β-ketoester reductions with whole cells of recombinant *Saccharomyces cerevisiae*. *Enzyme Microb. Technol.* **2006**; 38:536-544.

[238] **Kratzer R., Egger S., Nidetzky B.** Integration of enzyme, strain and reaction engineering to overcome limitations of baker's yeast in the asymmetric reduction of α-keto esters. *Biotechnol. Bioeng.* **2008**; 101:1094-1101.

[239] **Katz M., Frejd T., Hahn-Hägerdal B., Gorwa-Grauslund M.F.** Efficient anaerobic whole cell stereoselective bioreduction with recombinant *Saccharomyces cerevisiae*. *Biotechnol. Bioeng.* **2003**; 84:573-582.

[240] **Johanson T., Carlquist M., Olsson C., Rudolf A., Frejd T., Gorwa-Grauslund M.F.** Reaction and strain engineering for improved stereo-selective whole-cell reduction of a bicyclic diketone. *Appl. Microbiol. Biotechnol.* **2008**; 77:1111-1118.

[241] **Turner N.J.** Directed evolution drives the next generation of biocatalysts. *Nat. Chem. Biol.* **2009**; 5:568-574.

[242] **Schmid A., Dordick J.S., Hauer B., Kiener A., Wubbolts M., Witholt B.** Industrial biocatalysis today and tomorrow. *Nature* **2001**; 409:258-268.

[243] **Davids T., Schmidt M., Böttcher D., Bornscheuer U.T.** Strategies for the discovery and engineering of enzymes for biocatalysis. *Curr. Opin. Chem. Biol.* **2013**; 17:215-220.

[244] **Uchiyama T., Watanabe K.** The SIGEX scheme: High throughput screening of environmental metagenomes for the isolation of novel catabolic genes. *Biotechnol. Genet. Eng. Rev.* **2007**; 24:107-116.

[245] **Handelsman J.** Metagenomics: Application of genomics to uncultured microorganisms. *Microbiol. Mol. Biol. Rev.* **2004**; 68:669-686.

[246] **Knietsch A., Waschkowitz T., Bowien S., Henne A., Daniel R.** Metagenomes of complex microbial consortia derived from different soils as sources for novel genes conferring formation of carbonyls from short-chain polyols on *Escherichia coli*. *J. Mol. Microbiol. Biotechnol.* **2003**; 5:46–56.

[247] **Valencia A.** Automatic annotation of protein function. *Curr. Opin. Struct. Biol.* **2005**; 15:267-274.

[248] **Wackett L.P.** Novel biocatalysis by database mining. *Curr. Opin. Biotechnol.* **2004**; 15:280-284.

[249] **Labesse G.** MulBlast 1.0: A multiple alignment of BLAST output to boost protein sequence similarity analysis. *Comput. Appl. Biosci.* **1996**; 12:463-467.

[250] **Chen Y., Chen C., Wu X.** Dicarbonyl reduction by single enzyme for the preparation of chiral diols. *Chem. Soc. Rev.* **2012**; 41:1742-1753.

[251] **Hoyos P., Sinisterra J.V., Molinari F., Alcántara A.R., De María P.D.** Biocatalytic strategies for the asymmetric synthesis of α-hydroxy ketones. *Accounts Chem. Res.* **2010**; 43:288-299.

[252] **Adam W., Lazarus M., Saha-Möller C.R., Schreier P.** Biocatalytic synthesis of optically active α-oxyfunctionalized carbonyl compounds. *Accounts Chem. Res.* **1999**; 32:837-845.

[253] **Evans D.A., Connell B.T.** Synthesis of the antifungal macrolide antibiotic (+)-roxaticin. *J. Am. Chem. Soc.* **2003**; 125:10899-10905.

[254] **Eustache F., Dalko P.I., Cossy J.** Enantioselective monoreduction of 2-alkyl 1,3-diketones using chiral ruthenium catalysts. Synthesis of the C14-C25 fragment of bafilomycin A_1. *Tetrahedron Lett.* **2003**; 44:8823-8826.

[255] **Scheid G., Ruijter E., Konarzycka-Bessler M., Bornscheuer U.T., Wessjohann L.A.** Synthesis and resolution of a key building block for epothilones: a comparison of asymmetric synthesis, chemical and enzymatic resolution. *Tetrahedron: Asymmetry* **2004**; 15:2861-2869.

[256] **Andrus M.B., Hicken E.J., Stephens J.C., Bedke D.K.** Total synthesis of the hydroxyketone Kurasoin A using asymmetric phase-transfer alkylation. *J. Org. Chem.* **2006**; 71:8651-8654.

[257] **Christiansen M.A., Butler A.W., Hill A.R., Andrus M.B.** Synthesis of Kurasoin B using phase-transfer-catalyzed acylimidazole alkylation. *Synlett* **2009**:653-657

[258] **Ray A.M., Swift I.P., Moreira J.A., Millar J.G., Hanks L.M.** (*R*)-3-Hydroxyhexan-2-one is a major pheromone component of *Anelaphus inflaticollis* (Coleoptera: Cerambycidae). *Environ. Entomol.* **2009**; 38:1462-1466.

[259] **Schröder F., Fettköther R., Noldt U., Dettner K., König W.A., Francke W.** Synthesis of (3*R*)-3-hydroxy-2-hexanone, (2*R*,3*R*)-2,3-hexanediol and (2*S*,3*R*)-2,3-hexanediol, the male sex pheromone of *Hylotrupes bajulus* and *Pyrrhidium sanguineum* (Cerambycidae). *Liebigs Ann. Chem.* **1994**:1211-1218.

[260] **Bel-Rhlid R., Fauve A., Veschambre H.** Synthesis of the pheromone components of the grape borer *Xylotrechus pyrrhoderus* by microbiological reduction of an α-diketone. *J. Org. Chem.* **1989**; 54:3221-3223.

[261] **Fang Q.K., Han Z., Grover P., Kessler D., Senanayake C.H., Wald S.A.** Rapid access to enantiopure bupropion and its major metabolite by stereospecific nucleophilic substitution on an α-ketotriflate. *Tetrahedron: Asymmetry* **2000**; 11:3659-3663.

[262] **Banwell M.G., Blakey S., Harfoot G., Longmore R.W.** *cis*-1,2-dihydrocatechols in chemical synthesis: First synthesis of L-ascorbic acid (vitamin C) from a non-carbohydrate source. *Aust. J. Chem.* **1999**; 52:137-142.

[263] **Gavrilov K.N., Zheglov S.V., Gavrilova M.N., Chuchelkin I.V., Groshkin N.N., Rastorguev E.A., Davankov V.A.** Phosphoramidites based on phenyl-substituted 1,2-diols as ligands in palladium-catalyzed asymmetric allylations: The contribution of steric demand and chiral centers to the enantioselectivity. *Tetrahedron Lett.* **2011**; 52:5706-5710.

[264] **Bhowmick K.C., Joshi N.N.** Syntheses and applications of C_2-symmetric chiral diols. *Tetrahedron: Asymmetry* **2006**; 17:1901-1929.

[265] **Frost C.G., Williams J.M.J.** Enantiomerically pure acetals as ligands for asymmetric catalysis. *Synlett* **1994**; 7:551-552.

[266] **MacNeil P.A., Roberts N.K., Bosnich B.** Asymmetric synthesis: Asymmetric catalytic hydrogenation using chiral chelating six-membered ring diphosphines. *J. Am. Chem. Soc.* **1981**; 103:2273-2280.

[267] **Fryzuk M.D., Bosnich B.** Asymmetric synthesis: Production of optically-active amino-acids by catalytic-hydrogenation. *J. Am. Chem. Soc.* **1977**; 99:6262-6267.

[268] **Kadyrov R., Koenigs R.M., Brinkmann C., Voigtlaender D., Rueping M.** Efficient enantioselective synthesis of optically active diols by asymmetric hydrogenation with modular chiral metal catalysts. *Angew. Chem., Int. Ed.* **2009**; 48:7556-7559.

[269] **Roche C., Labeeuw O., Haddad M., Ayad T., Genet J.P., Ratovelomanana-Vidal V., Phansavath P.** Synthesis of anti-1,3-diols through $RuCl_3$/PPh_3-mediated hydrogenation of β-hydroxy ketones: An alternative to organoboron reagents. *Eur. J. Org. Chem.* **2009**:3977-3986.

[270] **Koike T., Murata K., Ikariya T.** Stereoselective synthesis of optically active α-hydroxy ketones and *anti*-1,2-diols *via* asymmetric transfer hydrogenation of unsymmetrically substituted 1,2-diketones. *Org. Lett.* **2000**; 2:3833-3836.

[271] **Fan Q.H., Yeung C.H., Chan A.S.C.** An improved synthesis of chiral diols *via* the asymmetric catalytic hydrogenation of prochiral diones. *Tetrahedron: Asymmetry* **1997**; 8:4041-4045.

[272] **Husain S.M., Stillger T., Dünkelmann P., Lödige M., Walter L., Breitling E., Pohl M., Bürchner M., Krossing I., Müller M., Romano D., Molinari F.** Stereoselective reduction of 2-hydroxy ketones towards syn- and *anti*-1,2-diols. *Adv. Synth. Catal.* **2011**; 353:2359-2362.

[273] **Bartoli G., Bosco M., Marcantoni E., Massaccesi M., Rinaldi S., Sambri L.** A highly diastereoselective TiCl$_4$-mediated reduction of *β*-hydroxy ketones with BH$_3$·py: A very efficient and general synthesis of *syn*-1,3-diols. *Eur. J. Org. Chem.* **2001**; Eur. J. Org. Chem.:4679-4684.

[274] **Quallich G.J., Keavey K.N., Woodall T.M.** Enantioselective synthesis of *C*$_2$-symmetrical diols. *Tetrahedron Lett.* **1995**; 36:4729-4732.

[275] **Evans D.A., Hoveyda A.H.** Reduction of *β*-hydroxy ketones with catecholborane. A stereoselective approach to the synthesis of *syn* 1,3-diols. *J. Org. Chem.* **1990**; 55:5190-5192.

[276] **Minato D., Arimoto H., Nagasue Y., Demizu Y., Onomura O.** Asymmetric electrochemical oxidation of 1,2-diols, aminoalcohols, and aminoaldehydes in the presence of chiral copper catalyst. *Tetrahedron* **2008**; 64:6675-6683.

[277] **Kawashima M., Hirayama A.** Direct optical resolution of vicinal diols and an *α*-hydroxy oxime with a vicinal diamine. *Chem. Lett.* **1991**:763-766.

[278] **Muthupandi P., Alamsetti S.K., Sekar G.** Chiral iron complex catalyzed enantioselective oxidation of racemic benzoins. *Chem. Commun.* **2009**:3288-3290.

[279] **Kuwano R., Sawamura M., Shirai J., Takahashi M., Ito Y.** Asymmetric hydrosilylation of symmetrical diketones catalyzed by a rhodium complex with trans-chelating chiral diphosphine EtTRAP. *Tetrahedron Lett.* **1995**; 36:5239-5242.

[280] **Enders D., Kallfass U.** An efficient nucleophilic carbene catalyst for the asymmetric benzoin condensation. *Angew. Chem., Int. Ed.* **2002**; 41:1743-1745.

[281] **Mei Y., Dissanayake P., Allen M.J.** A new class of ligands for aqueous, lanthanide-catalyzed, enantioselective Mukaiyama aldol reactions. *J. Am. Chem. Soc.* **2010**; 132:12871-12873.

[282] **Davis F.A., Chen B.C.** Asymmetric hydroxylation of enolates with *N*-Suifonyloxaziridines. *Chsm. Rev.* **1992**; 92:919-934.

[283] **Gibson D.T., Parales R.E.** Aromatic hydrocarbon dioxygenases in environmental biotechnology. *Curr. Opin. Biotechnol.* **2000**; 11:236–243.

[284] **Zhao L., Han B., Huang Z., Miller M., Huang H., Malashock D.S., Zhu Z., Milan A., Robertson D.E., Weiner D.P., Burk M.J.** Epoxide hydrolase-catalyzed enantioselective synthesis of chiral 1,2-diols via desymmetrization of *meso*-epoxides. *J. Am. Chem. Soc.* **2004**; 126:11156-11157.

[285] **Zeng A.P., Sabra W.** Microbial production of diols as platform chemicals: Recent progresses. *Curr. Opin. Biotechnol.* **2011**; 22:749–757.

[286] **Bertau M., Bürli M.** Enantioselective microbial reduction with baker's yeast on an industrial scale. *Chimia* **2000**; 54:503-507.

[287] **Short R.P., Kennedy R.M., Masamune S.** An improved synthesis of (-)-(2*R*,5*R*)-2,5-dimethylpyrrolidine. *J. Org. Chem.* **1989**; 54:1755-1756.

[288] **Noyori R.** Asymmetric catalysis: Science and opportunities (Nobel lecture). *Angew. Chem.-Int. Edit.* **2002**; 41:2008-2022.

[289] **Díez E., Fernández R., Marqués-López E., Martín-Zamora E., Lassaletta J.M.** Asymmetric synthesis of *trans*-3-amino-4-alkylazetidin-2-ones from chiral *N,N*-dialkylhydrazones. *Org. Lett.* **2004**; 6:2749-2752.

[290] **Cowart M., Pratt J.K., Stewart A.O., Bennani Y.L., Esbenshade T.A., Hancock A.A.** A new class of potent non-imidazole H$_3$ antagonists: 2-Aminoethylbenzofurans. *Bioorg. Med. Chem. Lett.* **2004**; 14:689-693.

[291] **Takada H., Metzner P., Philouze C.** First chiral selenium ylides used for asymmetric conversion of aldehydes into epoxides. *Chem. Commun.* **2001**:2350-2351.

[292] **Julienne K., Metzner P., Henryon V., Greiner A.** A simple C_2 symmetrical sulfide for a one-pot asymmetric conversion of aldehydes into oxiranes. *J. Org. Chem.* **1998**; 63:4532-4534.

[293] **Ahrens H., Paetow M., Hoppe D.** Stereoselective generation of 1,3-dioxy-substituted and 1,4-dioxy-substituted carbanions by sparteine-assisted deprotonation of chiral precursors: Substrate or reagent control in the synthesis of α,γ-diols and α,δ-diols. *Tetrahedron Lett.* **1992**; 33:5327-5330.

[294] **Kim M.J., Lee I.S.** Combined chemical and enzymatic synthesis of (*S,S*)-2,5-dimethylpyrrolidine. *Synlett* **1993**; 10:767-768.

[295] **Al-Masum M., Kumaraswamy G., Livinghouse T.** A new synthetic route to *P*-chiral phosphine-boranes of high enantiopurity via stereocontrolled Pd(0)-Cu(I) cocatalyzed aromatic phosphorylation. *J. Org. Chem.* **2000**; 65:4776-4778.

[296] **Burk M.J., Feaster J.E., Harlow R.L.** New chiral phospholanes: Synthesis, characterization, and use in asymmetric hydrogenation reactions. *Tetrahedron: Asymmetry* **1991**; 2:569-592.

[297] **Lake F., Moberg C.** Ti-mediated addition of diethylzinc to benzaldehyde. The effect of chiral additives. *Tetrahedron: Asymmetry* **2001**; 12:755-760.

[298] **Fehring V., Selke R.** Highly enantioselective complex-catalyzed reduction of ketones: Now with purely aliphatic derivatives too. *Angew. Chem. Int. Ed.* **1998**; 37:1827-1830.

[299] **Brunel J.M., Faure B.** Enantioselective palladium catalyzed allylic substitution with a new phosphite ligand issued from (2*S*,5*S*)-hexanediol. *J. Mol. Catal. A: Chem.* **2004**; 212:61-64.

[300] **Noyori R., Ohkuma T., Kitamura M., Takaya H., Sayo N., Kumobayashi H., Akutagawa S.** Asymmetric hydrogenation of β-keto carboxylic esters: A practical, purely chemical access to β-hydroxy esters in high enantiomeric purity. *J. Am. Chem. Soc.* **1987**; 109:5856-5858.

[301] **Burk M.J., Feaster J.E., Harlow R.L.** New electron-rich chiral phosphines for asymmetric catalysis. *Organometallics* **1990**; 9:2653-2655.

[302] **Nagai H., Morimoto T., Achiwa K.** Facile enzymatic synthesis of optically active 2,5-hexanediol derivatives and its application to the preparation of optically pure cyclic sulfate for chiral ligands. *Synlett* **1994**:289-290.

[303] **Hummel W., Riebel B.** *Alcohol dehydrogenase and its use in the enzymatic production of chiral hydroxy-compounds*. **1997**. EP0796914 A2

[304] **Schroer K., Lütz S.** A continuously operated bimembrane reactor process for the biocatalytic production of (2*R*,5*R*)-hexanediol. *Org. Process Res. Dev.* **2009**; 13:1202-1205.

[305] **Giaever G., Chu A.M., Ni L., Connelly C., Riles L., Véronneau S., Dow S., Lucau-Danila A., Anderson K., André B., Arkin A.P., Astromoff A., El Bakkoury M., Bangham R., Benito R., Brachat S., Campanaro S., Curtiss M., Davis K., Deutschbauer A., Entian K.D., Flaherty P., Foury F., Garfinkel D.J., Gerstein M., Gotte D., Güldener U., Hegemann J.H., Hempel S., Herman Z., Jaramillo D.F., Kelly D.E., Kelly S.L., Kötter P., LaBonte D., Lamb D.C., Lan N., Liang H., Liao H., Liu L., Luo C.Y., Lussier M., Mao R., Menard P., Ooi S.L., Revuelta J.L., Roberts C.J., Rose M., Ross-Macdonald P., Scherens B., Schimmack G., Shafer B.,**

Shoemaker D.D., Sookhai-Mahadeo S., Storms R.K., Strathern J.N., Valle G., Voet M., Volckaert G., Wang C.Y., Ward T.R., Wilhelmy J., Winzeler E.A., Yang Y., Yen G., Youngman E., Yu K., Bussey H., Boeke J.D., Snyder M., Philippsen P., Davis R.W., Johnston M. Functional profiling of the *Saccharomyces cerevisiae* genome. *Nature* **2002**; 418:387-391.

[306] **Martzen M.R., McCraith S.M., Spinelli S.L., Torres F.M., Fields S., Grayhack E.J., Phizicky E.M. A** biochemical genomics approach for identifying genes by the activity of their products. *Science* **1999**; 286:1153-1155.

[307] **Katz M., Hahn-Hägerdal B., Gorwa-Grauslund M.F.** Screening of two complementary collections of *Saccharomyces cerevisiae* to identify enzymes involved in stereo-selective reductions of specific carbonyl compounds: An alternative to protein purification. *Enzyme Microb. Technol.* **2003**; 33:163-172.

[308] **Sybesma W.F.H., Straathof A.J.J., Jongejan J.A., Pronk J.T., Heijnen J.J.** Reductions of 3-oxo esters by baker's yeast: Current status. *Biocatal. Biotransform.* **1998**; 16:95-134.

[309] **Perrone M.G., Santandrea E., Scilimati A., Syldatk C.** Stereoselective prostereogenic 3-oxo ester reduction mediated by a novel yeast alcohol dehydrogenase derived from Kluyveromyces marxianus CBS 6556. *Adv. Synth. Catal.* **2007**; 349:1111-1118.

[310] **Soni P., Kansal H., Banerjee U.C.** Purification and characterization of an enantioselective carbonyl reductase from *Candida viswanathii* MTCC 5158. *Process Biochem.* **2007**; 42:1632-1640.

[311] **Chen C.N., Porubleva L., Shearer G., Svrakic M., Holden L.G., Dover J.L., Johnston M., Chitnis P.R., Kohl D.H.** Associating protein activities with their genes: Rapid identification of a gene encoding a methylglyoxal reductase in the yeast *Saccharomyces cerevisiae*. *Yeast* **2003**; 20:545-554.

[312] **Goffeau A., Barrell B.G., Bussey H., Davis R.W., Dujon B., Feldmann H., Galibert F., Hoheisel J.D., Jacq C., Johnston M., Louis E.J., Mewes H.W., Murakami Y., Philippsen P., Tettelin H., Oliver S.G.** Life with 6000 genes. *Science* **1996**; 274:546-567.

[313] **Stewart J.D.** *Genomes as resources for biocatalysis*. In: Advances in Applied Microbiology. Edited by: Laskin AI, Bennett JW, Gadd GM. Academic Press; **2006**. pp. 31-52.

[314] **Stewart J.D., Rodriguez S., Kayser M.M.** *Cloning, structure, and activity of ketone reductases from baker's yeast*. In: Enzyme technology for pharmaceutical and biotechnological applications. Edited by: Kirst HA, Yeh WK. Marcel Dekker New York; **2001**. pp. 175-207.

[315] **Baneyx F.** Recombinant protein expression in *Escherichia coli*. *Curr. Opin. Biotechnol.* **1999**; 10:411-421.

[316] **Thielges M.C., Chung J.K., Axup J.Y., Fayer M.D.** Influence of histidine tag attachment on picosecond protein dynamics. *Biochemistry* **2011**; 50:5799-5805.

[317] **Freydank A.C., Brandt W., Dräger B.** Protein structure modeling indicates hexahistidine-tag interference with enzyme activity. *Proteins* **2008**; 72:173-183.

[318] **Wu J., Filutowicz M.** Hexahistidine (His$_6$)-tag dependent protein dimerization: A cautionary tale. *Acta Biochim. Pol.* **1999**; 46:591-599.

[319] **González E., Fernández M.R., Marco D., Calam E., Sumoy L., Parés X., Dequin S., Biosca J.A.** Role of *Saccharomyces cerevisiae* oxidoreductases Bdh1p and Ara1p in the metabolism of acetoin and 2,3-butanediol. *Appl. Environ. Microbiol.* **2010**; 76:670-679.

[320] **Bell P.A.** *E.coli expression systems*. In: Molecular biology problem solver: A laboratory guide. Edited by: Gerstein AS. New York, USA: John Wiley & Sons, Inc.; **2001**. pp. 461-490.

[321] **Sahdev S., Khattar S.K., Saini K.S.** Production of active eukaryotic proteins through bacterial expression systems: A review of the existing biotechnology strategies. *Mol. Cell Biochem.* **2008**; 307:249-264.

[322] **Abokitse K.** Biochemische und molekularbiologische Charakterisierung von Alkoholdehydrogenasen und einer Oxygenase aus *Rhodococcus* Spezies: Doktorarbeit Mathematisch-Naturwissenschaftlichen Fakultät, Heinrich-Heine-Universität Düsseldorf; **2004**.

[323] **Chang A.C., Cohen S.N.** Construction and characterization of amplifiable multicopy DNA cloning vehicles derived from the P15A cryptic miniplasmid. *J. Bacteriol.* **1978**; 134:1141-1156.

[324] **Betenbaugh M.J., Beaty C., Dhurjati P.** Effects of plasmid amplification and recombinant gene expression on the growth kinetics of recombinant *E. coli*. *Biotechnol. Bioeng.* **1989**; 33:1425-1436.

[325] **Camps M.** Modulation of ColE1-like plasmid replication for recombinant gene expression. *Recent Pat. DNA Gene Seq.* **2010**; 4:58-73.

[326] **Hoffmann F., Rinas U.** *Stress induced by recombinant protein production in Escherichia coli*. In: Physiological stress responses in bioprocesses. Edited by: Scheper T. Berlin: Springer-Verlag; **2004**. pp. 73–92.

[327] **Sørensen H.P., Mortensen K.K.** Advanced genetic strategies for recombinant protein expression in *Escherichia coli*. *J. Biotechnol.* **2005**; 115:113-128.

[328] **Studier F.W., Moffatt B.A.** Use of bacteriophage T7 RNA polymerase to direct selective high-level expression of cloned genes. *J. Mol. Biol.* **1986**; 189:113-130.

[329] **Lee C., Kim J., Shin S.G., Hwang S.** Absolute and relative QPCR quantification of plasmid copy number in *Escherichia coli*. *J. Biotechnol.* **2006**; 123:273-280.

[330] **Lin-Chao S., Bremer H.** Effect of the bacterial growth rate on replication control of plasmid pBR322 in *Escherichia coli*. *Mol. Gen. Genet.* **1986**; 203:143-149.

[331] **Sharp P.M., Li W.H.** The codon Adaptation Index: A measure of directional synonymous codon usage bias, and its potential applications. *Nucleic Acids Res.* **1987**; 15:1281-1295.

[332] **Chen D., Texada D.E.** Low-usage codons and rare codons of *Escherichia coli*. *Gene Ther. Mol. Biol.* **2006**; 10:1-12.

[333] **Kane J.F.** Effects of rare codon clusters on high-level expression of heterologous proteins in *Escherichia coli*. *Curr. Opin. Biotechnol.* **1995**; 6:494-500.

[334] **Kurland C., Gallant J.** Errors of heterologous protein expression. *Curr. Opin. Biotechnol.* **1996**; 7:489-493.

[335] **McNulty D.E., Claffee B.A., Huddleston M.J., Porter M.L., Cavnar K.M., Kane J.F.** Mistranslational errors associated with the rare arginine codon CGG in *Escherichia coli*. *Protein Expression Purif.* **2003**; 27:365-374.

[336] **Katzberg M., Skorupa Parachin N., Gorwa-Grauslund M.F., Bertau M.** Engineering cofactor preference of ketone reducing biocatalysts: A mutagenesis study on a γ-diketone reductase from the yeast *Saccharomyces cerevisiae* serving as an example. *Int. J. Mol. Sci.* **2010**; 11:1735-1758.

[337] **Knepper A., Schleicher M., Klauke M., Weuster-Botz D.** Enhancement of the NAD(P)(H) pool in *Saccharomyces cerevisiae*. *Eng. Life Sci.* **2008**; 8:381-389.

[338] **Bruinenberg P.M.** The NADP(H) redox couple in yeast metabolism. *Antonie van Leeuwenhoek* **1986**; 52:411-429.

[339] **Loftus T.M., Hall L.V., Anderson S.L., McAlister-Henn L.** Isolation, characterization, and disruption of the yeast gene encoding cytosolic NADP-specific isocitrate dehydrogenase. *Biochemistry* **1994**; 33:9661-9667.

[340] **Grabowska D., Chelstowska A.** The *ALD6* gene product is indispensable for providing NADPH in yeast cells lacking glucose-6-phosphate dehydrogenase activity. *J. Biol. Chem.* **2003**; 278:13984-13988.

[341] **De Smet M.J., Kingma J., Witholt B.** The effect of toluene on the structure and permeability of the outer and cytoplasmic membranes of *Escherichia coli*. *BBA-Proteins Proteomics* **1978**; 506:64-80.

[342] **Weckbecker A.** Entwicklung von Ganzzellbiokatalysatoren zur Synthese von chiralen Alkoholen: Doktorarbeit Mathematisch-Naturwissenschaftlichen Fakultät, Heinrich-Heine-Universität Düsseldorf; **2005**.

[343] **Bruinenberg P.M., Vandijken J.P., Scheffers W.A.** A radiorespirometric study on the contribution of the hexose-monophosphate pathway to glucose-metabolism in *Candida utilis* CBS 621 grown in glucose-limited chemostat cultures. *J. Gen. Microbiol.* **1986**; 132:221-229.

[344] **Katz M., Sarvary I., Frejd T., Hahn-Hägerdal B., Gorwa-Grauslund M.F.** An improved stereoselective reduction of a bicyclic diketone by *Saccharomyces cerevisiae* combining process optimization and strain engineering. *Appl. Microbiol. Biotechnol.* **2002**; 59:641-648.

[345] **Deeley M.C.** Adenine deaminase and adenine utilization in *Saccharomyces cerevisiae*. *J. Bacteriol.* **1992**; 174:3102-3110.

[346] **Polak A., Grenson M.** Evidence for a common transport system for cytosine, adenine and hypoxanthine in *Saccharomyces cerevisiae* and *Candida albicans*. *Eur. J. Biochem.* **1973**; 32:276-282.

[347] **van Dijken J.P., Scheffers W.A.** Redox balances in the metabolism of sugars by yeasts. *FEMS Microbiol. Lett.* **1986**; 32:199-224.

[348] **Meitian X., Jing Y., Yawu Z., Yayan H.** Reaction characteristics of asymmetric synthesis of (2*S*,5*S*)-2,5-hexanediol catalyzed with baker's yeast number 6. *Chin. J. Chem. Eng.* **2009**; 17:493-499.

[349] **Tufvesson P., Fu W., Jensen J.S., Woodley J.M.** Process considerations for the scale-up and implementation of biocatalysis. *Food Bioprod. Process* **2010**; 88:3-11.

[350] **Chmiel H.** *Bioprozesstechnik* Spektrum Akademischer Verlag, Heidelberg:; **2011**.

[351] **Gupta A., Tschentscher A., Bobkova M.** *Method of enantioselective enzymatic reduction of keto compounds.* **2008**. EP 1926821 A1

[352] **Schäfer T., Borchert T.W., Nielsen V.S., Skagerlind P., Gibson K., Wenger K., Hatzack F., Nilsson L.D., Salmons S., Pedersen S., Heldt-Hansen H.P., Poulsen P.B., Lund H., Oxenboll K.M., Wu G.F., Pedersen H.H., Xu H.** *Industrial enzymes*. In: White Biotechnology Springer-Verlag, Berlin; **2007**. pp. 59-131.

[353] **Weiß M., Gröger H.** Practical, highly enantioselective chemoenzymatic one-pot synthesis of short-chain aliphatic β-amino acid esters. *Synlett* **2009**:1251-1254.

[354] **Burda E., Hummel W., Gröger H.** Modular chemoenzymatic one-pot syntheses in aqueous media: Combination of a palladium-catalyzed cross-coupling with an asymmetric biotransformation. *Angew. Chem., Int. Ed.* **2008**; 47:9551-9554.

[355] **Sheldon R.A.** Fundamentals of green chemistry: Efficiency in reaction design. *Chem. Soc. Rev.* **2012**; 41:1437-1451.

[356] **Sheldon R. A.** Atom utilisation, E factors and the catalytic solution. *Acad. Sci. Paris, IIc, Chimie/Chemistry* **2000**; 3:541-551.

[357] **Prelog V.** Specification of the stereospecificity of some oxido-reductases by diamond lattice sections. *Pure Appl. Chem.* **1964**; 9:119-130.

[358] **Schlieben N.H., Niefind K., Müller J., Riebel B., Hummel W., Schomburg D.** Atomic resolution structures of *R*-specific alcohol dehydrogenase from *Lactobacillus brevis* provide the structural bases of its substrate and cosubstrate specificity. *J. Mol. Biol.* **2005**; 349:801-813.

[359] **Kurina-Sanz M., Bisogno F.R., Lavandera I., Orden A.A., Gotor V.** Promiscuous substrate binding explains the enzymatic stereo- and regiocontrolled synthesis of enantiopure hydroxy ketones and diols. *Adv. Synth. Catal.* **2009**; 351:1842-1848.

[360] **Nanduri V.B., Banerjee A., Howell J.M., Brzozowski D.B., Eiring R.F., Patel R.N.** Purification of a stereospecific 2-ketoreductase from *Gluconobacter oxydans*. *J. Ind. Microbiol. Biotechnol.* **2000**; 25:171-175.

[361] **Patel R.N., Banerjee A., Nanduri V., Goswami A., Comezoglu F.T.** Enzymatic resolution of racemic secondary alcohols by lipase B from *Candida antarctica*. *J. Am. Oil Chem. Soc.* **2000**; 77:1015-1019.

[362] **Hauser M., Horn P., Tournu H., Hauser N.C., Hoheisel J.D., Brown A.J.P., Dickinson J.R.** A transcriptome analysis of isoamyl alcohol-induced filamentation in yeast reveals a novel role for Gre2p as isovaleraldehyde reductase. *FEMS Yeast Res.* **2007**; 7:84-92.

[363] **Takatsume Y., Izawa S., Inoue Y.** Methylglyoxal as a signal initiator for activation of the stress-activated protein kinase cascade in the fission yeast *Schizosaccharomyces pombe*. *J. Biol. Chem.* **2006**; 281:9086-9092.

[364] **Moon J., Liu Z.L.** Engineered NADH-dependent *GRE2* from *Saccharomyces cerevisiae* by directed enzyme evolution enhances HMF reduction using additional cofactor NADPH. *Enzyme. Microb. Technol.* **2012**; 50:115-120.

[365] **Cai C.M., Zhang T., Kumar R., Wyman C.E.** Integrated furfural production as a renewable fuel and chemical platform from lignocellulosic biomass. *J. Chem. Technol. Biotechnol.* **2014**; 89:2-10.

[366] **Heer D., Heine D., Sauer U.** Resistance of *Saccharomyces cerevisiae* to high concentrations of furfural is based on NADPH-dependent reduction by at least two oxireductases. *Appl. Environ. Microbiol.* **2009**; 75:7631-7638.

[367] **Jörnvall H.** MDR and SDR gene and protein superfamilies. *Cell. Mol. Life Sci.* **2008**; 65:3875-3878.

[368] **Persson B., Kallberg Y., Bray J.E., Bruford E., Dellaporta S.L., Favia A.D., Duarte R.G., Jörnvall H., Kavanagh K.L., Kedishvili N., Kisiela M., Maser E., Mindnich R., Orchard S., Penning T.M., Thornton J.M., Adamski J., Oppermann U.** The SDR (short-chain dehydrogenase/reductase and related enzymes) nomenclature initiative. *Chem.-Biol. Interact.* **2009**; 178:94-98.

[369] **Filling C., Berndt K.D., Benach J., Knapp S., Prozorovski T., Nordling E., Ladenstein R., Jörnvall H., Oppermann U.** Critical residues for structure and catalysis in short-chain dehydrogenases/reductases. *J. Biol. Chem.* **2002**; 277:25677-25684.

[370] **Jörnvall H., Persson B., Krook M., Atrian S., Gonzàlez-Duarte R., Jeffery J., Ghosh D.** Short-chain dehydrogenase/Reductases (SDR). *Biochemistry* **1995**; 34:6003-6013.

[371] **Kavanagh K., Jörnvall H., Persson B., Oppermann U.** The SDR superfamily: Functional and structural diversity within a family of metabolic and regulatory enzymes. *Cell. Mol. Life Sci.* **2008**; 65:3895-3906.

[372] **Hedlund J., Jörnvall H., Persson B.** Subdivision of the MDR superfamily of medium-chain dehydrogenases/reductases through iterative hidden Markov model refinement. *BMC Bioinformatics* **2010**; 11:534.

[373] **Kallberg Y., Oppermann U., Persson B.** Classification of the short-chain dehydrogenase/reductase superfamily using hidden Markov models. *FEBS J.* **2010**; 277:2375-2386.

[374] **Rossmann M.G., Moras D., Olsen K.W.** Chemical and biological evolution of a nucleotide-binding protein. *Nature* **1974**; 250:194-199.

[375] **Jin Y., Penning T.M.** Aldo-keto reductases and bioactivation/detoxication. *Annu. Rev. Pharmacol. Toxicol.* **2007**; 47:263-292.

[376] **Hayashi M., Takahashi H., Tamura K., Huang J., Yu L.H., Kawai-Yamada M., Tezuka T., Uchimiya H.** Enhanced dihydroflavonol-4-reductase activity and NAD homeostasis leading to cell death tolerance in transgenic rice. *Proc. Natl. Acad. Sci. USA* **2005**; 102:7020-7025.

[377] **Warringer J., Blomberg A.** Involvement of yeast YOL151W/*GRE2* in ergosterol metabolism. *Yeast* **2006**; 23:389-398.

[378] **Kamitori S., Iguchi A., Ohtaki A., Yamada M., Kita K.** X-ray structures of NADPH-dependent carbonyl reductase from *Sporobolomyces salmonicolor* provide insights into stereoselective reductions of carbonyl compounds. *J. Mol. Biol.* **2005**; 352:551-558.

[379] **Guo P.C., Bao Z.Z., Ma X.X., Xia Q., Li W.F.** Structural insights into the cofactor-assisted substrate recognition of yeast methylglyoxal/isovaleraldehyde reductase Gre2. *BBA-Proteins Proteomics* **2014** DOI: 10.1016/j.bbapap.2014.05.008.

Ich versichere an Eides Statt, dass die hier vorgelegte Dissertation von mir selbstständig und ohne unzulässige fremde Hilfe unter Beachtung der "Grundsätze zur Sicherung guter wissenschaftlicher Praxis" an der Heinrich-Heine Universität Düsseldorf erstellt worden ist. Die Dissertation wurde in der vorgelegten oder in ähnlicher Form noch bei keiner anderen Institution eingereicht. Ich habe bisher keine erfolglosen Promotionsversuche unternommen.